Thèse de Xinzhe Wu, Université de Lille, 2019

Université de Lille

UNIVERSITÉ DE LILLE

École doctorale Sciences Pour l'Ingénieur Université Lille Nord-de-France
Centre de Recherche en Informatique, Signal et Automatique de Lille

THÈSE

préparée et soutenue publiquement

PAR

Xinzhe WU

à la Maison de la Simulation, Saclay, le 22 Mars 2019

pour obtenir le grade de Docteur en **Informatique et applications**

Contribution à l'émergence de nouvelles méthodes parallèles et reparties intelligentes utilisant un paradigme de programmation multi-niveaux pour le calcul extrême

---

Thèse dirigée par Serge G. Petiton, Université de Lille

Membres du jury:

Présidente	Sophie Tison	Professeure à l'Université de Lille
Rapporteurs	Michel Daydé	Professeur à l'ENSEEIHT
	Michael A. Heroux	Directeur de Rercherche Laboratoires National de Sandia, États-Unis
Examinateurs	Barbara Chapman	Professeure à l'Université de Stony Brook, États-Unis
	Michaël Krajecki	Professeur à l'Université de Reims Champagne-Ardenne
	France Boillod-Cerneux	Docteur, Ingénieure de Recherche au CEA Saclay
Directeur	Serge G. Petiton	Professeur à l'Université de Lille

© 2019 Tous droits réservés.

lilliad.univ-lille.fr

© 2019 Tous droits réservés.

lilliad.univ-lille.fr

Thèse de Xinzhe Wu, Université de Lille, 2019

Université de Lille

UNIVERSITY OF LILLE

Doctoral School of Sciences for Engineering University Lille Nord-de-France
Research Center in Computer Science, Signal and Automation of Lille

THESIS

prepared and publicly defended

BY

Xinzhe WU

at Maison de la Simulation, Saclay, March 22, 2019

to obtain the title Ph.D. of **Computer Science**

Contribution to the Emergence of New Intelligent Parallel and Distributed Methods Using a Multi-level Programming Paradigm for Extreme Computing

---

Thesis supervised by Serge G. Petiton, University of Lille

Members of the jury:

President	Sophie Tison	Professor at University of Lille
Reviewers	Michel Daydé	Professor at ENSEEIHT
	Michael A. Heroux	Senior Scientist Sandia National Laboratories, USA
Examinators	Barbara Chapman	Professor at Stony Brook University, USA
	Michaël Krajecki	Professor at University of Reims Champagne-Ardenne
	France Boillod-Cerneux	Doctor, Scientist at CEA Saclay
Director	Serge G. Petiton	Professor at University of Lille

© 2019 Tous droits réservés.

lilliad.univ-lille.fr

© 2019 Tous droits réservés.

lilliad.univ-lille.fr

謹以此文獻給我的祖母劉占仙（*1928-2015*）

This thesis is dedicated to my grandmother. Hope you can hear in the heaven.

© 2019 Tous droits réservés.

lilliad.univ-lille.fr

© 2019 Tous droits réservés.

lilliad.univ-lille.fr

Acknowledgement

First and foremost, I would like to express my gratitude to my advisor of the thesis, Prof. Serge G. Petiton, for the continuous support of my Ph.D. study and related research, for his patience, motivation, and immense knowledge. He enlightens me in the field of parallel computing and numerical algorithms. In addition, he has taught me how to conduct academic research in the past three years. I am grateful for his wise guidance and inclusiveness throughout my three years' study. I feel so lucky to work under his supervision.

I warmly thank Michel Daydé, professor at ENSEEIHT, and Michael A. Heroux, senior scientist at Sandia National Laboratories. I feel honored that they can be the reviewers of my thesis. Thanks for their revisions and relevant remarks. I would also like to thank all the members of the committee, Barbara Chapman, Sophie Tison, Michaël Krajecki and France Boillod-Cerneux for joining my defense of the thesis.

My sincere thanks also go to the MYX project and CNRS for funding my thesis. I am grateful for the warm welcome shown by the Maison de la Simulation, especially Edouard Audit, for accepting me to study at this laboratory and funding me for several international conferences. I would also thank Valérie Belle and all secretary members for helping me with numerous administrative work.

I have been privileged to visit with the National Supercomputing Center in Guangzhou. I want to thank them, especially Prof. Yutong Lu for sharing their knowledge and I have benefited from the fruitful discussion with them.

I would like to thank ROMEO HPC Center, Université de Reims Champagne-Ardenne. They provide me the access to their supercomputer ROMEO (both 2013 and 2018 versions), which are the major platforms for the experimentation within my dissertation. I appreciate Dr. Arnaud RENARD and his engineering team for their technique supports.

Special thanks to my lovely friends in Paris for their help and encouragement. I am very thankful to have these friends who enrich my life with great happiness. It is hard to forget the days of drinking Chinese liquor together, which eased my homesickness.

I also want to thank those who are dear to me. Their attention and encouragements have accompanied me throughout this journey. I thank my parents for their support and unfailing confidence. Words cannot express how grateful I am to my mother and father for all of the sacrifices that you've made on my behalf. Thanks to my sister Kunze for being present at every moment.

At the end of this journey, I thank Yuxin for being able to accompany me in the best way and to continue to inspire me daily.

© 2019 Tous droits réservés.

lilliad.univ-lille.fr

© 2019 Tous droits réservés.

lilliad.univ-lille.fr

Thèse de Xinzhe Wu, Université de Lille, 2019

Abstract

Krylov iterative methods are frequently used on High-Performance Computing (HPC) systems to solve the extremely large sparse linear systems and eigenvalue problems from science and engineering fields. With the increase of both number of computing units and the heterogeneity of supercomputers, time spent in the global communication and synchronization severely damage the parallel performance of iterative methods. Programming on supercomputers tends to become distributed and parallel. Algorithm development should consider the principles: 1) multi-granularity parallelism; 2) hierarchical memory; 3) minimization of global communication; 4) promotion of the asynchronicity; 5) proposition of multi-level scheduling strategies and manager engines to handle huge traffic and improve the fault tolerance.

In response to these goals, we present a distributed and parallel multi-level programming paradigm for Krylov methods on HPC platforms. The first part of our work focuses on an implementation of a scalable matrix generator to create test matrices with customized eigenvalue for benchmarking iterative methods on supercomputers. In the second part, we aim to study the numerical and parallel performance of proposed distributed and parallel iterative method. Its implementation with a manager engine and runtime can handle the huge communication traffic, fault tolerance, and reusability. In the third part, an auto-tuning scheme is introduced for the smart selection of its parameters at runtime. Finally, we analyse the possibility to implement the distributed and parallel paradigm by a graph-based workflow runtime environment.

Keywords:

Distributed and parallel programming Krylov iterative methods Linear systems High Performance Computing Preconditioning Techniques Asynchronous communication Heterogeneous and homogenous architectures Exascale supercomputer

© 2019 Tous droits réservés.

lilliad.univ-lille.fr

© 2019 Tous droits réservés.

lilliad.univ-lille.fr

Thèse de Xinzhe Wu, Université de Lille, 2019

Résumé

Les méthodes itératives de Krylov sont utilisées sur les plate-formes de Calcul Haute Performance (CHP) pour résoudre les grands systèmes linéaires issus des domaines de la science et de l'ingénierie. Avec l'augmentation du nombre de cœurs et de l'hétérogénéité des superordinateurs, le temps consacré à la communication et synchronisation globales nuit gravement aux leurs performances parallèles. La programmation tend à être distribuée et parallèle. Le développement d'algorithmes devrait prendre en compte les principes: 1) parallélisme avec multi-granularité; 2) mémoire hiérarchique; 3) minimisation de la communication globale; 4) promotion de l'asynchronicité; 5) proposition de stratégies d'ordonnancement et de moteurs de gestion pour gérer les trafic et la tolérance aux pannes.

En réponse à ces objectifs, nous présentons un paradigme de programmation multi-niveaux distribués et parallèls pour les méthodes de Krylov sur les plates-formes de CHP. La première partie porte sur la mise en œuvre d'un générateur de matrices avec des valeurs propres prescrites pour la référence des méthodes itératives. Dans la deuxiéme partie, nous étudions les performances numériques et parallèles de la méthode itérative proposée. Son implémentation avec un moteur de gestion peut gérer le communication, la tolérance aux pannes et la réutilisabilité. Dans la troisième partie, un schéma de réglage automatique est introduit pour la sélection intelligente de ses paramètres lors de l'exécution. Enfin, nous étudions la possibilité d'implémenter ce paradigme dans un environnement d'exécution de flux de travail.

Keywords:

Programmation distribuée et parallèle Méthodes itératives de Krylov Systèmes linéaires Calcul Haute Performance Techniques de préconditionnement Communications asynchrones Architectures hétérogeènes et homogènes Superordinateur exascale

© 2019 Tous droits réservés.

lilliad.univ-lille.fr

© 2019 Tous droits réservés.

lilliad.univ-lille.fr

Contents

© 2019 Tous droits réservés.

lilliad.univ-lille.fr

Thèse de Xinzhe Wu, Université de Lille, 2019

© 2019 Tous droits réservés.

lilliad.univ-lille.fr

Thèse de Xinzhe Wu, Université de Lille, 2019

© 2019 Tous droits réservés.

lilliad.univ-lille.fr

Thèse de Xinzhe Wu, Université de Lille, 2019

© 2019 Tous droits réservés.

lilliad.univ-lille.fr

Thèse de Xinzhe Wu, Université de Lille, 2019

© 2019 Tous droits réservés.

lilliad.univ-lille.fr

CONTENTS

© 2019 Tous droits réservés.

lilliad.univ-lille.fr

List of Figures

© 2019 Tous droits réservés.

Thèse de Xinzhe Wu, Université de Lille, 2019

© 2019 Tous droits réservés.

lilliad.univ-lille.fr

Thèse de Xinzhe Wu, Université de Lille, 2019

© 2019 Tous droits réservés.

lilliad.univ-lille.fr

Thèse de Xinzhe Wu, Université de Lille, 2019

© 2019 Tous droits réservés.

lilliad.univ-lille.fr

List of Tables

© 2019 Tous droits réservés.

lilliad.univ-lille.fr

Thèse de Xinzhe Wu, Université de Lille, 2019

© 2019 Tous droits réservés.

lilliad.univ-lille.fr

List of Algorithms

© 2019 Tous droits réservés.

lilliad.univ-lille.fr

Thèse de Xinzhe Wu, Université de Lille, 2019

© 2019 Tous droits réservés.

lilliad.univ-lille.fr

Thèse de Xinzhe Wu, Université de Lille, 2019

List of Symbols

The next list describes several symbols that will be later used within the body of the document

ADLB	Asynchronous Dynamic Load Balancing
AI	Artificial Intelligence
ALU	Arithmetic Logic Unit
AMG	Algebraic Multigrid
API	Application Programming Interface
ARM	Advanced RISC Machine
BiCGSTAB	Biconjugate Gradient Stabilized Method
BLAS	Basic Linear Algebra Subprograms
BLAS3	Basic Linear Algebra Subprograms - Level 3
CAF	Coarray Fortran
CFD	Computational Fluid Dynamics
CG	Conjugate Gradient Method
COO	Coordinate Matrix Format
CPE	Compute-Processing Element
CPU	Central Processing Unit
CSR	Compressed Sparse Row Matrix Format
CUDA	Compute Unified Device Architecture
DAG	Directed Acyclic Graph
DIA	Diagonal Matrix Format
DRAM	Dynamic Radom-Acess Memory
DSP	Digital Signal Processor

© 2019 Tous droits réservés.

lilliad.univ-lille.fr

Thèse de Xinzhe Wu, Université de Lille, 2019

ERAM	Explicitly Restarted Arnoldi Method
FDA	Fisher Discriminant Analysis
FEM	Finite element method
FLOPS	Floating-point Operations Per Second
FPGA	Field-Programmable Gate Array
GCRO-DR	Generalized Conjugate Residual method with inner Orthogonalization and Deflated Restarting
GMG	Geometric Multigrid
GMRES	Generalized Minimal Residual Method
GMRES-DR	Deflated GMRES
GPDSP	General-Purpose Digital Signal Processor
GPGPU	General-Purpose Computing on Graphics Processing Units
GPU	Graphic Processing Unit
GUI	Graphic User Interface
HPC	High-Performance Computing
HPCG	High-Performance Conjugate Gradients
HPL	High-Performance LINPACK
I/O	Input/Output
IDL	Interface Description Language
IDR	Induced dimension reduction
ILU	Incomplete LU Factorization
IRAM	Implicitly Restarted Arnoldi Method
LAPACK	Linear Algebra PACKage
MERAM	Multiple Explicitly Restarted Arnoldi method
MG	Multigrid method
MIC	Many Integrated Cores
MINRES	Minimal Residual
MPE	Management Processing Element

© 2019 Tous droits réservés.

lilliad.univ-lille.fr

Thèse de Xinzhe Wu, Université de Lille, 2019

MPI	Message Passing Interface
NUMA	Non-Uniform Memory Access
OpenACC	Open Accelerators
OpenCL	Open Computing Language
OpenMP	Open Multi-Processing
OS	Operating system
PCA	Principal Component Analysis
PDE	Partial Differential Equation
PETSc	Portable, Extensible Toolkit for Scientific Computation
PGAS	Partitioned Global Address Space
Pthreads	POSIX Threads
QCD	Lattice Quantum Chromodynamics
QMR	Quasi Minimal Residual
RAM	Random Access Memory
RHS	Right-hand Sides
RISC	Reduced Instruction Set Computer
ScaLAPACK	Scalable Linear Algebra PACKage
SIMD	Single Instruction Multiple Data
SIMT	Single Instruction Multiple Thread
SLEPc	Scalable Library for Eigenvalue Problem Computations
SMP	Symmetric Multiprocessor
SOR	Successive Overrelaxation
SpGEMM	Sparse Matrix Matrix Multiplication
SPMD	Single Program Multiple Data
SpMV	Sparse Matrix Vector Multiplication
SSOR	Symmetric Successive Overrelaxation
SVD	Singular Value Decomposition
SWIG	Simplified Wrapper and Interface Generator

© 2019 Tous droits réservés.

lilliad.univ-lille.fr

Thèse de Xinzhe Wu, Université de Lille, 2019

TFQMR	Transpose-free Quasi Minimal Residual
UMA	Uniform Memory Access
XMP	XcalableMP

© 2019 Tous droits réservés.

lilliad.univ-lille.fr

Chapter 1

Introduction

1.1 Motivations

HPC provides much larger computing power that cannot achieve with the typical desktop computers or workstations. At the early age, the HPC clusters are constructed in the UMA and NUMA models, in which all the computing units are able to access the gobal memory. That is the shared memory architecture of supercomputers, which provides a user-friendly parallel programming paradigm for the users. With the evolution of supercomputers, the lack of scalability between memory and CPUs made it difficult to construct much larger supercomputers. Therefore, the distributed memory architecture was introduced for modern supercomputing, in which each processor has its local memory. This architecture can scale the supercomputers with millions cores and more. The parallel programming for users on distributed memory architecture is much more complicated, since it is the users' responsability to explicitly define the data communication methologies between different computing units.

Nowadays, the exascale era of HPC will come soon, and the first exascale machine will be available around 2020, in which, the researchers hope to make unprecedented advancements in many fields of science and industry. In fact, the world's most powerful machine now has already more than a million cores. With the introduction of GPUs and other accelerators on the distributed memory architecture, HPC cluster systems will not only continue to expand the number of compute nodes and CPU cores, but will also increase the heterogeneity of components. This causes the trend of transition to multi- and many cores within compute nodes that communicate explicitly through a faster interconnected network. The heterogeneity of computing units on supercomputers introduces hierarchical memory and communications. Applications on these hierarchical supercomputers can be seen as the intersection of distributed and parallel computing. Nevertheless, due to the lack of good scalability on extreme large clusters, only a few applications may achieve sustainable performance.

Many scientific and industrial applications can be formulated as linear systems. A linear system can be described by an operator matrix A, an input x and an output b. The linear solvers which aim to solve these systems, are the kernels of many applications and softwares. When the operator matrix A is sparse, a collection of Krylov subspace methods, such as GMRES, CG, and BiCGSTAB, are widely used methods for solving linear systems. The Krylov subspace methods approximate the exact solution of a linear system from a given initial guess vector

© 2019 Tous droits réservés.

lilliad.univ-lille.fr

Thèse de Xinzhe Wu, Université de Lille, 2019

through the Krylov subspace.

Linear systems are associated with the real-world applications, such as the fusion reactions, earthquake, and weather forecast. As the complexity of applications increases, their dimension grows rapidly. For example, linear systems for seismic simulations have more than 10 billions unknowns. Therefore, Krylov subspace methods are deployed on supercomputing platforms to solve such large-scale linear systems in parallel. Nowadays, with the increase of the number of computing units and the heterogeneity of supercomputers, the communication of overall reduction and global synchronization of Krylov subspace methods become the bottleneck, which seriously damages their parallel performance. In detail, when a large-scale problem is solved by Krylov subspace methods on parallel architectures, their cost per iteration becomes the most significant concern, typically due to communication and synchronization overhead. Consequently, large scalar products, overall synchronization, and other operations involving communications among all cores have to be avoided. Parallel implementations of numerical algorithms should be optimized for more local communications and less global communications. In order to efficiently utilize the full computing power of such hierarchical computing systems, it is central to explore novel parallel methods and models for solving linear systems. These methods should not only accelerate convergence, but also have the ability to accommodate multiple granularity, multi-level memory, improve fault tolerance, reduce synchronization, and promote asynchronization.

1.2 Objectives and Contributions

The subject of my dissertation is related to this research context, and it focuses on the proposition and analysis of a distributed and parallel programming paradigm for smart hybrid Krylov methods targeting at the exascale computing. Since more than thirty years ago, different hybrid Krylov methods were introduced to accelerate the convergence of iterative solvers by using the selected eigenvalues of systems, e.g., Chebyshev polynomial preconditioned hybrid ERAM presented by Saad [182] to accelerate the convergence of ERAM to solve eigenvalue problems; another implementation of hybrid Chebyshev Krylov subspace algorithm introuced by Elman et al. [82], which uses the Arnoldi method to simultaneously compute the required eigenvalues; a hybrid GMRES algorithm via a Richardson iteration with Leja ordering presented by Nachtigal et al. [155] and an approach introduced by Brezinski et al. [44] for solving linear systems by the combination of two arbitrary approximate solutions of two methods. The research of this thesis relies on the Unite and Conquer approach proposed by Emad et al. [83], which is a model for the design of numerical methods that combines different computational components by asynchronous communication to work for the same objective. These different components can be deployed on different platforms such as P2P, cloud and the supercomputer systems, or different processors on the same platform. The ingredients of this dissertation on building a Unite and Conquer linear solver come from previous research, e.g., the hybrid methods firstly implemented by Edjlali et al. [79] on network of heterogeneous parallel computers to solve eigenvalue problem, and a hybrid gmres/ls-arnoldi method firstly introduced by Essai et al. [86]. Unite and Conquer approach is suitable to design a new programming paradigm for iterative methods with distributed and parallel computing on modern supercomputers.

Before investigating the Krylov subspace methods for solving linear systems, the first con-

© 2019 Tous droits réservés.

lilliad.univ-lille.fr

Thèse de Xinzhe Wu, Université de Lille, 2019

tribution of this work is to develop SMG2S[1]: a Scalable Matrix Generator with Given Spectra, due to the importance of spectral distribution for the convergence of iterative methods. SMG2S allows the generation of large-scale non-Hermitian matrices using user-given eigenvalues. These generated matrices are also non-Hermitian and non-trivial, with very high dimensions. Recent research on social networking, big data, machine learning, and AI has increased the necessity for non-Hermitian solvers associated with much larger sparse matrices and graphs. For decades, iterative linear algebra methods have been an important part of the overall computation time of applications in various fields. The analysis of their behaviors is complex, and it is necessary to evaluate their numerical and parallel performances to solve the extremely large non-Hermitian eigenvalue and linear problems on parallel and/or distributed machines. Since the properties of spectra have impacts on the convergence of iterative methods, it is critical to generate large matrices with known spectra to benchmark them. The motivation for proposing SMG2S is also that there is currently no set of test matrices with large dimensions and different kinds of spectral characteristics to benchmark the linear solvers on supercomputers. Throughout my thesis, SMG2S serves as an important tool for studying the performance of newly designed iterative methods.

After the implementation of SMG2S, the second contribution of my dissertation is to design and implement an distributed and parallel UCGLE (Unite and Conquer GMRES/LS-ERAM) method based on the Unite and Conquer approach. UCGLE is proposed to solve large-scale non-Hermitian linear systems with the reduction of global communications. Most hybrid and deflated iterative methods are able to be transformed into distributed and parallel scheme based on Unite and Conquer approach. However, this dissertation only implements UCGLE as an example, which is based on a hybrid GMRES method preconditioned by Least Squares polynomial. UCGLE consists of three computational components: ERAM Component, GMRES Component, and LSP (Least Squares Polynomial) Component. GMRES Component is used to solve the systems, LSP Component and ERAM Component serve as the preconditioning part. The information used to speed up convergence are the eigenvalues. The key feature of UCGLE is asynchronous communication between these three components, which reduces the number of synchronization points and minimizes global communication. There are three levels of parallelisms in UCGLE method to explore the hierarchical computing architectures. The convergence acceleration of UCGLE is similar to a normal hybrid preconditioner. The difference between them is that the improvement of the former one is intrinsic to the methods. It means that in the conventional hybrid methods, for each preconditioning, the solving procedure should stop and wait for the temporary preconditioning procedure using the information from previous Arnoldi reduction procedure. The latter's asynchronous communication can cover the synchronization overhead. Asynchronous communications between different computational components also improve the fault tolerance and the reusability of this method. Separating the procedure for calculating the preconditioning information (dominant eigenvalues in UCGLE) to be a component independent of the solution procedure can improve the flexibility of preconditioning, and this leads to a further improvement in numerical performance.

Moreover, both the mathematical model and the implementation of UCGLE have been ex-

1. https://smg2s.github.io

© 2019 Tous droits réservés.

lilliad.univ-lille.fr

Thèse de Xinzhe Wu, Université de Lille, 2019

tended to solve linear systems in sequence which share the same operator matrix but have different RHSs. This extension is even suitable for a series of linear systems with different operator matrices, which share a same portion of dominant eigenvalues. The eigenvalues obtained by UCGLE in solving previous systems can be recycled, improved on the fly and applied to construct new initial guess vectors for subsequent linear systems, which can achieve continuous acceleration to solve linear systems in sequence. Numerical experiments on supercomputers using different test matrices indicate a substantial decrease in both computation time and iteration steps for solving sequences of linear systems, when approximate eigenvalues are recycled to generate initial guess vectors.

Afterwards, since many problems in the field of science and engineering often require to solve simultaneously large-scale linear systems with multiple RHSs, we proposed another extension of UCGLE by combining it with block version of GMRES. This variant of UCGLE is implemented with newly designed manager engine, which is capable of allocating multiple block GMRES at the same time, each block GMRES solving the linear systems with a subset of RHSs and accelerating the convergence using the eigenvalues approximated by eigensolvers. Dividing the block linear system with multiple RHSs into subsets and solving them simultaneously using different allocated linear solvers allow localizing calculations, reducing global communication, and improving parallel performance.

An adaptive UCGLE is proposed with an auto-tuning scheme for selected parameters, that have the influence on its numerical and parallel performance. This work was achieved by analyzing the impacts of different parameters on the convergence.

1.3 Outline

The dissertation is organized as follows. In Chapter 2, we will give the state-of-the-art of HPC, including the modern computing architectures for supercomputers (e.g., CPU, Nvidia GPGPU, and Intel MIC) and the parallel programming models (including OpenMP, CUDA, MPI, PGAS, the task/graph based programming, etc.). Finally, in this chapter, we will discuss the challenges of the upcoming exascale supercomputers that the whole HPC community faces.

Chapter 3 covers the existing iterative methods for solving linear systems and eigenvalue problems, especially the Krylov Subspace methods. At the beginning, this chapter gives a brief introduction of the stationary and non-stationary iterative methods. Then different Krylov Subspace methods will be presented and compared. Apart from the basic introduction to methods, different preconditioners used to accelerate the convergence will be discussed, in particular the Least Squares polynomial method for constructing UCGLE will be described in detail. The relation between the convergence of Krylov subspace methods for solving linear systems and the spectral information of operator matrix A will also be analyzed in this chapter. Finally, we give an introduction of the parallel implementation of the Krylov subspace methods on modern distributed memory systems, then discuss the challenges of iterative methods facing on the coming of exascale platforms, and finally summarize the recent efforts to fit the numerical methods to much larger supercomputers.

In Chapter 4, we present the parallel implementation and numerical performance evaluation of SMG2S. It is implemented on CPUs and multi-GPU platforms with specially optimized

© 2019 Tous droits réservés.

lilliad.univ-lille.fr

Thèse de Xinzhe Wu, Université de Lille, 2019

communications. Efficient strong and weak scaling performance is obtained on several supercomputers. We have also proposed a method to verify its ability to guarantee the given spectra with high accuracy based on the Shift Inverse Power method. SMG2S is a released open source software developed using MPI and C++11. Moreover, the packaging, the interfaces to other programming languages and scientific libraries, and the GUI for verification are introduced. In the final part, we give an example to evaluate the numerical performance of different Krylov iterative methods using SMG2S .

In Chapter 5, the implementation of UCGLE based on the scientific libraries PETSc and SLEPc for both CPUs and GPUs are presented. In this chapter, we describe the implementation of components, the manager engine, and the distributed and parallel asynchronous communications. After implementation, the selected parameters, the convergence, the impact of spectral distribution, the scalability and fault tolerance are evaluated on several supercomputers.

Chapter 6 describes the extension of UCGLE for solving linear systems in sequence with different RHSs by recycling the eigenvalues. We give a survey on existing algorithms, including the seed and Krylov subspace recycling methods, and then develop the mathematical model and manager engine of UCGLE to solve linear systems in sequence. This chapter also shows the results of experiments on different supercomputers.

In Chapter 7, the variant of UCGLE to solve simultaneously linear systems with multiple RHSs is presented, which is denoted as m-UCGLE. This chapter introduces the existing block methods for solving linear systems with multiple RHSs, and then analyzes the limitations of block methods on large-scale platforms. After that, a mathematical extension of Least Squares polynomial for multiple RHSs is given, and then a special novel manager engine is developed. This engine allows allocating a user-defined number of computational components at the same time. This special version of UCGLE is implemented with the linear and eigen solvers provided by the Belos and Anasazi packages of Trilinos. Finally, we give the experimental results on large-scale machines.

UCGLE is a hybrid method with the combination of three different numerical methods. Thus the auto-tuning of different parameters is very important. In Chapter 8, we propose the strategy of auto-tuning for selected parameters in UCGLE. The auto-tuning heuristic is able to select the optimal parameter value for each restart of GMRES Component at runtime. Experimental results demonstrate the effectiveness of this auto-tuning scheme.

All Unite and Conquer methods, including UCGLE, are able to use the workflow/task-based programming runtimes to manage the fault tolerance, load balance and asynchronous communication of signals, arrays and vectors. In Chapter 9, we give a glance at the YML framework, and then analyze the workflow of UCGLE and the limitations of YML for Unite and Conquer approach. Finally, we propose the solutions for YML syntax and implementation, including the dynamic graph grammar, and the mechanism of exiting a parallel branch.

In Chapter 10, we summarize the key results obtained in this thesis and present our concluding remarks. Finally, we suggest some possible paths to future research.

© 2019 Tous droits réservés.

lilliad.univ-lille.fr

Thèse de Xinzhe Wu, Université de Lille, 2019

© 2019 Tous droits réservés.

lilliad.univ-lille.fr

Chapter 2

State-of-the-art in High-Performance Computing

High-Performance Computing most generally refers to the practice of aggregating computing power in a way that provides much higher performance than typical desktop computers or workstations to solve large-scale problems in science, engineering, or business. HPC is one of the most active areas of research in Computer Science because it is strategically essential to solve the large challenge problems that arise in scientific and industrial applications. The development of HPC relies on the efforts from multi-disciplines, including the computer architecture design, the parallel algorithms, and programming models, etc. This chapter gives the state-of-the-art of HPC: its history, modern computing architectures, and parallel programming models. Finally, with the advent of exascale supercomputers, we discuss the key challenges that the entire HPC community faces.

2.1 Timeline of HPC

The terms *high-performance computing* and *supercomputing* are sometimes used interchangeably. A supercomputer is a computing platform with a high level of performance, that consists of a large number of computing units connected by a local high-speed computer bus. HPC technology is implemented in a variety of computationally intensive applications in the multidisciplinary fields, including biosciences, geographical simulation, electronic design, climate research, neuroscience, quantum mechanics, molecular modeling, nuclear fusion, etc. Supercomputers were introduced in the 1960s, and the performance of a supercomputer is measured in FLOPS. Since the first generation of supercomputers, the *megascale* performance was reached in the 1970s, and the *gigascale* performance was passed in less than decade. Finally, the *terascale* performance was achieved in the 1990s, and then the *petascale* performance was crossed in 2008 with the installation of IBM Roadrunner at Los Alamos National Laboratory in the United States. Fig. 2.1 shows the peak performance of the fastest computer every year since the 1960s.

Since 1993, the TOP500 project[1] ranks and details the 500 most powerful supercomputing

1. https://www.top500.org

© 2019 Tous droits réservés.

lilliad.univ-lille.fr

Thèse de Xinzhe Wu, Université de Lille, 2019

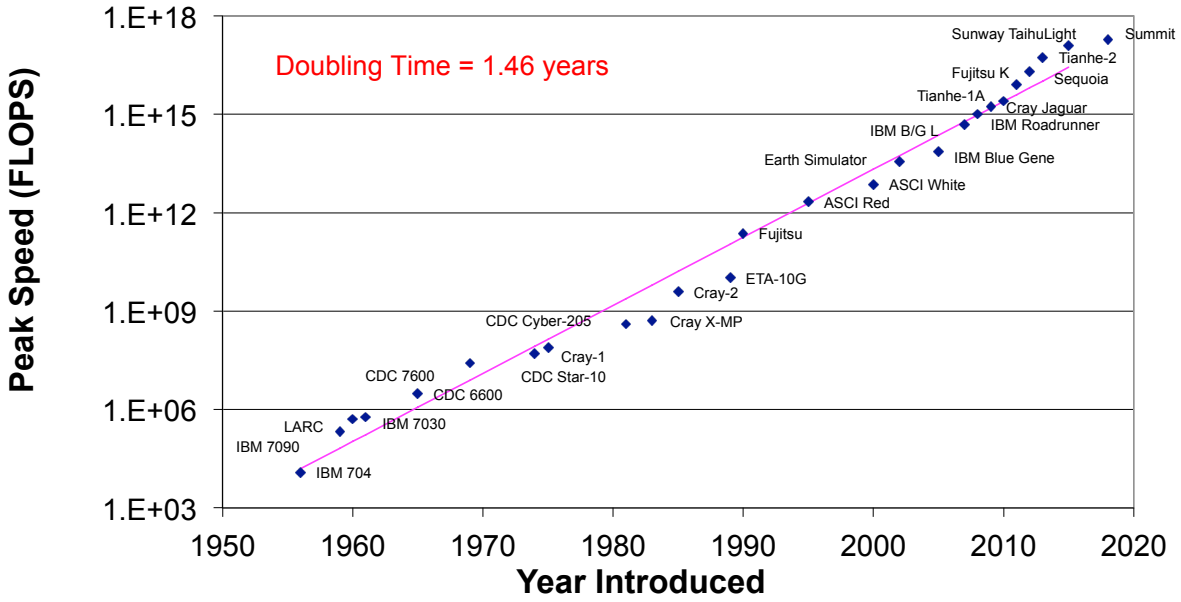

Figure 2.1 – Peak performance of the fastest computer every year since the 1960s. [175]

systems in the world and publishes an updated list of the supercomputers twice a year. The project aims to provide a reliable basis for tracking and detecting trends in HPC and bases rankings on HPL [76], a portable implementation of the high-performance LINPACK benchmark written in Fortran for distributed-memory computers. HPL is a software package that solves a (random) dense linear system in double precision (64 bits) arithmetic on distributed-memory computers. The algorithm used by HPL can be summarized by the following keywords:

- two-dimensional block-cyclic data distribution;
- right-looking variant of the LU factorization with row partial pivoting featuring multiple look-ahead depths;
- recursive panel factorization with pivot search and column broadcast combined;
- various virtual panel broadcast topologies;
- bandwidth reducing swap-broadcast algorithm;
- backward substitution with look-ahead of depth 1.

According to the latest Top500 list in November 2018, the fastest supercomputer is the Summit of the United States, with a LINPACK benchmark score of 122.3 PFLOPS. Sunway TaihuLight, Sierra and Tianhe-2A follow closely the Summit, with the performance respectively 93 PFLOPS, 71.6 PFLOPS, and 61.4 PFLOPS. Fig. 2.2 gives the No. 1 machine of HPL performance every year since 1993.

The next barrier for the HPC community to overcome is the *exascale* computing, which refers to the computing systems capable of at least one exaFLOPS (10^{18} floating point operations per second). This capacity represents a thousandfold increase over the first petascale computer which came into operation in 2008. The world first exascale supercomputer will be launched around

© 2019 Tous droits réservés.

lilliad.univ-lille.fr

Thèse de Xinzhe Wu, Université de Lille, 2019

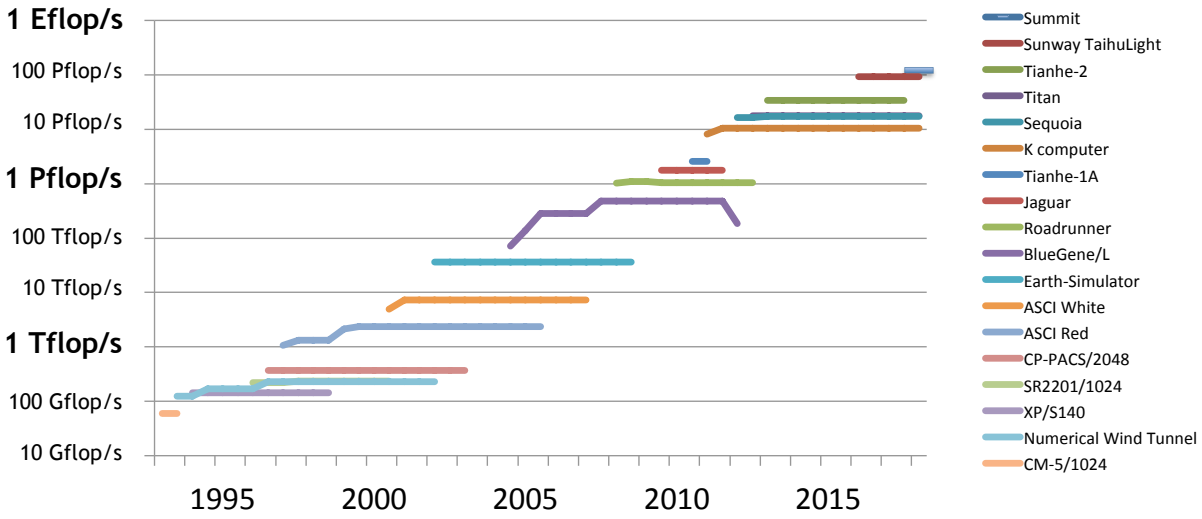

Figure 2.2 – No. 1 machine of HPL Performance each year since 1993. [209]

2020. China's first exascale supercomputer will be put into use by 2020. First exascale computer of United States is planned to be built by 2021 at Argonne National Laboratory. The post-K announced by Japan, public services will begin around 2021, and the first exascale supercomputer in Europe will appear around 2022. Exascale computing would be considered as a significant achievement in computer engineering, for it is estimated to be the order of processing power of the human brain at the neural level.

Considering the development of HPC, there are always two questions proposed by the users who want to develop applications on supercomputers:

- *How to build such powerful supercomputers?*
- *How to develop the applications to effectively utilize the total computational power of a supercomputer?*

In order to answer the above two questions, firstly, Section 2.2 outlines the modern computing architectures for building supercomputers. Different parallel programming models for developing applications on supercomputers are given in Section 2.3.

2.2 Modern Computing Architectures

Different architectures of computing units are designed to build the supercomputers. In this section, the state-of-the-art of modern CPUs and accelerators will be reviewed.

2.2.1 CPU Architectures and Memory Access

The development of modern CPUs is based on the *Von Neumann architecture*. The proposition of this computer architecture is based on the description by the mathematician and physicist *John von Neumann* and others in the *First Draft of a Report on the EDVAC* [214]. All the modern computing units are related to this concept, which consists of five parts:

© 2019 Tous droits réservés.

lilliad.univ-lille.fr

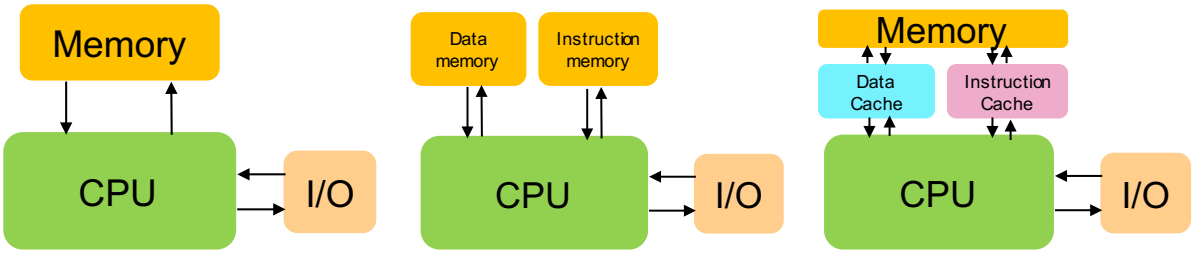

(a) Von Neumann architecture. (b) Harvard architecture. (c) Modified Harvard architecture.

Figure 2.3 – Computer architectures.

- A *processing unit* that contains an arithmetic logic unit and processor registers;
- A *control unit* that contains an instruction register and program counter;
- *Memory* that stores data and instructions;
- External mass *storage*;
- *Input/output* mechanisms.

As shown in Fig. 2.3a, the *Von Neumann architecture* uses the shared bus between the program memory and data memory, which leads to its bottleneck. Since the single bus can only access one of the two types of memory at a time, the data transfer rate between the CPU and memory is rather low. With the increase of CPU speed and memory size, the bottleneck has become more of a problem.

The *Harvard architecture* is another computer architecture that physically separates the storage and bus of the instructions and data. As shown in Fig. 2.3b, the limitation of a pure *Harvard architecture* is that the mechanisms must be provided to load the programs to be executed into the instruction memory and load any data onto the input memory. Additionally, read-only technology of the instruction memory allows the computer to begin executing a pre-loaded program as soon as it is powered up. The data memory will now be in an unknown state, so it is not possible to provide any kind of pre-defined data values to the program.

Today, most processors implement the separate pathways like the Harvard architecture to support the higher performance concurrent data and instruction access, meanwhile loosen the strictly separated storage between code and data. That is named as the *Modified Harvard architecture* (shown as Fig. 2.3c). This model can be seen as the combination of the Von Neumann architecture and Harvard architecture.

Modified Harvard architecture provides a hardware pathway and machine language instructions so that the contents of the instruction memory can be read as if they were data. Initial data values can then be copied from the instruction memory into data memory when the program starts. If the data is not to be modified, it can be accessed by the running program directly from instruction memory without taking up space in the data memory. Nowadays, most CPUs have Von Neumann like unified address space and separate instruction and data caches as well as memory protection, making them more Harvard-like, and so they could be classified more as modified Harvard architecture even using unified address space.

© 2019 Tous droits réservés.

lilliad.univ-lille.fr

Thèse de Xinzhe Wu, Université de Lille, 2019

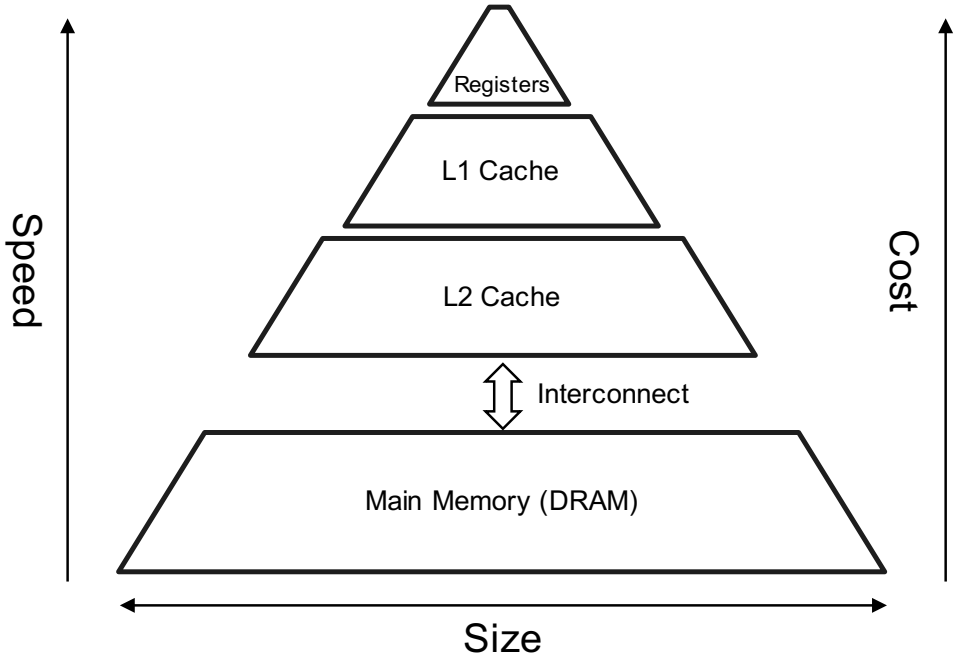

Figure 2.4 – Memory Hierarchy.

The most common modification of modified Harvard architecture for modern CPUs is to build a memory hierarchy with a CPU cache separating instructions and data based on response time. As shown in Fig. 2.4, the top of the memory hierarchy which provides the fastest data transfer rate are the registers. Target data with arithmetic and logic operations will be temporarily held in the register to perform the computations. The number of registers is limited due to the cost. CPU cache is the hardware that the CPU uses to reduce the average cost (time or energy) of accessing data from main memory. A cache is a smaller, faster memory, closer to a processor core, which stores copies of the data from frequently used main memory locations. Most CPUs have different independent caches, including instruction and data caches, where data cache is usually organized as a hierarchy of more cache levels. The lowest level is main memory, which is made of DRAM with the lowest bandwidth and the highest latency compared to registers and caches.

2.2.2 Parallel Computer Memory Architectures

The parallel computer memory architectures can be divided into shared and distributed memory types. Shared memory parallel computers come in many types, but typically have the ability to access all of the memory as a global address space for all processors. Multiple processors can operate independently but share the same memory resources. Changes in a memory location affected by one processor are visible to all other processors. Historically, shared memory machines have been classified as *UMA* (shown as 2.5a) and *NUMA* (shown as 2.5b), based upon memory access times. UMA is most commonly represented today by SMP machines with identical processors. These processors require the same memory access time. NUMA is often made by physically linking two or more SMPs, one SMP can directly access memory of another SMP. Not

© 2019 Tous droits réservés.

lilliad.univ-lille.fr

Thèse de Xinzhe Wu, Université de Lille, 2019

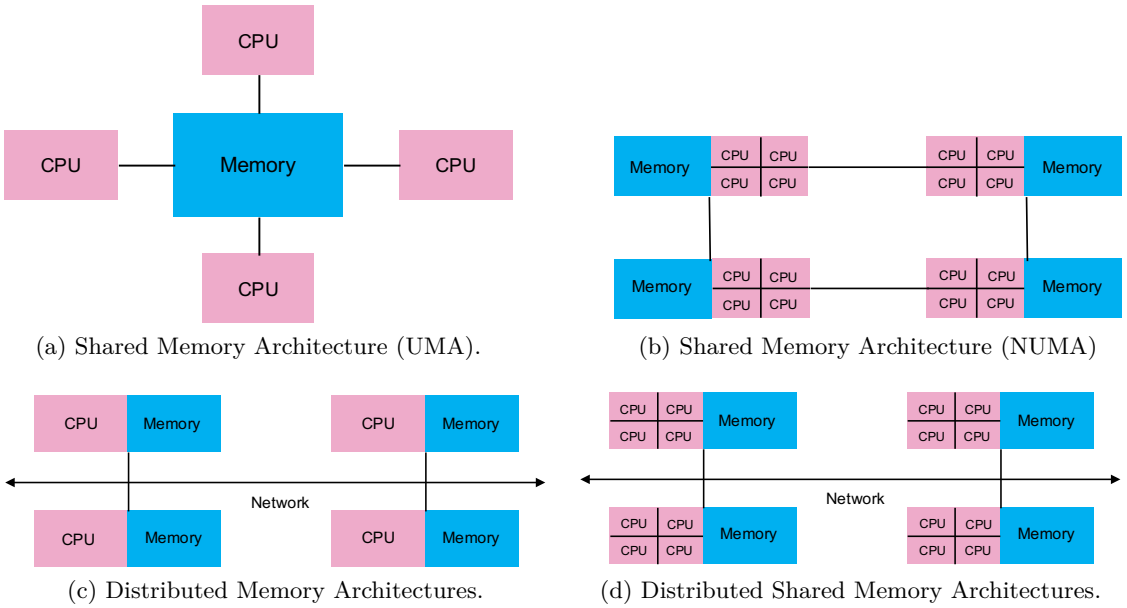

(a) Shared Memory Architecture (UMA).

(b) Shared Memory Architecture (NUMA)

(c) Distributed Memory Architectures.

(d) Distributed Shared Memory Architectures.

Figure 2.5 – Parallel Computer Memory Architectures.

all processors have equal access time to all memories, memory access across the link is slower. The advantages of shared memory architectures are:

(1) global address space provides a user-friendly programming perspective to memory;

(2) due to the proximity of the memory to the CPU, data sharing between tasks is fast and uniform.

The disadvantages are:

(1) lack of scalability between memory and CPUs, in fact, adding more CPUs can geometrically increase traffic on the shared memory-CPU path, and for cache coherent systems, geometrically increase traffic associated with cache/memory management;

(2) programmers' responsibility for synchronization operations that ensure *correct* access of global memory. It is impossible to construct today's multi-petaflop supercomputers with hundreds of thousands of CPU-cores.

The distributed-memory architecture was then proposed, which takes many multicore computers and connects them using a network. With a fast enough network, we can in principle extend this approach to millions of CPU cores and higher. As shown in Fig. 2.5c, inside distributed memory system, processors have their local memory. Memory addresses in one processor do not map to another processor, so there is no concept of global address space across all processors. Because each processor has its local memory, it operates independently. Changes made to its local memory do not affect the memory of other processors. Therefore, the concept of cache coherency does not apply. When a processor needs to access data in another processor, it is usually the task of programmers to explicitly define how and when data is communicated. Synchronization between tasks is likewise also programmers' responsibility. The advantages of distributed memory architecture are:

© 2019 Tous droits réservés.

lilliad.univ-lille.fr

Thèse de Xinzhe Wu, Université de Lille, 2019

(1) Memory is scalable with the number of processors. The number of processors and the size of memory increases proportionally;

(2) Each processor can quickly access its memory without interference, and there is no overhead incurred in trying to maintain global cache coherency;

(3) Cost-effectiveness.

The disadvantages are:

(1) the programmers are responsible for many of the details associated with data communication between processors;

(2) mapping existing data structures based on global memory to the distributed memory organization can be difficult;

(3) data that resides on the remote node requiring longer access time than the local node.

Nowadays, the largest and fastest computers in the world employ both shared and distributed memory architectures (shown as Fig. 2.5d). The shared memory component can be a shared memory machine and/or GPU. The distributed memory component is a network of multiple shared memory/GPU machines, which know only about their memory - not the memory on another computer. Therefore, network communications are required to move data from one machine to another. The current trend indicates that this type of memory architecture will continue to dominate and grow at HPC for the foreseeable future.

In a word, shared-memory systems are challenging to build but easy to use and are ideal for laptops and desktops. Distributed-shared memory systems are easier to build but harder to use, including many shared-memory nodes with their separate memory. Distributed-shared memory systems introduce much more hierarchical memory and computing with multi-level of parallelism. The critical advantage of distributed-shared memory architectures is increasing scalability, and the important drawback is the added complexity of the program.

2.2.3 Nvidia GPGPU

GPGPUs use GPUs, which typically only process computer graphics calculations to perform more general computation of complex applications that are traditionally processed by CPUs. Modern GPUs are very efficient at manipulating computer graphics and image processing. Due to its special features, GPGPU can be used as an accelerator for CPUs to improve the overall performance of the computer. Nowadays, it is becoming increasingly common to use GPGPU to build supercomputers. According to the latest list of the Top500 in November 2018, five of the top ten supercomputers in the world use GPGPUs.

As shown in Figure 2.6, the architectures of CPU and GPU are different: the CPU has a small number of complex cores and massive caches while the GPU has thousands of simple cores and small caches. The massive ALUs of GPU are simple, data-parallel, multi-threaded which offer high computing power and large memory bandwidth. In brief, graphics chips are designed for parallel computations with lots of arithmetic operations, while CPUs are for general complex

© 2019 Tous droits réservés.

lilliad.univ-lille.fr

Thèse de Xinzhe Wu, Université de Lille, 2019

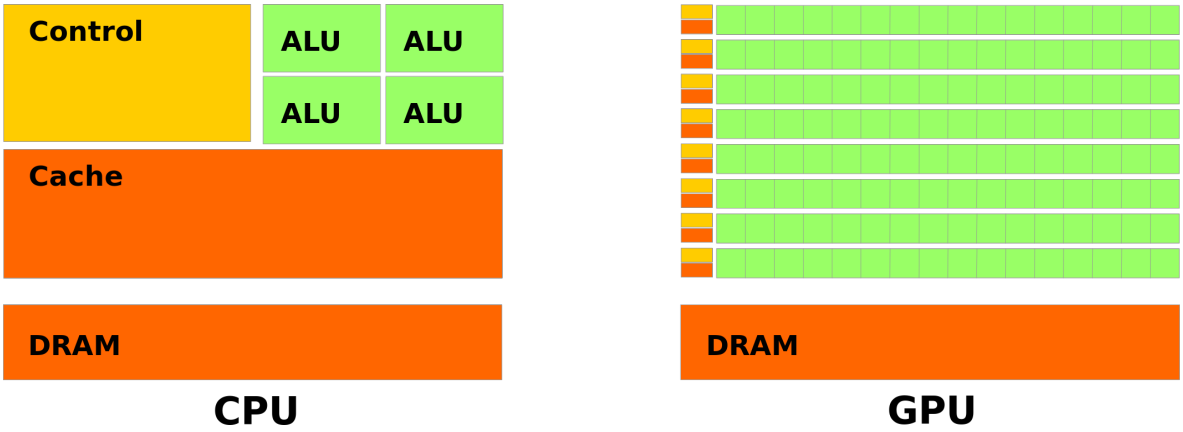

Figure 2.6 – CPU vs GPU architectures [163].

applications. The host character of CPU requires complex kernels and deep pipelines to deal with all kinds of operations. It usually runs at a higher frequency and supports branch prediction. The GPU only focuses on simple data-parallel operations thus the pipeline is shallow. The same instructions are used on large datasets in parallel with thousands of hardware cores, so the branch prediction is not necessary, and important arithmetic operations instead of caching hide memory access latency. GPGPU is also regarded as a powerful backup to overcome the *power wall*.

Introduced in mid-2017, the newest *Tesla V100* card can deliver 7.8 TFLOPS in double-precision floating point and 15.7 TFLOPS in single-precision floating point.

2.2.4 Intel Many Integrated Cores

The performance improvement of processors comes from the increasing number of computing units within the small chip area. Thanks to advanced semiconductor processes, more transistors can be built in one shared-memory system to perform multiple operations simultaneously. From a programmer's perspective, this can be realized in two ways: different data or tasks execute in multiple individual computing units (multi-thread) or long uniform instruction decoders (vectorization).

In 2013, Intel officially first revealed the latest MIC codenamed *Knights Landing (KNL)*, its organization is given as Fig. 2.7a. Being available as a coprocessor like previous boards, KNL can also serve as a self-boot MIC processor that is binary compatible with standard CPUs and boot standard OS. These second generation chips could be used as a standalone CPU, rather than just as an add-in card. Another key feature is the on-card high-bandwidth memory which provides high bandwidth and large capacity to run large HPC workloads. Due to the memory wall, memory bandwidth is one of the common performance bottlenecks in computing applications. KNL implements a two-level memory system to address this issue. Shown as Fig. 2.7b, it provides three types of memory modes, including the cache mode, the flat mode and the hybrid mode. The main difference between Xeon Phi and a GPGPU like Nvidia Tesla is that Xeon Phi with x86-compatible cores can run software originally targeted at a standard x86 CPU with less modification.

© 2019 Tous droits réservés.

lilliad.univ-lille.fr

Thèse de Xinzhe Wu, Université de Lille, 2019

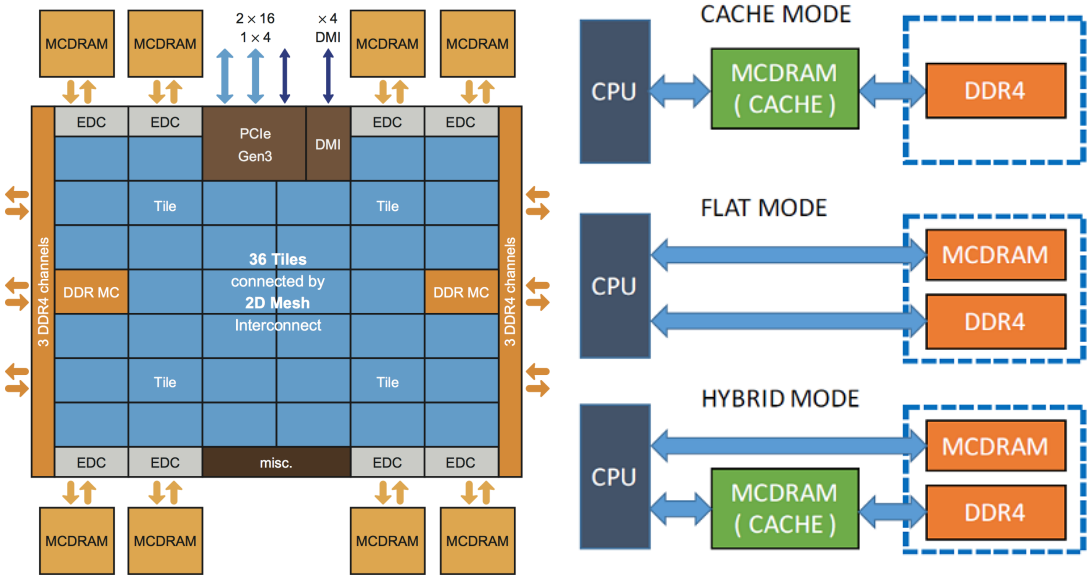

(a) KNL organization [177].

(b) KNL cache modes [223].

Figure 2.7 – Architecture and memory modes of Intel Knights Landing processor.

2.2.5 RISC-based (Co)processors

A RISC is such a processor that has a small set of simple and general instructions instead of a bunch of complex and specialized instructions. A type of well-known RISC-based computing units are the ARM architecture processors. In the 21st century, the use of smartphones and tablet computers provides a broad user base for RISC-based systems. Since the installation of Sunway TaihuLight[2], RISC processors also start to be used in supercomputers. RISC-based supercomputers enable low energy consumption per core and cheaper chips since they do not contain complex instruction sets. In this section, we list two types of RISC based (co)processors for the supercomputers.

The first type of processor is sw26010, which is a 260-core manycore processor [95] designed by the National High-Performance Integrated Circuit Design Center in Shanghai. It implements the Sunway architecture, a 64-bit RISC architecture designed by China. As shown in Fig. 2.8, the sw26010 has four clusters of 64 CPEs which are arranged in an eight-by-eight array. The CPEs support SIMD instructions and are capable of performing eight double-precision floating-point operations per cycle. Each cluster is accompanied by a more conventional general-purpose core called the MPE that provides supervisory functions. Each cluster has its own dedicated DDR3 SDRAM controller and a memory bank with its own address space. The processor runs at a clock speed of 1.45.

Matrix-2000 [219] is a 64-bit 128-core many-core processor designed by NUDT and introduced in 2017. This chip was specifically designed as an accelerator for China's Tianhe-2A supercomputer installed in the National Supercomputing Center in Guangzhou[3] to upgrade and replace

2. http://www.nsccwx.cn
3. http://www.nscc-gz.cn

© 2019 Tous droits réservés.

lilliad.univ-lille.fr

Thèse de Xinzhe Wu, Université de Lille, 2019

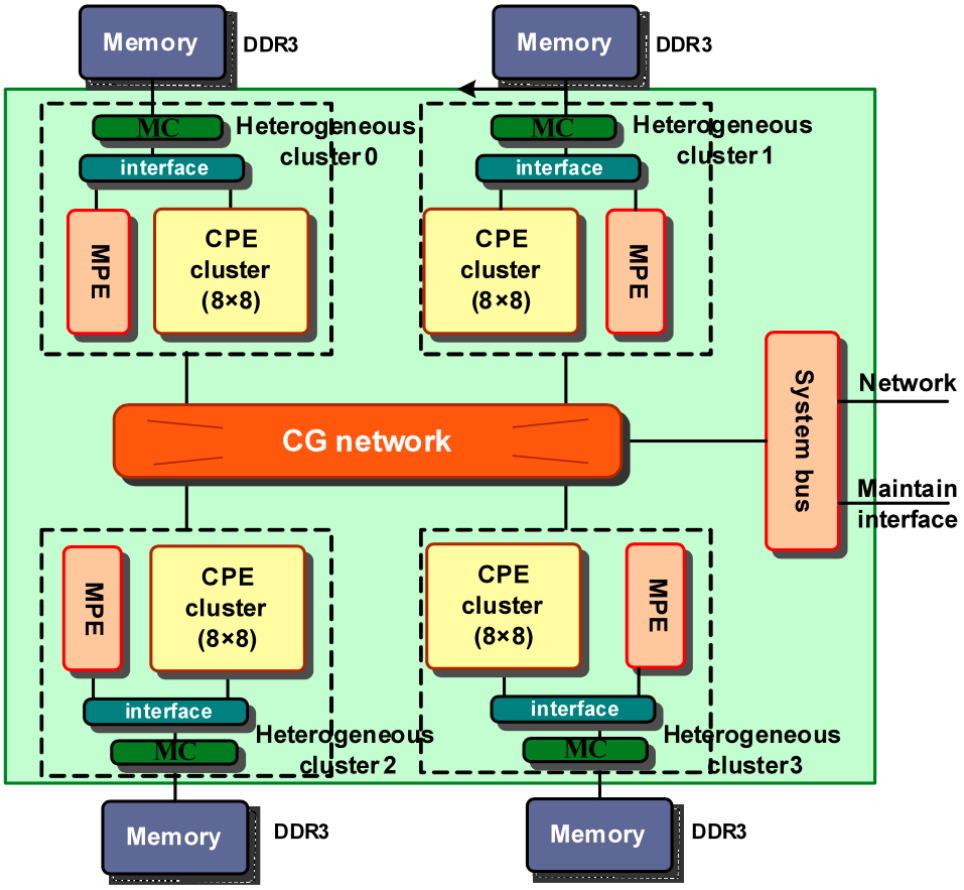

Figure 2.8 – The architecture of a sw26010 manycore processor. [95]

the aging Intel Knights Corner accelerators. The Matrix-2000 has 128 RISC cores operating at 1.2 GHz, reaching 2.46 and 4.92 TFLOPS respectively for double-precision and single-precision floating point, with a peak power dissipation of 240W. The Matrix-2000 consists of 128 cores, eight DDR4 memory channels, and 16 PCIe lanes. The chip consists of four supernodes consisting of 32 cores each operating at 1.2 GHz with a peak power dissipation of 240 Watts.

The applications and codes should also be implemented and optimized for modern RISC processors, e.g., Daydé et al. introduced efficient code design on high-performance RISC processors for both full and sparse linear solvers [65], and they presented also a blocked implementation of level 3 BLAS for RISC processors [66].

2.2.6 FPGA

FPGA is an integrated circuit designed to be configured with an array of programmable logic blocks and reconfigurable interconnects. The FPGA architecture provides the flexibility to create a massive array of application-specified ALUs that enable both instruction and data-level parallelism. FPGA has very high energy efficiency because it requires the low frequency and unused computing blocs do not consume energy. FPGAs can serve as accelerators on the supercomputers, e.g., Paderborn Center for Parallel Computing[4] installed several prototype hybrid machines by combining FPGAs with Intel Xeon CPUs. FPGAs are by no means anything new

4. https://pc2.uni-paderborn.de

© 2019 Tous droits réservés.

lilliad.univ-lille.fr

Thèse de Xinzhe Wu, Université de Lille, 2019

in the HPC sector – ten years ago they were all the rage but proved very difficult to program, and now they are coming back in vogue because the C, C++ and Fortran applications for these devices have become easier.

2.3 Parallel Programming Model

After introducing the hardware architectures, this section describes the parallel programming models for developing applications on supercomputers. Most modern supercomputers are of distributed shared memory architectures that introduce multi-level parallel programming models, including shared memory/thread-level parallel models, distributed memory/process-level parallel models, PGAS models, and task/workflow-based parallelism models.

2.3.1 Shared Memory Level Parallelism

In this section, we introduce various runtimes developed to support the shared memory parallelism of different computing architectures.

2.3.1.1 OpenMP

OpenMP [62] is an API that supports multi-platform shared memory parallel programming in C, C++, and Fortran. OpenMP supports most platforms, instruction set architectures, and operating systems. It consists of a set of compiler directives, library routines, and environment variables. OpenMP provides the ability to progressively parallelize serial programs by inserting specific directives. The compiler can ignore these directives, and the application can be executed in a sequential way when target machines do not support OpenMP. OpenMP is designed for multi-processor/core, shared memory machines. The underlying architecture can be shared memory UMA or NUMA. OpenMP programs accomplish parallelism exclusively through the use of threads.

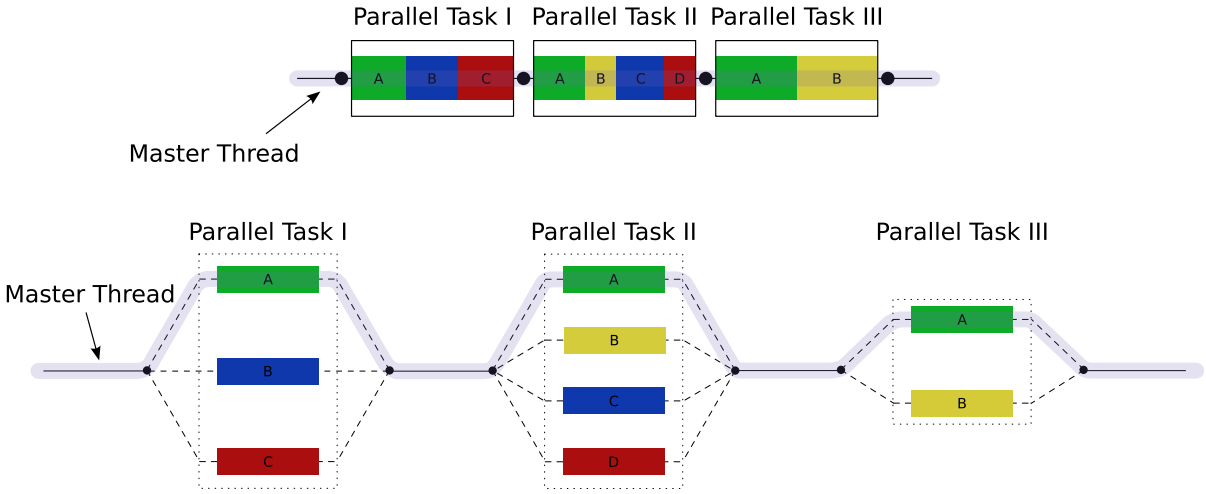

Figure 2.9 – OpenMP *fork-join* Model [220].

As shown in Fig. 2.9, OpenMP uses the *fork-join* model to support parallel execution. All OpenMP programs begin with a single process that continues until sequentially the first parallel

© 2019 Tous droits réservés.

lilliad.univ-lille.fr

Thèse de Xinzhe Wu, Université de Lille, 2019

region construct is encountered. Then this thread creates a team of parallel threads and assigns the workload to them and make them work at the same time. When the team threads complete the statements in the parallel region construct, they are synchronized and terminated, leaving only the main thread. The new released OpenMP begins to support task scheduling strategies, the SIMD directives for high-level vectorization and the *offload* directives for heterogeneous systems.

2.3.1.2 CUDA

CUDA [164] is a parallel programming platform and application programming interface model created by Nvidia. It allows software developers and engineers to perform general processing using GPUs that support CUDA. The CUDA software layer provides direct access to GPU's virtual instruction set and parallel computational elements to execute the compute kernels. The CUDA platform is designed to work with programming languages such as C, C++, and Fortran. This accessibility makes it easier for parallel programming specialists to use GPU resources. Fig. 2.10 gives the four steps of processing flow on CUDA:

(1) Copy the processing data from main memory to memory for GPU;

(2) Load the executable from CPU to GPUs;

(3) Execute the operations in each core in parallel;

(4) Copy back the results from memory for GPU to the main memory.

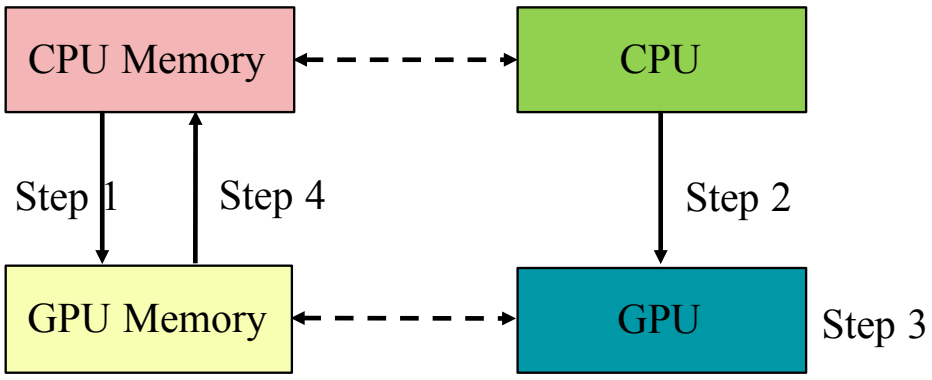

Figure 2.10 – Processing flow on CUDA.

2.3.1.3 OpenCL

OpenCL [152] is a framework for writing programs that execute across heterogeneous platforms consisting of CPUs, GPUs, DSPs, FPGAs, and other processors or hardware accelerators. OpenCL specifies programming languages (based on C99 and C++11) for programming these devices and APIs to control the platform and execute programs on the compute devices. OpenCL provides a standard interface for parallel computing using task- and data-based parallelism.

© 2019 Tous droits réservés.

lilliad.univ-lille.fr

2.3.1.4 OpenACC

OpenACC [218] is a programming standard for parallel computing developed by Cray, CAPS, Nvidia and PGI. The standard is designed to simplify parallel programming of heterogeneous CPU/GPU systems. As in OpenMP, the programmer can annotate C, C++ and Fortran source code to identify the areas that should be accelerated using compiler directives and additional functions. Like OpenMP 4.0 and newer, OpenACC can target both the CPU and GPU architectures and launch computational code on them.

2.3.1.5 Kokkos

Kokkos [81] implements a programming model in C++ for writing performance portable applications for all major HPC platforms. To this end, it provides abstractions for parallel executions of code and data management. Kokkos is designed for complex node architectures with N-level memory hierarchies and multiple types of execution resources. It currently uses OpenMP, Pthreads, and CUDA as backend programming models.

2.3.2 Distributed Memory Level Parallelism

In the distributed memory platforms, each processor owns a private memory that cannot be accessed from other processors. The only way for processors to exchange data is to use explicit communication to send and receive messages.

2.3.2.1 Message Passing Interface

MPI [104] is a standardized and portable message-passing standard designed by a group of researchers from academia and industry to support a variety of parallel computing architectures. MPI provides basic users with an easy-to-use, portable interface that is powerful enough to allow programmers to use the high-performance messaging operations available on advanced computers. Most MPI implementations consist of a specific set of routines that can be called directly from C, C++, Fortran, and any languages that interface with these libraries. MPI library functions include, but are not limited to, basic point-to-point send/receive operations, aggregate functions involving communication between all processes, synchronous nodes (barrier operations), one-way communication, dynamic process management, I/O, and so on.

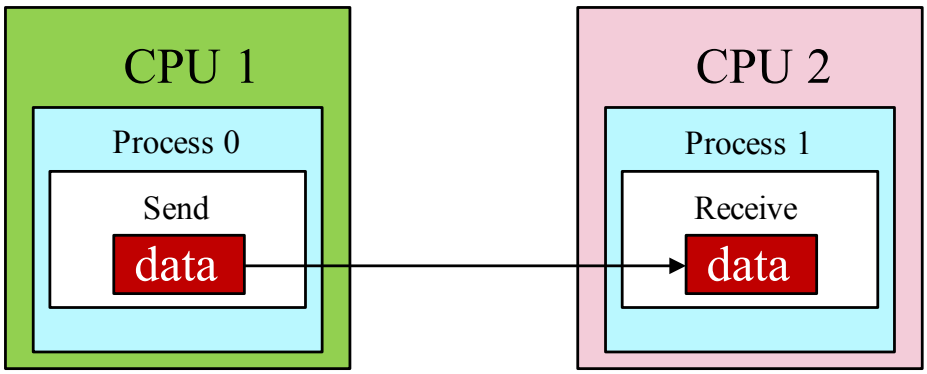

Figure 2.11 – MPI point to point send and receive Model.

© 2019 Tous droits réservés.

Thèse de Xinzhe Wu, Université de Lille, 2019

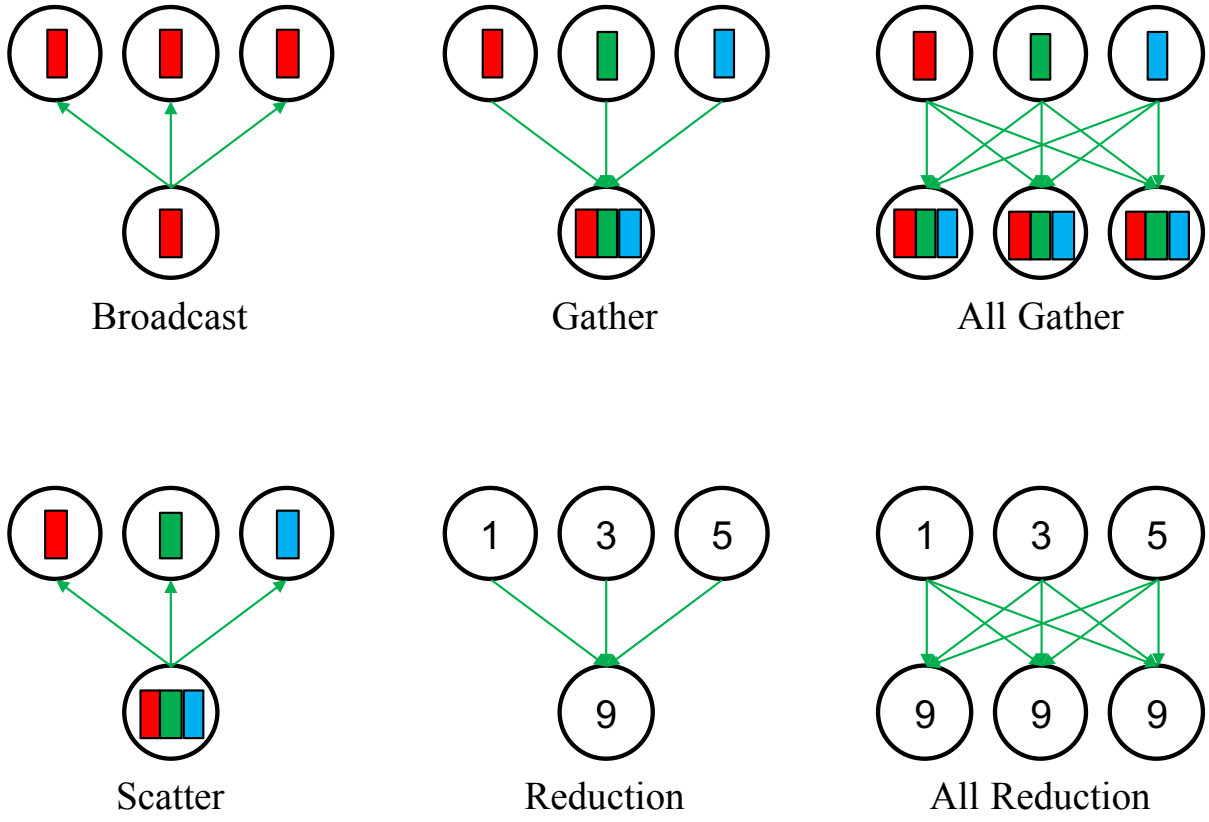

Figure 2.12 – Different modes of collective operations provided by MPI.

As shown in Fig. 2.11, *point-to-point operations* support the communication in both synchronous and asynchronous ways. Point-to-point operations, as these are called, are particularly useful in irregular communication, for example, a master-slave architecture in which the master sends new task data to a slave whenever the prior task is completed. MPI supports mechanisms for both blocking and non-blocking point-to-point communication mechanisms, as well as the so-called 'ready-send' mechanism whereby a send request can be made only when the matching receive request has already been made.

Collective functions (shown as Fig. 2.12) involve communication among all processes in a process group (which can mean the entire process pool or a program-defined subset). A typical function is the MPI_Bcast call (short for "broadcast"). This function takes data from one node and sends it to all processes in the process group. A reverse operation is the MPI_Reduce call, which takes data from all processes in a group, operates (such as summing), and stores the results on one node. MPI_Reduce is often useful at the start or end of a largely distributed calculation, where each processor operates on the part of the data and then combines it into a result. Fig. 2.12 gives six modes of collective communications, including broadcast, scatter, gather, reduction, all gather and all reduction.

In modern computing platforms with multiple shared-memory nodes, the shared memory programming models such as OpenMP and message passing programming such as MPI can be considered as complementary programming approaches, and can be used together in a hybrid way. This hybrid model is called *MPI+X*.

© 2019 Tous droits réservés.

lilliad.univ-lille.fr

Thèse de Xinzhe Wu, Université de Lille, 2019

2.3.3 Partitioned Global Address Space

In computer science, PGAS is a parallel programming model. Shown as Fig. 2.13, it assumes a global memory address space that is logically partitioned and a portion of it is local to each process, thread, or processing element. The novelty of PGAS is that the portions of shared memory space may have an affinity for a particular process, thereby exploiting locality of reference. There are different implementation based on PGAS model, such as Unified Parallel C, CAF, Chapel, X10, UPC++, DASH, XcalableMP, etc. PGAS attempts to combine the advantages of an SPMD programming style for distributed memory systems (as employed by MPI) with the data referencing semantics of shared memory systems. This is more realistic than the traditional shared memory approach of one flat address space because hardware-specific data locality can be modeled in the partitioning of the address space.

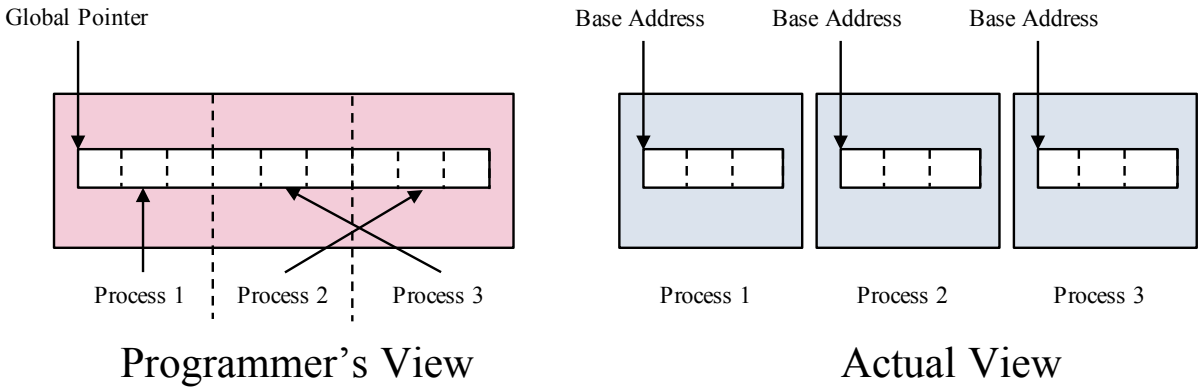

Figure 2.13 – Programmer's and actual views of memory address in the PGAS languages.

2.3.3.1 XcalableMP

XcalableMP [131] is a PGAS language extension of C and Fortran for parallel programming on distributed memory systems that helps users reduce programming efforts. XcalableMP provides two programming models.

- *Global view model*, which supports typical parallelization based on the data and task parallel paradigm, and enables parallelizing the original sequential code using minimal modification with simple, OpenMP-like directives. In the global view model, users specify the collective behaviors of nodes in the target program to parallelize them. The compiler is responsible for doing this when the user specifies the data and how the calculations are distributed across the nodes. This model is suitable for regular applications, such as domain-decomposition problems, where each node works in a similar way.

- *Local view model*, which allows using CAF-like expressions to describe inter-node communication. In the local-view mode, users specify the behavior of each node, just like MPI. Communications in this model can be specified in a one-sided manner based on CAF. This model is suitable for applications where each node performs a different task.

© 2019 Tous droits réservés.

lilliad.univ-lille.fr

Thèse de Xinzhe Wu, Université de Lille, 2019

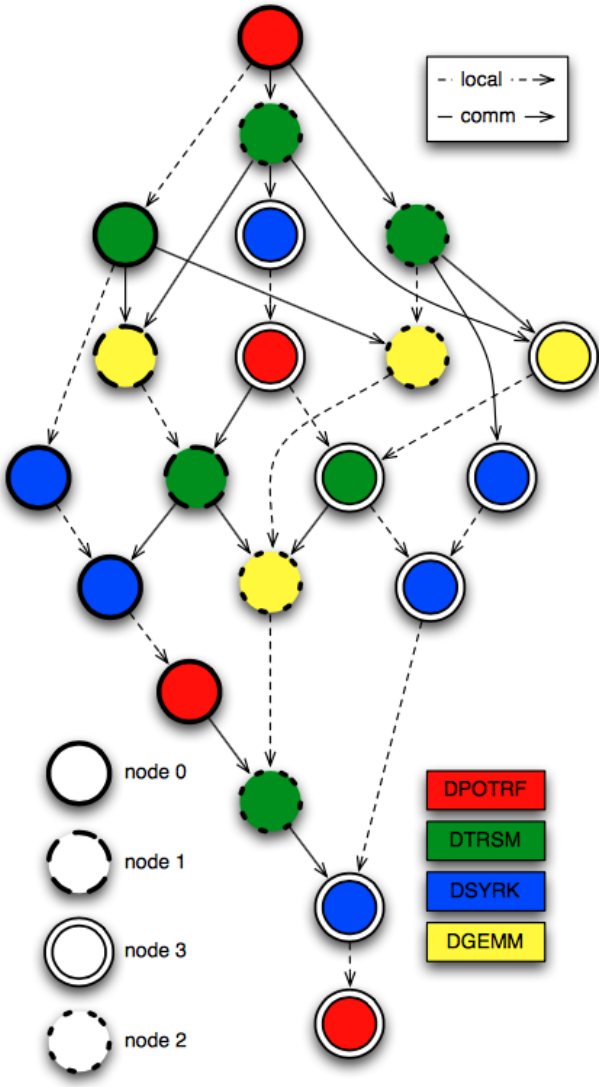

Figure 2.14 – Workflow of Cholesky factorization for a 4×4 tile matrix on a 2×2 grid of processors. Figure by Bosilca et al. [41]

2.3.4 Task/Graph Based Parallel Programming

As the complexity of applications on supercomputers increases, it becomes increasingly difficult for developers to maintain parallel code on modern computing architectures. The task/-graph based parallel programming models are proposed to express the task parallelism and data dependencies of complex codes. An application can be divided temporally and spatially into inter-dependent tasks of different natures. A good scheduler can manage the complex tasks efficiently across a large number of cores on the supercomputing systems, e.g., a parallelization on an MIMD computer with real-time scheduler was introduced with Gauss-Jordan method as an example [170]. Fig. 2.14 gives a workflow of Cholesky factorization for a 4×4 tile matrix on a 2×2 grid of processors proposed by Bosilca et al. [41].

The concept of granularity is introduced to describe the amount of work or task that can be performed before communicating or synchronizing with others. The choice of grain size is important for the parallel applications. In fact, for coarse-grained tasks, there may not be enough par-

© 2019 Tous droits réservés.

lilliad.univ-lille.fr

Thèse de Xinzhe Wu, Université de Lille, 2019

allel execution. In contrast, a large number of fine-grained tasks will cause unnecessary parallel overhead. Modern applications on supercomputers should consider multi-levels of granularities to accommodate hierarchical systems. In this section, we list several well-known task/graph based parallel programming runtime environments that were developed to support coarse-grained or fine-grained tasks.

2.3.4.1 StarPU

StarPU[5] [17] is a task programming library for hybrid architectures with shared memory. The application provides algorithms and constraints both the CPU/GPU implementations of tasks and the graphs of tasks, using either the StarPU's high-level GCC plugin pragmas, StarPU's rich C/C++ API, or OpenMP pragmas. StarPU handles runtime issues: task dependencies, optimized heterogeneous scheduling, optimized data transfer/replication between main and discrete memories, and optimized cluster communication.

2.3.4.2 OmpSs

OmpSs[6] is a task-based programming environment which covers both heterogeneous and homogeneous architectures. Its target is the programming of multi-GPU or many-core architectures and offers asynchronous parallelism in the execution of the tasks [78]. OmpSs is built on top of Mercurium compiler [23] and Nanos++ runtime system [172]. Nanos++ is able to schedule and run these tasks, taking care of the required data transfers and synchronizations on the accurate resources. Tasks in OmpSs are annotated with data directionality clauses that specify the use of data, and how it will be used (read, write or read & write). Dependencies are then deduced at runtime from user-supplied annotations of data accesses which are translated into a format that can be exploited by Nanos++. Nanos++ proposes several scheduling policies that define how ready tasks are executed.

2.3.4.3 YML

YML[7] [71, 72, 69] was introduced and designed in May 2000 by Serge Petiton and Olivier Delannoy, while Olivier Delannoy was beginning his Master internship at the CNRS laboratory *Application du Calcul Scientific Intensif (ACSI)* of the National CNRS Supercomputer Center IDRIS in Saclay. A first prototype was developed by Olivier Delannoy during his intership and evaluated on some block dense linear algebra methods [70]. Since 2001, YML is developed, improved, and evaluated on several methods and platforms (including P2P platforms, Grids, cloud and supercomputing) by researchers worldwide. The website and the main team are now hosted by the University of Versailles and led by Nahid Emad. International collaborations with researchers from Japan and Germany are supported by the national agencies of these countries. The French side is led by Serge Petiton.

YML can describe a complex parallel application regardless of the execution platform. The YvetteML language is used to express the task graph of applications. The nodes of the graph are

5. http://starpu.gforge.inria.fr
6. https://pm.bsc.es/ompss
7. http://yml.prism.uvsq.fr

© 2019 Tous droits réservés.

lilliad.univ-lille.fr

Thèse de Xinzhe Wu, Université de Lille, 2019

the tasks described by components, and the edges correspond to dependencies or communications. The components are written in XML. Each component implementation can contain C++, XMP-C, XMP-FORTRAN or other code. Each component implementation can be expressed in parallel with finer grain. The combination of YML, XMP and StarPU provides a three-level parallelism programming paradigm to develop applications on supercomputers. YML will be discussed in detail in Chapter 9.

2.3.4.4 Swift

Swift[8] [221] is a data-flow oriented coarse-grained scripting language that supports dataset typing and mapping, dataset iteration, conditional branches, and procedural composition. Swift scripts are primarily concerned with processing (possibly large) collections of data files, by invoking programs to do that processing. Swift handles execution of such programs at remote sites by choosing sites, handling the staging of input and output files to and from the chosen sites and remote execution of programs. Swift/T is an implementation of the Swift language for HPC, which translate the Swift script into an MPI program that uses the Turbine and ADLB runtime libraries[9] for highly scalable dataflow processing over MPI, without single-node bottlenecks.

2.3.4.5 Legion

Legion[10] [103] is a data-centric parallel programming system for writing portable high performance programs for distributed heterogeneous architectures. Legion provides abstractions which allow programmers to describe properties of program data (e.g., independence, locality). By making the Legion programming system aware of the structure of program data, it can automate many of the tedious tasks programmers face today, including correctly extracting task- and data-level parallelism and moving data around complex memory hierarchies. A novel mapping interface provides explicit programmer controlled data placement in the memory hierarchy and assignment of tasks to processors in a manner that is orthogonal to correctness, making the Legion application easy to port and tune to the new architecture.

2.4 Exascale Challenges of Supercomputers

The era of exascale computing is coming. In this section, we will analyze the increasing trend of heterogeneity in modern supercomputers and then summarize the challenges of parallel programming for exascale systems.

2.4.1 Increase of Heterogeneity for Supercomputers

Hardware architectures have great impacts on the development of supercomputers. In the early days, processor performance was primarily improved by increasing the number of transistors per integrated circuit. According to *Moore's law*, the number of transistors per integrated circuit doubles every 18 months. This means that the size of the transistor is reduced to half, which

8. http://swift-lang.org
9. https://cs.mtsu.edu/ rbutler/adlb
10. http://legion.stanford.edu

© 2019 Tous droits réservés.

lilliad.univ-lille.fr

Thèse de Xinzhe Wu, Université de Lille, 2019

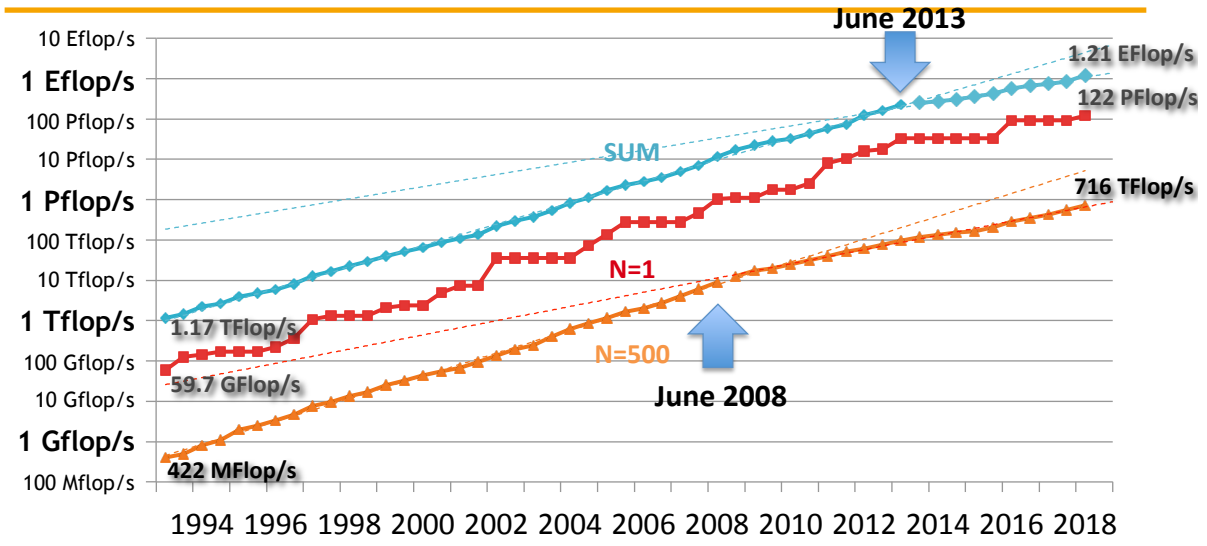

Figure 2.15 – HPL Performance in Top500 by year. [209]

allows for a faster clock rate. Before 2002, *Moore's law* was found to be totally acceptable. Since then, the overheating introduced by higher frequency reaches the limit of air cooling. This is the famous *power wall*. Fig. 2.15 shows the HPL performance by year in Top500 List. *Moore's law* is not totally acceptable in recent years, where the performance's development of supercomputer has slowed down. Since then, modern computing architectures tend to have multiple processors on-chip, lower operating frequency and hierarchical architectures, such as the GPGPU, Intel MIC, the many-core sw26010, and Matrix-2000 GPDSP, etc. Moreover, Europe (Mont-Blanc [176], CEA and Atos [87]) and Japan (RIKEN and Fujitsu [88]) are now pushing the development of ARM supercomputers. Fig. 2.16 shows the trend of supercomputers equipped with accelerators by year. According to the Top 500 list in November 2018, 137 of 500 systems use accelerator or co-processor technology. The introduction of accelerators on the supercomputers with a large number of cores extremely increases their heterogeneity of communications, memory and computing units.

Compared with the traditional computing architectures such as Intel, AMD CPUs which dedicate to multiple different purposes that result in lousy energy efficiency in HPC, the introduction of low frequency and/or less complex architecture improve the energy efficiency. In the Green500 list[11] of November 2016, 8 out of 10 the most efficient supercomputers are equipped with the Nvidia GPGPU, and the No.1 machine of Green500 list *ZettaScaler-2.2* installed by RIKEN is powered by the Intel low-frequency processor (*Xeon D-1571 16C 1.3GHz*).

2.4.2 Potential Architecture of Exascale Supercomputer

This section attempts to create a blueprint (shown as Fig. 2.17) for the upcoming exascale machine, which is based on the future Aurora Exascale system architecture discussed in [208].

As shown in Fig. 2.17, the exascale supercomputers will consist of more than 100,000 interconnected nodes. Each compute node is packed with the thin cores and fat cores. The fat cores refer to the Intel, AMD X86 CPUs dedicated to more complex operations. The thin cores can be

11. https://www.top500.org/green500/

© 2019 Tous droits réservés.

lilliad.univ-lille.fr

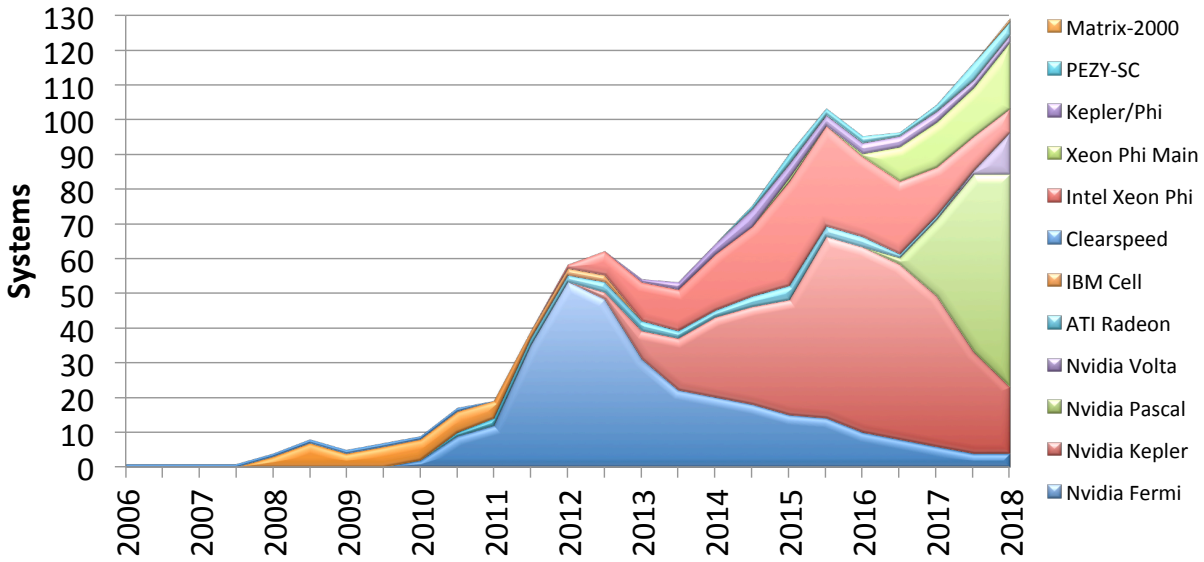

Figure 2.16 – Number of systems each year boosted by accelerators. [209]

the accelerators and co-processors (e.g., GPGPU, Matrix-2000, FPGA, etc.) with low frequency and/or less complex operations. A typical fat-thin mode is the Nvidia *Host* and *device* architecture. The fat cores are connected with RAM which has high capacity and low bandwidth, and the thin cores are connected with the memory which has low capacity and high bandwidth.

This fat core-thin core hybrid approach can also be found in the sw26010 processor deployed in the Sunway TaihuLight supercomputer. As shown in Fig. 2.8, this processor is designed with one fat core (MPE) which provides supervisory functions, and four auxiliary meshes of skinny cores (CPEs) conducted to computing operations, each with 64 cores, for a total of 260 cores.

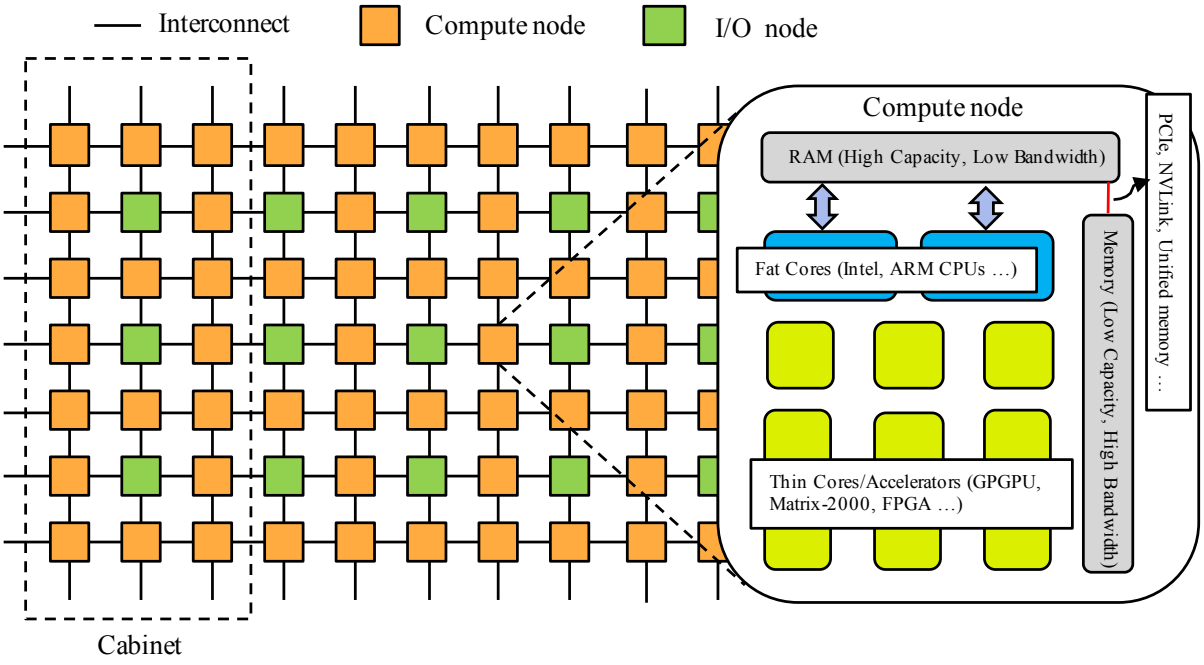

Figure 2.17 – Multi-level parallelism and hierarchical architectures in supercomputers.

© 2019 Tous droits réservés.

These hierarchical computing architectures introduces multiple level parallelism:

(1) 1^{st} level is the *inter-node parallelism* between compute nodes: MPI is the considered model to manage the communication among the compute nodes, manager engine or other complex software stacks are required to handle huge traffic and failure of applications;

(2) 2^{nd} level is the *intra-node parallelism*, including:

- shared memory parallelism with NUMA among cores and/or sockets in each compute node;
- heterogeneous computing with different accelerators, memory space, and bandwidth;

(3) 3^{rd} level are the *vectorization* techniques, which can compute a full vector of data with the same set of operations simultaneously. These techniques include the SIMD vectorization on CPUs, and the SIMT vectorization on GPGPUs, etc.

2.4.3 Parallel Programming Challenges

As the number of cores and compute nodes in a supercomputer increases, communication time will exceed computation time and become a huge bottleneck for modern applications using supercomputers. Facing the challenges, parallel programming should consider highly hierarchical computation and memory architectures, increasing levels and degrees of parallelism, the heterogeneity of computing, memory and scalability. HPL benchmark is a little outdated, which cannot represent the common operations and applications on modern supercomputers.

HPCG List	Top500 List	Computer	HPCG [Pflop/s]	Rpeak [Pflop/s]	Rmax [Pflop/s]	HPCG/Peak	HPCG/HPL
1	1	Summit	2.93	200.79	143.50	1.50%	2.04%
2	2	Sierra	1.80	125.71	94.64	1.40%	1.90%
3	18	K computer	0.60	11.28	10.50	5.3%	5.70%
4	6	Trinity	0.55	41.46	20.16	1.33%	2.70%
5	7	AI Bridging Cloud Infrastructure	0.51	32.58	19.88	1.57%	2.57%
6	5	Piz Daint	0.50	27.15	21.23	1.84%	2.36%
7	3	Sunway TaihuLight	0.48	125.44	93.01	0.40%	0.50%
8	13	Nurion	0.39	25.71	13.93	1.52%	2.80%
9	14	Oakforest-PACS	0.39	24.91	13.56	1.56%	2.88%
10	12	Cori	0.36	27.88	14.01	1.29%	2.57%

Figure 2.18 – Top10 HPCG list in the November 2018. **Source**: https://www.top500.org

© 2019 Tous droits réservés.

Thèse de Xinzhe Wu, Université de Lille, 2019

Thus, HPCG benchmark [75] was proposed by Dongarra et al. in 2015. In mathematics, the CG method is an algorithm for numerical solutions of particular linear systems, namely those whose matrix is symmetric and positive-definite. These linear systems are typically modeled by PDEs and are used to simulate many aspects of the physical world. CG can be considered a good representation of modern applications on supercomputers. HPCG project aims to create a new metric for ranking HPC systems, which is intended to complement the HPL benchmark. HPL's computing and data access models still represent some important scalable applications, but not all. HPCG is designed to exercise computational and data access patterns that more closely match a different and broad set of important applications, and to give incentive to computer system designers to invest in capabilities that will have the impact on the collective performance of these applications.

HPCG is a complete, stand-alone code that measures the performance of basic operations in a unified code:

- Sparse matrix-vector multiplication.
- Vector updates.
- Global dot products.
- Local symmetric Gauss-Seidel smoother.
- Sparse triangular solve (as part of the Gauss-Seidel smoother).
- Driven by multigrid preconditioned conjugate gradient algorithm that exercises the key kernels on a nested set of coarse grids.
- Reference implementation is written in C++ with MPI and OpenMP support.

Fig. 2.18 lists the Top10 computers in the HPCG List of November 2018. We could conclude that the HPCG tests on the world most powerful machines typically only achieve an extremely tiny fraction of the peak FLOPS of computers. Lots of modern algorithms are much more complex than the HPCG, and their parallel performance tends to be even worse. Therefore, the programming paradigm for parallel applications should be re-considered and re-designed.

In fact, as the heterogeneity of supercomputers increases, HPC tends to be somewhat similar to Grid computing, which uses a widely distributed computer resource connected to a network (private, public, or Internet) to achieve a common goal. Grid computing is distinguished from HPC systems in that Grid computers have each node set to perform a different task/application. The geographically dispersed of Grid computers leads in many heterogeneous properties compared with HPC systems. Due to its heterogeneity, coordinating Grid computing applications can be a complex task, especially when coordinating information flows across distributed computing resources. Hence workflow management systems have been developed specifically to compose and execute a series of computational or data manipulation steps, or a workflow. Current parallel applications can be seen as the intersection of distributed and parallel computing.

The parallel performance of a common application in HPC is measured by the scalability (also referred as the scaling efficiency). This measurement indicates how efficient an application is

© 2019 Tous droits réservés.

lilliad.univ-lille.fr

Thèse de Xinzhe Wu, Université de Lille, 2019

when using increasing numbers of parallel processing elements (CPUs/cores/processes/threads, etc.). There are two basic ways to measure the parallel performance of a given application, depending on whether or not one is CPU-bound or memory-bound. These are referred to as strong and weak scaling, respectively:

- *strong scaling* which is defined as how the solution time varies with the number of processors for a fixed total problem size;
- *weak scaling* which is defined as how the solution time varies with the number of processors for a fixed problem size per processor.

In order to improve parallel performance and achieve optimal scalability on modern supercomputers, several principles should be considered for the development of applications:

(1) Algorithms should have multiple grain parallelism to accommodate the heterogeneity of the computer architecture.

(2) Applications should be able to adapt to the hierarchical memory on supercomputers.

(3) The data movements should be limited, and the amount of global communications should be minimized.

(4) The parallel programming should reduce synchronizations and promote the asynchronicity;

(5) Multi-level scheduling strategies should be proposed, and the manager engine or other complex software stacks should be implemented to handle large amounts of traffic and improve the fault tolerance and resilience, similarly to Grid computing.

In the following sections, we will focus on the design and implementation of new numerical methods for modern supercomputers following these principles.

© 2019 Tous droits réservés.

lilliad.univ-lille.fr

© 2019 Tous droits réservés.

lilliad.univ-lille.fr

Thèse de Xinzhe Wu, Université de Lille, 2019

Chapter 3

Krylov Subspace Methods

An important application on supercomputers is to solve the linear systems and eigenvalue problems. The chapter gives an overview of the relevant iterative methods to solve these problems with large-scale non-Hermitian operator matrices. Many applications in science and engineering fields can be formulated as such problems with large dimensions. Large matrices that arise in most applications are almost sparse. That is, the vast majority of their entries are zero. In numerical linear algebra, these systems are often solved by iterative methods. An iterative method is a mathematical procedure that uses an initial guess to generate a sequence of improved approximate solutions for a class of problems, in which the n-th approximation is derived from the previous ones. Krylov subspace methods are very useful and popular iterative methods to solve large-scale sparse systems because of their simplicity and generality. In this chapter, firstly we give a summary on the existing stationary and non-stationary iterative methods, especially the Krylov subspace methods. Then, the mathematical definitions of GMRES to solve non-Hermitian linear systems and Arnoldi methods to solve non-Hermitian eigenvalue problems are given in detail. The convergence properties of GMRES is also described by the spectral information of operator matrix. For some applications, the convergence of conventional Krylov subspace methods cannot always be guaranteed. Thus various kinds of preconditioners are introduced to accelerate the convergence. In the end, this chapter gives a survey on the parallel implementation of Krylov subspace methods on distributed memory platforms, and also the related challenges on the upcoming exascale supercomputers. The material covered in this chapter will be helpful in establishing the mathematical base of this dissertation. Additionally, a large part of constant efforts in this field are reviewed, even some of them have less connection with the motivation of this thesis.

3.1 Linear Systems and Eigenvalue Problems

Given a matrix $A \in \mathbb{C}^{n\times n}$ and a n-vector $b \in \mathbb{C}^n$, the problem considered is: find $x \in \mathbb{C}^n$ such that:

$$Ax = b. \tag{3.1}$$

© 2019 Tous droits réservés.

lilliad.univ-lille.fr

Thèse de Xinzhe Wu, Université de Lille, 2019

This problem is a *linear system*, A is the coefficient matrix, b is the *RHS*, and x is the *vector of unknowns*. In most cases, the linear systems are constructed by solving complex PDE systems. In general, the discretization of these PDEs into a cell-centered Finite Volume scheme in space and a Euler implicit method in time, leads to a nonlinear system which can be solved with a Newton's method. For each Newton step by time, the system is linearized then solved using a linear solver.

Eigenvalue problems occur in many areas of science and engineering, such as structural analysis [196, 195, 124], wave modes simulations [138, 137, 166, 139] and electromagnetic applications [46, 135, 58], and *eigenvalues* are also important in analyzing numerical methods. The standard eigenvalue problem can be defined as: given a matrix $A \in \mathbb{C}^{n\times n}$, find scalar $\lambda \in \mathbb{C}$ and nonzero vector $v \in \mathbb{C}$ such that:

$$Av = \lambda v. \tag{3.2}$$

In this formula, λ is an *eigenvalue* of A, and v is its corresponding *eigenvector*, λ may be complex even if A is real. The *spectrum* of A is the set of all eigenvalues of A, denoted it as $\lambda(A)$, and the *Spectral radius* of A $\rho(A)$ is $\max\{|\lambda| : \lambda \in \lambda(A)\}$.

3.2 Iterative Methods

Iterative methods approach the solution x of Equation (3.1) by a number of iterative steps. Compared with the direct methods such as LU and Gauss Jordan which need an overall computational cost of the order $\frac{2}{3}n^3$, the cost of iterative methods is the order of n^2 operations for each iteration. Iterative methods are especially competitive with direct methods in the case of large sparse matrices, to avoid the potential introduction of the dramatic fill-in by the direct methods. This section gives an overview of both stationary and non-stationary iterative methods.

3.2.1 Stationary and Multigrid Methods

The iterate of stationary methods to solve Equation (3.1) can be expressed in the simple form

$$x_k = Bx_{k-1} + c, \tag{3.3}$$

where neither B nor c depends upon the iteration count k. The four well-known stationary methods are the *Jacobi method* [230], *Gauss-Seidel method* [232], *SOR method* [3], and *SSOR method* [18]. Beginning with an initial guess vector, these methods modify one or a few components of the approximation at each iterative step, until the convergence is reached. These modifications are called relaxation steps. Theoretically, the stationary methods are applicable for all linear systems, but they are more efficient only for the applications arising from the finite difference discretization of Ellipse PDEs. Though the inefficiency of stationary methods for most linear problems, they are often used by combining with the more efficient methods described later in this chapter.

For *Jacobi method*, the Formula (3.3) is extended as:

© 2019 Tous droits réservés.

lilliad.univ-lille.fr

Thèse de Xinzhe Wu, Université de Lille, 2019

$$x_k = D^{-1}(L+U)x_{k-1} + D^{-1}b,$$

where the matrices D, $-L$, and $-U$ represent the diagonal, strictly lower triangular, and strictly upper triangular parts of A, respectively.

The convergence condition for the Jacobi method is the situation that the spectral radius of the matrix $D^{-1}(L+U)$ is less than 1:

$$\rho(D^{-1}(L+U)) < 1.$$

For general cases, the convergence of Jacobi method can be slow. A sufficient (but not necessary) condition for the convergence is that the matrix A is strictly or irreducibly diagonally dominant.

For *Gauss-Seidel method*, the Formula (3.3) is extended as:

$$x_k = (D-L)^{-1}(Ux_{k-1} + b).$$

The Gauss-Seidel method is similar to the Jacobi method except that it uses updated values as soon as they are available. It generally converges faster than the Jacobi method, although still relatively slow.

The Gauss-Seidel method can converge if either:

(1) The matrix A is strictly or irreducibly diagonally dominant;

(2) A is symmetric positive-definite.

For *SOR method*, the Formula (3.3) is extended as:

$$x_k = (D-\omega L)^{-1}[\omega U + (1-\omega)D]x_{k-1} + \omega(D-\omega L)^{-1}b,$$

The SOR method can be derived from the Gauss-Seidel method by introducing an extrapolation parameter ω. If $\omega = 1$, the SOR method can be simplified to the Gauss-Seidel method. A theorem due to Kahan [119] shows that SOR fails to converge if ω is outside the interval $(0, 2)$. In general, it is not possible to compute in advance the value of ω that will maximize the rate of convergence of SOR. This method can converge faster than Gauss-Seidel by an order of magnitude.

Finally, *SSOR method* is useful as a preconditioner for other methods. However, it has no advantage over the SOR method as a stand-alone iterative method.

In general, many stationary methods have the smoothing property, where oscillatory modes with short wave-length of the errors of linear systems can be eliminated effectively, but the smooth modes with long wave-length are damped very slowly. Thus *MG methods* [117, 115, 27] are introduced for solving differential equations using a hierarchy of discretizations. The main idea of MG methods is to accelerate the convergence of stationary iterative methods (known as relaxation process) by a global correction on the approximative solution of the fine grid from time to time. This global correction is achieved by solving a coarse problem. The coarse grids

© 2019 Tous droits réservés.

lilliad.univ-lille.fr

Thèse de Xinzhe Wu, Université de Lille, 2019

can be used to compute an improved initial guess for the fine-grid processes. The reason for the coarse grid are:

(1) Relaxation on the coarse-grid is much cheaper;

(2) Relaxation on the coarse-grid has a marginally better convergence rate;

(3) Smooth error is relatively more oscillatory in the coarse-grid processes, and the relaxation will be more effective

The steps 2-4 in Algorithm 1 is the kernel of MG method, which gives the restriction-coarse solution-interpolation processes. The involved matrices in this algorithm are:

$$A = A_h = orginal\ matrix$$

$$R = R_h^{2h} = restriction\ matrix$$

$$I = I_h^{2h} = interpolation\ matrix$$

$$A_{2h} = R_h^{2h} A_h I_{2h}^h = RAI = coarse\ grid\ matrix$$

Algorithm 1 Fine-coarse-fine loop of MG method

1: Relaxion **Iterate** on $A_h u = b_h$ by stationary methods to reach u_k.
2: **Restrict** the residual $r_h = b_h - A_h u_h$ to the coarse grid by $r_{2h} = R_h^{2h} r_h$.
3: **Solve** $A_{2h} E_{2h} = r_{2h}$.
4: **Interpolate** E_{2h} as $E_h = I_{2h}^h E_{2h}$. Add E_h to u_h.
5: **Iterative** more times on $A_h u = b_h$ starting from the improved $u_h + E_h$.

One extension of MG method is the *AMG* [179, 212, 42, 43]. AMG constructs their restriction, interpolation, and coarse grid matrices directly from the matrix of a linear system. AMG is regarded as advantageous when GMG is too difficult to apply, e.g., unstructured meshes, graph problem, etc. Fig. 3.1 gives an example of hierarchical multi-level AMG.

3.2.2 Non-stationary Methods

In practice, the stationary methods talked in the previous section cannot always get the convergence quickly for more general matrices which are not constructed from PDEs. The GMG and AMG which use the relaxation steps of stationary methods can speed up the convergence for more general matrices, but the construction of restriction, interpolation, and coarse matrices either from geometric PDE problems or the operator matrix A is far more difficult, and these operations matter the convergence. There is no free lunch for AMG which is hard to *control* and get optimal performance. In my dissertation, I will talk about the *non-stationary methods* which are easy to implement and have better convergence performance than the stationary methods. The difference of non-stationary methods compared with stationary methods is that the involved computational information changes at each step of the iteration. The most well-known non-stationary methods are the suite of *Krylov subspace methods*.

© 2019 Tous droits réservés.

lilliad.univ-lille.fr

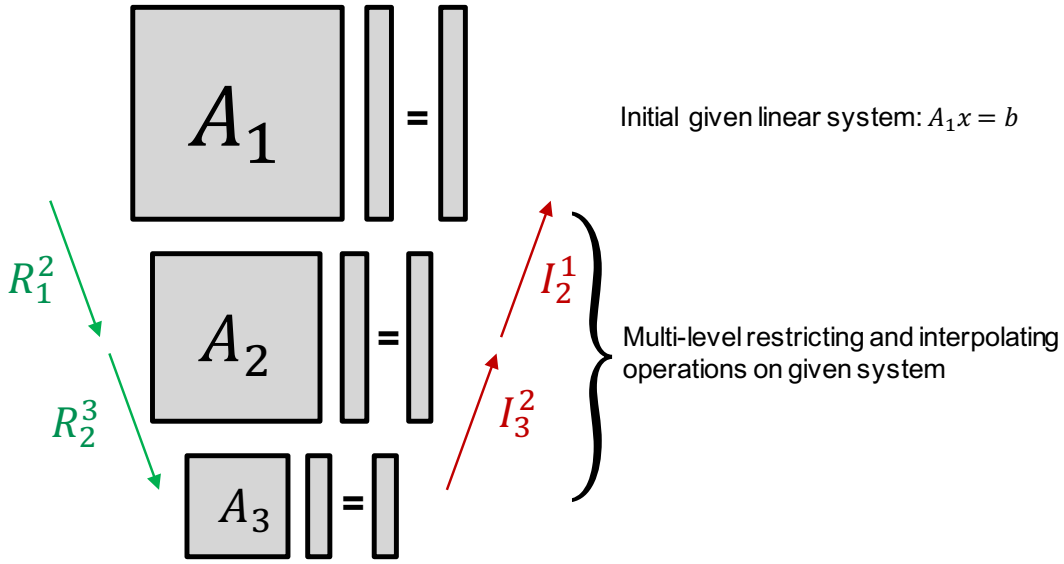

Figure 3.1 – Algebraic multigrid hierarchy.

3.3 Krylov Subspace methods

This section presents the Krylov Subspace projection and the basic Arnoldi reduction in the Krylov subspace.

3.3.1 Krylov Subspace

In linear algebra, the m-order Krylov subspace [186] generated by a $n \times n$ matrix $A \in \mathbb{C}^{n \times n}$ and a vector $b \in \mathbb{C}^n$ is the linear subspace spanned by the images of b under the first m powers of A, that is

$$K_m(A, b) = span(b, Ab, A^2 b, \cdots, A^{m-1} b).$$

The Krylov subspace provides the ability to extract the approximations from an m-dimensional subspace K_m. Since K_m is the subspace of all vectors in $\mathbb{C}^n$, for all $x \in K_m$, it can be written as $x = p(A)b$, with p a polynomial of degree not exceeding $m - 1$.

3.3.2 Basic Arnoldi Reduction

Arnoldi reduction is well used to build an orthogonal basis of the Krylov subspace K_m. One variant of basic Arnoldi reduction algorithm is given in Algorithm 2. In this algorithm, at each step of Arnoldi reduction, the algorithm times the previous Arnoldi vector ω_j by matrix A, and get an orthogonal vector ω_j against all previous ω_i by a standard Gram-Schmit procedure. It will stop if the vector computed in line 9 is zero. Then the vectors $\omega_1, \omega_2 . \cdots, \omega_m$ form an orthonormal basis of the Krylov Subspace.

Denote by Ω_m, the $n \times m$ matrix with column vectors $\omega_1, \omega_2 . \cdots, \omega_m$, by $\overline{H}_m$, the $(m+1) \times m$ Hessenberg matrix whose nonzero entries $h_{i,j}$ are defined by Algorithm 2, then note H_m as the matrix obtained from $\overline{H}_m$ by deleting its last row (shown as Fig. 3.2). The following relations are given:

© 2019 Tous droits réservés.

Thèse de Xinzhe Wu, Université de Lille, 2019

Algorithm 2 Arnoldi Reduction

1: **function** AR($input$:A, m, ν, $output$: H_m, Ω_m)
2: $\omega_1 = \nu/||\nu||_2$
3: **for** $j = 1, 2, \cdots, m$ **do**
4: **for** $i = 1, 2, \cdots, j$ **do**
5: $h_{i,j} = (A\omega_j, \omega_i)$
6: **end for**
7: $\omega_j = A\omega_j - \sum_{i=1}^{j} h_{i,j}\omega_i$
8: $h_{j+1,j} = ||\omega_j||_2$
9: **if** $h_{j+1,j} = 0$ **then** Stop
10: **end if**
11: $\omega_{j+1} = \omega_j/h_{j+1,j}$
12: **end for**
13: **end function**

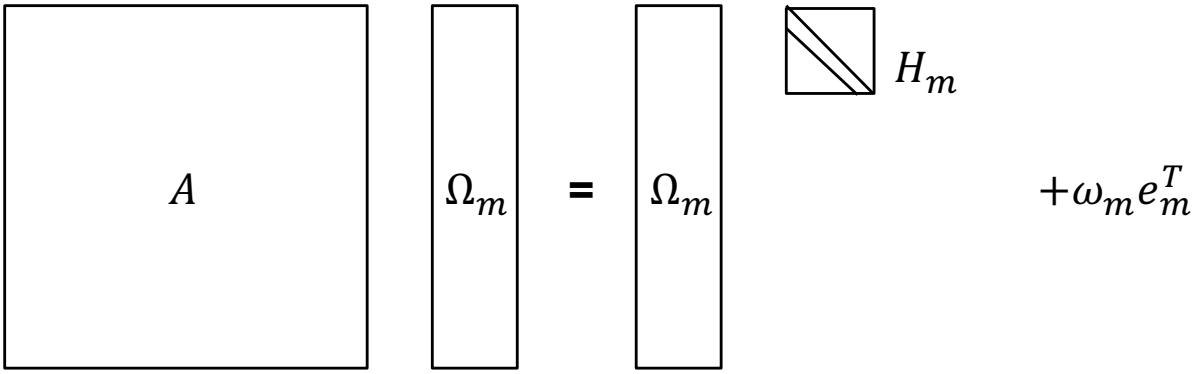

Figure 3.2 – The action of A on V_m gives $V_m H_m$ plus a rank-one matrix.

$$A\Omega_m = \Omega_m H_m + \omega_m e_m^T = \Omega_{m+1}\overline{H}_m. \tag{3.4}$$

$$\Omega_m^T A \Omega_m = H_m. \tag{3.5}$$

In case that the norm of ω_j in line 9 of Algorithm 2 vanishes at a certain step j, the next vector ω_{j+1} cannot be computed and the algorithm steps, H_m turns to be H_j with dimension $j \times j$.

3.3.3 Orthogonalization

There are different orthogonalization schemes to construct the orthogonal basis of Krylov subspace, in this section, we list four variants.

(1) *Classic Gram-Schmit Orthogonalization*: Algorithm 2 gives an example of Arnoldi reduction using the Classic Gram-Schmit Orthogonalization to create a basis vector by vector. The benefit of Classic Gram-Schmit Orthogonalization is the parallelism in computing $h_{i,j}$ and ω_j in steps 5 and 7.

(2) *Modified Gram-Schmit Orthogonalization*: An alternative (See Algorithm 3), in which the number of subtractions is reduced, resulting in a less chance of cancellations. Though

© 2019 Tous droits réservés.

lilliad.univ-lille.fr

Thèse de Xinzhe Wu, Université de Lille, 2019

Algorithm 3 Arnoldi Reduction with Modified Gram-Schmidt process

```
1: function AR-MGS(input:A, m, ν, output: H_m, Ω_m)
2:     ω_1 = ν/||ν||_2
3:     for j = 1, 2, ··· , m do
4:         for i = j, 2, ··· , j do
5:             h_{i,j} = (Aω_j, ω_i)
6:             ω_j = ω_j − h_{i,j} v_i
7:         end for
8:         h_{j+1,j} = ||ω_j||_2
9:         if h_{j+1,j} = 0 then Stop
10:        end if
11:        ω_{j+1} = ω_j / h_{j+1,j}
12:    end for
13: end function
```

Modified Gram-Schmit Orthogonalization is more stable than Classic Gram-Schmit Orthogonalization, it is less parallelizable than Classic Gram-Schmit Orthogonalization. In Classic Gram-Schmit Orthogonalization, the orthogonalization process from line 5 to 7 can be overlapped, while the same process of Modified Gram-Schmit Orthogonalization has a data dependency. Thus the parallel implementation of Arnoldi reduction still prefers Classic Gram-Schmit Orthogonalization, and a preconditioner or a reorthogonalization process can compensate its deficiency of numerical stability.

(3) *Householder Orthogonalization*: the Arnoldi reduction can also be operated by the Householder orthogonalization, which is more numerically robust than the Gram-Schmit orthogonalization.

(4) *Incomplete Orthogonalization*: The orthogonalization process in Arnoldi is expensive because each vector accumulated in the basis is orthogonalized against all previous ones. Thereby, the orthogonalization process number of iterations k is bounded to the Krylov subspace size, thus higher values of m will imply more computations and memory space in order to create the Krylov orthonormalized vector basis. With the aim to reduce the cost induced by the Arnoldi orthogonalization process, it is possible to truncate it by orthogonalizing each vector against a subset of the basis vectors, i.e., the q precedent basis vectors (Algorithm 4). In this case, the resulting upper Hessenberg matrix H_m is not fully orthogonalized and has the propriety to be banded of bandwidth q. Incomplete orthogonalization can speed up the construction of Krylov subspace basis, with the loose of numerical accuracy.

3.3.4 Different Krylov Subspace Methods

Different variants of Krylov subspace methods are developed, such as the Arnoldi [215], Lanczos [217], CG [129], IDR(s) [211], GMRES, BiCGSTAB [198], QMR [94], TFQMR [29], and MINRES [167] methods. This dissertation concentrates on GMRES which is used to solve non-Hermitian linear systems.

© 2019 Tous droits réservés.

lilliad.univ-lille.fr

Thèse de Xinzhe Wu, Université de Lille, 2019

Algorithm 4 Arnoldi Reduction with Incomplete Orthogonalization process

function AR-INCOMPLETE(*input*:A, m, ν, *output*: H_m, Ω_m)
  $\omega_1 = \nu/||\nu||_2$
  for $j = 1, 2, \cdots, m$ **do**
    for $i = max\{1, j-q+1\}, \cdots, j$ **do**
      $h_{i,j} = (A\omega_j, \omega_i)$
      $\omega_j = \omega_j - h_{i,j}v_i$
    end for
    $h_{j+1,j} = ||\omega_j||_2$
    if $h_{j+1,j} = 0$ **then** Stop
    end if
    $\omega_{j+1} = \omega_j/h_{j+1,j}$
  end for
end function

3.4 GMRES for Non-Hermitian Linear Systems

GMRES is a well-known Krylov iterative method to solve non-Hermitian linear systems $Ax = b$. This section gives an introduction in-depth about the fundamentals of GMRES.

3.4.1 Basic GMRES Method

GMRES (Algorithm 5) is a kind of projection method which extracts an approximate solution x_m of given problem in a well-selected m-dimensional Krylov subspace $K_m(A, v)$ from a given initial guess vector x_0. GMRES method was introduced by Saad and Schultz in 1986 [185].

Algorithm 5 Basic GMRES method

function BASICGMRES(*input*: A, m, x_0, b, *output*: x_m)
  $r_0 = b - Ax_0, \beta = ||r_0||_2$, and $\nu_1 = r_0/\beta$
  Compute an AR(*input*:A, m, ν_1, *output*: H_m, Ω_m)
  Compute y_m which minimizes $||\beta e_1 - H_m y||_2$
  $x_m = x_0 + \Omega_m y_m$
end function

In fact, any vector x in subspace $x_0 + K_m$ can be written as

$$x = x_0 + \Omega_m y, \tag{3.6}$$

with y a m-dimensional vector, Ω_m an orthonormal basis of the Krylov Subspace K_m. The norm of residual $R(y)$ of $Ax = b$ is given as:

$$\begin{aligned} R(y) &= ||b - Ax||_2 = ||b - A(x_0 + \Omega_m y)||_2 \\ &= ||\Omega_{m+1}(\beta e_i - \overline{H}_m y)||_2 = ||\beta e_i - \overline{H}_m y||_2. \end{aligned} \tag{3.7}$$

The approximation of GMRES x_m can be obtained as $x_m = x_0 + \Omega_m y_m$ where $y_m = \text{argmin}_y||\beta e_i - \overline{H}_m y||_2$. The minimizer y_m is inexpensive to compute since it requires the solution of an $(m+1) \times m$ Least Squares problem if m is typically small. This gives the basic GMRES method as Algorithm 5.

© 2019 Tous droits réservés.

lilliad.univ-lille.fr

Thèse de Xinzhe Wu, Université de Lille, 2019

If m is very large, GMRES can be restarted after some iterations, to avoid large memory and computational requirements with the increase of Krylov subspace projection number. It is called the restarted GMRES. The restarted GMRES will not stop until the condition $||b-Ax_m|| < \epsilon_g$ is satisfied. See Algorithm 6 for restarted GMRES algorithm in detail. A well-known difficulty with the restarted GMRES algorithm is that it can stagnate when the matrix is not positive definite. A typical method is to use preconditioning techniques whose goal is to reduce the number of required iteration steps for the convergence.

Algorithm 6 Restarted GMRES method

```
1: function RESTARTEDGMRES(input: A, m, x_0, b, ε_g, output: x_m)
2:     BASICGMRES(input: A, m, x_0, b, output: x_m)
3:     if (||b − Ax_m||_2 < ε_g) then
4:         Stop
5:     else
6:         set x_0 = x_m and GOTO 2
7:     end if
8: end function
```

3.4.2 Variants of GMRES

Several variants of GMRES are proposed, such as:

(1) *Restarted GMRES* [150]: the cost of the iterations grow as $\mathcal{O}(n^2)$, where n is the iteration number. Therefore, the method is sometimes restarted after a number, say k, of iterations, with x_k as an initial guess. The resulting method is called restarted GMRES. This method suffers from stagnation in convergence as the restarted subspace is often close to the earlier subspace.

(2) *Truncated GMRES* [68]: a version of GMRES with incomplete orthogonalization, which reduces the computing and memory requirement of the Arnoldi process in GMRES with the cost of the accuracy of orthogonalization.

(3) *Deflated GMRES* [85]: Restarted GMRES with deflation. As we have just seen, restarting of GMRES results in a loss of useful information, which might slow down the convergence after a restart. To overcome this problem, restarted GMRES with deflation (GMRES-DR) was introduced. The deflation in GMRES-DR makes restarted GMRES more robust and makes it converge much faster for tough problems with small eigenvalues.

(4) *Pipelined GMRES* [100]: A particular variant of GMRES which hides the global communication latency for parallel implementation.

(5) *FGMRES* [93]: Flexible GMRES is a variant of GMRES with the advantage of being able to switch preconditioners on the fly according to specific heuristics in the GMRES process without any additional computation. This method is interesting because it allows developing robust and easily parallelizable methods. FGMRES is developed based on the right-preconditioner which will be presented later in Section 3.5.1.1.

© 2019 Tous droits réservés.

lilliad.univ-lille.fr

Thèse de Xinzhe Wu, Université de Lille, 2019

3.4.3 GMRES Convergence Description by Spectral Information

After the brief introduction of GMRES algorithm, in this section, we will review the recent research to describe the convergence behavior of GMRES. This analysis makes it possible for the users to select suitable linear solvers according to their applications and problems. Different techniques are used to give the upper and lower bound for the convergence of GMRES, mainly including the spectral information, the ϵ-pseudospectrum and the polynomial hull.

3.4.3.1 Spectral Information and Convergence

In this section, we will briefly review how spectral information influences the convergence behavior of GMRES. This introduction benefits from the previous work of Liesen et al. [134, 133].

For a linear systems $Ax = b$ with a general nonsingular matrix A, the initial residual of GMRES is given as $r_0 = b - Ax_0$. For the n-th step of GMRES, the projection process assure a Least Squares problem (Algorithm 5 step 4), and the optimal property is:

$$||r_n||_2 = \min_{x_n \in x_0 + K_n(A, r_0)} ||b - Ax_n||_2. \tag{3.8}$$

The Formula (3.8) can be transformed into the formula below with a *residual polynomial* R_d

$$||r_n||_2 = \min_{\substack{R_d(0)=1,\\ d \leq n}} ||R_d(A) r_0||_2. \tag{3.9}$$

A can be decomposed as $A = SJS^{-1}$, with $J = diag(J_1, \cdots, J_k)$ a matrix in Jordan Canonical form. Then (3.9) leads to a GMRES convergence bound as:

$$\begin{aligned} ||r_n||_2 &= \min_{\substack{R_d(0)=1,\\ d \leq n}} ||R_d(A) r_0||_2 = \min_{\substack{R_d(0)=1,\\ d \leq n}} ||S R_d(J) S^{-1} r_0||_2 && \text{(3.10a)} \\ &\leq ||S||_2 ||S^{-1} r_0||_2 \min_{\substack{R_d(0)=1,\\ d \leq n}} \max_{1 \leq i \leq k} ||R_d(J_i)||_2 && \text{(3.10b)} \\ &\leq \kappa(S) ||r_0||_2 \min_{\substack{R_d(0)=1,\\ d \leq n}} \max_{1 \leq i \leq k} ||R_d(J_i)||_2, && \text{(3.10c)} \end{aligned}$$

where $\kappa(S)$ is the condition number of S. Thus the relative residual in the GMRES can be bounded as:

$$\frac{||r_n||_2}{||r_0||_2} \leq \kappa(S) \min_{\substack{R_d(0)=1,\\ d \leq n}} \max_{1 \leq i \leq k} ||R_d(J_i)||_2. \tag{3.11}$$

If A is a normal matrix, which is unitarily diagonalisable $A = U \Lambda U^*$, with eigenvalues $\lambda_1, \cdots, \lambda_k$, then $\kappa(S) = \kappa(U) = 1$, and this leads to the formula below:

$$\frac{||r_n||_2}{||r_0||_2} \leq \min_{\substack{R_d(0)=1,\\ d \leq n}} \max_{1 \leq i \leq k} |R_d(\lambda_i)|. \tag{3.12}$$

Hermitian Indefinite Matrix: For A is Hermitan Indefinite, it has positive and negative

© 2019 Tous droits réservés.

lilliad.univ-lille.fr

Thèse de Xinzhe Wu, Université de Lille, 2019

real eigenvalues, and these egenvalues can be described as the unition of two intervals containing them and excluding the origin, denoted as $I^- \cup I^+ = [\lambda_{min}, \lambda_s] \cup [\lambda_{s+1}, \lambda_{max}]$ with $\lambda_{min} \leq \lambda_s < 0 < \lambda_{s+1} \leq \lambda_{max}$. Note that if one or several eigenvalues of A are zero, then the maximum-minimum problem (3.12) would be constant for all d, which results that this bound would be useless.

The maximum-minimum problem in (3.12) leads to the bound

$$\min_{\substack{R_d(0)=1,\\ d\leq n}} \max_{1\leq i\leq k} |R_d(\lambda_i)| \leq \min_{\substack{R_d(0)=1,\\ d\leq n}} \max_{z\in I^-\cup I^+} |R_d(z)|. \tag{3.13}$$

When both intervals I^- and I^+ are of the same length, Liesen [134] gives an upper bound as

$$\min_{\substack{R_d(0)=1,\\ d\leq n}} \max_{z\in I^-\cup I^+} |R_d(z)| \leq 2\left(\frac{\sqrt{|\lambda_{min}\lambda_{max}|}-\sqrt{|\lambda_s\lambda_{s+1}|}}{\sqrt{|\lambda_{min}\lambda_{max}|}+\sqrt{|\lambda_s\lambda_{s+1}|}}\right)^{[n/2]}, \tag{3.14}$$

where $[n/2]$ denotes the integer part of $n/2$.

Set $\alpha^2 = \min(\lambda_{max}, |\lambda_{min}|)$ and $\beta^2 = \max(\lambda_s, |\lambda_{s+1}|)$, the right-hand side of formula (3.14) can be reduced to

$$2\left(\frac{\alpha\kappa(A)-\beta}{\alpha\kappa(A)+\beta}\right)^{[n/2]}, \tag{3.15}$$

with $\kappa(A)$ the condition number of matrix A.

In the general case when the two intervals I^- and I^+ have different lengths, the explicit solution of this minimum-maximum approximation problem on $I^- \cup I^+$ becomes quite complicated, no explicit and straightforward bound on its value is known.

For this general case, we set also $\gamma^2 = \max(\lambda_{max}, |\lambda_{min}|)$ and $\delta^2 = \min(\lambda_s, |\lambda_{s+1}|)$, and a superset Δ of $I^- \cup I^+$ can be defined as $[-\gamma^2, -\delta^2] \cup [\delta^2, \gamma^2]$, where the two intervals have the same length. Thus we have

$$\min_{\substack{R_d(0)=1,\\ d\leq n}} \max_{z\in I^-\cup I^+} |R_d(z)| \leq \min_{\substack{R_d(0)=1,\\ d\leq n}} \max_{z\in\Delta} |R_d(z)| \leq 2\left(\frac{\gamma\kappa(A)-\delta}{\gamma\kappa(A)+\delta}\right)^{[n/2]}. \tag{3.16}$$

A particular case for the real eigenvalues are all positive or negatives. Denote respectively the maximum and minimum eigenvalues as λ_{max} and λ_{min}, the maximum-minimum problem in (3.12) leads to the bound

$$\min_{\substack{R_d(0)=1,\\ d\leq n}} \max_{1\leq i\leq k} |R_d(\lambda_i)| \leq \min_{\substack{R_d(0)=1,\\ d\leq n}} \max_{z\in[\lambda_{min},\lambda_{max}]} |R_d(z)|. \tag{3.17}$$

© 2019 Tous droits réservés.

lilliad.univ-lille.fr

Thèse de Xinzhe Wu, Université de Lille, 2019

A upper bound of this formula can be given as

$$\min_{\substack{R_d(0)=1,\\ d\leq n}} \max_{z\in[\lambda_{min},\lambda_{max}]} |R_d(z)| \leq 2\left(\frac{|\sqrt{|\lambda_{max}|}-\sqrt{|\lambda_{min}|}|}{\sqrt{|\lambda_{max}|}+\sqrt{|\lambda_{min}|}}\right)^n \tag{3.18a}$$

$$= 2\left(\frac{\sqrt{\kappa(A)}-1}{\sqrt{\kappa(A)}+1}\right)^n. \tag{3.18b}$$

With the upper bounds defined as 3.15, 3.16 and 3.18, the effects of spectral information for Hermitian Indefinite matrices can be described in different ways:

(1) the eigenvalues close to the origin point damage the convergence rate of GMRES. If it exists $\lambda \approx 0$, GMRES cannot achieve the convergence. Therefore, the preconditioners can be constructed which can remove or deflate the eigenvalues which are close to 0;

(2) the dominant eigenvalues with large Euclidean norm accelerate the convergence of GMRES. For the eigenvalue with largest and smallest Euclidean norm having a fixed distance, larger Euclidean norm makes the defined upper bounds much smaller than 1, which signifies much larger convergence rate for each iteration in GMRES;

(3) the condition number $\kappa(A)$ of matrix A can also be used to qualify the convergence of GMRES. Large $\kappa(A)$ slows down the convergence of GMRES. Hence, the preconditioning can also be constructed by transforming the matrix A to another one with smaller condition number. This impact of $\kappa(A)$ can also be translated as the clustering of eigenvalues stimulating the convergence. Thus, the preconditioning techniques can be constructed by enlarging the Euclidean norm of dominant eigenvalues, or transforming the spectral distribution of A with more clustering properties.

General Normal Matrix: for the case that A is a general normal matrix (or is close to normal with $\kappa(S) \approx 1$), the bound (3.12) still makes sense, which signifies that the right-hand sides of (3.11) depend entirely (or mostly) on the eigenvalues of A. In such cases, the eigenvalues can be used to obtain a reasonable estimate of the worst-case convergence behavior of GMRES. Similarly, it is necessary to solve a maximum-minimum problem for a set of complex eigenvalues in the real-complex plain. It is much more difficult to give an explicit formula for this problem, but it can be approximated by the good selection of optimal polynomials. Usually one works with connected inclusion sets since polynomial approximation on disconnected sets is not well understood (even in the case of two disjoint intervals; see above). Because of the normalization of the polynomials at zero, the set should not include the origin.

The simplest result is obtained when the spectrum of A is contained in a disk π_n in the complex plane (that excludes the origin), say with radius $r > 0$ and center at $c \in \mathbb{C}$. Then the polynomial $R_n(z) = (\frac{c-z}{c})^n \in \pi_n$ can be used to show that

$$\min_{R\in\pi_n} \max_k |R(\lambda_k)| \leq |\frac{r}{c}|^n. \tag{3.19}$$

© 2019 Tous droits réservés.

lilliad.univ-lille.fr

Thèse de Xinzhe Wu, Université de Lille, 2019

In particular, a disk of a small radius that is far from the origin guarantees fast convergence of the GMRES residual norms. More refined bounds can be obtained using the convex hull Ξ of of an ellipse instead of a disk. For example, suppose that the spectrum is contained in an ellipse with center at $c \in \mathbb{R}$, focal distance $d > 0$ and major semi axis $a > 0$. If $0 \notin \Xi$, it can be shown that:

$$\min_{R \in \pi_n} \max_k |R(\lambda_k)| \leq \frac{C_n(a/d)}{|C_n(c/d)|} \approx \left(\frac{a + \sqrt{a^2 - d^2}}{c + \sqrt{c^2 - d^2}} \right)^n , \tag{3.20}$$

where $C_n(z)$ denotes the n-th complex Chebyshev polynomial, for details in [188]. These polynomials are able to predict the correct rate of convergence of this minimum-maximum approximation problem. With the definition of this upper bound for the general (quasi-)normal matrix, the similar remarks with Hermitian Indefinite matrix can also be given as below

(1) the eigenvalues close to the origin point damage the convergence rate of GMRES. The eigenvalues with too small Euclidean norm make GMRES be difficult to obtain the convergence;

(2) the dominant eigenvalues with large Euclidean norm accelerate the convergence of GMRES. The dominant eigenvalues are the ones far from the origin point in the real-imaginary plane. If the refined ellipse by the dominant eigenvalues has small focal distance d and major semi axis a, and large $|c|$ for its center, GMRES can quickly converge. This can also be translated as the clustering of eigenvalues stimulating the convergence.

(3) of course, one would like to find a set Ξ in the complex plane that yields the smallest possible upper bound. Both a disk and the convex hull of an ellipse are convex, so one can probably improve the convergence bound by using the smallest convex set containing all the eigenvalues, i.e., the convex hull of the eigenvalues. However, all convex inclusion sets Ξ are limited in their applicability by the strict requirement that $0 \notin \Xi$, in particular, if zero is inside the convex hull of the eigenvalues of A, then no convex inclusion set for these points can be used. Moreover, if the convex hull is close to the origin, then any bound derived from this set will be poor, regardless of the distance of the eigenvalues to the origin.

Non-normal Matrix: Finally, if A is far from normal in the sense that $\kappa(S)$ is very large, then the bound (3.12) may fail to provide any reasonable information about the actual behavior of convergence of GMRES. When S is ill-conditioned, the transition from (3.10b) to (3.10c) is over-amplified. Consequently, this minimization problem can lack any relationship with the problem that is minimized by GMRES.

It should be clear by now that in the non-normal case the GMRES convergence behavior is significantly more difficult to analyze than in the normal case. A general approach to understand the worst-case GMRES convergence in the non-normal case is to replace the complicated minimization problem by another one that is easier to analyze. Natural bounds on the GMRES residual norm arise by excluding the influence of the initial residual r_0. Some approaches for

© 2019 Tous droits réservés.

lilliad.univ-lille.fr

Thèse de Xinzhe Wu, Université de Lille, 2019

understanding at least the worst-case convergence of GMRES for non-normal matrices are based on the following upper bounds.

$$\frac{||r_n||_2}{||r_0||_2} = \min_{R\in\pi_n} \frac{||R(A)r_0||_2}{r_0} \qquad \text{(GMRES)} \tag{3.21a}$$

$$\leq \max_{||v||_2=1} \min_{R\in\pi_n} ||R(A)v||_2 \qquad \text{(worst-case GMRES)} \tag{3.21b}$$

$$\leq \min_{R\in\pi_n} ||R(A)||_2 \qquad \text{(ideal GMRES)} \tag{3.21c}$$

The approach of analyzing the worst-case GMRES via bounding the ideal GMRES approximation problem is certainly useful to obtain a priori convergence estimates in terms of some properties of A, and possibly to analyze the effectiveness of preconditioning techniques. However, none of the bounds stated above indeed characterizes (concerning properties of A) the convergence behavior of GMRES in the non-normal case. In the following section, we will describe a different approach to investigate the link between spectral information and GMRES.

3.4.3.2 ϵ-pseudospectrum

A possible way to approximate the value of the matrix approximation problem (3.21c) is to determine sets $\Xi \in \mathbb{C}$ and $\hat{\Xi} \in \mathbb{C}$, that are somehow associated with A, and that provide lower and upper bounds on (3.21c), i.e.,

$$c \min_{\substack{R_d(0)=1,\\ d\leq n}} \max_{\lambda\in\Xi} |R_d(\lambda)| \leq \min_{\substack{R_d(0)=1,\\ d\leq n}} ||R_d(A)||_2 \leq \hat{c} \min_{\substack{R_d(0)=1,\\ d\leq n}} \max_{\lambda\in\hat{\Xi}} |R_d(\lambda)|. \tag{3.22}$$

Here c and $\hat{c}$ should be some (moderate size) constants depending on A and possibly on n. This approach represents a generalization of the idea for normal matrices, where the appropriate set associated with A is the spectrum of A and $c = \hat{c} = 1$.

Trefethen [210] has suggested taking $\hat{\Xi}$ to be the ϵ-pseudospectrum of A,

$$\Lambda_\epsilon(A) = \{z \in \mathbb{C} : ||(zI - A)^{-1}||_2 \geq \epsilon^{-1}\}. \tag{3.23}$$

Denote by L the arc length of the boundary of $\Lambda_\epsilon(A)$, the following bound can be derived

$$\min_{\substack{R_d(0)=1,\\ d\leq n}} ||R_d(A)||_2 \leq \frac{L}{2\pi\epsilon} \min_{\substack{R_d(0)=1,\\ d\leq n}} \max_{\lambda\in\Lambda_\epsilon(A)} |R_d(\lambda)|. \tag{3.24}$$

The parameter ϵ gives some flexibility, but choosing a good value can be tricky. Note that in order to make the right-hand side of (3.24) reasonably small, one must select ϵ large enough to make the constant $\frac{L}{2\pi\epsilon}$ small, but small enough to make the set $\Lambda_\epsilon(A)$ not too large. This bound only works well for some situations.

3.4.3.3 Field of Values and Polynomial Hull

Another approach is based on the field of values of A, which is defined by

© 2019 Tous droits réservés.

lilliad.univ-lille.fr

Thèse de Xinzhe Wu, Université de Lille, 2019

$$F(A) \equiv v^* A v : ||v||_2 = 1, v \in \mathbb{C}^m. \tag{3.25}$$

The distance of $F(A)$ from the origin in the complex plane is

$$v(F(A)) \equiv \min_{\lambda \in F(A)} |A|. \tag{3.26}$$

We will not give in detail of this approach, but only take the result from [202] as below:

$$\min_{\substack{R_d(0)=1,\\ d \leq n}} ||R_d(A)||_2 \leq (1 - v(F(A))v(F(A^{-1})))^{n/2}. \tag{3.27}$$

The field of values analysis can be advantageous when the given linear system comes from the discretization of elliptic PDEs by the Galerkin finite element method.

A generalization of the field of values of A is the polynomial numerical hull, introduced by Nevanlinna [159] and defined as

$$\mathcal{H}_n(A) = \lambda \in \mathbb{C} : ||R_d(A)||_2 \geq |R_d(\lambda)|, \forall \text{ polynomials } R_d \text{ of degree} \leq n. \tag{3.28}$$

It can be shown that $\mathcal{H}_1(A) = F(A)$, and the set $\mathcal{H}_n(A)$ provides the lower bound:

$$\min_{\substack{R_d(0)=1,\\ d \leq n}} \max_{\lambda \in \mathcal{H}_n(A)} |R_d(\lambda)| \leq \min_{\substack{R_d(0)=1,\\ d \leq n}} ||R_d(A)||_2. \tag{3.29}$$

3.4.3.4 Summary

For the general normal (or quasi-normal) matrices, the relation between the convergence of GMRES and the spectral information of operator matrix is clear. The spectrum of A can be used to give an acceptable upper bound for the convergence of GMRES. For the linear systems which are difficult to achieve the convergence by GMRES, different preconditioners can be constructed to either transform the spectral distribution into another one with smaller condition number, deflate the smallest eigenvalues or enlarge the dominant eigenvalues to accelerate the convergence. Different preconditioning techniques will be presented in the Section 3.5.

In many practical applications, one can observe a correlation between the eigenvalues of a general non-normal matrix A and the convergence rate of GMRES. Considering the results in this section, linking eigenvalues and the convergence of GMRES for a non-normal matrix A must always be based on convincing arguments. They can consist of, e.g., demonstrating a special relationship between the initial residual (or the right-hand side if $x_0 = 0$) and the eigenvectors of A. Such connection may compensate for the influence of ill-conditioned eigenvectors, so that the approximation problem actually solved by GMRES is indeed (close to) an approximation problem on the eigenvalues of A. In some cases, ϵ-pseudospectra, the field of values or the polynomial numerical hull can be used to find close estimates of the norm of $R_d(A)$ and hence of the ideal GMRES approximation. The convergence behaviors of GMRES for non-normal matrices are far more complicated, the conventional preconditioners which focus on the operations on the smallest or largest eigenvalues, might be not acceptable. However the preconditoners might be built based on the ϵ-pseudospectrum, the field of values and polynomial hull for special cases.

© 2019 Tous droits réservés.

lilliad.univ-lille.fr

Thèse de Xinzhe Wu, Université de Lille, 2019

3.5 Preconditioners for GMRES

In practice, one weakness of GMRES discussed in the previous section is the lack of robustness, it is likely to suffer from slow convergence for some problems. Preconditioning is a kind of techniques to accelerate the convergence of Krylov subspace methods by transforming the original linear systems from one to another. The conventional preconditioners are effective by removing and deflating the smallest eigenvalues, enlarging the dominant eigenvalues and decreasing the condition number of operator matrix. In this section, we summarize different types of existing preconditioners, including the preconditioning by a selected matrix, by the deflation, and by a selected polynomial.

3.5.1 Preconditioning by Selected Matrix

The first alternative is to use the preconditioning matrix M. This M can be defined in many different ways, and it makes it much easier to solve linear systems $Mx = b$ compared with the original linear systems $Ax = b$. After the selection of M, there are three ways to apply this preconditioning matrix M to the original systems: the left, right and split preconditioning. This type of preconditioners are general more used for the linear systems with normal and quasi-normal matrices. They are effective to accelerate the convergence of iterative methods by changing the spectral properties of operator matrices.

3.5.1.1 Left, Right and Split Preconditioning

The *left preconditioning* of matrix on the original linear system can be defined as:

$$M^{-1}Ax = M^{-1}b. \tag{3.30}$$

GMRES is applied to solve the Equation (3.30) instead of the original matrix. The left preconditioned version GMRES is given as Algorithm 7.

Algorithm 7 Left-Preconditioned GMRES

$r_0 = M^{-1}(b - Ax_0), \beta = ||r_0||_2$, and $\nu_1 = r_0/\beta$
for $i = 0, \cdots, m-1$ **do**
  $z \leftarrow M^{-1}A\nu_i$
  $h_{j,i} \leftarrow \langle z, \nu_j \rangle$, $z = z - h_{j,i}\nu_j$ $j = 1, \cdots, i$
  if $h_{j+1,j} == 0$ **then**
    stop
  else
    $\nu_{i+1} = z/h_{i+1,i}$, and $h_{i+1,i} = ||z||_2$
  end if
end for
Compute y_m which minimizes $||\beta e_1 - H_m y||_2$
$x_m = x_0 + V_m y_m$

As shown in Algorithm 7, M is applied to each step of GMRES iteration, and the Krylov subspace constructed by the Arnoldi process tends to be:

© 2019 Tous droits réservés.

lilliad.univ-lille.fr

Thèse de Xinzhe Wu, Université de Lille, 2019

$$span\{r_0, M^{-1}Ar_0, \cdots, (M^{-1}A)^{m-1}r_0\}. \tag{3.31}$$

The residual vectors in this algorithm can be defined as $r_m = M^{-1}(b - Ax_m)$, instead of the unpreconditioned one $b - Ax_m$.

The *right preconditioning* of M makes GMRES solve linear systems as follows instead of the original systems:

$$AM^{-1}u = b, \qquad u = Mx. \tag{3.32}$$

The right-preconditioned GMRES is given as Algorithm 8. As shown in this algorithm, the Krylov subspace spanned by the right preconditioning can be defined as:

Algorithm 8 Right-Preconditioned GMRES

$r_0 = b - Ax_0, \beta = ||r_0||_2$, and $\nu_1 = r_0/\beta$
for $i = 0, \cdots, m-1$ **do**
    $z \leftarrow AM^{-1}\nu_i$
    $h_{j,i} \leftarrow \langle z, \nu_j \rangle$, $z = z - h_{j,i}\nu_j$ $j = 1, \cdots, i$
    if $h_{j+1,j} == 0$ **then**
        stop
    else
        $\nu_{i+1} = z/h_{i+1,i}$, and $h_{i+1,i} = ||z||_2$
    end if
end for
Compute y_m which minimizes $||\beta e_1 - H_m y||_2$
$x_m = x_0 + M^{-1}V_m y_m$

$$Span\{r_0, AM^{-1}r_0, \cdots, (AM^{-1})^{m-1}r_0\}. \tag{3.33}$$

The essential difference of right preconditioning compared with left preconditioning is that the residual vectors can be obtained as $b - Ax_m = b - AM^{-1}u_m$, which is equal the ones of unpreconditioned systems, and independent from the selection of M. Thus this preconditioning matrix can vary with different selections for each iteration of GMRES, that is the flexible GMRES, which can be useful for several linear systems.

Another alternative is to use the *split preconditioning*, which can be seen as a combination of left and right preconditioning. Suppose that a preconditioning matrix M can be factorized as the form:

$$M = LU. \tag{3.34}$$

Then, the split preconditioned linear systems to be solved by GMRES can be defined as:

$$L^{-1}AU^{-1}u = L^{-1}b, \qquad x = U^{-1}u. \tag{3.35}$$

The residual vectors of this type of GMRES is that form $L^{-1}(b - Ax_m)$. In fact, a split preconditioner may be much better if A is nearly symmetric.

© 2019 Tous droits réservés.

lilliad.univ-lille.fr

Thèse de Xinzhe Wu, Université de Lille, 2019

3.5.1.2 Jacobi, SOR, and SSOR Preconditioners

The preconditioners are able to be constructed based on stationary methods, such as Jacobi, SOR and SSOR.

Their general form for the preconditioning can be given as:

$$x_{k+1} = M^{-1}Nx_k + M^{-1}b, \tag{3.36}$$

where M and N are created by the splitting of A as:

$$A = M - N. \tag{3.37}$$

The above formula can be rewritten as:

$$x_{k+1} = Gx_k + f, \tag{3.38}$$

with $f = M^{-1}b$ and $G = M^{-1}N = I - M^{-1}A$.
The Expression (3.38) attempts to solve:

$$(I - G)x = f. \tag{3.39}$$

which can be rewritten as:

$$M^{-1}Ax = M^{-1}b. \tag{3.40}$$

For *Jacobi Preconditioner*, the preconditioning matrix M can be defined as:

$$M_{Jacobi} = D^{-1}. \tag{3.41}$$

For *Gauss-Seidel Preconditioner*, the preconditioning matrix M can be defined as:

$$M_{Gauss} = (D - E)D^{-1}(D - F). \tag{3.42}$$

For *SSOR preconditioner*, the preconditioning matrix M can be defined as:

$$M_{SSOR} = (D - \omega E)D^{-1}(D - \omega F). \tag{3.43}$$

3.5.1.3 Imcomplete LU Preconditioners

In numerical linear algebra, an ILU of a matrix is a sparse approximation of the LU factorization. It is often used as a preconditioner.

For a linear system $Ax = b$, it is often solved by computing the factorization $A = LU$, with L a lower triangular and U upper triangular. One then solves efficiently $Ly = b$ and $Ux = y$ in sequence since U, and L are all triangular. It is well known that usually in the factorization procedure, the matrices L and U have more non zero entries then A. These extra entries are called fill-in entries.

© 2019 Tous droits réservés.

lilliad.univ-lille.fr

Thèse de Xinzhe Wu, Université de Lille, 2019

An incomplete factorization [187, 194, 130, 140] instead seeks triangular matrices L and U such that

$$A \approx LU.$$

An example of ILU is given as Algorithm 9. For a typical sparse matrix, the LU factors can be much less sparse than the original matrix - a phenomenon called fill-in. The memory requirements for using a direct solver can then become a bottleneck in solving linear systems. One can combat this problem by using fill-reducing reorderings of the matrix's unknowns.

Algorithm 9 Incomplete LU Factorization Algorithm

```
for i = 2, ··· , n do
    for k = 1, ··· , i − 1 do
        if (i, k) ∉ P then
            a_{i,k} = a_{i,k} / a_{k,k}
            for j = k + 1, ··· , n do
                if (i, j) ∉ P then
                    a_{i,j} = a_{i,j} − a_{i,k} a_{k,j}
                end if
            end for
        end if
    end for
end for
```

Let S be a subset of all positions of the original matrix generally including the main diagonal, and $\forall(i,j)$ such that $a_{i,j} \neq 0$. An incomplete LU factorization of A only allows fill-in positions which are in S, which is designated by the elements to drop at each step. S has to be specified in advance statically by defining a zero pattern which must exclude the main diagonal. Therefore, for any zero patterns P, such that

$$P \subset \{(i,j)|i \neq j; 1 \leq i,j \leq n\} \tag{3.44}$$

Solving for $LUx = b$ can be done quickly but does not hield the exact solution to the given problem. So a matrix is

$$M_{LU} = LU,$$

often used as a preconditioner for another iterative method such as GMRES. For an incomplete factorization with no-fill, named ILU(0), we define the pattern P as the zero patterns of A. However, more accurate factorization can be obtained by allowing some fill-in, denoted by ILU(p) where p stands for the desired level of fill. This class of preconditioners have some difficulties to converge in a reasonable number of iterations for ill-conditioned systems.

3.5.1.4 Preconditioning by Multigrid Solvers

MG methods, including GMG and AMG, are the most complex preconditioners. The MG methods speed up the convergence of stationary iterative methods by smoothing the low-frequency modes of the errors of linear systems with the construction of a series of coarse representations. The main difference between the GMG and AMG is the strategy to construct the restriction

© 2019 Tous droits réservés.

lilliad.univ-lille.fr

Thèse de Xinzhe Wu, Université de Lille, 2019

and coarse matrices. AMG preconditioners need an amount of time for the pre-processing, but they can accelerate convergence much more significantly.

When AMG is applied as a preconditioner (e.g. [173, 132, 229, 145]), the setup phase of restriction matrix R_h^{2h} and the interpolation matrix I_h^{2h} need to be complex as the standalone AMG solvers. The creation of a given number of sub-domains, and each domain representing by only one value at the coarse level is enough. After dividing the nodes of mesh into groups, the projection matrix can be defined as W. W is used to build the coarse-system matrix A_{2h} of an original matrix A:

$$A_{2h} = W^T A W. \tag{3.45}$$

Thus, W is the restriction operation R_h^{2h} , and W^T is the interpolation matrix I_h^{2h}. After the creation of transfer operation W, it can be applied into the fine-coarse-fine loop of MG method to generate an approximate solution of original linear systems. Algorithm 10 gives an example of AMG preconditioned GMRES.

Algorithm 10 AMG-Preconditioned GMRES

$r_0 = b - Ax_0, \beta = ||r_0||_2$, and $\nu_1 = r_0/\beta$
for $i = 0, \cdots, m-1$ **do**
    Get u_p by p **relaxions** on $Au = \nu_i$ starting from u_0 using stationary methods.
    Find the residual: $r_p = \nu_i - Au_p$.
    Project r_p one the coarse level: $r_pc = W^T r_p$.
    Solve the coarse-level residual system: $A_{2h}E_{pc} = r_{pc}$.
    Project back E_{pc} the fine level: $E_p = We_{pc}$.
    Correct the fine-level approximation: $u_p = u_p + E_p$.
    Iterate p times on $Au = \nu_i$ starting from u_p, get the final approximation $\hat{u}$.
    set $\nu_i = \hat{u}$.
    $z \leftarrow A\nu_i$
    $h_{j,i} \leftarrow \langle z, \nu_j \rangle$, $z = z - h_{j,i}\nu_j$ $j = 1, \cdots, i$
    if $h_{j+1,j} == 0$ **then**
        stop
    else
        $\nu_{i+1} = z/h_{i+1,i}$, and $h_{i+1,i} = ||z||_2$
    end if
end for
Compute y_m which minimizes $||\beta e_1 - H_m y||_2$
$x_m = x_0 + M^{-1}V_m y_m$

3.5.2 Preconditioning by Deflation

As discussed in Section 3.4.3, it is not always true, but the convergence of Krylov subspace methods for most (normal and quasi-normal) linear systems depends on the distribution of eigenvalues. The removing or deflation of the small eigenvalues might greatly improve the convergence performance. If the dimension of Krylov subspace is large enough, some deflation occurs automatically. But for the restarted GMRES, the limitation of the dimension of Krylov subspace is not enough for these deflations, and convergence cannot be achieved accordingly. Thus deflation schemes should be constructed for each cycle of the restart, and this technique is called

© 2019 Tous droits réservés.

lilliad.univ-lille.fr

Thèse de Xinzhe Wu, Université de Lille, 2019

the deflated preconditioners. Kharchenko et al. [122] built a deflation preconditioner using the approximate eigenvectors. In [85], Erhel et al. developed a deflation technique based on an invariant subspace approach; Burrage et al. [47] improved this deflation technique by considering the eigenpairs outside the Krylov subspace of GMRES. Both Chapman et al. [52] and Gaul et al. [99] presented the deflated and augmented Krylov subspace techniques. Giraud et al. [102] proposed a novel algorithm that attempts to combine the numerical features of deflated GMRES, and the flexibility of FGMRES. Kutsukake et al. [128] developed a new deflated flexible GMERS which uses an approximate inverse preconditioner.

In this section, we give a example of deflated GMRES(m, k) (denoted as GMRES-DR(m, k)) developed by Morgan et al. [151]. GMRES-DR is a deflation preconditioned GMRES uses the thick restarting iterations. It has two parameters m and k, where m is the restart size of GMRES, and k is the number of eigenvectors used for the deflation during the restart. The first cycle is the same as GMRES(m), which is able to generate V_m and H_m. The k smallest eigenpairs (λ_k, g_k) of matrix $H_m + \beta H_m^{-T} e_m e_m^T$ can be calculated. Then a matrix G_k can be formulated as:

$$G_k = [g_1, g_2, \cdots, g_k], \tag{3.46}$$

and then G_{k+1} can be generated as:

$$G_{k+1} = ((G_k), c - \bar{H}_m y). \tag{3.47}$$

Q_{k+1} can be gotten from G_{k+1}, hence V_{k+1} and H_k are generated, where V_{k+1} is a $n \times (k+1)$ matrix and H_k is a $k \times k$ matrix. Therefore, it becomes necessary to extend V_{k+1} and H_k to V_m and H_m by the Arnoldi method that starts at the $(k+1)$-th iteration. This method is shown in Algorithm 11. GMRES-DR is efficient and numerical stable for deflating the small eigenvalues and accelerating the convergence.

3.5.3 Preconditioning by Polynomials - A Detailed Introduction on Least Squares Polynomial Method

In the context of iterative methods for solving linear systems, polynomial preconditioners have been studied extensively. In this section, we recall some of the results regarding simple polynomial preconditioners, and then give an introduction about the Least Squares Polynomial preconditioner.

3.5.3.1 Polynomial Preconditioners for Linear Solvers

In order to approximate the solution of linear system

$$Ax = b,$$

one approach is to get the inverse of A, denote it as A^{-1}, and then the solution can be easily obtained as

$$x = A^{-1}b.$$

.

© 2019 Tous droits réservés.

lilliad.univ-lille.fr

Thèse de Xinzhe Wu, Université de Lille, 2019

Algorithm 11 GMRES-DR(A, m, k, x_0)

$r_0 = b - Ax_0, \beta = ||r_0||_2$, and $\nu_1 = r_0/\beta$
for $i = 0, \cdots, m-1$ **do**
    $z \leftarrow A\nu_i$
    $h_{j,i} \leftarrow \langle z, \nu_j \rangle$, $z = z - h_{j,i}\nu_j$ $j = 1, \cdots, i$
    if $h_{j+1,j} == 0$ **then**
        stop
    else
        $\nu_{i+1} = z/h_{i+1,i}$, and $h_{i+1,i} = ||z||_2$
    end if
end for
Compute y_m which minimizes $||\beta e_1 - H_m y||_2$
Compute the k smallest eigenpairs (λ_k, g_k) of $H_m + \beta H_m^{-T} e_m e_m^T$
Set $G_k = [g_1, g_2, \cdots, g_k]$
Orthonormalize G_k into Q_k which is a $n \times k$ matrix
Extend Q_k to length $m+1$ by appending a zero entry to each. Then orthonormalize the vector $c - \bar{H}_m d$ against them to form q_{k+1}. Note $c - \bar{H}_m d$ is a vector of length $m+1$, Q_{k+1} can be formulated by combining Q_k and q_{k+1}
Set $V_{k+1}^{new} = V_{k+1}Q_{k+1}$ and $\bar{H_k}^{new} = Q_{k+1}^H \bar{H}_m$
Reorthogonalize v_{k+1} against the earlier columns of V_{k+1}^{new}
Apply the Arnoldi iteration from this point to form the rest of V_{m+1} and $\bar{H}_m$, with $\beta = h_{m+1,m}$
Set $c = V_{m+1}^T r_0$ and solve $\min ||c - \bar{H}_m d||_2$ for d
Set $x_m = x_0 + V_m d$, $r_m = b - Ax_m = V_{m+1}(c - \bar{H}_m d)$
if $||r_m|| < tol$ **then**
    Stop
end if
Compute the k smallest eigenpairs (λ_k, g_k) of $H_m + \beta H_m^{-T} e_m e_m^T$
set $x_0 = x_m$ and Go to Step 1

Suppose that the characteristic polynomial for A:

$$q(A) = \gamma_n A^n + \gamma_{n-1} A^{n-1} + \cdots + \gamma_1 A + \gamma_0 I = 0. \tag{3.48}$$

The polynomial representation of A^{-1} with $\gamma_0 \neq 0$ can be given as:

$$A^{-1} = \frac{1}{\gamma_0}(-\gamma_n A^{n-1} - \gamma_{n-1} A^{n-1} - \cdots - \gamma_1 I) = p(A). \tag{3.49}$$

Therefore, it makes sense to approximate A^{-1} by a polynomial in A. Better selection of this kind of polynomial can approximate more quickly the solution of linear systems.

3.5.3.2 Neumann series polynomials

The simplest p is the polynomial with the Neumann series expansion:

$$I + N^1 + N^2 + \cdots, \tag{3.50}$$

with:

© 2019 Tous droits réservés.

lilliad.univ-lille.fr

Thèse de Xinzhe Wu, Université de Lille, 2019

$$N = I - \omega A, \tag{3.51}$$

and ω is a scaling parameter. The above series can be obtained by the expansion of the inverse of ωA:

$$\begin{aligned}(\omega A)^{-1} &= [D - (D - \omega D^{-1}A)]^{-1} \\ &= [I - (I - \omega D^{-1}A)]^{-1}D^{-1},\end{aligned} \tag{3.52}$$

where D can be the Identity matrix I, the diagonal of A, or even a block diagonal of A. Setting:

$$N = I - \omega D^{-1}A, \tag{3.53}$$

and truncating this series, a polynomial preconditioner of degree k can be defined as:

$$p_k(A) = [I + N^1 + N^2 + \cdots + N^k]D^{-1}. \tag{3.54}$$

Denote the exact solution of $Ax = b$ as $x = A^{-1}b$ and the approximate solution by $p_k(A)$ as $x' = p_k(A)b$. The error of between x' and x is bounded as:

$$\begin{aligned}||x - x'||_2 &= ||A^{-1}b - p_k(A)b||_2 \\ &= ||(I - p_k(A)A)A^{-1}b||_2 \\ &= ||N^{k+1}A^{-1}b||_2 \leq ||N||_2^{k+1}||A^{-1}b||_2.\end{aligned} \tag{3.55}$$

The performance of preconditioning by Neumann polynomial can be improved with the enlargement of polynomial degree of p_k, but matrix operation can be difficult numerically for large k.

3.5.3.3 Chebyshev Polynomials

In order to accelerate the convergence with the degree k as small as possible, a kind of minimum-maximum polynomials are proposed. A polynomial preconditioner can be more abstractly defined as any polynomial $P_d(A)$ of degree $d - 1$.

The iterates of this polynomial to approximate the solution can be written as

$$x_d = x_0 + P_d(A)r_0, \tag{3.56}$$

where x_0 is a selected initial approximation to the solution, and r_0 the corresponding residual norm. A polynomial of d degree R_d can be set such that

$$R_d(\lambda) = 1 - \lambda P_d(\lambda). \tag{3.57}$$

R_d is called the *residual polynomial*. The residual r_d generated by a d degree polynomial can be expressed as equation

$$r_d = R_d(A)r_0, \tag{3.58}$$

© 2019 Tous droits réservés.

lilliad.univ-lille.fr

Thèse de Xinzhe Wu, Université de Lille, 2019

with the constraint $R_d(0) = 1$. It is necessary to find a kind of polynomial which can minimize $||R_d(A)r_0||_2$, with $||.||_2$ the Euclidean norm.

If A is a $n \times n$ diagonalizable matrix with its spectrum denoted as $\sigma(A) = \lambda_1, \cdots, \lambda_n$, and the associated eigenvectors $u_1, \cdots, u_n$. Expanding the initial residual vector r_0 in the basis of these eigenvectors as

$$r_0 = \sum_{i=1}^{n} \rho_i u_i. \tag{3.59}$$

Moreover, then the residual vector r_d can be expanded in this basis of these eigenvectors as

$$r_d = \sum_{i=1}^{n} R_d(\lambda_i)\rho_i u_i, \tag{3.60}$$

which allows getting the upper limit of $||r_d||_2$ as

$$||r_d||_2 \leq ||r_0||_2 \max_{\lambda \in \sigma(A)} |R_d(\lambda)|. \tag{3.61}$$

In order to minimize the norm of r_d, it is possible to find a polynomial P_d which can minimize the Equation (3.61). And it tends to be a minimum-maximum problem with the constraint $R_d(0) = 1$ and $\lambda \in \sigma(A)$

$$min\ max_{\lambda \in \sigma(A)} |R_d(\lambda)|. \tag{3.62}$$

This mimimum-maximum problem can be expressed as

$$min\ max_{\lambda \in H} |R_d(\lambda)|, \tag{3.63}$$

where H is taken to be an ellipse with center c and focal distance f, which contains the convex hull of $\lambda(A)$. In order to solve the last problem, a well known method is the Chebyshev polynomial iterative method, If the origin is outside of this ellipse, the minimal polynomial can be reduced to a scaled and shifed Chebyshev polynomial:

$$R_d(\lambda) = \frac{T_d(\frac{c-\lambda}{f})}{T_d(\frac{c}{f})}, \tag{3.64}$$

with T_d a Chebyshev polynomial. The three-term recurrence for the Chebyshev polynomials results in the following three-term recurrences

$$T_{k+1}(\frac{c}{f}) = 2\frac{c}{f}T_k(\frac{c}{f}) - T_{k-1}(\frac{c}{f}),\ k = 1, 2, 3, \cdots, \tag{3.65}$$

with

$$T_0(\frac{c}{f}) = 1,\ T_1(\frac{c}{f}) = \frac{c}{f}. \tag{3.66}$$

and

© 2019 Tous droits réservés.

lilliad.univ-lille.fr

Thèse de Xinzhe Wu, Université de Lille, 2019

$$\begin{aligned} R_{k+1}(\lambda) &= \frac{1}{T_{k+1}(\frac{c}{f})}\left[2\frac{c-\lambda}{f}T_k(\frac{c}{f})R_k(\lambda) - T_{k-1}(\frac{c}{f})R_{k-1}(\lambda)\right] \\ &= \frac{T_k(\frac{c}{f})}{T_{k+1}(\frac{c}{f})}\left[2\frac{c-\lambda}{f}R_k(\lambda) - \frac{T_{k-1}(\frac{c}{f})}{T_k(\frac{c}{f})}R_{k-1}(\lambda)\right],\ k \geq 1, \end{aligned} \tag{3.67}$$

with

$$R_0(\lambda) = 1,\ R_1(\lambda) = 1 - \frac{\lambda}{c}. \tag{3.68}$$

Denote

$$\rho_k = \frac{T_k(\frac{c}{f})}{T_{k+1}(\frac{c}{f})},\ k = 1, 2, 3, \cdots \tag{3.69}$$

We have

$$\begin{cases} \rho_k = \dfrac{1}{2\frac{c}{f} - \rho_{k-1}} \\ R_{k+1}(\lambda) = \rho_k\left[2(\dfrac{c}{f} - \dfrac{\lambda}{f})R_k(\lambda) - \rho_{k-1}R_{k-1}(\lambda)\right], k \geq 1 \end{cases} \tag{3.70}$$

After the construction of three-term recurrence for R_d by the optimal ellipse H, the difference between two successive residual vectors can be given as

$$r_{k+1} - r_k = (R_{k+1}(A) - R_k(A))r_0. \tag{3.71}$$

Thus for the approximated solution x_{k+1} and x_k corresponding respectively to r_{k+1} and r_k, we have

$$x_{k+1} - x_k = \rho_k\left[\rho_{k-1}(x_k - x_{k-1}) + \frac{2}{f}(b - Ax_k)\right]. \tag{3.72}$$

A Chebyshev polynomial preconditioned GMRES is given as Algorithm 12. After m-steps GMRES with approximate solution $\tilde{x}$, a new ellipse can be refined with the newly gotten eigenvalues from the Hessenberg matrix. Denote this optimal ellipse as $ellipse(a, c, f)$, with a the major axis, c the center, and f the focal. A new solution can be updated by the recurrence of Chebyshev polynomial from $\tilde{x}$, and it will be used as an initial vector for the next restart of GMRES.

3.5.3.4 Least Squares Polynomial Method

An important drawback for Chebyshev polynomial preconditioner is that the optimal ellipse which encloses the spectrum often does not accurately represent the spectrum. This might result in slow convergence. Based on the normalized Chebyshev polynomial, the Least Squares polynomial methods are introduced. The spectrum of A is discrete, it is possible to introduce one or more polygonal regions without the origin, which has a relatively small number of edges instead of ellipses [200]. The problem tends to find a polynomial P_d on the boundary of H which we note as ∂H, that maximizes the modulus of $|1 - \lambda P_d(\lambda)|$. Then we get the Least Squares

© 2019 Tous droits réservés.

lilliad.univ-lille.fr

Thèse de Xinzhe Wu, Université de Lille, 2019

Algorithm 12 Chebyshev Polynomial Preconditioned GMRES

1: Compute current residual vector $r = b - A\tilde{x}$
2: Run m steps of GMRES for solving $Ad = r$.
3: Update $\tilde{x}$ by $\tilde{x} = \tilde{x} + d$.
4: Get eigenvalue estimates from the eigenvalues of the Hessenberg matrix.
5: Refine a new ellipse $ellipse(a, c, f)$ with novel eigenvalue estimates.
6: Compute the current residual vector $r_0 = b - A\tilde{x}$, $\rho_0 = \frac{f}{c}$, $d = \frac{1}{c}r_0$;
7: **for** $k = 0, 1, \cdots = d - 1$ **do**
8: $\quad x_{k+1} = x_k + d_k$
9: $\quad r_{k+1} = r_k - Ad_k$
10: $\quad \rho_{k+1} = (2\frac{c}{f} - \rho_k)^{-1}$
11: $\quad d_{k+1} = \rho_{k+1}\rho_k d_k + \frac{2\rho_{k+1}}{f} r_{k+1}$
12: **end for**
13: Update $\tilde{x}$ as $\tilde{x} = x_d$.
14: Test for convergence.
15: If solution converged then STOP, else GOTO 1.

problem with respect to some weight $w(\lambda)$ on the boundary of H and the constraint $R_d(0) = 1$.

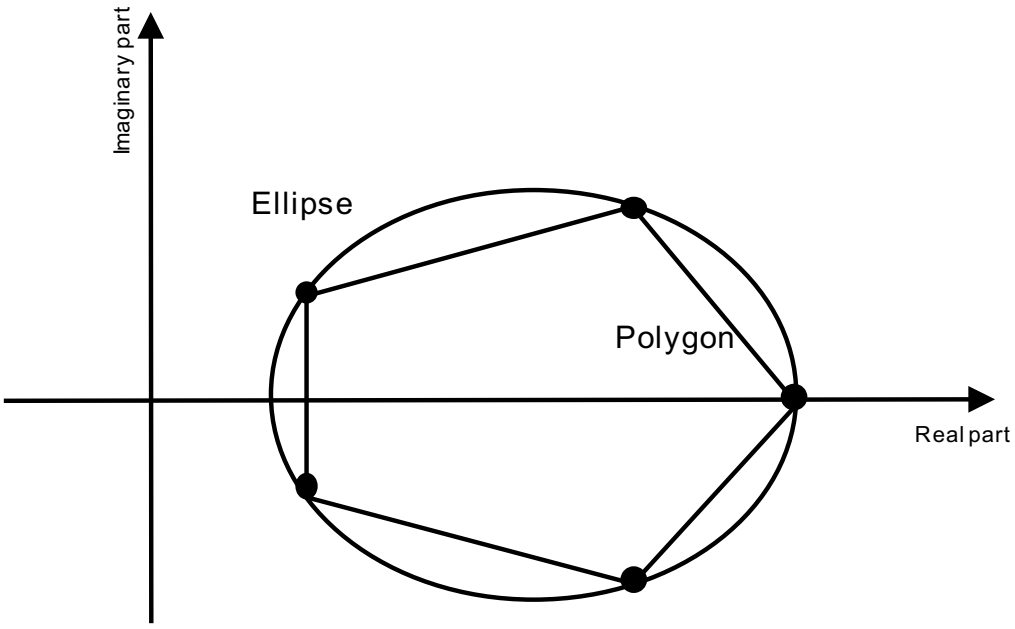

Figure 3.3 – The polygon of samllest area containing the convex hull of $\lambda(A)$.

Weight Function and Gram Matrix: Suppose that matrix A is real, we know that its spectrum is symmetric with the real axis, which means we will only need the upper half part H^+ of the convex hull H.

Suppose that ∂H^+ the upper part of boundary H and $v = 1, \cdots, \mu$ that $\partial H^+ = \cup_{v=1}^{\mu} E_v$. And then, suppose c_v and f_v, the center and focal distance of edge E_v. The inner product of two complex polynomials p and q associated with the weight function ω_v on the edge E_v can be expressed as.

© 2019 Tous droits réservés.

lilliad.univ-lille.fr

Thèse de Xinzhe Wu, Université de Lille, 2019

$$(p,q)_w = 2\Re\Big[\sum_{v=1}^{v}\int_{E_v} p(\lambda)\overline{q(\lambda)}w_v(\lambda)\mathrm{d}\lambda\Big]. \tag{3.73}$$

$$w_v(\lambda) = \frac{2}{\pi}|f_v^2 - (\lambda - c_v)^2|^{-\frac{1}{2}}. \tag{3.74}$$

This function is the weight function of one edge E_v generated by the basis of Chebyshev polynomials, which facilitates to calculate the inner product.

And then, each polynomial $t_i(\lambda)$ can be expressed in terms of the Chebyshev polynomial (3.75) constructed by the ellipse $\xi(a, c_v, f_v)$ with $i \geq 0$ as the Fourmule (3.76).

$$T_l(\frac{\lambda - c_v}{f_v}). \tag{3.75}$$

$$t_i(\lambda) = \sum_{l=0}^{i}\gamma_{l,v}^{(i)}T_l(\frac{\lambda - c_v}{f_v}). \tag{3.76}$$

Since the polygon have μ different edges, thus each polynomial $t_i(\lambda)$ will have μ different expressions in terms of Formula (3.76), on each edge E_v. Clearly, one of these expressions is normally enough to fully determine the polynomial $t_i(\lambda)$. However, we construct it with a linear combination of them, which allows stably performing an efficient computation.

With this polynomial basis, a so-called modified Gram matrix $M_d = m_{i,j}$ can be obtained, which is well-conditioned. The entries $m_{i,j}$ of M_d defined as the relation below where $i, j \in 1, \cdots, d+1$

$$m_{i,j} = (t_{i-1}, t_{j-1})_\omega \tag{3.77}$$

Thus the coefficients of the Gram matrix M_d are given by

$$m_{i+1,j+1} = 2\Re\Big[\sum_{v=1}^{\mu}\Big(2\gamma_{0,v}^{(i)}\overline{\gamma_{0,v}^{(j)}} + \sum_{l=1}^{j}\gamma_{l,v}^{(i)}\overline{\gamma_{l,v}^{(j)}}\Big)\Big], \tag{3.78}$$

for all i, j such that $0 \leq i \leq j \leq d$.

Because of the three term-recurrence of the Chebyshev polynomials, it is possible to carry the computation of these coefficients recursively. The recurrence relation for the shifted Chebyshev polynomials are rewritten in the form

$$\begin{aligned}\beta_{i+1}t_{i+1}(z) &= (z-a)t_i(z) - \delta_i t_{i-1}(z)\\ &= (z-\alpha_i)\sum_{l=0}^{i}\gamma_{l,v}^{(i)}T_l(\frac{z-c_v}{f_v}) - \delta_i\sum_{l=0}^{i-1}\gamma_{l,v}^{(i-1)}T_l(\frac{z-c_v}{f_v}),\end{aligned} \tag{3.79}$$

with the convention that $t_{-1} = 0$ and $\delta_0 = 0$. This formula provides the expressions for t_{i+1} from those of t_i and t_{i-1} by exploiting the following relations

$$\begin{cases}\dfrac{z-c_v}{f_v}T_l(\dfrac{z-c_v}{f_v}) = \dfrac{1}{2}[T_{l+1}(\dfrac{z-c_v}{f_v}) + T_{l-1}(\dfrac{z-c_v}{f_v})] \quad l > 0,\\ \dfrac{z-c_v}{f_v}T_0(\dfrac{z-c_v}{f_v}) = T_1(\dfrac{z-c_v}{f_v})\end{cases} \tag{3.80}$$

© 2019 Tous droits réservés.

lilliad.univ-lille.fr

Thèse de Xinzhe Wu, Université de Lille, 2019

Finally, for $v = 1, 2, \cdots, \mu$, the expansion coefficients $\gamma_{l,v}^{(i)}$ satisfy the recurrence relation

$$\beta_{i+1}\gamma_{l,v}^{(i+1)} = \frac{f_v}{2}\left[\gamma_{l+1,v}^{(i)} + \gamma_{l-1,v}^{(i)}\right] + (c_v - \alpha_i)\gamma_{l,v}^{(i)} - \delta_i\gamma_{l,v}^{(i-1)}, \tag{3.81}$$

for $l = 0, 1, \cdots, i+1$ with the notational convention,

$$\gamma_{-1,v}^{(i)} = \gamma_{1,v}^{(i)}, \quad \gamma_{l,v}^{(i)} = 0, \quad \forall l > i. \tag{3.82}$$

Compute the Best Polynomial: For two polynomials p and q of degree d, their inner product can be described as

$$(p, q)_\omega = (M_d\eta, \theta), \tag{3.83}$$

with $\eta = (\eta_1, \cdots, \eta_d)$ and $\theta = (\theta_1, \cdots, \theta_d)$, the coordinates of polynomials p and q in basis t_i.

Expanding the polynomial P_d of (3.56) into the Chebyshev basis, and then we can get R_d as equation below,

$$P_d = \sum_{i=0}^{d-1} \eta_i t_i. \tag{3.84}$$

The residual polynomial R_d can be expressed as

$$\begin{aligned} R_d(\lambda) &= 1 - \lambda P_d(\lambda) \\ &= 1 - \sum_{i=0}^{d-1} \eta_i \lambda t_i(\lambda) \end{aligned} \tag{3.85}$$

and in the end we obtain the following equations with the three terms recurrence (3.79):

$$R_d(\lambda) = t_0 - \sum_{i=0}^{d-1} \eta_i(\beta_{i+1}t_{i+1} + \alpha_i\eta_i + \delta_i\eta_{i+1})t_i. \tag{3.86}$$

Then R_d can be expressed into $e_1 - T_d\eta$ with its coordinations in the polynomial t_i, where T_d is a $(d+1) \times d$ matrix as

$$T_d = \begin{bmatrix} \alpha_0 & \delta_1 & & & & \\ \beta_1 & \alpha_1 & \delta_2 & & & \\ & \beta_2 & \alpha_2 & \delta_3 & & \\ & & & & & \\ & & & & & \delta_{d-1} \\ & & & & \beta_{d-1} & \alpha_{d-1} \\ & & & & & \beta_d \end{bmatrix} \tag{3.87}$$

With the definition of inner product in the polynomial basis, the function which needs to be minimized can be expressed under the form of the equation below.

$$\begin{aligned} R_d^2 &= (R_d, R_d)_\omega \\ &= (M_d(e_1 - T_dH_d), e - T_dH_d). \end{aligned} \tag{3.88}$$

© 2019 Tous droits réservés.

lilliad.univ-lille.fr

Thèse de Xinzhe Wu, Université de Lille, 2019

As M_d is symmetric, we can get the factorization of M_d under the form $M_d = L_d L_d^T$, and in the end we obtain the equation as below with $F_d = L_d^T T_k$ a $(d+1) \times d$ upper Hessenberg matrix.

$$\begin{aligned} R_d^2 &= (R_d, R_d)_\omega \\ &= (L_d^T(e_1 - T_d H_d), L_d^T(e_1 - T_d H_d)). \end{aligned} \tag{3.89}$$

In the end, $||R_d||_2$ can be defined as

$$\begin{aligned} ||R_d||_2 &= ||L_d^T(e_1 - T_d H_d)||_2 \\ &= ||l_{1,1} - F_d H_d||_2 \end{aligned} \tag{3.90}$$

The coefficients H_d are the solution of problem $\min ||l_{1,1}e_1 - F_d H_d||_2$ with $H_d \in IR^d$. This problem can maybe be solved easily by Givens rotations and QR factorization. The process to generate the Least Squares Polynomial's parameters by three terms recurrence using the eigenvalues are given in Algorithm 13.

Compute the Iteration Form: the iteration form of Least Squares polynomial is $x_d = x_0 + P_d(A)r_0$ with P_d the least square polynomial of degree $d-1$ under the Formula (3.91). The polynomial basis t_i meet the three terms recurrence relation (3.92).

$$P_d = \sum_{i=0}^{d-1} \eta_i t_i. \tag{3.91}$$

$$t_{i+1}(\lambda) = \frac{1}{\beta_{i+1}}[\lambda t_i(\lambda) - \alpha_i t_i(\lambda) - \delta_i t_{i-1}] \tag{3.92}$$

The parameters $H = (\eta_0, \eta_1, \cdots, \eta_{d-1})$ can be computed by a Least Squares problem of the formula

$$min \|l_{11}e_1 - F_d H_d\| \tag{3.93}$$

We therefore need to compute the vectors $\omega_i = t_i(A)r_0$, and get the linear combination of formula (3.91). The recurrence expression of ω_i is given as (3.94) and the final solution as (3.95). The hybrid GMRES preconditioned by least squares polynomial methods is given as Algorithm 14.

$$\omega_{i+1} = \frac{1}{\beta_{i+1}}(A\omega_i - \alpha_i\omega_i - \delta_i\omega_{i-1}) \tag{3.94}$$

$$\begin{aligned} x_d &= x_0 + P_d(A)r_0 \\ &= x_0 + \sum_{i=1}^{d-1} \eta_i \omega_i. \end{aligned} \tag{3.95}$$

Non-Hermitian Linear Systems: For the non-Hermitian linear systems, the acceleration of Least Squares polynomial preconditioner depends on the spectral distribution. If the polygon generated by the dominant eigenvalues is able to well approximate the spectral distribution, Least Squares polynomial might speed up the convergence efficiently. If the spectral distribution is far non-symmetric with the real-axis, the acceleration of Least Squares polynomial is limited.

© 2019 Tous droits réservés.

lilliad.univ-lille.fr

Thèse de Xinzhe Wu, Université de Lille, 2019

Algorithm 13 Least Square Polynomial Generation

function LSP-PRETREATMENT(*input*: A, b, d, Λ_r, *output*: A_d, B_d, Δ_d, H_d)
  construct the convex hull C by Λ_r
  construct $ellispe(a, c, f)$ by the convex hull C
  compute parameters A_d, B_d, Δ_d by $ellispe(a, c, f)$
  construct matrix T $(d+1) \times d$ matrix by A_d, B_d, Δ_d
  construct Gram matrix M_d by Chebyshev polynomials basis
  Cholesky factorization $M_d = LL^T$
  $F_d = L^T T$
  H_d satisfies min $\|l_{11}e_1 - F_d H_d\|$
end function

Algorithm 14 Hybrid GMRES Preconditioned by Least Squares Polynomial

Compute current residual vector $r = b - Ax$
Run m_1 steps of GMRES for solving $Ad = r$.
Update x by $x = x + d$.
Get eigenvalue estimates from the eigenvalues Λ_r of the Hessenberg matrix.
LSP-Pretreatment(*input*: A, b, d, Λ_r, *output*: A_d, B_d, Δ_d, H_d)
$r_0 = f - Ax_0$, $\omega_1 = r_0$ and $x_0 = 0$
for $k = 1, 2, \cdots, lsa$ **do**
  for $i = 1, 2, \cdots, d-1$ **do**
    $\omega_{i+1} = \frac{1}{\beta_{i+1}}[A\omega_i - \alpha_i\omega_i - \delta_i\omega_{i-1}]$
    $x_{i+1} = x_i + \eta_{i+1}\omega_{i+1}$
  end for
end for
set $x_0 = x_d$
Test for convergence.
If solution converged then Step, else GoTo 1.

Even for the general non-normal matrices, the Least Squares polynomial preconditioner might perform better than the conventional preconditioners. Since it is constructed by the polynomial hull, which might be effcient for several cases with non-normal matrices.

3.6 Arnoldi for Non-Hermitian Eigenvalue Problems

The dominant eigenvalues of a non-Hermitian eigenvalue problem can be approximated by the Arnoldi method. The dominant eigenvalues means the ones with large Euclidean norms. In the section, we present the basic algorithm of Arnoldi method and its variants.

3.6.1 Basic Arnoldi Methods

Arnoldi algorithm [13] is widely used to approximate the eigenvalues of large sparse matrices. The kernel of Arnoldi algorithm is the Arnoldi reduction, which gives an orthonormal basis $\Omega_m = (\omega_1, \omega_2, \cdots, \omega_m)$ of Krylov subspace $K_m(A, v)$, by the Gram-Schmidt orthogonalization, where A is $n \times n$ matrix, and ν is a n-dimensional vector. Since Arnoldi reduction can reduce a matrix A to be an upper Hessenberg matrix H_m with relation $\Omega_m^T A \Omega_m = H_m$, the eigenvalues of H_m are the approximated ones of A, which are called the *Ritz values* of A. With the Arnoldi

© 2019 Tous droits réservés.

lilliad.univ-lille.fr

Thèse de Xinzhe Wu, Université de Lille, 2019

reduction, the r desired Ritz values $\Lambda_r = (\lambda_1, \lambda_2, \cdots, \lambda_r)$, and the corresponding *Ritz vectors* $U_r = (u_1, u_2, \cdots, u_r)$ can be calculated by Basic Arnoldi method.

The numerical accuracy of the computed eigenpairs by basic Arnoldi method depends highly on the size of the Krylov subspace and the orthogonality of Ω_m. Generally, the larger the subspace is, the better the eigenpairs approximation is. The problem is that firstly the orthogonality of the computed Ω_m tends to degrade with each basis extension. Also, the larger the subspace size is, the larger the Ω_m matrix gets. Hence available memory may also limit the subspace size, and so the achievable accuracy of the Arnoldi process. To overcome this, Saad [189] proposed to restart the Arnoldi process, which is the ERAM. Inside ERAM, the subspace size is fixed as m, and only the starting vector will vary. After one restart of the Arnoldi process, the starting vector will be initialized by using information from the computed Ritz vectors. In this way, the vector will be forced to be in the desired invariant subspace. The Arnoldi process and this iterative scheme will be executed until a satisfactory solution is computed. The implementation of ERAM is given by Algorithm 15, where ϵ_a is a tolerance value, r is desired eigenvalues number and the function g defines the stopping criterion of iterations.

Algorithm 15 ERAM algorithm

1: **function** ERAM(*input*: A, r, m, ν, ϵ_a, *output*: Λ_r)
2: Compute an AR(*input*:A, m, v, *output*: H_m, Ω_m)
3: Compute r desired eigenvalues λ_i $(i \in [1, r])$ of H_m
4: Set $u_i = \Omega_m y_i$, for $i = 1, 2, \cdots, r$, the Ritz vectors
5: Compute $R_r = (\rho_1 . \cdots, \rho_r)$ with $\rho_i = ||\lambda_i u_i - A u_i||_2$
6: **if** $g(\rho_i) < \epsilon_a$ $(i \in [1, r])$ **then**
7: stop
8: **else**
9: set $v = \sum_{i=1}^{d} Re(\nu_i)$, and GOTO 2
10: **end if**
11: **end function**

3.6.2 Variants of Arnoldi Methods

There are various strategies to restart the basic Arnoldi method and to accelerate the convergence by the deflation of unwanted eigenvalues. This section lists three variants:

(1) **ERAM [149]**: Arnoldi algorithm restarted explicitly by the combination of Ritz values and vectors.

(2) **IRAM [201]**: IRAM is a variant of Arnoldi algorithm with deflation of unwanted eigenvalues. It can shift the unwanted eigenvalues of matrix implicitly without the explicit construction of filter polynomial during the process of Arnoldi reduction. The Algorithm 16 illustrates this method. The shift of unwanted values of matrix A can be transferred to be a shifted QR factorization of Hessenberg matrix H_m. IRAM can operate in parallel to solve the large problem without extra memory space.

(3) **Krylov-Schur Method [204]**: It is another implementation of Arnoldi algorithm with deflation of unwanted eigenvalues. Krylov-Schur method is mathematically equal to IRAM.

© 2019 Tous droits réservés.

lilliad.univ-lille.fr

Thèse de Xinzhe Wu, Université de Lille, 2019

Algorithm 16 IRAM algorithm

function IRAM(*input*: A, r, m, ν, ϵ_a, *output*: Λ_r)
  Compute an AR(*input*:A, m, v, *output*: H_m, Ω_m)
  Compute the spectrum of H_m: $\Lambda(H_m)$.
  if converge **then**
    stop
  else if
    thenselect set of p shifts $\mu_1, \mu_2, \cdots, \mu_p$
  end if
  $q^T = e_m^T$
  for $j = 1, 2, 3, \cdots, p$ **do**
    Factor $[Q_J, R_j] = QR(H_m - \mu_j I)$
    $H_m = q_j^T H_m Q_j$, $V_m = V_m Q_j$, $q^T = q^T Q_j$
  end for
  $f_k = v_{k+1} H_{m(k+1,k)} + f_m q^T(k)$, $V_k = V_{m(1:n,1:k)}$, $H_k = H_{m(1:k,1:k)}$
  Beginning with the k-step Arnoldi factorization, $AV_k = V_k H_k + f_k e_k^T$, apply p additional steps of the Arnoldi process to obtain a new m-step Arnoldi factorization as $AV_m = V_m H_m + f_m e_m^T$
end function

Algorithm 17 Krylov-Schur Method

function KRYLOV-SCHUR(*input*: A, x_1, m, *output*: Λ_k with $k \leq p$)
  Build an initial Krylov decomposition of order m
  Apply orthogonal transformations to get a Krylov-Schur decompostion
  Reorder the diagonal blocks of the Krylov-Schur decompostion
  Truncate to a Krylov-Schur decompostion of order p
  Extend to a Krylov decomposition of order m
  If not satisfied, go to step 3
end function

Its two advantages over IRAM: 1) it is easier to deflate converged Ritz vectors; 2) it avoids the potential forward instability of the QR algorithm. The Algorithm 17 gives this method. During the Arnoldi reduction procedure, the Hessenberg matrix H_m is decomposed by the Schur deposition as $H_m = S_m T_m S_m$ with unitary matrix S_m and upper triangular matrix T_m. The upper triangular form of T_m eases the analysis of Ritz pairs. The wanted and unwanted Ritz values in T_m can be reordered into two separate parts as T_{m-k} and T_k. T_{m-k} can be extended to m-dimension without unwanted values through further k steps of Krylov subspace projection.

3.7 Parallel Krylov Methods on Large-scale Supercomputers

Since decades, Krylov subspace methods are generally implemented in parallel on the supercomputers to solve very large linear systems and eigenvalue problems. In 1992, an implementation of parallel subspace was already introduced by Petiton for non-Hermitian eigen-problems on the Connection Machine 2 (CM2) [171]. This section discusses the scheme to implement Krylov methods in parallel on modern distributed memory systems.

© 2019 Tous droits réservés.

lilliad.univ-lille.fr

Thèse de Xinzhe Wu, Université de Lille, 2019

3.7.1 Core Operations in Krylov Methods

It is necessary to identify the main operations in Krylov methods before the parallel implementation. Considering the Algorithm 2, we identify four types of operations, which are:

- Matrix-vector products in line 5 of Algorithm 2;
- AXPY operation in line 7 of Algorithm 2;
- Dot products in line 8 of Algorithm 2;
- Orthogonalization of vector for the loop from line line 4 to line 6 in of Algorithm 2.

This section gives the parallel implementation of these four operations in detail.

3.7.1.1 AXPY Operation

AXPY is in the form:

$$y = \alpha x + y, \tag{3.96}$$

with x and y two vectors, and α is a scalar. This operation is used to *update vectors* inside Krylov subspace methods. On distributed memory platforms, it is necessary to assume that the vectors x and y should be distributed in the same manner across all the processor. The distributed AXPY is simple without requiring communication. It can be regarded as several AXPY of local vectors in serial on each processor.

3.7.1.2 Dot product and Global Reduction Operation

The dot product is the operation that use all the components of given vectors to compute a single floating-point scalar. In the Arnoldi reduction process, this scalar is always needed by all processors. Equation (3.97) gives the formula of dot product operation.

$$v \cdot w = \langle v_1, v_2, \cdots, v_n \rangle \cdot \langle w_1, w_2, \cdots, w_n \rangle = v_1 w_1 + v_2 w_2 + \cdots + v_n w_n. \tag{3.97}$$

The distributed version of the dot-product is needed to compute the inner product of two vectors v and w and then distribute the result across all the processors. This type of operations are termed the *All Reduction Operations*, which can be seen as the combination *Reduction Operations* and *Broadcast Operations*. In Krylov subspace methods, the dot-product operation is typically needed to perform the vector update on each processor. If the number of processors is large, this kind of operations can introduce enormous communication costs. The computation of the Euclidean norm of distributed vectors is also a global reduction operation which is similar to the dot-product.

3.7.1.3 Orthogonalization of Vector

In the Arnoldi reduction (as shown by Algorithm 2) for non-Hermitian matrices, the vector Av_i should be orthogonalized against all the previous vectors. In practice, the classic Gram-Schmidt process is preferred than the Modified Gram-Schmidt, even the presence of round-offs

© 2019 Tous droits réservés.

lilliad.univ-lille.fr

Thèse de Xinzhe Wu, Université de Lille, 2019

and cancellations within Classic Gram-Schmit orthogonalization diminish its numerical stability. In Classic Gram-Schmit orthogonalization, the orthogonalization process is overlapped, while the same process of Modified Gram-Schmit orthogonalization has a data dependency, which is not possible to get good parallel performance. A preconditioner or a reorthogonalization process can compensate for the deficiency of numerical stability.

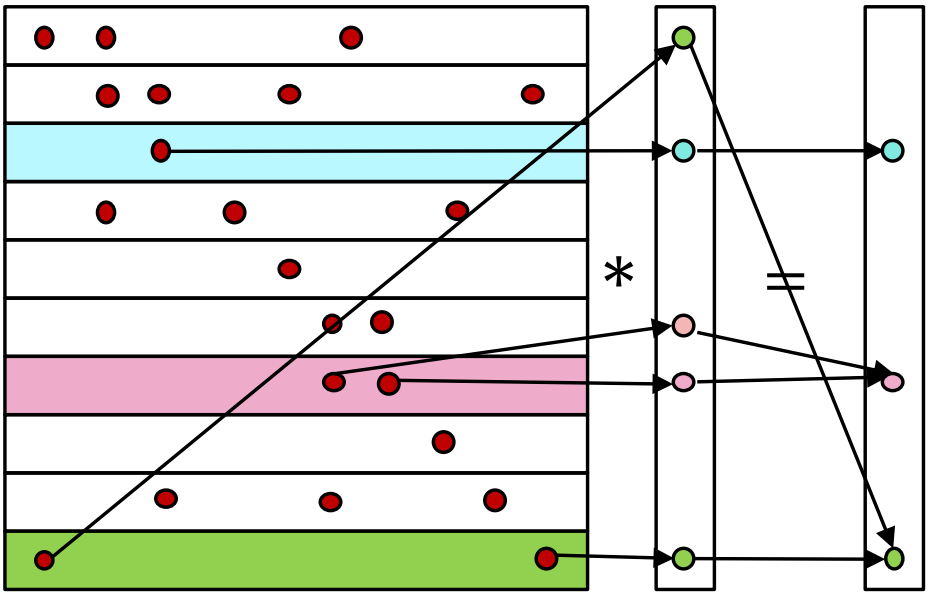

Figure 3.4 – Communication Scheme of SpMV.

3.7.1.4 SpMV Operation

In practice, the parallel version of Arnoldi orthogonalization is memory/communication bounded. The most critical operation with the high communication intensity is the substantial number of matrix-vector multiplications Av_i. The parallel implementation of Krylov iterative methods depends heavily on the data structure to store the matrix. Different distributed sparse matrix format introduces different matrix-vector implementation schemes and finally results in the different parallel performance.

The standard used sparse matrix storage format includes: COO which stores respectively the row index, column index and values into three arrays; CSR which stores respectively the row offset, the column index and data values into three arrays; ELLPACK which stores the column index and values into two two-dimensional arrays according their row index; and DIA which store the diagonal offsets into one-dimensional array, and the values sorted by diagonal into a two-dimensional array.

For the parallel implementation of SpMV on modern parallel systems, the matrix with selected storage format should be distributed across different processors with considering the load balance and reduction of communications. Fig. 3.4 gives the communication scheme of SpMV on distributed memory systems.

© 2019 Tous droits réservés.

lilliad.univ-lille.fr

Thèse de Xinzhe Wu, Université de Lille, 2019

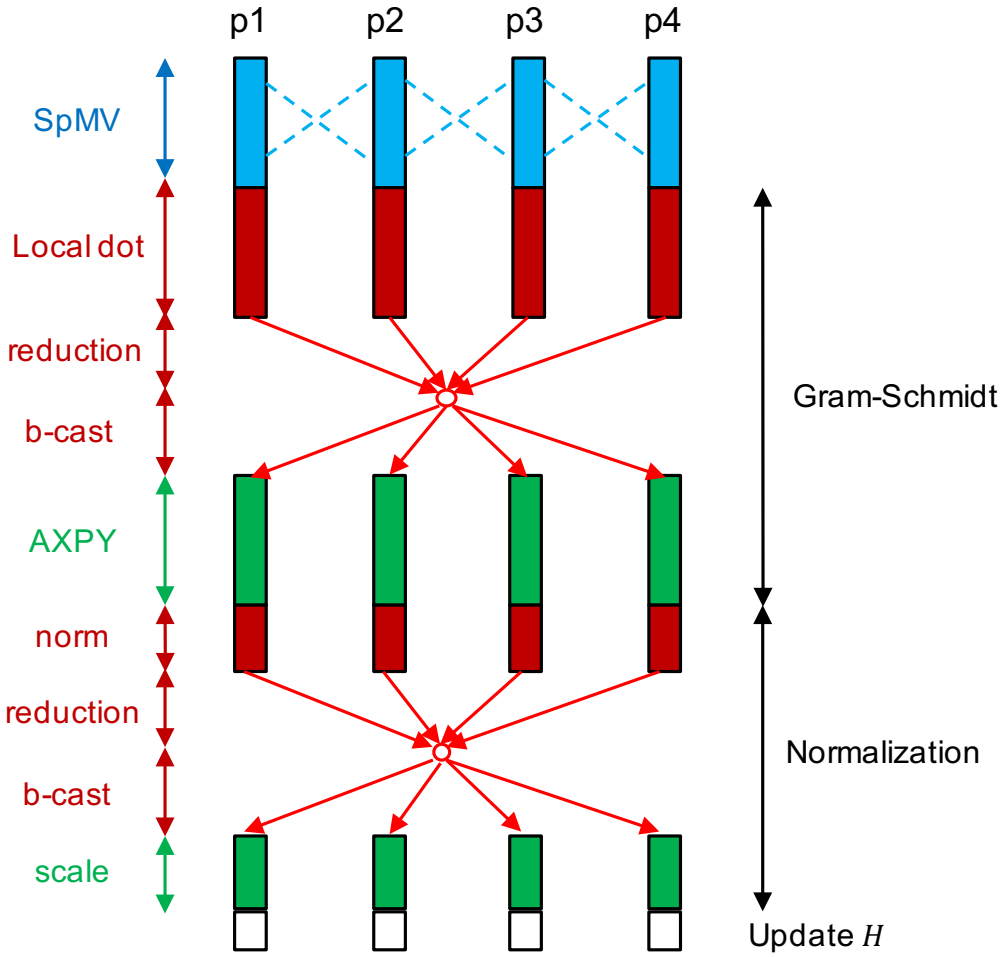

Figure 3.5 – Classic Parallel implementation of Arnoldi reduction.

3.7.2 Parallel Krylov Iterative Methods

Fig. 3.5 describes the parallel implementation of the Arnoldi reduction process inside GMRES. For each loop inside, it can be divided into two parts: the Gram-Schmidt and the normalization processes. The SpMV in Gram-Schmidt process is implemented in parallel with the communication among the processors, and the distributed version of dot-product operation is the combination of *Reduction* and *Broadcast* Operations, which introduce a synchronization point, and the AXPY is implemented in parallel without communications. In the normalization process, the computation of the norm of the distributed vectors also introduce the synchronization points. In the Arnoldi reduction, this loop is executed in sequence for m times to generate an orthonormal basis in the m-dimensional Krylov subspace. For large-scale supercomputers, the SpMV operations involving global communications, and the synchronization points produced by the *Reduction* and *Broadcast* operations become bottleneck.

3.7.3 Parallel Implementation of Preconditioners

On modern parallel computers, the preconditioning techniques should have a high degree of parallelism. The selection of preconditioners should consider not only their intrinsic numerical qualities, but also their ability to explore multi-level parallelism. In this section, we discuss the

© 2019 Tous droits réservés.

lilliad.univ-lille.fr

Thèse de Xinzhe Wu, Université de Lille, 2019

ability of different preconditioners presented in Section 3.5 to explore the parallelism.

3.7.3.1 Natural Parallelizable Preconditioners

Deflation and polynomial preconditioners for iterative methods are intrinsically parallel preconditioners, which means that they are parallelizable because of their mathematical scheme. The deflated and polynomial preconditioners take place after each restart of Krylov iterative methods. Their preconditioning procedure can be divided into two parts:

(1) the *iterative steps*, which are similar to the ones in the Arnoldi reduction, and their kernels are the parallel SpMV and AXPY operations;

(2) the *LAPACK operations* executed in serial redundantly on all computing units, such as the solution of small dimensional Least Squares problem and eigenvalue problems for different preconditioning techniques. The operations are always implemented with the *Allreduction* of MPI standard, which introduces extra synchronization points.

3.7.3.2 Non-Natural Parallelizable Preconditioners

There is a limited amount of parallelism can be extracted from the standard preconditioners such as ILU and SSOR. According to the conventional wisdom, these preconditioners are primarily serial in nature. The row-by-row, upward-looking factorizations for the ILU preconditioner, and the relaxation steps in SSOR preconditioner introduce a large number of task and data dependencies for all entries of matrices, which restrict their parallel performance on modern supercomputing systems. Thus, a number of alternative techniques are developed that are specifically targeted at parallel environments. *Block Jacobi preconditioner* is the simplest approach. The Jacobi method splits the coefficient matrix as $A = L + D + U$, with a diagonal matrix $D = (\{a_{ii}\})$, a lower triangular factor $L = (\{a_{ij}\} : i > j)$, and an upper triangular factor $U = (\{a_{ij}\} : i < j)$. The Block Jacobi method is an extension that gathers the diagonal blocks of A into $D = (D_1, D_2, \cdots, D_N)$, with $D_i \in \mathbb{R}^{m_i \times m_i}$, $i = 1, 2, \cdots, N$, and $n = \sum_{i=1}^{N} m_i$. The remaining elements of A are then partitioned into matrices L and U such that L contains the elements below the diagonal blocks in D, while U contains those above them. The Block Jacobi method is well defined if all diagonal blocks are nonsingular. The resulting preconditioner, $M = D$, is particularly effective if the blocks succeed in reflecting the nonzero structure of the coefficient matrix, which arises from PDEs [9]. Each block can set separately different iterative solvers and preconditioners.

Apart from the Block Jacobi preconditioner, there are also other more complex preconditioners which decompose the entire linear systems into several subdomains. For each local system, they can be solved either by a direct solver or using a standard preconditioned Krylov solver. They are the *Domain-Decomposition-Type preconditioners*, such as *Additive Schwarz preconditioners* [48] and *Schur-complement based preconditioners* [190], etc.

3.7.4 Existing Softwares

Recent years, there are several efforts to provide the parallel Krylov methods on different computing architectures. This section gives a glance at two famous ones of them.

© 2019 Tous droits réservés.

lilliad.univ-lille.fr

Thèse de Xinzhe Wu, Université de Lille, 2019

3.7.4.1 PETSc/SLEPc

PETSc [24], is a suite of data structures and routines developed by Argonne National Laboratory for the scalable (parallel) solution of scientific applications modeled by PDEs. It employs the MPI standard for all message-passing communication. PETSc provides many of the mechanisms needed within parallel application code, such as simple parallel matrix and vector assembly routines that allow the overlap of communication and computation. PETSc provides the parallel implementation of Krylov methods and several preconditioners.

SLEPc [111] is a software library for the parallel computation of eigenvalues and eigenvectors of large, sparse matrices. It can be seen as a module of PETSc that provides solvers for different types of eigenproblems, including linear (standard and generalized) and nonlinear (quadratic, polynomial and general), as well as the SVD. It also uses the MPI standard for parallelization. Both real and complex arithmetics are supported, with single, double and quadruple precision. When using SLEPc, the application programmer can use any of the PETSc's data structures and solvers. Other PETSc features are incorporated into SLEPc as well. The module *EPS* in SLEPc provides Krylov subspace methods such as Krylov-Schur, Arnoldi, and Lanczos to solve sparse eigenvalue problems.

3.7.4.2 Trilinos

Trilinos [113] is a collection of open source software libraries, intended to be used as building blocks for the development of scientific applications. Trilinos was developed at Sandia National Laboratories from a core group of existing algorithms and utilizes the functionality of software interfaces such as the BLAS, LAPACK, and MPI. Trilinos supports many different packages which are defined to implement the iterative linear and eigensolvers methods. There are some packages which are widely used as follows:

- *Kokkos* [81]: Kokkos implements a programming model in C++ for writing performance portable applications targeting all major HPC platforms. Kokkos is designed to target complex node architectures with N-level memory hierarchies and multiple types of execution resources. It currently can use OpenMP, Pthreads, and CUDA as backend programming models.

- *Epetra* [112]: Epetra provides the fundamental construction routines and services function that are required for serial and parallel linear algebra libraries. Epetra provides the underlying foundation for all Trilinos solvers. It implements linear algebra objects including sparse graphs, sparse matrices, and dense vectors.

- *Tpetra* [21]: Tpetra is the next version of Epetra with better support for shared-memory parallelism. Many Trilinos packages and applications are implemented based on Tpetra's linear algebra objects, or depend on Tpetra's parallel data redistribution facilities. Tpetra supports at least two levels of parallelism: MPI for distributed-memory parallelism and any of various shared-memory parallel programming models (OpenMP, Pthreads or Nvidia's CUDA) boosted by Kokkos package within an MPI process. Tpetra has the following unique features:

© 2019 Tous droits réservés.

lilliad.univ-lille.fr

Thèse de Xinzhe Wu, Université de Lille, 2019

  - Native support for representing and solving very large graphs, matrices, and vectors;
  - Matrices and vectors may contain many different kinds of data, such as floating-point types of different precision and complex-valued types;
  - Support for many different shared-memory parallel programming models based on Kokkos.

- *AztecOO* [114]: Preconditioners and Krylov subspace methods (CG, GMRES, etc.), compatible with Epetra only.
- *Belos* [31]: Classical and block Krylov subspace methods, including the implementations of CG, block CG, block GMRES, pseudo-block GMRES, block FGMRES, and GCRO-DR iterations). Belos is compatible with Epetra and Tpetra.
- *Anasazi* [20]: It provides algorithms for the numerical solution of large-scale eigenvalue problems. Anasazi is compatible with Epetra and Tpetra.
- *Komplex* [64]: Complex-valued system solver, Komplex is an add-on module to AztecOO that allows users to solve complex-valued linear systems. Komplex solves a complex-valued linear system by solving an equivalent real-valued system of twice the dimension.

3.8 Toward Extreme Computing, Some Correlated Goals

This section gives the challenges of numerical methods facing the development of HPC platforms. In Section 2.4, we discussed the trend of future exascale supercomputing architectures and the related challenges of parallel programming to develop the applications to profit efficiently from these supercomputers. The main objective for the parallel implementation of numerical methods is to minimize the global computing time. The global computing time of an algorithm can be reduced by either accelerating the convergence or improving its parallel scaling performance with much more computing units. In 2014, the mathematics and algorithms research opportunities which will enable scientific applications to harness the potential of exascale computing are identified by seventy members of the applied mathematics community [74]. In this section, we list more in detail the correlated goals of iterative methods toward the extreme computing:

(1) *Accelerate the convergence*: When solving linear systems by Krylov subspace, the convergence cannot be guaranteed for the ill-conditioned matrix or when the restart strategy is used. Thus, a critical issue for the iterative methods is to propose different kinds of preconditioners which have better speedup on the convergence, and also enough numerical stability. Moreover, facing the upcoming exascale computing, the proposed preconditioners should either with better parallel performance across a large number of cores or be able to promote the asynchronicity and benefit from the more complex architectures of modern supercomputers. In summary, the novel preconditioners should be proposed either to be stronger or with better parallel performance.

(2) *Minimize the number of communications*: When solving huge problems on parallel architectures, the most significant concern becomes the cost per iteration of the method – typically

© 2019 Tous droits réservés.

lilliad.univ-lille.fr

Thèse de Xinzhe Wu, Université de Lille, 2019

because of communication and synchronization overheads. In general, the complexity of algorithms (number of operations performed) is used to express their performance rather than the quantity of data movement and communications. In fact, on the exascale computers, the global communications across millions of cores are very expensive, and the computing operations inside each core will be nearly free. To address the critical issue of communication costs, researchers need to investigate algorithms that minimize communication. For the Arnoldi reduction process inside Krylov iterative methods such as GMRES, CG, and Lanczos, the operations of loop inside introduce much more global communications.

When matrix A in Krylov subspace methods is very sparse, the SpMV invokes even more communications. Hence, strategies for reducing communication overheads in Arnoldi orthogonalization have been proposed to address this bottleneck. In order to reduce the global communication of SpMV for sparse matrices, the first approach is to select the best sparse matrix storage format, which can produces less communications (e.g. [147, 136, 203, 144, 32, 33, 127, 15]). Another approach is to use the Hypergraph Partitioning Models to optimize the SpMV scheme on parallel computers, e.g., in 1999, Catalyurek et al. proposed two computational hypergraph models which avoid this crucial deficiency of the graph model for SpMV [51]; Vastenhouw et al. tried to reduce the communication volume of SpMV through a recursive bi-partitioning of the sparse matrix [213]; Chen et al. proposed a communication optimization scheme based on the hypergraph for basis computation of Krylov subspace methods on multi-GPUs [54]; a Locality-aware parallel sparse matrix-vector and matrix-transpose-vector multiplication on many-core processors is introduced by Karsavuran et al. [120]; and spatiotemporal graph and hypergraph partitioning models for SpMV on many-core architectures is presented by Abubaker et al. with better scaling performance through enhancing data locality in the operations [2], etc.

(3) *Promote the asynchronicity and reduce the synchronization points*: One algorithm often must do the synchronize operations during the computation. The global data synchronization across a number of cores in the distributed memory systems is expensive especially for a hybrid platform with accelerators. Inside Krylov subspace methods, the dot product is a good example which needs the global synchronization. For the extreme-scale platforms, synchronizations become bottlenecks. Hence, the algorithm should be designed with as few synchronization points as possible.

Attempts have been made to restructure existing algorithms for the exascale computing so that the number of synchronizations is reduced. Communication-avoiding and pipelined variants of Krylov solvers are critical for the scalability of linear system solvers on future exascale architectures. Firstly, the impact of global communication latency at extreme scales on Krylov methods are analyzed by Ashby et al. [16]. The strategy of hiding global synchronization latency in GMRES and the preconditioned CG was presented by Ghysels [101, 100]; Fujino et al. evaluated performance of parallel computing of revised BiCGSafe and BiCGStar-plus method, and made clear that the revised single synchronized BiCGSafe method outperforms other methods from the viewpoints of elapsed time and speed up on parallel computer with distributed memory [96]; Rupp et al. implemented pipelined

© 2019 Tous droits réservés.

lilliad.univ-lille.fr

Thèse de Xinzhe Wu, Université de Lille, 2019

iterative solvers with kernel fusion for GPUs [180]; Sanan et al. presented variants of CG, CR, GMRES which both pipelined and flexible [192]; Yamazaki et al. proposed to improve the performance of GMRES by reducing communication and pipelining global collectives [228]; Swirydowicz et al. presented low synchronization variants of iterated Classic Gram-Schmit orthogonalization and Modified Gram-Schmit orthogonalization algorithms that require one and two global reduction communication steps; the reduction operations are overlapped with computations and pipelined to optimize performance [206], etc. Moreover, an essential consideration for the restructuring an algorithm to reduce synchronization and communication is their numerical stability.

(4) *Mixed arithmetic*: In order to develop numerical methods for the exascale computing, it is important to identify and exploit the existence of mixed precision mathematics. Low-precision floating-point operation is a powerful tool for accelerating scientific computing applications, especially artificial intelligence. In fact, 32-bit operations can achieve at least twice the acceleration of 64-bit operational performance on the modern computing architectures. In addition, through the combination of 32-bit and 64-bit floating-point operations, the performance of many linear algebra algorithms can be significantly enhanced by 32-bit precision operations while maintaining the 64-bit precision of the final solution. The mixed arithmetic can be applied to different computing architectures, including traditional CPUs and accelerators such as GPUs. The creation of a mixed-precision algorithms allow for more efficient use of heterogeneous hardware. Minor modifications to existing code can provide significant acceleration by considering existing hardware attributes.

In 2014, Kouya et al. [126], evaluate the performance of Krylov subspace methods by using highly efficient multiple precision SpMV. They show that SpMV implemented in these functions can be more efficient. Yamazaki et al. [227] present a mixed-precision Cholesky factorization, which has 1.4× speedup over the standard approach on GPU. In 2018, Haidar et al. [108] investigate how HPC applications can be accelerated by the mixed arithmetic technique. In detail, they developed the architecture-specific algorithms and highly tuned implementations of a solver based on mixed-precision (FP16-FP64) iterative refinement for the general linear system, $Ax = b$, where A is a large dense matrix, and a double precision (FP64) solution is needed for accuracy. Their paper show how using half-precision Tensor Cores (FP16-TC) for the arithmetic can provide up to 4× speedup. Maynard et al. [143] present a mixed-precision implementation of Krylov solver for the numerical weather prediction and climate modeling, the beneficial effect on run-time and the impact on solver convergence. The complex interplay of errors arising from accumulated round-off in floating-point arithmetic and other numerical effects is discussed. They employ now the mixed-precision solver in the operational forecast to satisfy run-time constraints without compromising the accuracy of the solution.

(5) *Minimize energy consumption*: The generated heat also affects the performance of supercomputers such as the arising failure rate of hardware, and the energy consumption also becomes a tremendous financial burden for supercomputer centers, because it takes up a large portion in the total cost. That is the *Power wall*, another roadblock to approach

© 2019 Tous droits réservés.

lilliad.univ-lille.fr

Thèse de Xinzhe Wu, Université de Lille, 2019

the exascale computing. In recent years, the HPC community has begun to address this issue, and it is necessary to establish numerical methods and libraries for energy awareness, control and efficiency.

In 2013, an analysis of energy-optimized lattice-Boltzmann CFD simulations from the chip to the highly parallel level was introduced by Wittmann et al. [222]. Padoin et al. [165] evaluated the application performance and energy consumption on hybrid CPU/GPU architecture. In 2015, Anzt et al. [8] unveil some energy efficiency and performance frontiers for sparse computations on GPU-based supercomputers. Aliaga et al. [5] unveil the performance-energy trade-off in iterative linear system solvers for multithreaded processors. In order to gain insights about the benefits of hands-on optimizations, they analyze the runtime and energy efficiency results for both out-of-the-box usage relying exclusively on compiler optimizations, and implementations manually optimized for target architectures, that range from CPUs and DSPs to manycore GPUs.

(6) *Multi-level Parallelism*: The increase of heterogeneity of modern supercomputers introduces the multi-level parallelism of memory and communication. The implementation of numerical iterative methods should be considered to adapt to the multi-level parallelism. The multi-level parallelism includes the distributed memory level parallelism across the platforms, the shared memory level parallelism inside the thread or accelerator and the vectorization level parallelism.

(7) *Load balance*: For the exascale computing with millions of cores and accelerators, even naturally load-balanced algorithms on homogeneous hardware will present many of the same load-balancing problems. Dynamic scheduling based on DAGs has been identified as a path forward, but this approach will require new approaches to optimize for resource utilization without compromising spatial locality. The DAGs runtime environments such as StarPU, OmpSs are good candidatures for the fine-grained parallelism. The workflow runtime environment such as YML can be used for the coarse-grained parallelism.

(8) *Auto-tuning*: Current supercomputer have complex architectures, with millions of cores utilizing non-uniform memory access and hierarchical cases. The introduction of GPUs and other accelerators increases the heterogeneity of computers. Such adaptation must deal with the complexity of discovering and applying the best algorithm for diverse and rapidly evolving architectures. Thus, tuning the performance of softwares becomes difficult. Moreover, the science and industrial applications on the supercomputing systems tend to be more and more complex. It is necessary to propose strategies and methodologies to auto-tune them for achieving the best performance. Auto-tuning refers to the automatic generation of a search space of possible implementations of a computation that are evaluated through machine learning based models or empirical measurement to identify the most desirable implementation [22]. In general, the code variant in the libraries, the hardware and the parameters of algorithms are all necessary to be auto-tuned. The main goal of auto-tuning for the iterative methods is the minimization of the execution time of applications. The combination of different auto-tuning schemes might optimize the parallel performance, the energy efficiency and reliability of applications. Besides, auto-tuning

© 2019 Tous droits réservés.

lilliad.univ-lille.fr

Thèse de Xinzhe Wu, Université de Lille, 2019

has to be extended for the optimization of data layout (e.g., storage formats for sparse matrices, hypergraph strategies for SpMV kernels). Aquilanti et al. [12] present a general parallel auto-tuned linear solver approach based on the tuning of the Arnoldi incomplete orthogonalization process within GMRES by monitoring the convergence in order to reduce the time of computation needed for a solver to attain a solution. Katagiri et al. [121] presented a smart tuning strategy for restart frequency of GMRES with hierarchical cache sizes.

(9) *Fault tolerance, resilience*: Exascale computing poses the challenges for assessing and ensuring the correctness of numerical simulation results. Adaptability to failure has been identified as a key requirement for future HPC systems. The emergence of the exascale platforms is predicted to increase the error rate. The iterative approach is an important core of many simulations. These simulations can take days, weeks, or even months to complete, which increases the exposure of the calculation to the failure. The frequency of both hard and soft faults tends to be much higher. Uncorrected soft faults can damage the solution to the calculation. Hard faults require dynamic processing, which will be prohibitively expensive at the exascale. Dynamically recovering from either type of fault will introduce nondeterministic variability in resource usage. The checkpointing mechanism should be implemented for the iterative methods to improve the resilience to the faults. Fault management will require developments in hardware, programming environments, runtime systems, and programming models. The research will be required to devise efficient application-level fault-tolerance mechanisms and new procedures to verify code correctness at scale.

The work of this dissertation tries to propose a potential smart multi-level parallel programming with auto-tuning scheme for solving linear systems which address on the goals of accelerating the convergence, minimizing the number of communications, promoting the asynchronisity, reducing the synchronize points and fault tolerance.

© 2019 Tous droits réservés.

lilliad.univ-lille.fr

Chapter 4

Sparse Matrix Generator with Given Spectra

In Chapter 3, we have discussed the convergence of iterative methods and their relation to the spectral distribution of linear systems. Indeed, algorithms and applications from diverse fields can be formulated as eigenvalue problems. The eigenvalues are also extremely important for the analysis of preconditioners to solve linear systems. In machine learning, pattern recognition and AI, it is often demanded to solve the eigenvalue problems for both supervised and unsupervised learning algorithms, such as PCA [61], FDA [36], and clustering [89], etc. Insufficient precision and failure of the eigenvalue and linear solvers typically result in poor approximation of the original discrete problem and failure of the entire algorithm, respectively. A good selection of solvers becomes especially essential. Thus it is crucial to have the test matrices to benchmark the numerical performance and parallel efficiency of different methods. In this chapter, we present SMG2S, including its parallel implementation and optimization for both CPU and GPU clusters, the verification mechanism, and the release of open source package.

4.1 Demand of Large Matrices with Given Spectrum

As described in Chapter 3, the size of eigenvalue problems and the supercomputer systems continue to scale up. The entire ecosystem of HPC, especially linear system applications, should be adjusted to these large clusters. In this context, there are four special requirements for the test matrices to evaluate numerical algorithms on extreme-scale platforms:

(1) their spectra must be known and customizable;

(2) they should be both sparse, non-Hermitian and non-trivial;

(3) they could have a very high dimension, including the non-zero element numbers and/or the matrix dimension, to evaluate the numerical algorithms on large-scale systems, which means that the proposed matrix generator should be able to be parallelized to profit from the large distributed memory supercomputers.

© 2019 Tous droits réservés.

lilliad.univ-lille.fr

Thèse de Xinzhe Wu, Université de Lille, 2019

(4) their sparsity patterns should be controllable.

In order to provide numerically robust solvers of eigenvalue or linear system problems, the researchers need the matrices whose spectra are known, which help to analyze the numerical accuracy. Some scientific communities may be interested in matrices with clustered, conjugated eigenvalues, and the closest eigenvalues in random distribution or contained in a specified interval. It is significant to develop a suite of large non-Hermitian test matrices whose eigenvalues can be given.

The properties of being sparse, non-Hermitian and non-trivial together can add many mathematical features to simulate real-world matrices. Besides, the test matrices should be of very high size for experiments on large scale platforms. Furthermore, since the large matrices are generated in parallel, their different slices are already distributed on separate computing units, which can be used directly to evaluate the required linear and eigenvalue solvers, without having to consider loading large matrix files from the file systems. It can save time and improve the efficiency for applications.

In this chapter, we introduce SMG2S (Scalable Matrix Generator with Given Spectra) for testing the linear and eigenvalue solvers on large-scale platforms. In Section 4.2, we introduce the related work of proposing test matrix collections. In Section 4.3, we present the proof of mathematical models of SMG2S to generate matrices with given spectra. In Section 4.4, the numerical algorithm and practical implementation of SMG2S are given. In section 4.5, firstly, we provide an initial implementation of SMG2S based on PETSc for homogenous platforms and PETSc+CUDA for heterogeneous machines with multi-GPU. Then an open source package with specific communication optimization based on MPI and C++ is available. In Section 4.6, the evaluations of its scalability and the accuracy to keep the given spectra are presented on different supercomputing platforms. We propose to verify the capacity of the generated matrix to keep the given spectra based on the Shifted Inverse Power Method in Section 4.7, and the accuracy verification for various spectral distributions is also presented in this section. In Section 4.8, we introduce the SMG2S package as a released software, including interfaces to different programming languages and scientific computational libraries, and GUI for verification. Finally examples which evaluate the Krylov solvers using SMG2S are given in Section 4.9.

4.2 The Existing Collections

It is rare, but there are already several efforts to supply test matrix collections for linear problems.

4.2.1 Test Matrix Providers

SPARSEKIT [181] implemented by Saad contains a variety of simple matrix generation subroutines. Z. Bai et al. [19] presented a collection of test matrices for the development of numerical algorithms to solve nonsymmetric eigenvalue problems. There are also three widely spread matrix providers, the Hawell Boeing sparse matrix collection [77], the Tim Davis collection [63] and Matrix Market [40]. They all contain many matrices with various mathematical properties coming from different scientific fields. However, the spectra of matrices in these collections are fixed, and that cannot be whatever we want. A test matrix generation suite with given spectra

© 2019 Tous droits réservés.

lilliad.univ-lille.fr

Thèse de Xinzhe Wu, Université de Lille, 2019

was already introduced by Demmel et al. [73] in 1989 for the benchmark of LAPACK. They proposed a method of transferring a diagonal matrix with a given spectrum into a dense matrix with the same spectrum using an orthogonal matrix, and then reducing them to an asymmetric band by Householder transformation. This method requires $\mathcal{O}(n^3)$ time and $\mathcal{O}(n^2)$ storage even for generating a small bandwidth matrix. Moreover, this method was implemented for the shared memory systems, rather than for larger distributed memory systems. Therefore, it is difficult to generate large-scale test matrices that are customized for testing on extremely large scale clusters. As far as we know, this matrix generation suite is the only example which was implemented in parallel for generating test matrices with given spectra. This is our motivation for SMG2S, which can generate large-scale non-Hermitian matrices with a given spectrum on modern parallel platforms with less time and storage, and can be easily implemented in distributed memory systems.

4.2.2 Matrix Generators in LAPACK

In LAPACK, a suite of test matrix generation software is implementation, which generates random matrices with various controlled properties. The three mains routines are called xLATMR, xLATMS and xLATME.

4.2.2.1 xLATMR, xLATMS and xLATME

xLATMR [73] generates a random matrix with off-diagonal entries. It is the simplest and fastest routines in this suite, and permits no direct control over the eigenvalues of the generated matrices, the properties of xLATMR are given as:

- Elements of A formed from one of three distributions
- Symmetric or nonsymmetric.
- Optionally graded (by row and/or column), banded, "sparsified".
- Bandwidth optionally reduced to a specified value.

xLATMS [73] generates random real symmetric and complex Hermitian matrices with given eigenvalues and bandwidth, or a random nonsymmetric or complex symmetric matrix with given singular values and upper and lower bandwidth.

- Matrix of singular values specified by the user or chosen from one of six different distributions.
- A is formed as UDV^T, where V is random orthogonal.
- Bandwidth optionally reduced to a specified value by further unitary transformations (possibly combined with the previous step).

xLATME [73] generates a random nonsymmetric square matrix with specified eigenvalues. For example, xLATME is able to generate random Hessenberg matrices with given eigenvalues

© 2019 Tous droits réservés.

lilliad.univ-lille.fr

Thèse de Xinzhe Wu, Université de Lille, 2019

and sensitivities, and this is useful for testing QR factorization algorithms for nonsymmetric eigenproblems. xLATME is able to generate the dense matrix with prescribed eigenvalues, and this matrix can be reduced into band with user-defined upper and lower bandwidth by a series of Householder transformation operations.

- Matrix of singular values specified by the user or chosen from one of seven different distributions:

  (1) Input by users;

  (2) $D(1) = 1$ and the other $D(i) = \frac{1}{COND}$, where $COND$ is the condition number specified by the users;

  (3) $D(n) = \frac{1}{COND}$ and the other $D(i) = 1$;

  (4) The $D(i)$ form a geometric sequence from 1 to $\frac{1}{COND}$;

  (5) The $D(i)$ form a arithmetic sequence from 1 to $\frac{1}{COND}$;

  (6) The $D(i)$ are random in the range $[\frac{1}{COND}, 1]$ with uniformly distributed logarithms;

  (7) The $D(i)$ are random with the same distribution as the other matrix entries;

  Additionally, each $D(i)$ may optionally be multiplied by a random number with absolute value 1.

- A is formed as $USVDV'S^{-1}VU'$, where (V, V') and (U, U') are two pairs of randomly generated unitary matrices. Here A is generated as a dense matrix with given spectra.

- Bandwidth optionally reduced to a specified value by further Householder transformations.

4.2.2.2 Procedure of xLATME

The implementation of xLATME in LAPACK is given as Algorithm 18. The procedure of generation matrix by xLATME can be given as follows:

(1) Specify the diagonal of A by $D = diag(\lambda_i)$, and the entries of D can be computed by one of the provided modes;

(2) The upper triangle of A is filled with random numbers;

(3) Generate randomly the unitary matrix pairs (V, V') and (U, U');

(4) Generate a singular matrix S by one of the provided modes. Thus S is a random dense nonsymmetric matrix whose singular values may be chosen with the same options as D;

(5) pre-multiply and post-multiply the unitary matrices and singular matrix on A, thus $A = USVDV'S^{-1}VU'$. A is a dense matrix generated with a given spectrum;

(6) If the user so specifies, either the upper or lower bandwidth (but not both) is reduced to any positive value desired;

(7) Scale A, if desired, to have a given maximum absolute entry.

© 2019 Tous droits réservés.

lilliad.univ-lille.fr

Thèse de Xinzhe Wu, Université de Lille, 2019

Algorithm 18 xLATME Implementation in LAPACK

1: Generate a complex array D by a selected mode containing n eigenvalues
2: Setup the diagonal of A by D
3: Setup the upper triangle of A to random numbers
4: Generate a real array S by a selected mode containing n singular values
5: Generate random n-dimensional unitary matrix V and V', with $VV' = I$
6: Compute $A = VAV'$
7: Compute $A = SAS^{-1}$
8: Generate random n-dimensional unitary matrix U and U', with $UU' = I$
9: Compute $A = UAU'$, then A is a dense matrix containing given eigenvalues
10: **for** $i = lbandwidth + 1, \cdots, n-1$ **do**
11: Householder transformation to reduce the column of number $n + lbandwidth - i$ in A
12: **end for**
13: **for** $j = ubandwidth + 1, \cdots, n-1$ **do**
14: Householder transformation to reduce the row of number $n + ubandwidth - j$ in A
15: **end for**

In practice, xLATME is implemented with the subroutines provided by LAPACK. Thus only the dense matrix storage format is supported. xLATME uses $n^2 + \mathcal{O}(n)$ space and $\mathcal{O}(n^3)$ time even for generating a very small bandwidth matrix. xLATME cannot fufill our requirements. The reasons are not only its existing parallel implementation on shared memory architectures but also the difficulty to implement its mathematical scheme with good scaling performance on modern supercomputers. In next section, we will propose a technique to generate test matrices in parallel with given spectra which requires less time and operations. A mechanism to verify the capacity of the generated matrices to keep the given spectra is also proposed in this chapter.

4.3 Mathematical Framework of SMG2S

In this section, we summarize this theorem and related proof based on preliminary theoretical research of Gachlier et al. [98], and the initial introduction of this theorem can also be found in the dissertation of Boillod-Cerneux [37].

Theorem 4.3.1. *Let's consider the matrix $A \in \mathbb{C}^{n\times n}$, $M_0 \in \mathbb{C}^{n\times n}$, $n \in \mathbb{N}^*$. If M verifies:*

$$\begin{cases} \dfrac{dM(t)}{dt} = AM(t) - M(t)A, \\ M(t=0) = M_0. \end{cases}$$

Then the matrices $M(t)$ and M_0 are similar, $\forall A \in \mathbb{C}^{n\times n}$.

Proof. Denote respectively $\sigma(M_0)$ and $\sigma(M_t)$ the spectra of M_0 and M_t. If M_0 is a diagonalisable matrix, $\forall \lambda \in \sigma(M_0)$, it exists an eigenvector $v \neq 0$ satisfies the relation:

$$M_0 v = \lambda v. \tag{4.1}$$

Denote $v(t)$ by the matrix $B \in I_n$:

$$v(t) = B_t v = e^{tA} B v. \tag{4.2}$$

© 2019 Tous droits réservés.

lilliad.univ-lille.fr

Thèse de Xinzhe Wu, Université de Lille, 2019

We can get:

$$\begin{aligned}\frac{d(M_t v(t) - \lambda v(t))}{dt} &= \frac{dM_t}{dt}v(t) + M_t\frac{dv(t)}{dt} - \lambda\frac{dv(t)}{dt} \\ &= A(M_t v(t) - \lambda v(t)) + \lambda A v(t) \\ &- M_t A v(t) + M_t\frac{dB_t}{dt}v - \lambda\frac{dB_t}{dt}v.\end{aligned} \tag{4.3}$$

With the definition of B_t in Equation (4.2), we have:

$$\frac{dB_t}{dt} = AB_t. \tag{4.4}$$

Thus the Equation (4.3) can be simplified as

$$\frac{d(M_t v(t) - \lambda v(t))}{dt} = A(M_t v(t) - \lambda v(t)). \tag{4.5}$$

The initial condition for the Equation (4.5) is:

$$\begin{aligned}M_t v(t) - \lambda v(t)|_{t=0} &= M_0 B v - \lambda B v \\ &= M_0 v - \lambda v \\ &= 0.\end{aligned} \tag{4.6}$$

Hence the solution of the differential Equation (4.5) is 0 and $\forall\lambda \in \sigma(M_0)$, we have $\lambda \in \sigma(M_t)$. Since $dim(M_0) = dim(M_t)$, we have $\sigma(M_0) = \sigma(M_t)$. Thus, M_0 and M_t are similiar with same eigenvalues, but different eigenvectors.

□

4.4 Numerical Algorithm of SMG2S

Based on the previous mathematical work by Gachlier at al., a matrix M_0 with given spectra can be transferred to another one $M(t)$ that verifies *Theorem* 4.3.1 and keeps the spectra of M_0. We propose a matrix generation method by selecting many parameters including the matrices A and M_0.

4.4.1 Matrix Generation Method

The idea is to impose the desired spectra to M_0 and obtain a M_t matrix that verifies the Theorem 4.3.1 and our hypothesis. The M_t spectrum is the same as M_0, however we recall that the M_t eigenvectors are not the same as M_0. The idea may seem very simple, but many parameters need to be determined to achieve our objective.

Firstly, we define the linear operator $\widetilde{A_A}$ such that:

$$\begin{cases}\widetilde{A_A} : M_{n\times n} \to M_{n\times n}, \\ \qquad M \to AM - MA.\end{cases} \tag{4.7}$$

At the present time, we did not imposed any conditions on the matrix A. The $\widetilde{A_A}$ operator verifies that:

© 2019 Tous droits réservés.

lilliad.univ-lille.fr

Thèse de Xinzhe Wu, Université de Lille, 2019

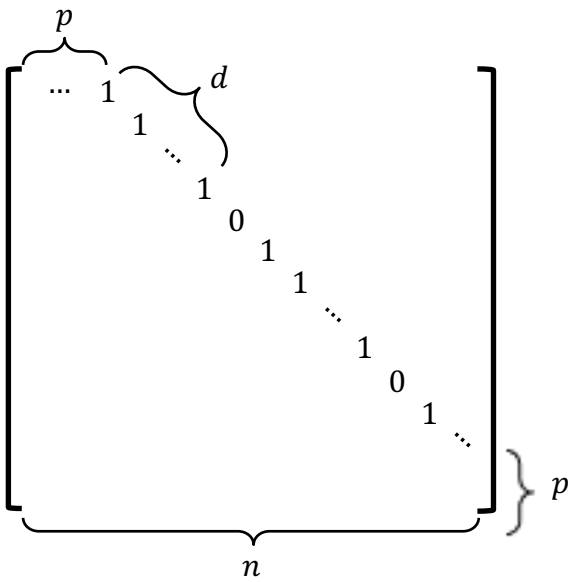

Figure 4.1 – Nilpotent Matrix. p off-diagonal offset, d number of continuous 1, and n matrix dimension.

$$\widetilde{A_A}(I_d) = 0, \forall A \in M_{n\times n}. \tag{4.8}$$

Based on the Theorem 4.3.1 and the linear operator $\widetilde{A_A}$ definition, we can rewrite the ordinary differential equation such that:

$$\begin{cases} \dfrac{dM(t)}{dt} = \widetilde{A_A}(M(t)), \\ M(t=0) = M_0. \end{cases} \tag{4.9}$$

We apply the exponential operator (which is possible as $\widetilde{A_A}$ has no time dependency) to Equation (4.9). This leads to the fact that the solution of Equation (4.9), can be expressed as follows:

$$\begin{cases} M_t = e^{(\widetilde{A_A}t)}M_0, \\ M_t = \sum\limits_{k=0}^{\infty} \dfrac{t^k}{k!}(\widetilde{A_A})^k M_0. \end{cases} \tag{4.10}$$

The k-times power operation of $\widetilde{A_A}(M_0)$ can be given as

$$(\widetilde{A_A})^k(M_0) = \sum_{m=0}^{k} (-1)^m C_k^m A^{k-m} M_0 A^m. \tag{4.11}$$

With the loop

$$M_{i+1} = M_i + \frac{1}{i!}(\widetilde{A_A})^i(M_0), i \in (0, +\infty), \tag{4.12}$$

a very simple initial matrix $M_0 \in \mathbb{C}^{n\times n}$ can be converted into a new sparse, non-trivial and non-Hermitian matrix $M_{+\infty} \in \mathbb{C}^{n\times n}$, which has the same spectra but different eigenvectors with M_0.

© 2019 Tous droits réservés.

lilliad.univ-lille.fr

Thèse de Xinzhe Wu, Université de Lille, 2019

However, it is unreasonable to generate a matrix through an infinite number of iterations. Therefore, a good selection matrix A which can make $\widetilde{(A_A)}^i$ tend to $\mathbf{0}$ in limited steps is very necessary. We define the matrix A as the formula $A = Q^{-1}PQ$ with $Q \in \mathbb{R}^{n\times n}$ and $P \in \mathbb{N}^{n\times n}$. Besides, P is set to be a nilpotent matrix, which means that there is an integer k such that: $P^i = 0$ for all $i \geq k$. Such k is called the nilpotency of P. In this chapter, we set the matrix Q to be the identity matrix $I \in \mathbb{N}^{n\times n}$ for simplification. Thus A is also a nilpotent matrix. The selection of a nilpotent matrix will affect the sparsity pattern of the upper band of the generated matrix.

The exact shape of A is given in Fig. 4.1. Inside an $n \times n$ matrix A, its entries default to 0, except in except for the upper diagonal of the distance p from the diagonal. In this diagonal, its entries begin with d continuous 1 and a 0, this pattern is repeated until the end. Matrix A should be nilpotent with good choices of the parameters p, d and n. The determination of this series of matrices to be nilpotent or not might be difficult, but the cases that $p = 1$ or $p = 2$ are straightforward, which can completely fulfill our demands.

If $p = 1$, with $d \in \mathbb{N}^*$, or $p = 2$ with $d \in \mathbb{N}^*$ to be even, the nilpotency of A and the upper band's bandwidth of generated matrix are respectively $d+1$ and $2pd$. Obviously, there is another constraint that the matrix size n should be greater or equal to the upper band's width $2pd$. For $p = 2$, if d is odd, the matrix A will not be nilpotent, thus we do not take it into account.

4.4.2 Numerical Algorithm

As shown in Algorithm 19, the procedure of SMG2S is simple. Firstly, it reads an array $Spec_{in} \in \mathbb{C}^n$, as the given eigenvalues. Then it inserts the elements in h lower diagonals of the initial matrix M_0 according to the parameters p and d, and sets its diagonal to be $Spec_{in}$, and scales it with $(2d)!$. Meanwhile, it generates a nilpotent matrix A with the parameters d, p and n. The final matrix M_t can be generated as $M_t = \frac{1}{(2d)!}M_{2d}$, where M_{2d} is the result after $2d$ times of loop $M_{i+1} = M_i + (\prod_{k=i+1}^{2d} k)(\widetilde{A_A})^i(M_0)$. The slight modification of the loop formula is to reduce the potential rounding errors coming from numerous division operations on modern computer systems.

Algorithm 19 Matrix Generation Method

1: **function** MATGEN(*input*:$Spec_{in} \in \mathbb{C}^n$, h, d, *output*: $M_t \in \mathbb{C}^{n\times n}$)
2: Insert the entries in h lower diagonals of $M_o \in \mathbb{N}^{n\times n}$
3: Insert $Spec_{in}$ on the diagonal of M_0
4: $M_0 = (2d)!M_0$
5: Generate nilpotent matrix $A \in \mathbb{C}^{n\times n}$ with selected parameters d, p and n
6: **for** $i = 0, \cdots, 2d-1$ **do**
7: $M_{i+1} = M_i + (\prod_{k=i+1}^{2d} k)(\widetilde{A_A})^i(M_0)$
8: **end for**
9: $M_t = \frac{1}{(2d)!}M_{2d}$
10: **end function**

For M_t, if M_0 is a lower triangular matrix having h non zero diagonals, it will be a band diagonal matrix, whose number of new diagonals in the upper triangular zone will be at most $2pd-1$. Thus the maximal number of the bandwidth of matrix M_t is: $width = h+2pd-1$, as in

© 2019 Tous droits réservés.

lilliad.univ-lille.fr

Thèse de Xinzhe Wu, Université de Lille, 2019

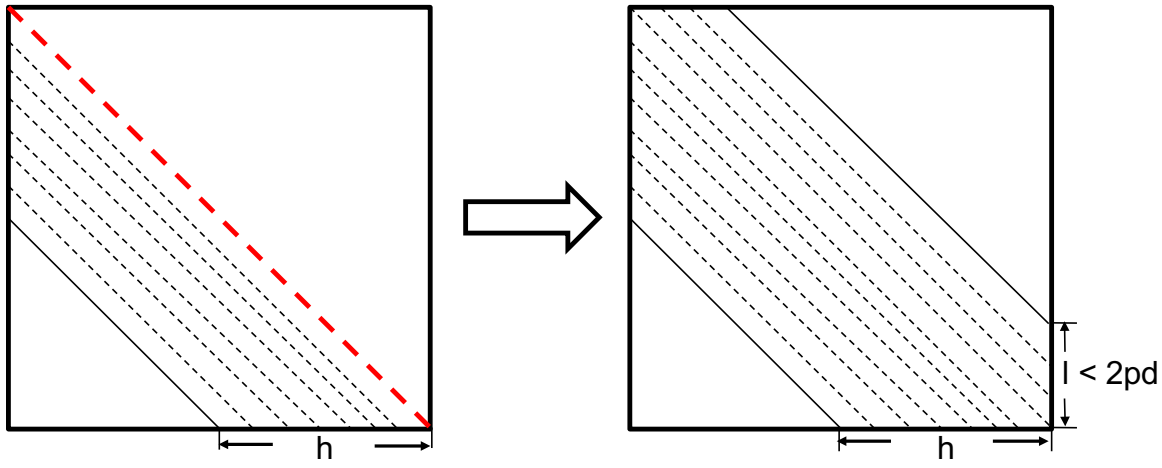

Figure 4.2 – Matrix Generation. The left is the initial matrix M_0 with given spectrum on the diagonal, and the h lower diagonals with random values; the right is the generated matrix M_t with nilpotency matrix determined by the parameters d and p.

Fig. 4.2. In general, researchers use these matrices to test the iterative methods for sparse linear systems. The h lower diagonals of the initial matrix can set to be sparse, which ensures the sparsity of the final generated matrix, as shown in Fig. 4.3. Moreover, the permutation matrix can also be applied to change the sparsity of the generated matrix further.

The operations complexity C of Algorithm 19 is given as:

$$C \approx 2(2d^2 + (4h-2)d - (h+5))n - h(h+1)(h+4d-4). \tag{4.13}$$

In Equation (4.13), the complexity of SMG2S is $\max(\mathcal{O}(hdn), \mathcal{O}(d^2n))$. The worst case would be an $\mathcal{O}(n^3)$ problem for operations with large d and h, and it would require $\mathcal{O}(n^2)$ memory storage. But if we want to generate a band matrix with small bandwidth which means $d \ll n$ and $h \ll n$, it turns to be a $\mathcal{O}(n)$ problem with good potential scalability and to consume $\mathcal{O}(n)$ memory storage. Table 4.1 gives the comparison of memory and operation requirement between SMG2S and xLATME in LAPACK for generating a large-scale matrix with a very small bandwidth.

Table 4.1 – Comparison of memory and operation requirement between SMG2S and xLATME in LAPACK for generating a large-scale matrix with a very small bandwidth.

Methods	Memory Requirment	Operation Requirement
SMG2S	$\mathcal{O}(n)$	$\mathcal{O}(n)$
xLATME	$\mathcal{O}(n^2)$	$\mathcal{O}(n^3)$

4.5 Our Parallel Impementation

In this section, we will introduce parallel implementations of SMG2S on homogeneous and heterogeneous supercomputing platforms. The first prototype of this method introduced by Hervé

© 2019 Tous droits réservés.

lilliad.univ-lille.fr

Thèse de Xinzhe Wu, Université de Lille, 2019

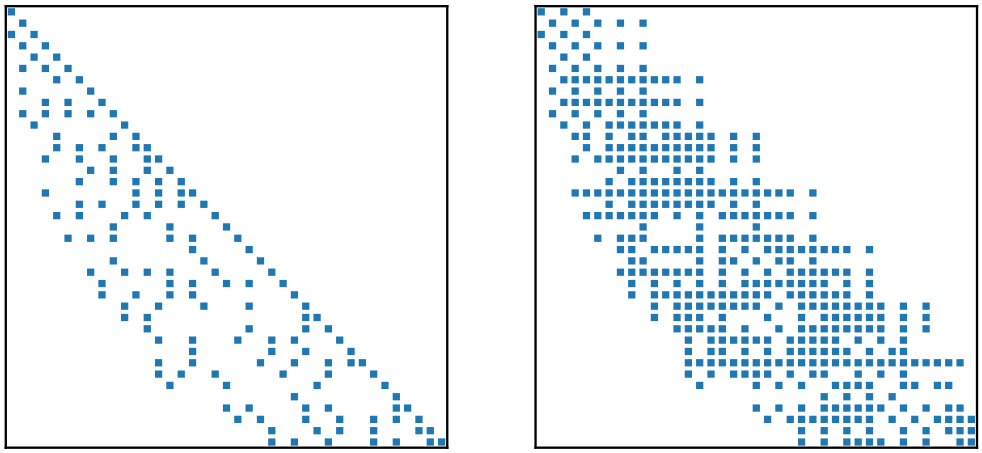

Figure 4.3 – Matrix generation pattern example. The initial and generated matrices have same spectrum.

Galicher to generate a non-Hermitian matrices with given eigenvalues was developed by Boillod-Cerneux during her PhD thesis [37]. She implemented initially this method based on PETSc for multi-CPU systems. It was part of a French-Japanese project FP3C [7] supported by the French ANR and the Japanese JST. She proposed also to evaluate the spectrum conservation accuracy by computing a small subset of the dominant eigenvalues using Arnoldi and Krylov-Schur eigensolvers provided by SLEPc. Based on previous research, we would like implement this matrix generator as a complete and standard software with better parallel performance which is able to be accessed and reused by all the researchers in the fields of numerical algorithms. We implemented PETSc-based SMG2S on the CPUs and then another version for multi-GPUs based on MPI, CUDA and PETSc. We chose PETSc for the initial implementation because it provides the basic operations optimized for different computer architectures. An open source parallel software with specific optimized communication is also implemented based on MPI and C++, which can generate the test matrices with less time. The accuracy verification for all the given eigenvalues based on Shift Inverse Power method will be introduced in Section 4.7. Compared with the mechanism proposed by Boillod-Cerneux based on Krylov solver, this accuracy verification based on Shift Inverse Power method is able to evaluate the spectrum conservation accuracy for all given eigenvalues, which is not a classical eigenvalue problem researchers have to solve.

4.5.1 Basic Implementation on CPUs

For the initial CPU implementation, we chose PETSc instead of ScaLAPACK because we would like to evaluate the solvers for sparse linear systems. As shown in Algorithm 19, the kernel of generation is the SpGEMM operation of AM and MA, and the matrix-matrix addition (AYPX operation) as $AM - MA$. All the sparse matrices during the generation procedure are stored by the block CSR format which is provided by PETSc by default. We use the matrix operations supported by PETSc to facilitate implementation. The block diagonal parallel matrix based on MPI are partitioned and stored into several sub-matrices. For example, if there are three MPI process: $proc1$, $proc2$ and $proc3$, the matrix can be divided into blocks as the Formula (4.14).

© 2019 Tous droits réservés.

lilliad.univ-lille.fr

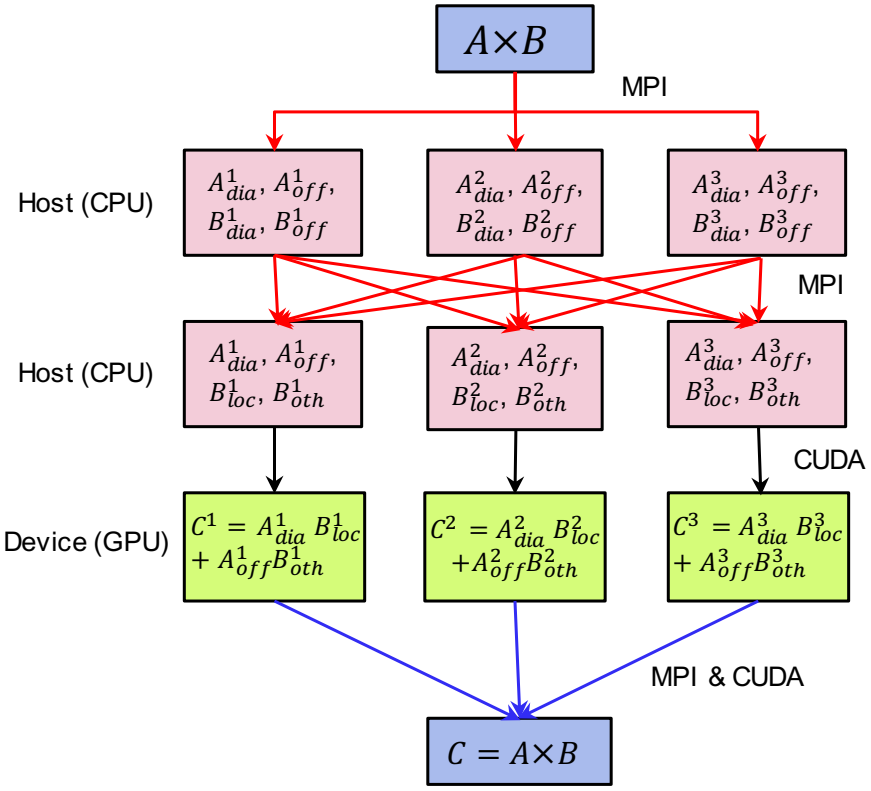

Figure 4.4 – The structure of a CPU-GPU implementation of SpGEMM, where each GPU is attached to a CPU. The GPU is in charge of the computation, while the CPU handles the MPI communication among processes.

The sub-matrices A, B and C are stored in $proc1$, D, E and F in $proc2$, and G, H and I is stored in $proc3$. In each process, the diagonal and the off-diagonal parts are separately stored into two sequence block matrices. The parallel SpGEMM and AXPY operations for CPUs are already supported by PETSc [25]. We use these functions directly to facilitate the implementation.

$$\left[\begin{array}{c|c|c} A & B & C \\ \hline D & E & F \\ \hline G & H & I \end{array}\right] \tag{4.14}$$

4.5.2 Implementation on Multi-GPU

PETSc does not supply the SpGEMM and AXPY operations for GPU clusters. Thus we implemented them using MPI, CUDA and cuSPARSE library based on the PETSc data structure definitions. The structure of implementation is given in Fig. 4.4 which uses sparse matrix A and B multiplication as an example. Firstly, the same as in PETSc, A and B are divided into slices, and each slice is saved in a process. In each process numbered i, the local matrices are all saved as two separate sequence matrix, labeled as A^i_{dia} and A^i_{off} for matrix A^i, B^i_{dia} and B^i_{off}

© 2019 Tous droits réservés.

Thèse de Xinzhe Wu, Université de Lille, 2019

for matrix B^i. Then B^i_{dia} and B^i_{off} are combined together as a novel sequence matrix noted as B^i_{loc} in each process i. Using MPI features, each CPU collects all the remote data of matrix B from the other processes, and construct them into a new sequence matrix B^i_{oth}. Copy these matrices from each process to one attached GPU, and calculate $C^i = A^i_{dia}B^i_{loc} + A^i_{off}B^i_{oth}$. The matrix operations on each GPU device is supported by the cuSPARSE. The final result C can be obtained by gathering all slices C_i from all devices.

4.5.3 Communication Optimized Implementation with MPI

In fact, the parallel SpGEMM kernel's communication can be specifically optimized based on the particular property of nilpotent matrix A. Since A is determined by three parameters p, d and n as we mentioned in Section 4.4, it is not necessary to implement this nilpotent matrix in parallel. We note this nilpotent matrix as $A(p, d, n)$. Denote $J(i, j)$ the entry in row i and column j of matrix J; $J(i, :)$ all the entries of row i; and $J(:, j)$ all the entries of column j. As shown in Fig. 4.5a, the right-multiplication $A(p, d, n)$ will cause all the entries of the first $n - p$ columns of M to shift right by an offset p. Denote MA the result gotten by the right-multiplying A on M. We have $MA(:, j) = M(:, j - p), \forall j \in p, \cdots, n-1$, and $MA(:, j) = 0, \forall j \in 0, \cdots, p-1$. Similarly, the left-multiplying $A(p, d, n)$ on M will shift up the whole entries of last $n - p$ rows by an offset p. Denote AM the matrix gotten by the left-multiplying A on M. We have $AM(i, :) = M(i + p, :), \forall i \in 0, \cdots, n - p - 1$, and $AM(i :,) = 0, \forall i \in p, \cdots, n - 1$. Moreover, the parameter d decides that $MA(:, r(d + 1)) = 0$ and $AM(r(d + 1), :) = 0$ with $r \in 1, \cdots, \lfloor \frac{n}{d+1} \rfloor$.

For the parallel implementation on distributed memory systems, the three parameters p, d and n are distributed across all MPI processes, then operations AM and MA are different from a general parallel SpGEMM. Firstly, the matrix M is one-dimensional distributed by row across m MPI process. As shown in Fig. 4.5b, for MA, there is no communication between different MPI processes since the data are moved inside each row. Ensure that $\lfloor \frac{n}{m} \rfloor \geq p$, for AM, the intercommunication of MPI takes place when the MPI process k ($k \in 1, \cdots, m - 1$) should send the first p rows of their sub-matrix to the closest previous MPI process numbering $k - 1$. The communication complexity for each process is $\mathcal{O}(np)$. When generating the band matrix with low bandwidth b, it tends to be a $\mathcal{O}(bp)$ with $p = 1$ or 2. The MPI-based optimization implementations of AM and MA are respectively given by Algorithm 20 and 21. The communication between MPI process is implemented by the asynchronous sending and receiving functions. In this algorithm, M_k, MA_k and AM_k imply the sub-matrices on process k with t rows. The rows and columns of these sub-matrices in Algorithm 20 and 21 are all indexed by the local indices.

The communication-optimized SMG2S is implemented based on MPI and C++. The submatrix on each process is stored in ELLPACK format, using the key-value map containers provided by C++. The key-value map implementation facilitates the indexing and moving of the rows and columns. We did not implement a GPU version of SMG2S with this kind of communication optimization since its core is the data movement among different computing units, which is not well suitable for the multi-GPU architecture.

© 2019 Tous droits réservés.

lilliad.univ-lille.fr

Thèse de Xinzhe Wu, Université de Lille, 2019

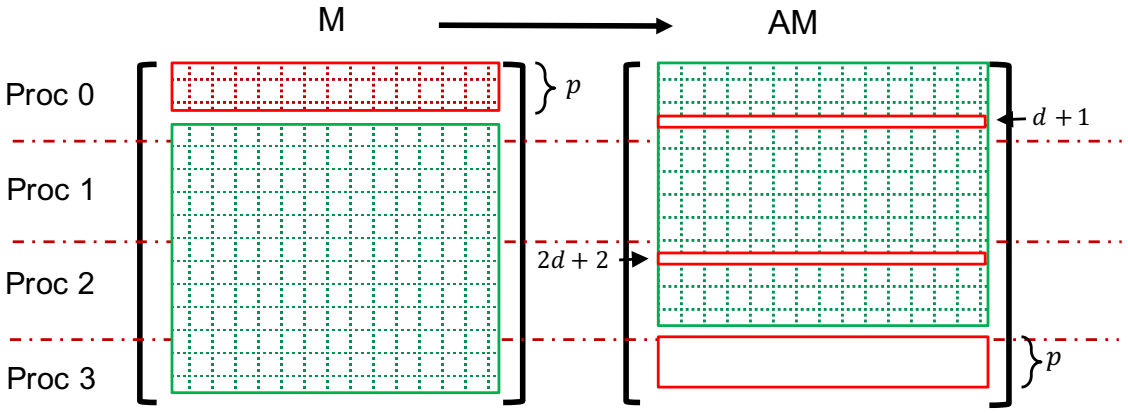

(a) AM Operation.

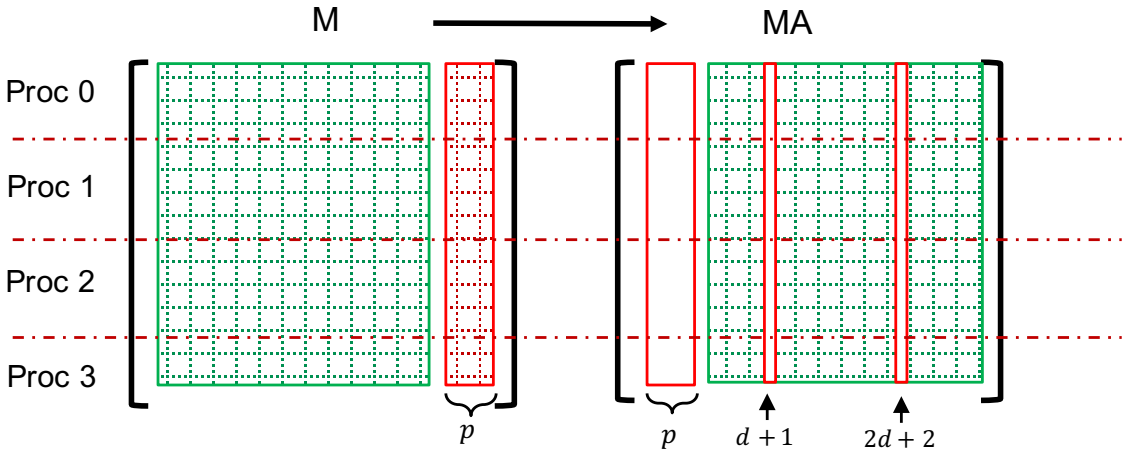

(b) MA Operation.

Figure 4.5 – AM and MA operations.

4.6 Parallel Performance Evaluation

In this section, we present the parallel performance of SMG2S on the supercomputing systems.

4.6.1 Hardware

We implement SMG2S on the supercomputers *Tianhe-2* and *Romeo-2013*. *Tianhe-2* system ranked first in the Top500 rankings six times, which is installed at the National Super Computer Center in Guangzhou of China. It is a heterogeneous system made of Intel Xeon CPUs and Intel Knights Corner (KNC), with 16000 compute nodes in total. Each node composes 2 Intel Ivy Bridge 12 cores @ 2.2 GHz.

Romeo-2013 is located at University of Reims Champagne-Ardenne, France. It is also a heterogeneous system made of Xeon CPUs and Nvidia GPUs, with 130 BullX R421 nodes. Each node composes 2 Intel Ivy Bridge 8 cores @ 2.6 GHz and 2 NVIDIA Tesla K20x GPUs.

4.6.2 Strong and Weak Scalability Evaluation

In this section, we will use double-precision real and complex values to evaluate the strong and weak scalability of SMG2S's different implementations on multi-CPUs and multi-GPUs.

© 2019 Tous droits réservés.

lilliad.univ-lille.fr

Thèse de Xinzhe Wu, Université de Lille, 2019

Algorithm 20 Parallel MPI AM Implementation

function AM(*input*: matrix M, matrix row number n, p, d, proc number m; *output*: matrix AM)
  Distribute t row blocks M_k of M to MPI process k
  for $p+1 \leq i < t$ **do**
    for $0 \leq j < n$ **do**
      if $M(i,j) \neq 0$ **then**
        $AM_k(i-p, j) = M_k(i,j)$
      end if
    end for
  end for
  for $0 \leq i < p$ **do**
    if $k \neq 0$ **then**
      isend ith row $M_k(i)$ to $k-1$
    end if
    if $k \neq m-1$ **then**
      irecv ith row $M_k(i)$ from $k+1$
      $AM_k(t-p+i) = M_k(i)$
    end if
  end for
end function

Algorithm 21 Parallel MPI MA Implementation

function MA(*input*: matrix M, matrix row number n, p, d, proc number m; *output*: matrix MA)
  Distribute t row blocks M_k of M to process k
  for $0 \leq i < t$ **do**
    for $p+1 \leq j < n$ **do**
      if $M_k(i,j) \neq 0$ **then**
        $MA_k(i, j+p) = M_k(i,j)$
      end if
    end for
  end for
end function

All the test matrices in this chapter are generated with h set to be 10 and d to be 7. The details of the weak scaling experiments are given in Table 4.2. The matrix size of the strong scaling experiments on *Tianhe-2* with CPUs, *Romeo-2013* with CPUs and, *Romeo-2013* with GPUs are respectively 1.6×10^7, 3.2×10^6 and 8.0×10^5. The results are given in Fig. 4.6, Fig. 4.7 and Fig. 4.8. The weak scaling for the PETSc implementation of SMG2S on *Tianhe-2* trends to be bad when MPI processes number is greater than 768, with communication overhead becoming more and more important compared to the required time for computation. However, for communication-optimized SMG2S, both strong and weak extensions perform well when the number of MPI processes is greater than 768. Experiments show that SMG2S implemented with GPUs can still have good strong and weak scalability. In conclusion, SMG2S has always good strong scaling performance when d and h are much smaller than the dimension of the matrix n, because it turns to be a $\mathcal{O}(n)$ problem. The weak scalability is good enough for most cases. The reason is that the nilpotent matrix A in SpGEMM is simple with not many non-zero elements.

© 2019 Tous droits réservés.

lilliad.univ-lille.fr

Thèse de Xinzhe Wu, Université de Lille, 2019

Table 4.2 – Details for weak scaling and speedup evaluation.

(a) Matrix size for the CPU weak scaling tests on *Tianhe-2*.

CPU number	48	96	192	384	768	1536
matrix size	1×10^6	2×10^6	4×10^6	8×10^6	1.6×10^7	3.2×10^7

(b) Matrix size for the CPU weak scaling on *Romeo-2013*.

CPU number	16	32	64	128	256
matrix size	4×10^5	8×10^5	1.6×10^6	3.2×10^6	6.4×10^6

(c) Matrix size for the GPU weak scaling and speedup evaluation on *Romeo-2013*.

CPU or GPU number	16	32	64	128	256
matrix size	2×10^5	4×10^5	8×10^5	1.6×10^6	3.2×10^6

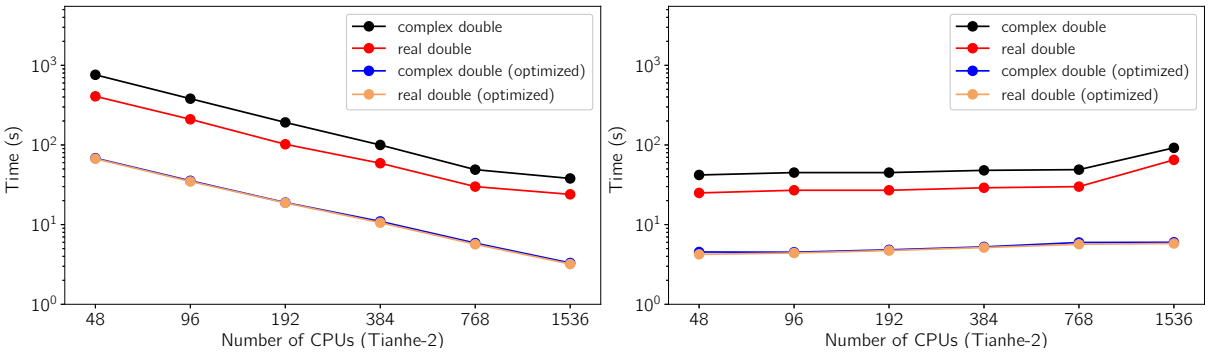

(a) CPU strong scaling on *Tianhe-2*. (b) CPU weak scaling on *Tianhe-2*.

Figure 4.6 – Strong and weak scaling results of SMG2S on *Tianhe-2*. A base 2 logarithmic scale is used for X-axis, and a base 10 logarithmic scale for Y-axis.

Therefore there is not enormous communication among different computing units. The weak scalability has its drawback in case that the computing unit number come to be huge for the SMG2S implementation based on PETSc, where the communication overhead become dominant. The specific implementation of communication-optimized SMG2S makes his strong and weak scalability better. The results show that for the basic SMG2S implementation, the time taken to generate a double-precision complex matrix is almost twice that of a double-precision real, but the time consumption of the complex and real-matrix generation with the optimized SMG2S seems similar. The reason is that there are no numerical value multiplications anymore in the optimized implementation of SMG2S.

4.6.3 Speedup Evaluation

The speedup of both SMG2S on multi-GPU and communication-optimized SMG2S on the CPUs compared with the PETSc-based implementation on CPU are also tested on *Romeo-2013*. Based on previous assessments that complex and real value types always have good scalability, we select

© 2019 Tous droits réservés.

lilliad.univ-lille.fr

Thèse de Xinzhe Wu, Université de Lille, 2019

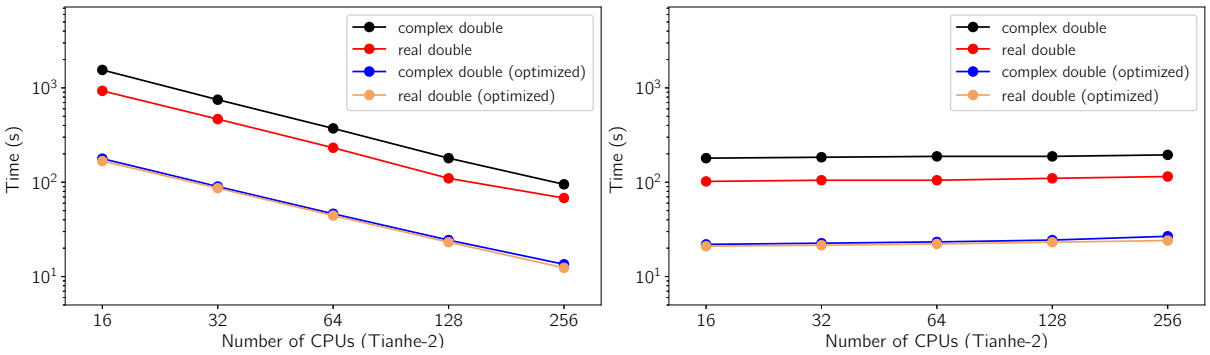

(a) CPU strong scaling on *Romeo-2013*. (b) CPU weak scaling on *Romeo-2013*.

Figure 4.7 – Strong and weak scaling results of SMG2S on *Romeo-2013*. A base 2 logarithmic scale is used for X-axis, and a base 10 logarithmic scale for Y-axis.

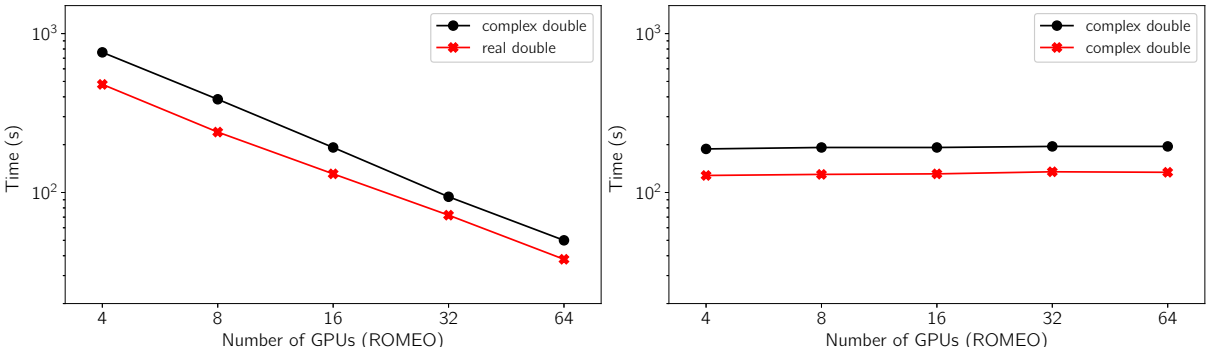

(a) GPU strong scaling on*Romeo-2013*. (b) GPU weak scaling on *Romeo-2013*.

Figure 4.8 – Strong and weak scaling results of SMG2S on *Romeo-2013* with multi-GPUs. A base 2 logarithmic scale is used for X-axis, and a base 10 logarithmic scale for Y-axis.

the double precision complex values for the speedup evaluation. Details of experiments are also given in Table 4.2c. The results are shown in Fig. 4.9. We can find that the GPU version of SMG2S has almost 1.9× speedup over the PETSc CPU version. The communication-optimized SMG2S on CPUs has about 8× speedup over the basic PETSc CPU version.

4.7 Accuracy Evaluation of the Eigenvalues of Generated Matrices with respect to the Given Ones

In the previous section, we showed the good parallel performance of SMG2S, and then it was necessary to verify that the generated matrices are able to maintain given spectra with sufficient accuracy.

4.7.1 Verification based on Shift Inverse Power Method

Generally, iterative eigenvalue solvers such as the Arnoldi or other Krylov methods are applied to approximate the dominant eigenvalues. However, this accuracy verification is an opposite case. The scenrio of accuracy verification for each given value can be summarized as finding its nearest eigenvalue, and verifying if this value is near enough to the given one. If yes, the accuracy for this

© 2019 Tous droits réservés.

lilliad.univ-lille.fr

Thèse de Xinzhe Wu, Université de Lille, 2019

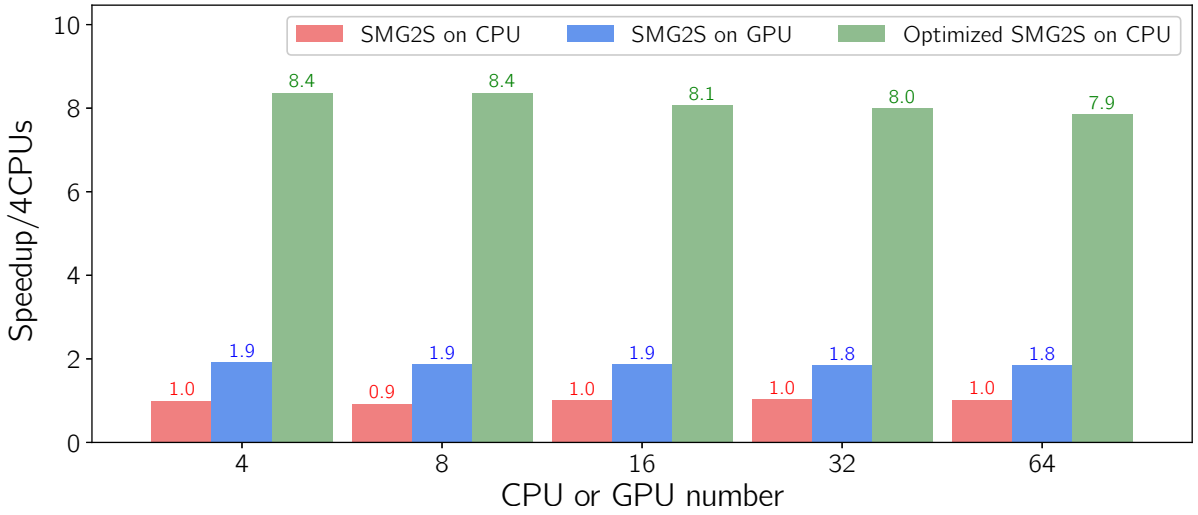

Figure 4.9 – Weak scaling speedup comparison over PETSc-based SMG2S with 4 CPUs on *Romeo-2013*.

Algorithm 22 Shifted Inverse Power method

1: **function** SIPM(*input*: Matrix A, initial guess for desired eigenvalue σ, initial vector v_0, *output*: Approximate eigenpair (θ, v))
2: $y = v_0$
3: **for** $i = 1, 2, 3 \cdots$ **do**
4: $\theta = ||y||_\infty$
5: $v = y/\theta$
6: Solve $(A - \sigma I)y = v$
7: **end for**
8: **end function**

value is acceptable, otherwise, this verfication cannot be approved. These iterative methods are not able to handle this validation directly and efficiently. In this section, we present a method for accuracy verification using the Shifted Inverse Power method, which can be easily implemented in parallel.

The Power method is an algorithm to approximate the greatest eigenvalue. Meanwhile, the Inverse Power method is a similar iterative algorithm to find the smallest eigenvalue. The middle eigenvalues can be obtained by the Shifted Inverse Power method [110]. This method is given in Algorithm 22. Its operation complexity is $\mathcal{O}(n^3)$. The Shifted Inverse Power method is used to compute the eigenvalue which is the nearest one to a given value in a few steps of iterations. The related eigenvector can be easily calculated by its definition and used to check if this given value is an eigenvalue of the matrix.

Fig. 4.10 gives the workflow of this verification operation. In detail, in order to check if the given value λ is the eigenvalue of a matrix, we choose a shift value σ which is close enough to λ. An eigenpair (λ', v') with the relation $Av' = \lambda' v'$ can be approximated in very few steps by Shifted Inverse Power method, with λ' is the closest eigenvalue to σ. Since σ is very close to λ, it should be that λ and λ' are the same eigenvalue of a system, and v' should be the eigenvector related to λ. In reality, even if the computed eigenvalue is very close to the true value, the associated eigenvector may be quite inaccurate. For the correct eigenpairs, the formula $Av' \approx \lambda v'$ should be

© 2019 Tous droits réservés.

lilliad.univ-lille.fr

Thèse de Xinzhe Wu, Université de Lille, 2019

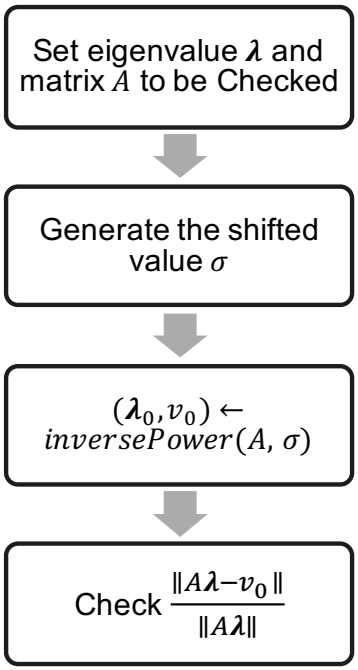

Figure 4.10 – SMG2S verification workflow.

satisfied. Based on this relationship, we define the relative error as Formula (4.15) to quantify the accuracy.

$$error = \frac{||Av' - \lambda v'||}{||Av'||} \tag{4.15}$$

If this *error* is 0, $\lambda' = \lambda$, if not, this generated matrix do not have an exact eigenvalue as λ. In real experiments, the exact solution cannot always be guaranteed with the arithmetic rounding errors of floating operations during the generation. A threshold could be set for accepting it or not.

Table 4.3 – Accuracy verification results.

Matrix N^o	Size	Spectra	Acceptance (%)	max *error*
1	100	*Spec*1	93	2×10^{-2}
2	100	*Spec*2	94	3×10^{-2}
3	100	*Spec*3	100	7×10^{-5}
4	100	*Spec*4	100	3×10^{-7}
5	100	*Spec*5	100	1×10^{-7}

4.7.2 Experimental Results

In the experiments, we test the accuracy of SMG2S with five selected cases among the various tests of different spectral distributions. Fig. 4.11 and Fig. 4.13 are cases of clustered eigenvalues with different scales. Fig. 4.12 is a special case with the dominant part of eigenvalues clustered in a small region. Fig. 4.14 is a case that composes the conjugate and closest pair eigenvalues.

© 2019 Tous droits réservés.

lilliad.univ-lille.fr

Thèse de Xinzhe Wu, Université de Lille, 2019

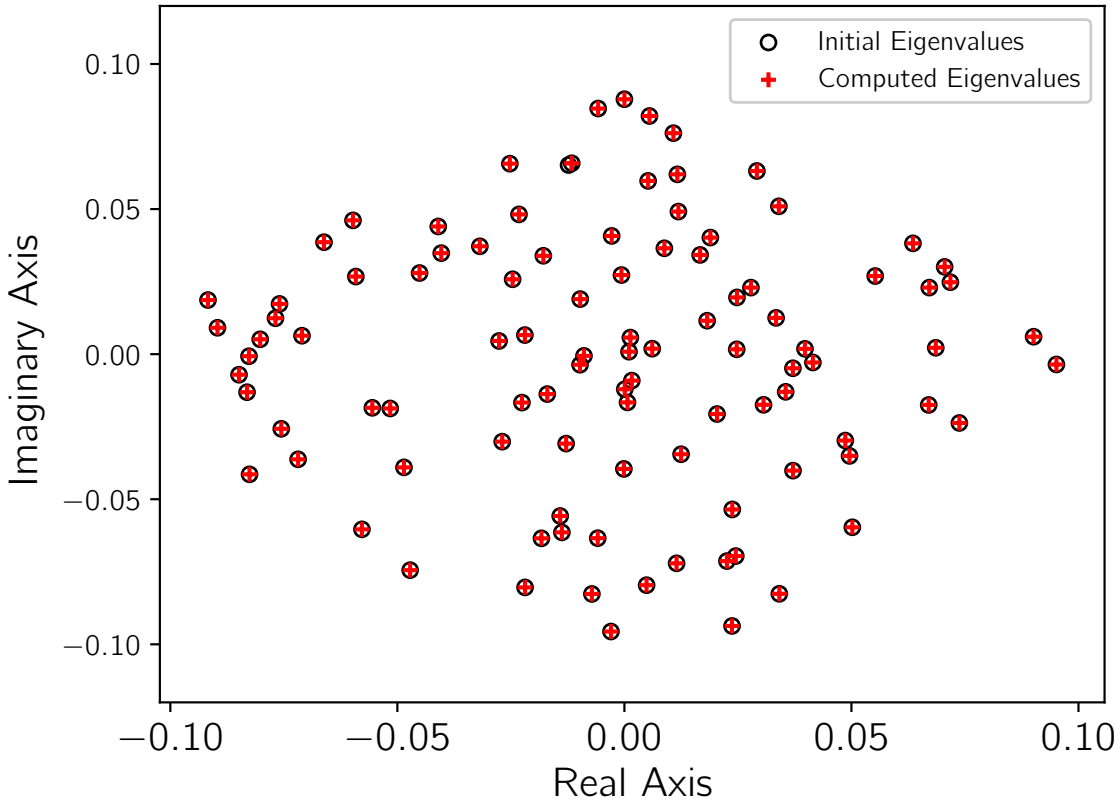

Figure 4.11 – Spec1: Clustered Eigenvalues I.

Fig. 4.15 is a case with discrete distribution of eigenvalues in the complex plain. These figures compare the difference between the given spectra (labeled as initial eigenvalues in the figures) and the approximated ones (labeled as computed eigenvalues) by the Shifted Inverse Power Method. Clearly, the matrices generated by SMG2S can keep almost all the given eigenvalues in the four cases even if they are very clustered. The acceptance threshold is set to be 1.0×10^{-3}.

This acceptance for cases of Fig. 4.11, Fig. 4.12, Fig. 4.13, Fig. 4.14 and Fig. 4.15 (shown as Table 4.3) are respectively 93%, 94%, 100%, 100% and 100%. The maximum *error* for them are respectively 2×10^{-2}, 3×10^{-2}, 7×10^{-5}, 3×10^{-7} and 1×10^{-7}. After the tests, we conclude that even for very concentrated and closest eigenvalues, SMG2S is able to accurately maintain given spectra. In some cases, a very small number of over-aggregated eigenvalues may result in inaccurate eigenvalues, but in general, the generated matrix satisfies the need to evaluate linear systems and eigenvalue solvers.

4.7.3 Arithmetic Precision Analysis

Any floating operation introduces rounding errors, which are not negligible for generating large matrices. Regarding the non-Hermitian matrix, its eigenvalues may be extremely sensitive to perturbation. This sensibility is bounded by

$$bound(\lambda) \leq ||E||_2 Cond(\lambda),$$

© 2019 Tous droits réservés.

lilliad.univ-lille.fr

Thèse de Xinzhe Wu, Université de Lille, 2019

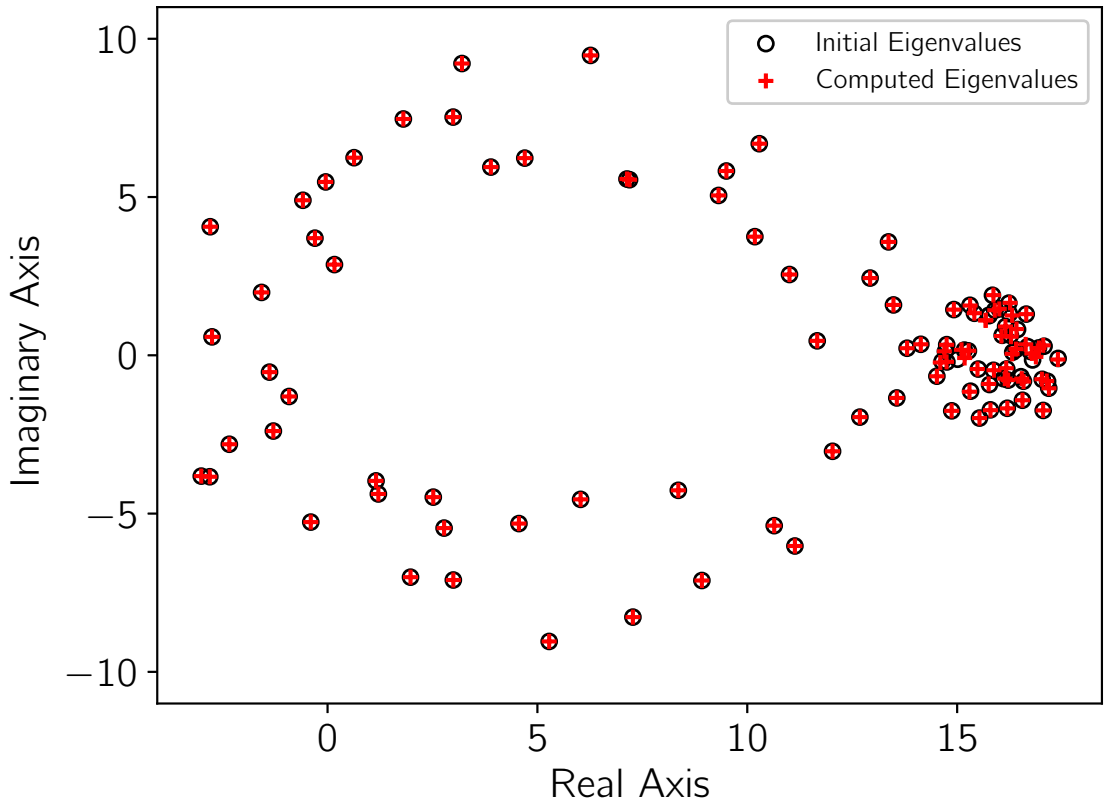

Figure 4.12 – Spec2: Clustered Eigenvalues II.

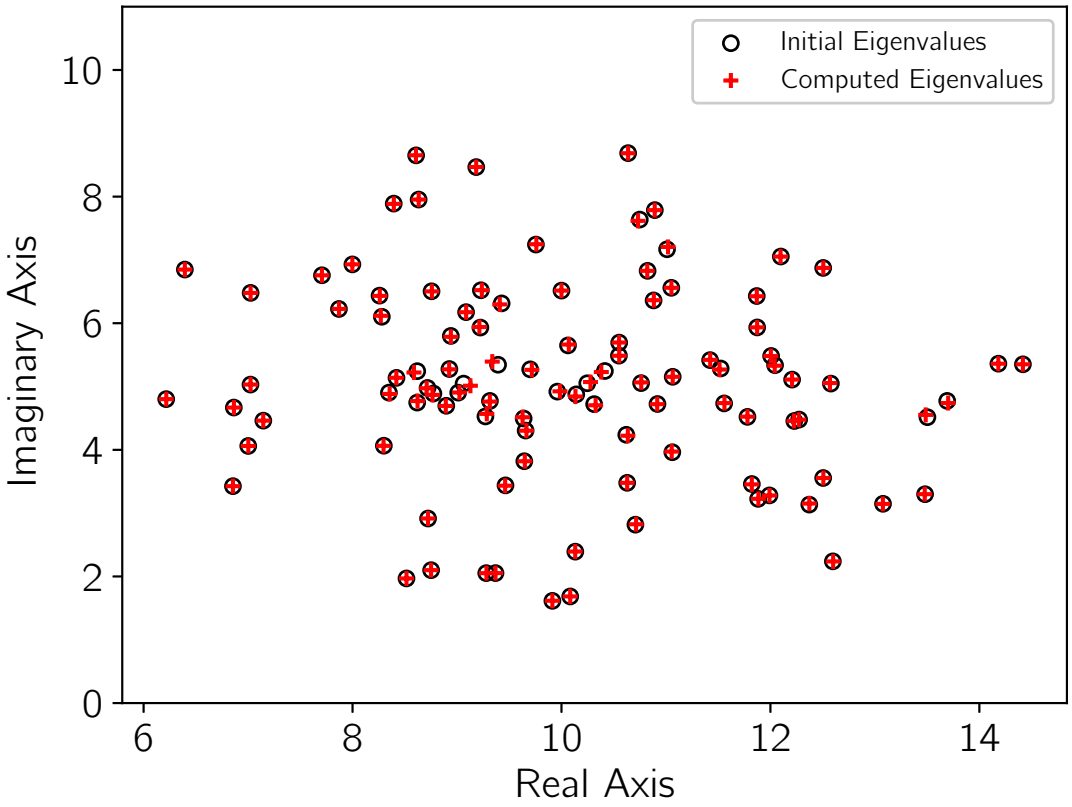

Figure 4.13 – Spec3: Clustered Eigenvalues III.

© 2019 Tous droits réservés.

lilliad.univ-lille.fr

Thèse de Xinzhe Wu, Université de Lille, 2019

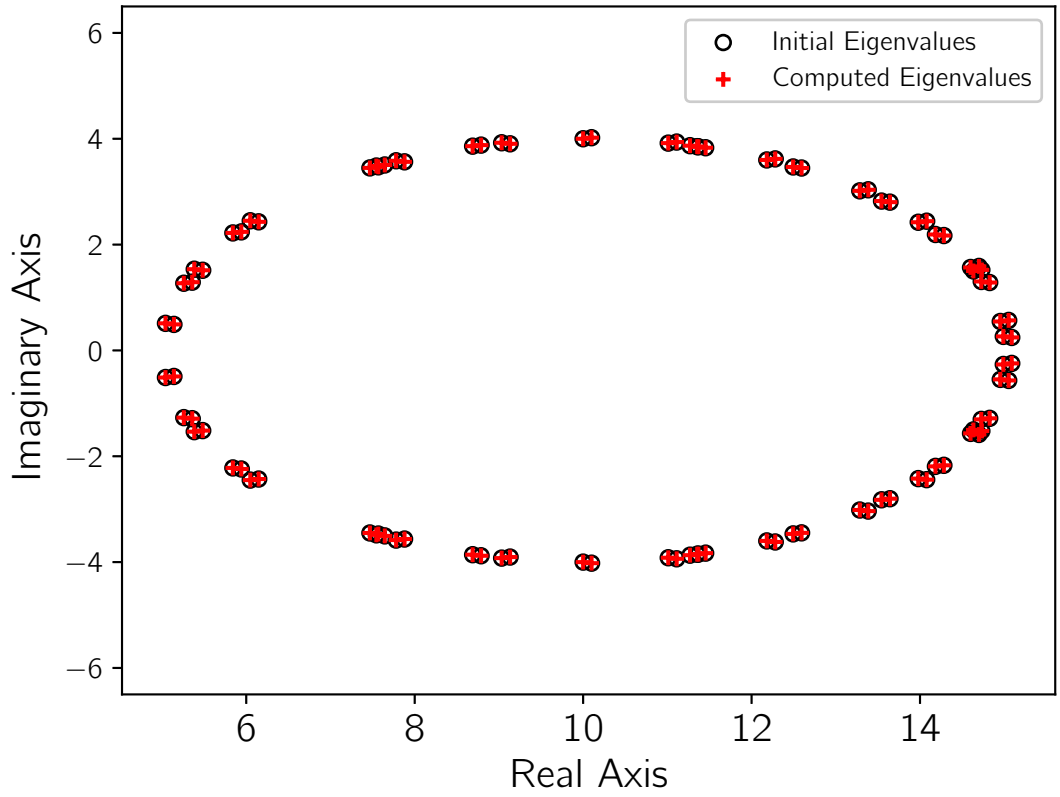

Figure 4.14 – Spec4: Conjugate and Closest Eigenvalues.

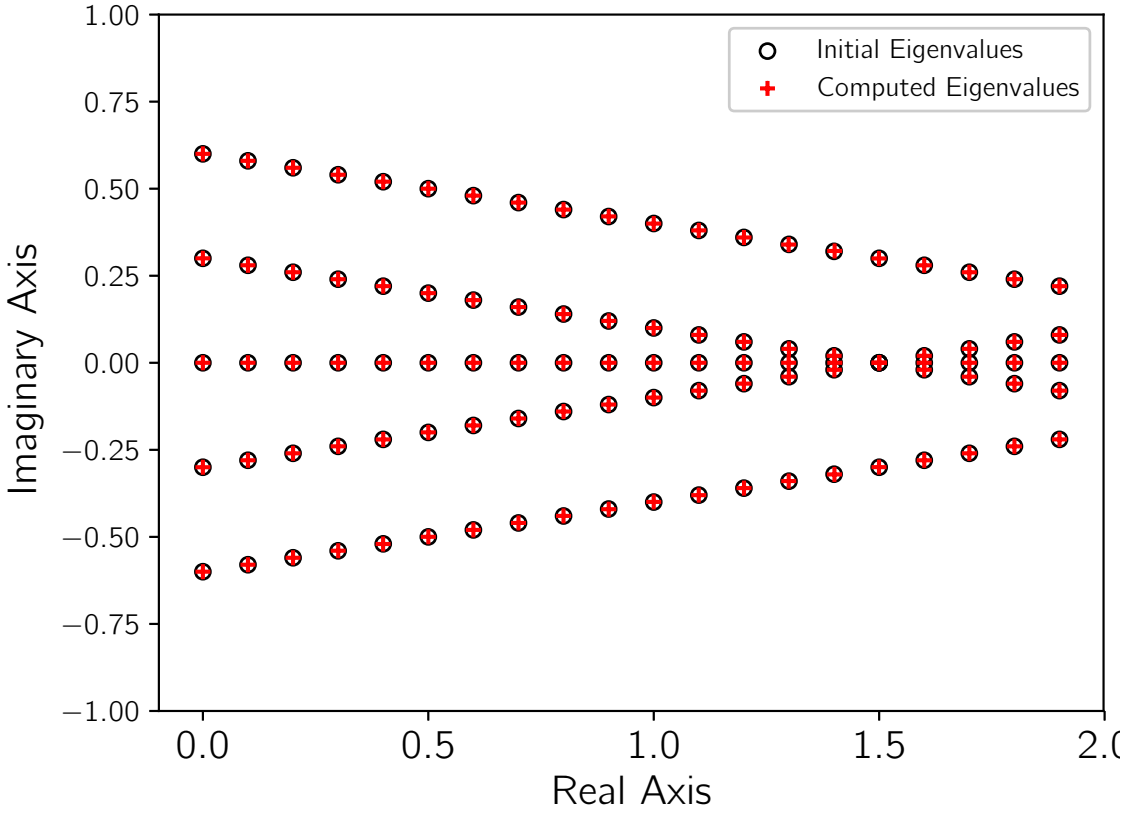

Figure 4.15 – Spec5: Distributed Eigenvalues.

© 2019 Tous droits réservés.

lilliad.univ-lille.fr

Thèse de Xinzhe Wu, Université de Lille, 2019

with $Cond(\lambda)$ the condition number of related eigenvalue λ and $||E||_2$ the Euclidean norm of errors [189]. $Cond(\lambda) = 1$ for the Hermitian matrices, but for the non-Hermitian ones, it can be excessively high. There are two solutions to solve this problem. The first one is to ensure the eigenvalues to be well-conditioned. The second is to use the integer values to generate matrices, since only integers and the operations $+$, $-$, and $\times$ on the microprocessor can make absolutely exact computations. As shown in Algorithm 19, most of the operations in SMG2S are $+$, $-$ and $\times$, except the step 9 with a division operation. Without step 9, we can introduce a special SMG2S fully using integers to avoid the risks of rounding errors [98]. The spectra of the generated matrix will be $(2d)!$ times of the given one. Moreover, the upper band's width of generated depends on the parameter d. The factorial of $2d$ can easily reach the limit of integer, even with unsigned long long type. Thus a special factorial function using multiple integers should be implemented in order to enlarge the upper band's width.

4.8 Package, Interface and Application

SMG2S is packaged and released as an open source software based on MPI and C++. In this section, we present the package information of SMG2S and its interface to various programming languages and scientific computational libraries. For more details on this package, please refer to the relevant manual [224]. Then, we give examples which use SMG2S to evaluate different Krylov solvers. The homepage of SMG2S is https://smg2s.github.io.

4.8.1 Package

4.8.1.1 Installation Prerequisites

The following packages and libraries should be available on the computer platform before using SMG2S:

(1) C++ compiler with c++11 support;

(2) MPI;

(3) CMake (version minimum 3.6);

(4) (Optional) PETSc and SLEPc are necessary for the verification of accuracy of generated matrices to keep the given spectra.

4.8.1.2 Functions

SMG2S provides the following subsets of functions:

- the setup of parallel matrix and vector;
- the construction of particular nilpotent matrix.
- the matrix generation function;
- the interfaces to other languages and libraries;

© 2019 Tous droits réservés.

lilliad.univ-lille.fr

Thèse de Xinzhe Wu, Université de Lille, 2019

- the mechanism of accuracy verification;

- the GUI facilitating the verification and comparison.

4.8.1.3 Generation Workflow

SMG2S is a collection of C++ header files. This section provides the workflow for SMG2S to generate test matrices. SMG2S's C++ template support allows the generation of matrices of different sizes, scalar types and precision. The workflow details as follow:

(1) Include the header file

```
#include <smg2s/smg2s.h>
```

(2) Generate the Nilpotent Matrix Object:

```
Nilpotency<int> nilp;
nilp.NilpType1(length,probSize);
```

(3) Create the parallel Sparse Matrix Object Mt:

```
parMatrixSparse<std::complex<double>,int> *Mt;
```

(4) Generate a new matrix by SMG2S:

```
MPI_Comm comm; //working MPI Communicator
Mt = smg2s<std::complex<double>,int>(probSize, nilp,
        lbandwidth, spectrum, comm);
```

Here, in step (4), the *probsize* parameter represents the matrix size, *nilp* is the nilpotency matrix object that we have declared previously in step 2, *lbandwidth* is the bandwidth of lower-diagonal band. *spectrum* is the file path of given spectra file, if *spectrum* is set as " ", SMG2S will use the internal function to generate the spectral distribution. *comm* is the basic MPI communicator that the processes for SMG2S are involved in.

The given spectra file is in *pseudo-Matrix Market Vector format*. For complex eigenvalues, the given spectrum is stored in three columns, as shown below, the first column are the coordinates, the second column are the real part of the complex values, and the third column are the imaginary part of the complex values.

© 2019 Tous droits réservés.

lilliad.univ-lille.fr

Thèse de Xinzhe Wu, Université de Lille, 2019


```
%%SMG2S given eigenvalues complex general
3 3 3
1 10 6.5154
2 10.6288 3.4790
3 10.7621 5.0540
```

For the real eigenvalues, the given spectrum is stored in two columns, as shown below, the first column are the coordinates. The second column are eigenvalue.

```
%%SMG2S given eigenvalues real general
3 3
1 10
2 10.6288
3 10.7621
```

If users want to generate the eigenvalues at the runtime without loading from local file, they can customize their eigenvalues generation by the function *specGen* in the file *./smg2s/specGen.h*, and set the parameter *spectrum* of *smg2s* to be *" "*.

```
template<typename T, typename S>
void parVector<T,S>::specGen(std::string spectrum)
```

In this function, the eigenvalues are stored by the distributed vector *parVector*. And the filling of values on this *parVector* can be done by the function *SetValueGlobal* implemented in *parVector*, which takes the global indices to set values.

We know that the bandwidth of lower band of initial matrix can be set by the parameter *lbandwidth* of *smg2s*. Additionaly, the distribution of entries of initial matrix can also be customized by the function *matInit* provided by the file *./smg2s/specGen.h*. In default, these entries are filled in random. The different mechanism to fill them will influence the sparsity of final generated sparse matrix.

```
template<typename T, typename S>
void matInit(
        parMatrixSparse<T,S> *Am,
        parMatrixSparse<T,S> *matAop,
        S probSize,
        S lbandwidth
)
```

In this function, distributed matrix *Am* and *matAop* should be filled with the same way. And these entries of matrix can be filled by the method *Loc_SetValue* implemented in *parMatrixSparse*. *Loc_SetValue* uses the *global indices* of matrix to set values.

© 2019 Tous droits réservés.

lilliad.univ-lille.fr

Thèse de Xinzhe Wu, Université de Lille, 2019

4.8.2 Interface to Other Programming Languages

Until now, SMG2S provides interfaces to programming languages C and Python.

4.8.2.1 Interface to C

SMG2S install command will generate a shared library *libsmg2s.so* (*libsmg2s2c.dylib* on OS X platform) into ${INSTALL_DIRECTORY}/lib. It can be used to profit the C wrapper of SMG2S.

A minimum example to use the interface of SMG2S to C is given as Listing 1. SMG2S provides the C interface to different data types. For the data type of matrix size, it can be either *int* or *longint*; for the data type of matrix entries, it can be either *complex* or *real* with *single* or *double* precision.

Listing 1 A minimum example of SMG2S's interface to C.

```
#include <interface/C/c_wrapper.h>

/*create Nilpotency object*/
struct NilpotencyInt *n;
n = newNilpotencyInt();
NilpType1(n, 2, 10);
/*create the parallel Sparse Matrix Object*/
struct parMatrixSparseRealDoubleInt *m;
m = newParMatrixSparseRealDoubleInt();
/*Generation by SMG2S*/
smg2sRealDoubleInt(m, 10, n, 3 ," ",MPI_COMM_WORLD);
/*Release Nilpotency Object and parMatrixSparse Object*/
ReleaseNilpotencyInt(&n);
ReleaseParMatrixSparseRealDoubleInt(&m);
```

C interface implements the Nilpotent Matrix object for both *int* and *long int* as below:

```
struct NilpotencyInt;
struct NilpotencyLongInt;
```

For all the public functions in parMatrixSparse Object and smg2s function, *SUFFIX* below can be added them to provides the implementations for different data types:

- *ComplexDoubleLongInt*;
- *ComplexDoubleInt*;
- *ComplexSingleLongInt*;
- *ComplexSingleInt*;
- *RealDoubleLongInt*;
- *RealDoubleInt*;
- *RealSingleLongInt*;
- *RealSignleInt*.

© 2019 Tous droits réservés.

lilliad.univ-lille.fr

Thèse de Xinzhe Wu, Université de Lille, 2019

4.8.2.2 Interface to Python

SMG2S uses SWIG[1] to generate its wrapper to Python. This interface is available through either the Python package management system *pip* or from a local installation.

Listing 2 Install SMG2S with Python supporting.

```
#install online from pypi
CC=mpicxx pip install smg2s

#bulid in local
cd ./interface/Python
CC=mpicxx python setup.py build_ext --inplace
#or
CC=mpicxx python setup.py build
#or
CC=mpicxx python setup.py install

#run
mpirun -np 2 python generate.py
```

Before the utilization, make sure that *mpi4py* is installed. A minimum example to use the interface of SMG2S to Python is given as Listing 3.

Listing 3 A minimum example of SMG2S's interface to Python.

```
from mpi4py import MPI
import smg2s

#create the nilpotent matrix
nilp = smg2s.NilpotencyInt()

#setup the nilpotent matrix: 2 = continous 1 nb, 10 = matrix size
nilp.NilpType1(2,10)

#Generate Mt by SMG2S
Mt = smg2s.parMatrixSparseDoubleInt()
Mt = smg2s.smg2sDoubleInt(10,nilp,lbandwidth," ", MPI.COMM_WORLD)
```

4.8.3 Interface to Scientific Libraries

One benefit of SMG2S is that the test matrices generated are already distributed onto different computing units across the whole platforms. These distributed data can be directly by users

1. http://www.swig.org

© 2019 Tous droits réservés.

lilliad.univ-lille.fr

Thèse de Xinzhe Wu, Université de Lille, 2019

to efficiently evaluate the numerical linear methods of the scientific libraries or their personal implementation without involving I/O operations, whose time consumption is enormous if the matrix size is large. In the package of SMG2S, we provide the interface to PETSc and Trilinos, which can convert the generated matrices into the sparse matrix storage format corresponding to these libraries.

4.8.3.1 Interface to PETSc and SLPEc

SMG2S provides the interface to scientific computational softwares PETSc and SLEPc. The way of usage is shown as follows:

(1) Include the header file:

```
#include <interface/PETSc/petsc_interface.h>
```

(2) Create parMatrixSparse type matrix :

```
parMatrixSparse<std::complex<double>,int> *Mt;
```

(3) Restore this matrix into CSR format :

```
Mt->Loc_ConvertToCSR();
```

(4) Create PETSc MAT type :

```
Mat A;
MatCreate(PETSC_COMM_WORLD,&A);
```

(5) Convert to PETSc MAT format :

```
A = ConvertToPETSCMat(Mt);
```

4.8.3.2 Interface to Trilinos/Teptra

SMG2S is able to convert its distributed matrix into the CSR format of distributed matrix defined by Teptra in Trilinos. The way of usage:

(1) Include header file

```
#include <interface/Trilinos/trilinos_interface.hpp>
```

(2) Create parMatrixSparse type matrix :

© 2019 Tous droits réservés.

lilliad.univ-lille.fr

Thèse de Xinzhe Wu, Université de Lille, 2019


```
parMatrixSparse<std::complex<double>,int> *Mt;
```

(3) Create Trilinos/Teptra MAT type :

```
Tpetra::CrsMatrix<std::complex<double>, int, int> K;
```

(4) Convert to Trilinos MAT format :

```
K = ConvertToTrilinosMat(Mt);
```

4.8.4 GUI for Verification

SMG2S provides a GUI for users to compare and verify the prescribed spectra and eigenvalues of generated matrices. This GUI is implemented by Python. When the users launch this GUI, a new window opens like Fig. 4.16.

Figure 4.16 – Home Screen

The files which store the original spectrum and final eigenvalues can be respectively loaded from local filesystems into the GUI. After that, you can click on *Display* to build and open the graphic on the right side of the window, as shown by Fig. 4.17.

This GUI also supports the zoom in/out operations of a small part of figures, which allows the users to see more details of spectral distribution. In addition, the display can also be done with the users' selected scale by inputting the minimum and maximum values for the x-axis and y-axis, as shown by Fig. 4.18.

© 2019 Tous droits réservés.

lilliad.univ-lille.fr

Figure 4.17 – Home Screen Plot Capture

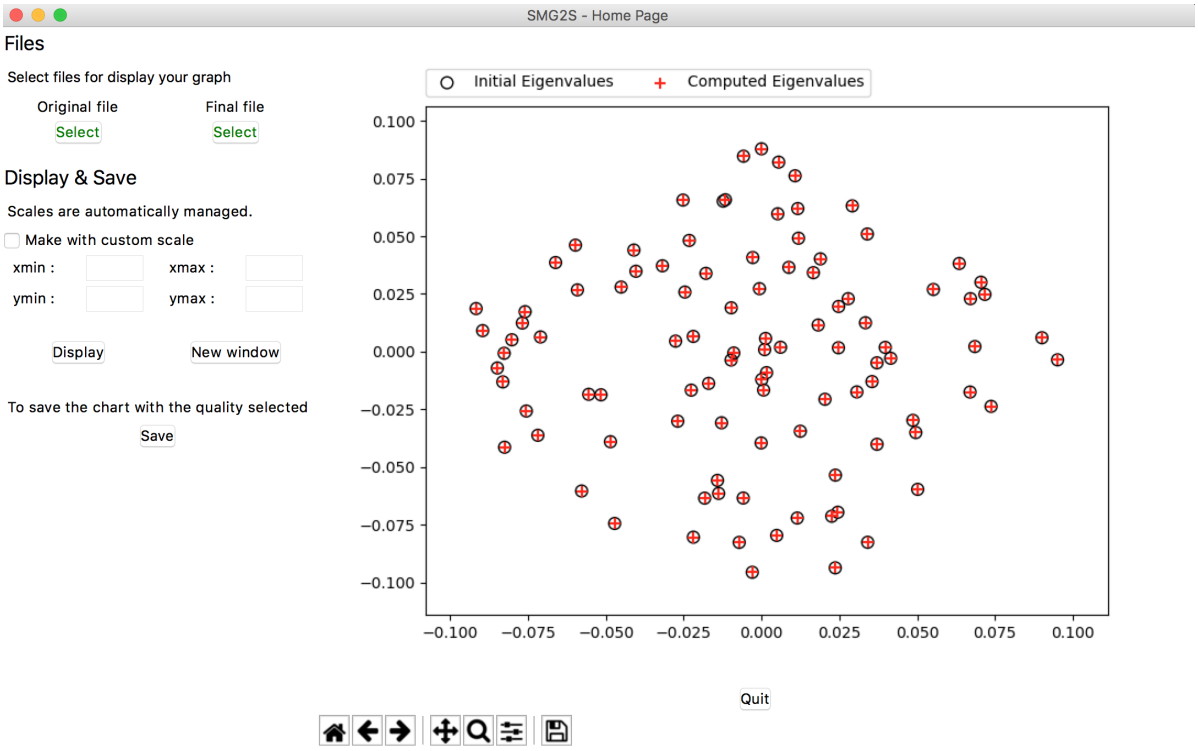

Figure 4.18 – Home Screen Custom

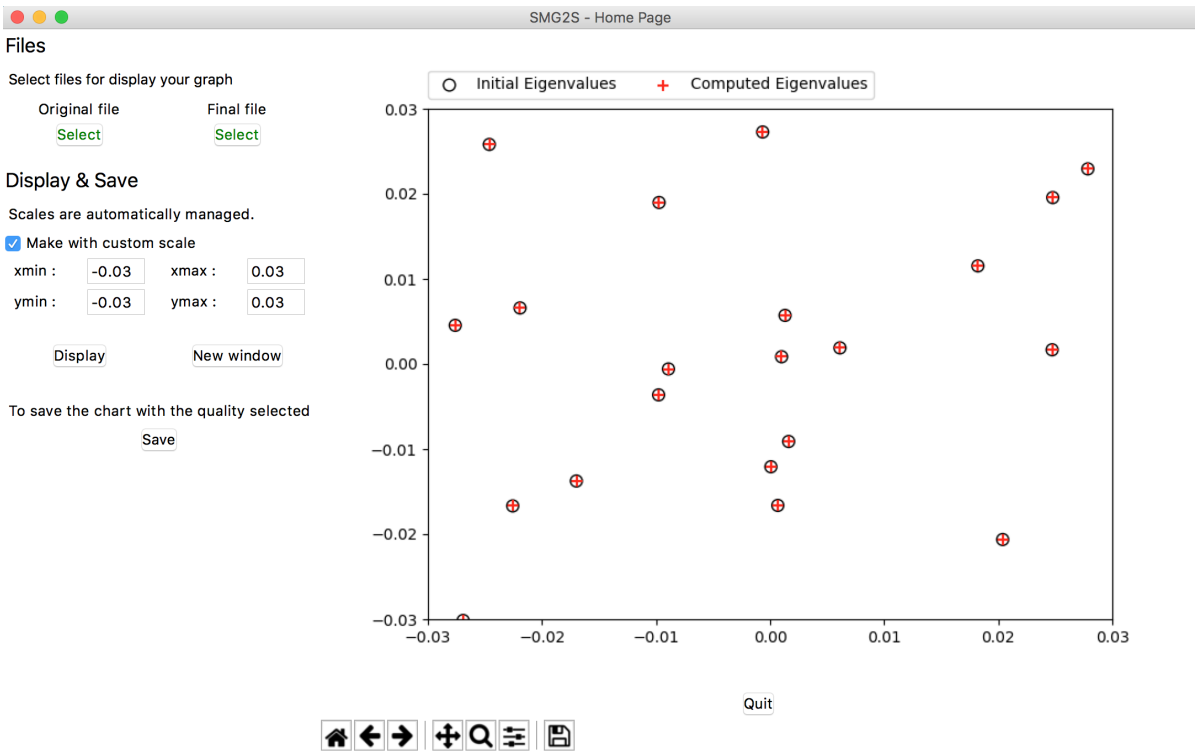

© 2019 Tous droits réservés.

Thèse de Xinzhe Wu, Université de Lille, 2019

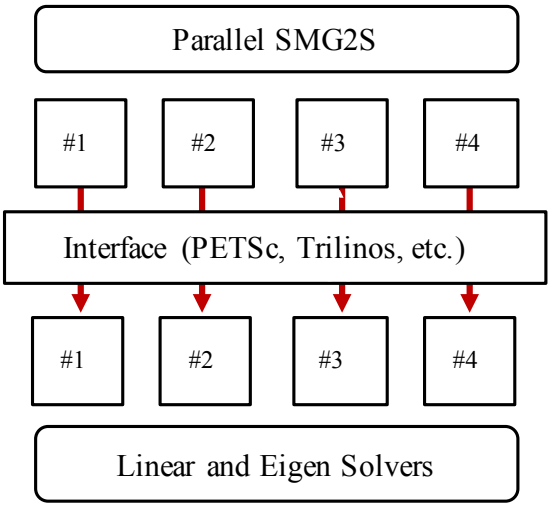

Figure 4.19 – SMG2S Workflow and Interface.

4.9 Krylov Solvers Evaluation using SMG2S

SMG2S is suitable to evaluate different kinds of linear system and eigenvalue solvers. We give some examples to demonstrate its workflow and ability to evaluate the Krylov solvers. In this section, we do not mean to propose new points on the Krylov methods, but to show the benefits of SMG2S. A class of Krylov subspace iterative methods is one of the most powerful tools to solve large and sparse linear systems. Convergence analysis of these methods is not only of great theoretical importance, but it can also help to answer practically relevant questions about improving their performance using the preconditioners. The convergence of Krylov solvers depends on the spectral distribution of matrices. And most preconditioners are applied to change the spectral distribution in order to accelerate the convergence. Anyway, the spectrum has a significant impact on the convergence of Krylov methods. We can use SMG2S to generate the test matrices with different spectral distributions and to study their influence on the convergence.

4.9.1 SMG2S workflow to evaluate Krylov Solvers

SMG2S workflow for evaluating the solvers is shown in Fig. 4.19. It generates the matrix in parallel. The interfaces provided to PETSc, Trilinos, and other public or personal parallel solvers, can restore the distributed data into the necessary data structures of different libraries. This feature can significantly reduce the I/O of applications and improve their efficiency to evaluate the numerical methods.

4.9.2 Experiments

Fig. 4.20 shows the comparison of conventional GMRES without preconditioning, GMRES preconditioned by Jacobi and SOR, and a hybrid GMRES with Least Squares polynomial, using the matrix generated SMG2S. This figure demonstrates that it is effective to evaluate the convergence of different implementation of GMRES with the matrices generated by SMG2S.

We evaluate also three different restarted Krylov linear system solvers using SMG2S. The test methods include GMRES, BiCGStab, and TFQMR, with/without the basic parallel precon-

© 2019 Tous droits réservés.

lilliad.univ-lille.fr

Thèse de Xinzhe Wu, Université de Lille, 2019

Figure 4.20 – Convergence Comparison using a matrix generated by SMG2S.

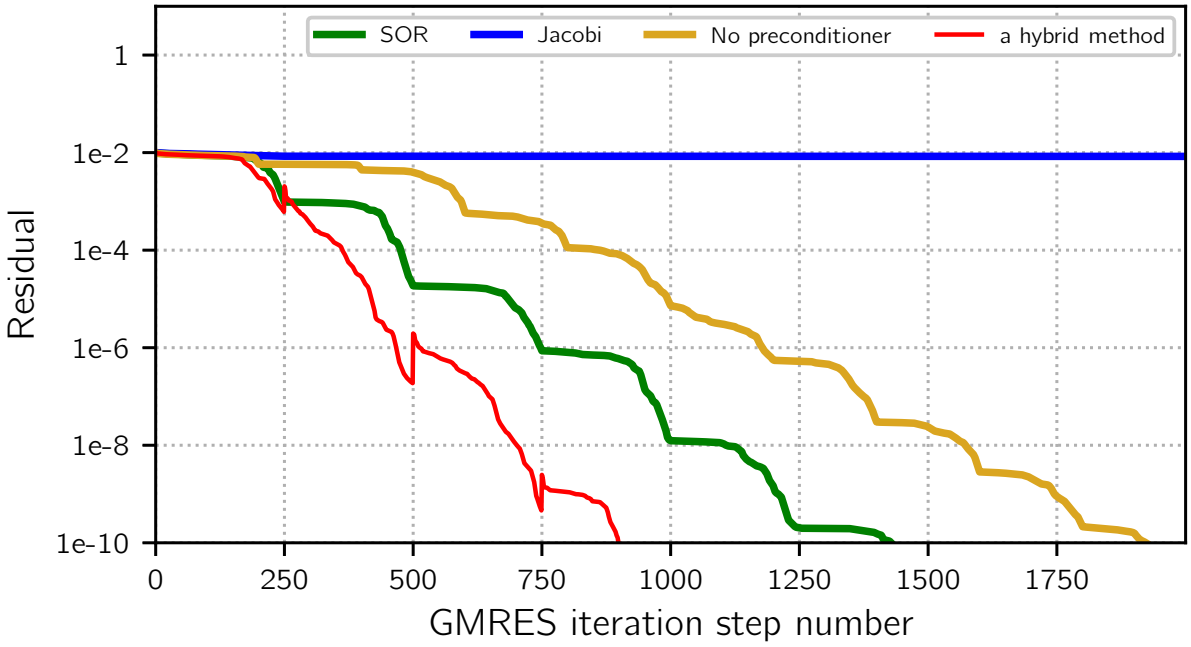

ditioners SOR or Jacobi. In the experiments, matrices with different spectral distributions are generated by SMG2S, including the clustered, closest, conjugate eigenvalues, eigenvalues with dominant values, etc. With the interface of SMG2S to PETSc, we use the parallel Krylov solvers and preconditioners provided by PETSc for the evaluations.

Table 4.4 shows iterative steps for convergence of different solvers. We can conclude that different matrices generated by SMG2S with different spectral distributions have different convergence performance with different solvers and preconditioners. The six cases listed in Table 4.4 are not cover much more different types of spectral distributions, and the tested preconditioners are relatively simple because it is not the primary purpose of this chapter. But we can say that SMG2S is a reliable tool which can be used to evaluate the different numerical methods, and in the future, we will make use of it to do more tests with different solvers and novel preconditioners and to analyse their performance with different spectral distributions.

4.10 Conclusion

In this chapter, we have presented a scalable matrix generator with the given spectra and its parallel implementation on homogeneous and heterogeneous clusters. This method allows generating large-scale test matrices with customized eigenvalues to evaluate the influence of spectra on the linear and eigenvalue solvers targeting the large-scale platform. SMG2S is designed with less memory requirement and operation complexity. We have evaluated its parallel scalability and the accuracy to keep the spectra of matrices generated by this matrix generator. The experiments proved that this method has good scalability and acceptable accuracy to keep the given spectra. One more important benefit of SMG2S is that the matrices are generated in parallel. Thus the data are already allocated to different processes. These distributed data can be used directly by users to efficiently evaluate the numerical linear methods of the scientific libraries or

© 2019 Tous droits réservés.

lilliad.univ-lille.fr

Thèse de Xinzhe Wu, Université de Lille, 2019

Table 4.4 – Krylov solvers evaluation by SMG2S with matrix row number = 1.0×10^5, convergence tolerance = 1×10^{-10} (dnc = do not converge in 8.0×10^4 iterations, the solvers and preconditioners are provided by PETSc.)

Krylov Methods	**Preconditioner**	**Case 1**	**Case 2**	**Case 3**	**Case 4**	**Case 5**	**Case 6**
GMRES	None	2160	dnc	dnc	dnc	50773	dnc
	Jacobi	17	dnc	129	dnc	12056	dnc
	SOR	3	dnc	4	dnc	dnc	dnc
BiCGStab	None	220	6859	dnc	771	53	dnc
	Jacobi	9	1097	66	214	56	dnc
	SOR	2	168	3	12	8	dnc
TFQMR	None	510	dnc	dnc	dnc	dnc	dnc
	Jacobi	18	dnc	128	dnc	dnc	dnc
	SOR	3	dnc	5	22	dnc	dnc

their personal implementation without concerning the I/O operation, whose time consumption is enormous if the matrix size is large. In the future, in order to augment the bandwidth of the generated matrix, a special data structure and function for the very large factorial operation should be implemented. And the interface to more scientific linear and eigenvalue solver libraries should be provided. The trend of computing units for the future exascale machines targeting at the AI applications with low-precision floating and integer operations requires the implementation of an variant of SMG2S with only integer operations, which has extremely high capacity to keep the accuracy of given spectra.

© 2019 Tous droits réservés.

lilliad.univ-lille.fr

Chapter 5

Unite and Conquer GMRES/ LS-ERAM Method

Facing with the challenges of numerical linear algebra methods on a large-scale machine discussed in Section 3, new programming models should be proposed with well-suited characteristics on modern architectures. These features should include optimized communications, asynchronicity, diversity of natural parallelism and fault tolerance. In such numerical methods, the avoidance of operations involving synchronous communications is the most important. Consequently, large scalar products and overall synchronization, and other operations involving communications between all cores have to be avoided. On the other hand, asynchronicity of communications has to be promoted. Indeed, this kind of communications could allow overlapping the computation operations inside a task and the tasks constituting these methods. The diversity of natural parallelism existing in such methods can be exploited to take advantage of heterogeneity of targeted architectures. Fault tolerance and reusability should be also important integral parts of these methods. These characteristics allow the improvement of the performance of applications built on the basis of existing methods. In this chapter, we present UCGLE, an asynchronous distributed and parallel method to solve sparse non-Hermitian systems on large platforms. The key feature of UCGLE compared with the classical hybrid methods using Least Squares polynomial preconditioner [86, 109] is its distributed and parallel asynchronous communication and the manager engine implementation between three components, which are specified for the extreme-scale supercomputing platforms. We summarize the Unite and Conquer approach in Section 5.1. In Section 5.2, we analyze the possibility to construct different iterative methods based on Unite and Conquer approach. The workflow of UCGLE is given in Section 5.3. In Section 5.4, we present its distributed and parallel implementation, including the computational components, the manager engine, and the asynchronous communications. The experimental results on different supercomputers which evaluate the convergence, the parameters, the impact of spectral distribution, the scalability, and the fault tolerance are shown in Section 5.5.

© 2019 Tous droits réservés.

lilliad.univ-lille.fr

Thèse de Xinzhe Wu, Université de Lille, 2019

5.1 Unite and Conquer Approach

As discussed in Section 1.2, Unite and Conquer approach is to make the collaboration of several iterative methods to accelerate the convergence of one of them. This approach is a model for the design of numerical methods by combining different computational components to work for the same objective, with asynchronous communication among them. *Unite* implies the combination of different computational components, and *conquer* represents different components work together to solve one problem. Different independent components with asynchronous communications can be deployed on various platforms such as P2P, cloud and the supercomputer systems. The idea of mixing asynchronously resarted Krylov methods using distributed and parallel computing was initially introduced by Guy Edjlali and Serge Petiton [79, 80] in 1991 at the *Etablissement Central de l'Armement* in Arcueil, France. They experimented those hybrid Krylov methods asynchronously on networks of heterogenous parallel computers (e.g., using two *Connection Machines*, a CM5 and a CM200 and a network of workstations). The concept of *Unite and Conquer* was introduced by Nahid Emad et al. [84, 83].

MERAM is an example of Unite and Conquer approach to solve eigenvalue problems based on an ERAM with multiple projections. MERAM was firstly implemented by Edjlali et al. on parallel computers [79], then more details of numerical evaluations of MERAM were presented in [84]. This method projects an eigenproblem on a set of subspaces and thus creates a whole range of differently parameterized ERAM processes which cooperate to compute a solution of this problem efficiently. As shown in Fig. 5.1, in MERAM, the restarting vector of each ERAM is updated by taking into account the interesting eigen-information obtained by the other ones. In detail, different ERAM processes inside MERAM begin with several subspaces spanned by a set of initial vectors and a set of subspace sizes. If the convergence does not occur for any of them, then the new subspaces will be defined with initial vectors updated by taking into account the intermediary solutions computed by all the ERAM processes. As shown in Fig. 5.2, which is an experimental results extracted from [84], MERAM is able to accelerate the convergence of ERAM. The numerical experiments have demonstrated that this variant of MERAM is often much more efficient than ERAM.

5.2 Iterative Methods based on Unite and Conquer Approach

Based on the Unite and Conquer approach, most of the hybrid and deflated iterative methods are able to be transformed into distributed and parallel schemes by dividing them into different computational components. In this section, we analyze the possibilities of building different iterative methods based on Unite and Conquer approach.

5.2.1 Preconditioning Techniques

As presented in Section 3.5, different preconditioning techniques are applied to accelerate the convergence. The reconstruction of iterative methods based on Unite and Conquer approach should take into account their preconditioners.

© 2019 Tous droits réservés.

lilliad.univ-lille.fr

Thèse de Xinzhe Wu, Université de Lille, 2019

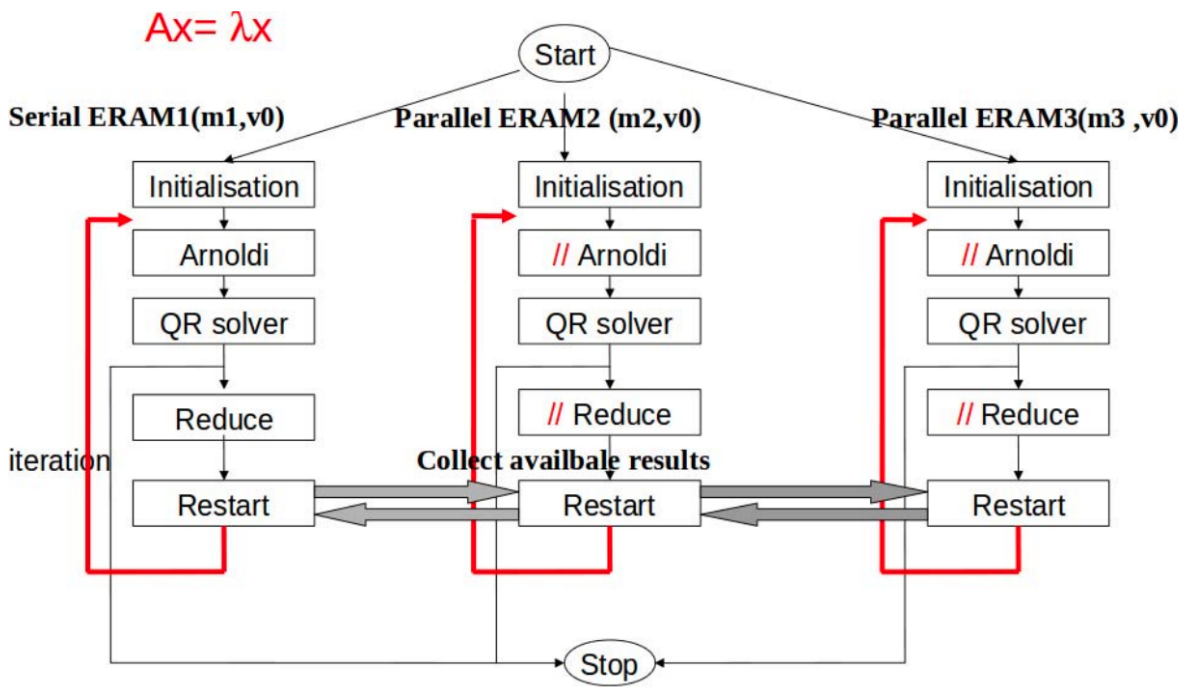

Figure 5.1 – An overview of MERAM, in which three ERAM communicate with each other by asynchronous communications [84].

5.2.1.1 Preconditioning by Matrix

The first alternative is to use the preconditioning matrix M, and replace the original system by $Mx = b$, which is much easier to be solved. M can be applied to the original systems either by the left, right or split preconditioning. Well-known preconditioners include SOR, Jacobi, AMG, ILU, etc.

5.2.1.2 Preconditioning by Deflation

As presented in Section 3.4.3, it is not always true, but in general, the convergence of Krylov subspace methods for solving linear systems depends on the distribution of eigenvalues. The removing or deflation of small eigenvalues might greatly improve the convergence performance. Hence deflated preconditioners should be constructed for each cycle of the restart. The small eigenvalues can be explicitly or implicitly deflated, e.g., the former uses the approximated Ritz pairs from H_m to construct new restart residual vectors for linear solvers; the latter implicitly deflates these eigenvalues by special operations on H_m and V_m [85, 47, 151]. For example, a deflated GMRES introduced in [151], firstly it approximates k smallest eigenpairs of $H_m + \beta H_m^{-T} e_m e_m^T$, secondly, these eigenpairs are used to construct new H_m and V_m with the implicit deflation of these smallest eigenvalues.

The iterative methods for solving eigenvalue problems can be explicitly deflated by the Ritz values and vectors approximated through previous Arnoldi reduction procedures. ERAM uses the Ritz pairs to construct a new restart vector, which can deflate the gotten eigenvalues and accelerate the convergence. Two well-known implicitly deflated Krylov subspace methods for eigenvalue problems are IRAM and Krylov-Schur method, which remove the unwanted eigen-

© 2019 Tous droits réservés.

lilliad.univ-lille.fr

Thèse de Xinzhe Wu, Université de Lille, 2019

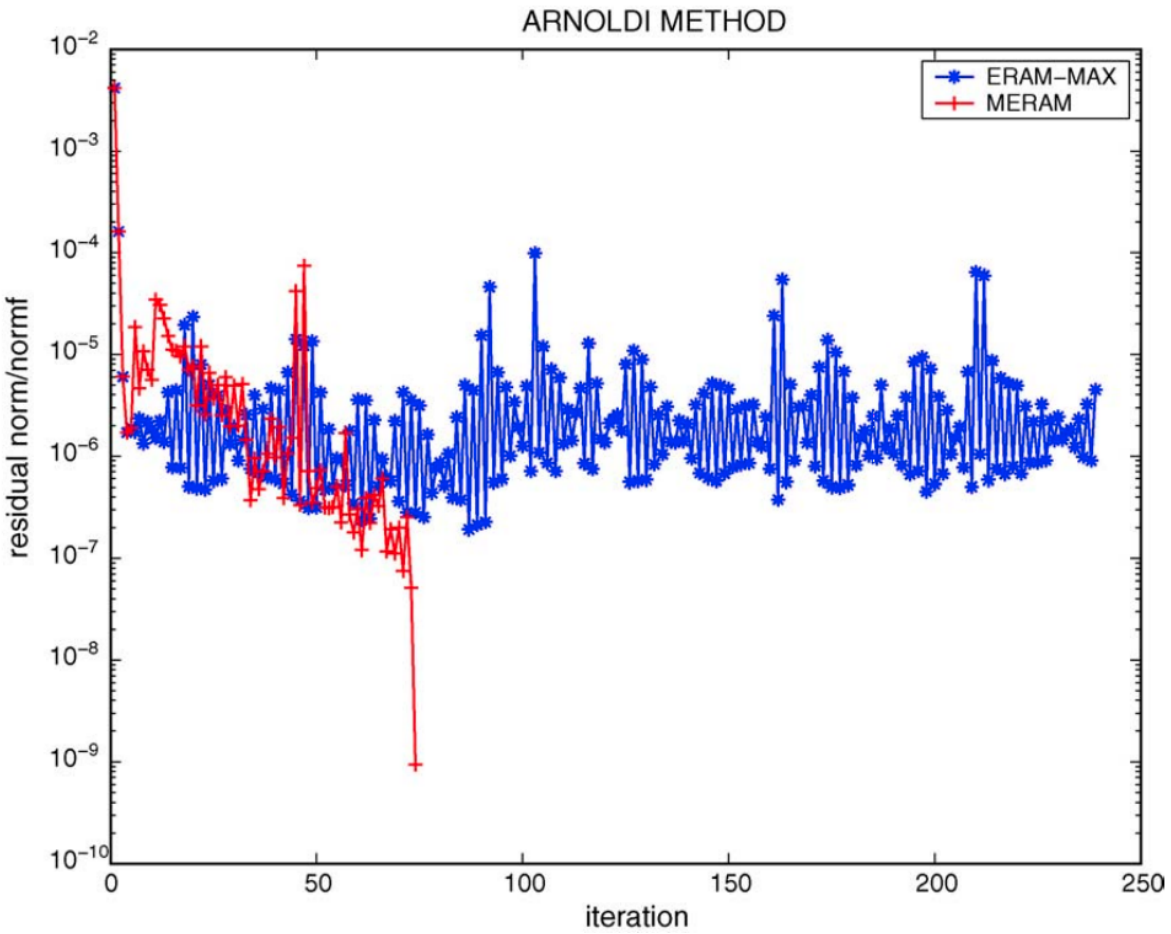

Figure 5.2 – An example of MERAM: MERAM(5,7,10) vs. ERAM(10) with af 23560.mtx matrix. MERAM converges in 74 restarts, ERAM does not converge after 240 restarts [84].

values implicitly by QR factorization and Krylov-Schur decomposition, respectively.

5.2.1.3 Preconditioning by Polynomial

In order to approximate the solution of linear system (3.1), one approach is to get the inverse of A, denote it as A^{-1}, and then an approximate solution can be easily obtained as $\tilde{x} = A^{-1}b$. $\tilde{x}$ can be applied as a new residual vector for the subsequent restart, that is the polynomial preconditioning for linear solvers. In detail, the cycle step of iterative methods is able to construct a Hessenberg matrix H_m by the Arnoldi reduction. Then some dominant eigenvalues are approximated through the Ritz values of H_m. The preconditioning step is to get the optimal polynomial p_k by these Ritz values to approximate A^{-1}, and p_k is used to generate a new $\tilde{x}$ for the next time restart of iterative methods.

The idea of polynomial preconditioning for the iterative solvers of eigenvalue problems is similar to the one for linear systems. In detail, a selected polynomial p_k can be constructed by the set of unwanted eigenvalues and new gotten Ritz values from previous Arnoldi reduction, and the operator A can be replaced by $B_k = p_k(A)$. This polynomial is able to amplify the wanted eigenvalues of A into the eigenvalues of B_k with much larger norms compared with other remaining eigenvalues, which will result in much faster convergence. The eigenvalues of A can

© 2019 Tous droits réservés.

lilliad.univ-lille.fr

Thèse de Xinzhe Wu, Université de Lille, 2019

be obtained from the ones of B_k by a Galerkin projection. The polynomial p_k can be formulated either by the Chebyshev basic with the best ellipse constructed by the unwanted and known eigenvalues[184], or by a polygon refined with these unwanted and known eigenvalues [142].

5.2.1.4 Preconditioning by Shift-Invert

Classic Krylov method is able to approximate the dominant eigenvalues. If the wanted values are not dominant, it is necessary to enlarge the Krylov subspace size, which requires larger memory and computational operations. One of the most effective techniques for solving such problems is to iterate with the shifted and inverted matrix $(A - \sigma I)^{-1}$. The eigenvalues approximated by this new operator are the ones around the given shift σ. Different fractions of eigenvalues can be efficiently calculated by changing σ.

5.2.1.5 Analysis

Table 5.1 summarizes the required information for the deflation, polynomial and Shift-Invert preconditioners of linear and eigensolvers. For the explicit deflation of iterative methods, the Ritz pair obtained from H_m are used to perform the preconditioning. The implicitly deflated solvers use directly the Hessenberg matrix H_m and the orthonormal basis of Krylov subspace V_m to accelerate the convergence. The polynomial preconditioners for solving linear systems use the dominant eigenvalues approximated from H_m to construct the best polynomial, and the unwanted Ritz values to formulate the preconditioning polynomial for solving eigenvalue problems. A special Shift-Invert preconditioner for eigenvalue problems is able to quickly approximate different parts of eigenvalues by selecting different shift value σ. The preconditioners implemented based on matrices is not listed in Table 5.1.

Table 5.1 – Information used by preconditioners to accelerate the convergence.

Info \ Solver / Precond	Linear Solver	Eigen Solver
Explicit Deflation	Ritz values and vectors	Ritz values and vectors
Implicit Deflation	H_m and V_m	H_m and V_m
polynomial	Dominant Ritz values	unwanted Ritz values
Shift-Invert	×	shift value σ

5.2.2 Separation of Components

As presented in Section 3.8, iterative methods for solving linear systems and eigenvalue problems on extreme-scale platforms should be modified and optimized by minimizing global communication, reducing synchronization points, and promoting asynchronicity. Recent studies have focused more on the optimization of different parts inside iterative methods, e.g., the communication

© 2019 Tous droits réservés.

lilliad.univ-lille.fr

Thèse de Xinzhe Wu, Université de Lille, 2019

avoiding techniques for linear algebra operations [116, 50] and pipelined strategies for Krylov methods [148, 60]. Since modern supercomputing can be seen as distributed and parallel computing, it is necessary to divide the applications into different complex components according to their functionalities. They should be implemented with asynchronous communications and controlled by a manager engine. The first step is to identify different components of preconditioned iterative methods.

5.2.2.1 Component Identification inside Iterative Methods

Based on Table 5.1, the mechanism to divide the numerical methods into different computational components is proposed. For the deflation and polynomial preconditioned iterative methods, the important information for the preconditioning is either H_m and V_m or the Ritz pairs obtained from H_m and V_m. Immediately, they can be divided into two parts: the solving and preconditioning parts. Moreover, a supplementary computational component should also be provided which is able to generate the information used by the preconditioners. Finally, these algorithms can be divided into three kinds of computational components:

- *Solver Component* for solving problems;
- *Information Generator Component* to generate this information used by the preconditioners;
- *Preconditioner Component* for the preconditioning pretreatment for the solvers.

Fig. 5.3 gives a cyclic relation of the proposed three components for the deflation and the polynomial preconditioned methods, which communicate with each other by asynchronous communications. Various existing algorithms can be transformed into the three types of components, e.g., for the polynomial preconditioned solver for linear systems, three types of computational components are:

(1) an iterative method to solve the systems;

(2) an eigensolver to approximate the dominant eigenvalues;

(3) a preconditioning pretreatment component to generate the preconditioning parameters, either by the ellipse or the refinement of polygon constructed by the approximated Ritz values.

and for the deflated eigensolvers, three types of computational components are:

(1) an eigensolver to solve the problems;

(2) another eigensolver with different settings (e.g., the Krylov subspace size, the shift value) to generate the information for preconditioning, such as H_m and V_m for the implicit deflation and Ritz pairs for the explicit deflation;

(3) best preconditioning information can be selected by the *Preconditioner Component* using the information of previous two components (e.g., for explicit deflation, the best information can be the combination of Ritz vectors from different components), and it can achieve better numerical performance than conventional deflated iterative methods.

© 2019 Tous droits réservés.

lilliad.univ-lille.fr

Thèse de Xinzhe Wu, Université de Lille, 2019

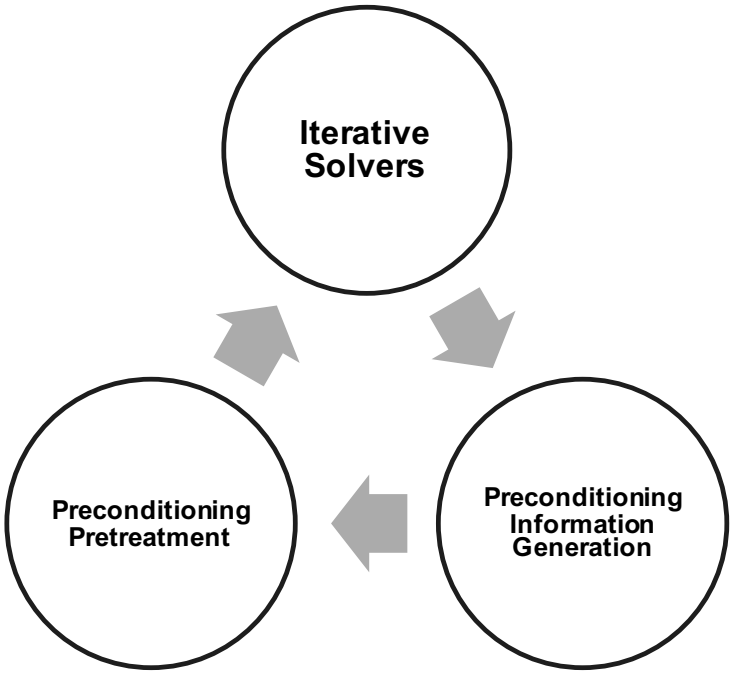

Figure 5.3 – Cyclic relation of three computational components.

For the shift-invert preconditioned eigensolvers, they can be divided into several similar solvers with different shift value σ. These components can be tickly restarted with much smaller Krylov subspace size to approximate a small fraction of wanted eigenvalues. The total wanted ones can be a combination the subsets of different components. This is similar to the spectrum slicing strategies for restarted Lanczos methods introduced by Campos et al. [49].

For the matrix preconditioned methods, it is difficult to divide the solver and preconditioning matrix into two independent components with asynchronous communications, since the preconditioned matrix M should be left or right multiplied with the operator A for each time projection inside the Arnoldi reduction process, which cannot be explicitly separated.

5.2.2.2 Distributed and Parallel Implementation of Components

By dividing the preconditioned iterative methods into different components, they can be implemented in a distributed manner. Each component can be implemented in parallel. These different components communicate with others by asynchronous communications. They can concentrate on their own tasks independently from other components unless the necessary data are asynchronously received from others. The dependencies of tasks for the preconditioning inside iterative methods can be reorganized in a more flexible way. For each component, it can be replaced by the implementation with the linear algebra operations optimized by the recent research, which introduce a potential improvement for the parallel performance of each component. The separation of components makes it easier to take advantage of current research to optimize linear algebra operations within iterative methods, thereby improving the parallel performance of each computational component.

© 2019 Tous droits réservés.

lilliad.univ-lille.fr

Thèse de Xinzhe Wu, Université de Lille, 2019

5.2.3 Benefits of Separating Components

Dividing iterative methods into components with asynchronous communication introduces both numerical and parallel benefits for them.

Numerical benefits: for conventional deflation and polynomial preconditioned methods, the information used is obtained from previous Arnoldi reduction, and it might be difficult to explore larger subspace. Therefore, the convergence might be slowed down. For the methods implemented with the proposed paradigm, the solving and preconditioning parts are independent, thus for the *Information Generator Component*, different Arnoldi reduction procedures can be implemented in the same time with much larger Krylov subspace or other parameters. This information applied to the deflation or polynomial preconditioned *Solver Components* can be different from their own Arnoldi reduction, which improve the flexibility the algorithms, e.g., much more eigenvalues and larger searching space for the deflation. Hence the limitation of spectral information caused by restarting might be broken down, and faster convergence might be obtained. The numerical benefits for linear and eigensolver are already respectively discussed in [225] and [84].

Parallel benefits: parallel performance of iterative methods can be improved by the promotion of asynchronization and reduction of synchronizations and global communications, especially the synchronization points for the preconditioning. Separating components improves also the fault tolerance and reusability of algorithms.

Multi-level parallelism: the iterative solvers implemented based on Unite and Conquer approach is able to explore multi-level parallelism of the distributed memory computing architectures. The three-level parallelism is listed below:

(1) *Coarse Grain/Component level*: this paradigm allows the distribution of different numerical components on different platforms, processors or computing nodes;

(2) *Medium Grain/Intra-component level*: each computational component is able to be deployed in parallel with a collection of cores/nodes on distributed memory systems;

(3) *Fine/Thread level for shared memory*: either the thread level parallelism in CPU or accelerator level parallelism if GPUs or other accelerators are available.

5.3 Proposition of UCGLE

In this section, we try to propose a new multi-level parallelism programming paradigm to solve linear systems based on the Unite and Conquer approach. We select the hybrid method preconditioned by the Least Squares polynomial to construct a distributed and parallel linear solver, that is the UCGLE method. Firstly, Section 5.3.1 present different computational components inside UCGLE. In Section 5.3.2, we give the workflow and implementation of UCGLE.

5.3.1 Selection of Components

We list the details of the three computational components in UCGLE as below,

(1) *Solver Component:* this component is implemented with restarted GMRES to solve non-Hermitian linear systems.

© 2019 Tous droits réservés.

lilliad.univ-lille.fr

Thèse de Xinzhe Wu, Université de Lille, 2019

(2) *Information Generator Component:* the materials for Least Squares polynomial preconditioner are the dominant eigenvalues, thus this type of component is implemented with ERAM to approximate the eigenvalues.

(3) *Preconditioner Component:* this component is to generate the Least Squares polynomial preconditioning parameters using the approximated eigenvalues by the ERAM Component. In this thesis, it is denoted as LSP component.

5.3.2 Workflow

In the conventional implementation of this hybrid method, the eigenvalues used to construct the Least Squares polynomials are computed by the Hessenberg matrix H_m after each time Arnoldi reduction cycle of GMRES. In UCGLE, the linear solver, the approximation of eigenvalues and the construction of Least Squares polynomials are separated into three different parts. These three computing components work independently with each other, and they share the necessary information by the asynchronous communications.

UCGLE method is mainly composed of two parts: the first part uses the restarted GMRES method to solve the linear systems; in the second part, it computes a certain number of approximated eigenvalues, and then applies them to the Least Squares polynomial method and gets a new preconditioned residual, as a new initial vector for restarted GMRES.

Figure 5.4 gives the workflow of UCGLE method with three computational components. ERAM Component and GMRES Component are implemented in parallel, and the communication between them is asynchronous. ERAM Component computes a desired number of eigenvalues, and then sends them to LSP Component; LSP Component uses these received eigenvalues to output the preconditioning parameters, and sends them to GMRES Component; GMRES Component uses these parameters to generate a new restarted initial vector for solving non-Hermitian linear systems.

5.4 Distributed and Parallel Implementation

This section gives the distributed and parallel implementation of UCGLE, including the components, the multi-level parallelism, the manager engine, and the asynchronous communications.

5.4.1 Component Implementation

This section describes the basic implementation and workflow of each component in UCGLE. Algorithm 23 details the entire implementation of UCGLE.

5.4.1.1 GMRES Component

GMRES Component aims to solve a linear system $Ax = b$. It takes an operator matrix A and two vectors, x the initial guess vector and b the related RHS as input. GMRES approximates the solution starting from this initial guess vector until the exact solution is found or if a stopping criterion is met, for example, that the residual norm is below a given threshold (e.g.,

© 2019 Tous droits réservés.

lilliad.univ-lille.fr

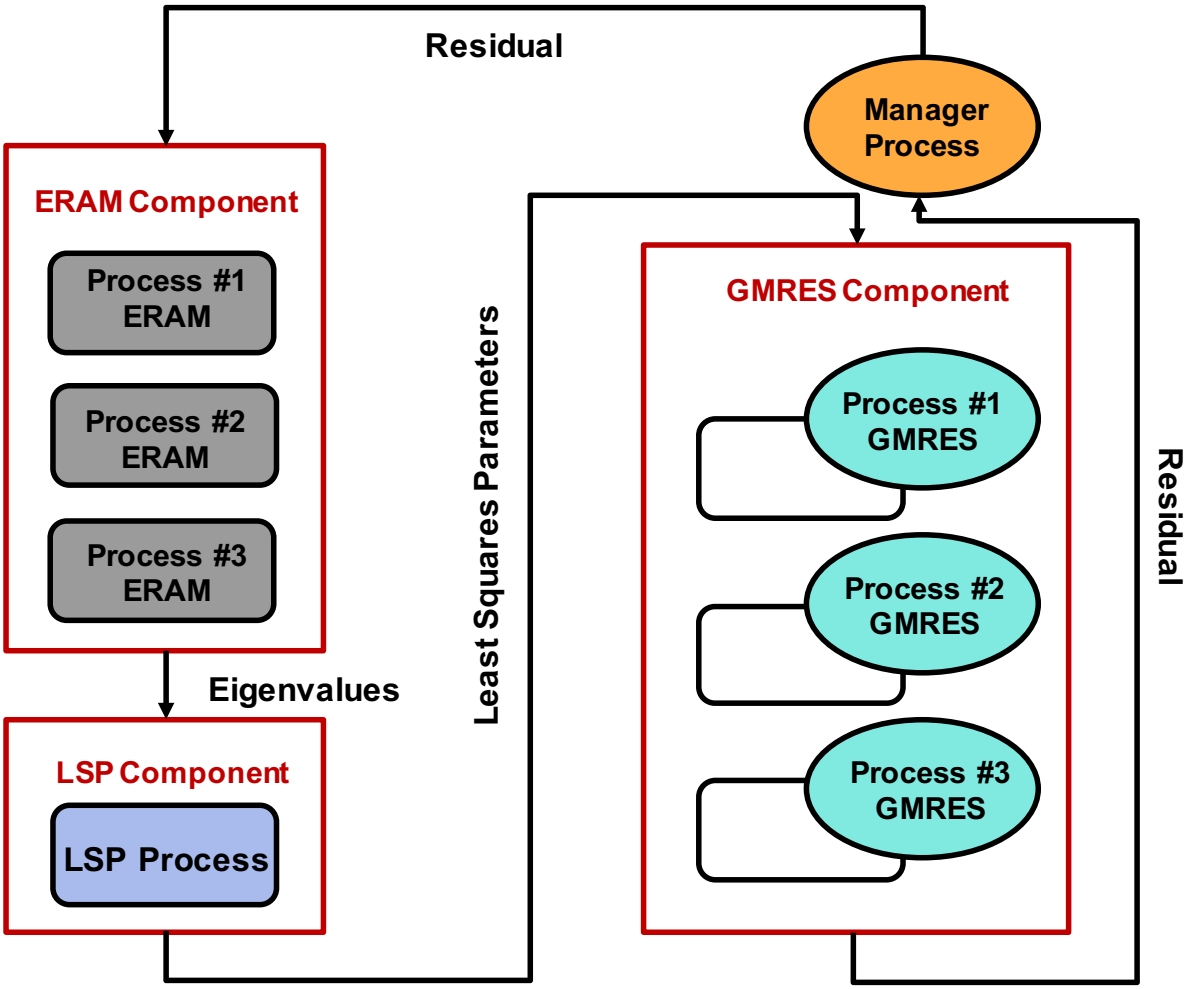

Figure 5.4 – Workflow of UCGLE method.

$||r||_2 \leq 10e^{-8}$). In practice, GMRES are restarted after m steps of iterations in order to reduce the memory requirement.

Fig. 5.5 gives the workflow of GMRES Component. GMRES Component loads the parameters $A, m_g, x_0, b, \epsilon_g, freq, lsa$ to solve the linear systems. At the beginning of execution, it behaves like the basic GMRES method. When it finishes the m^{th} iteration, it will check if the condition $||b - Ax_m|| < \epsilon_g$ is satisfied, if yes, x_m is the approximated solution of linear system $Ax = b$, or GMRES Component will be restarted using x_m as a new initial vector. A parameter *count* is used to count the times of restart. All these processes are similar to a restarted GMRES. However, when *count* is an integer multiple of $freq$ (number of GMRES restarts between two times preconditioning of Least Squares polynomial), it will check if it has received the parameters A_d, B_d, Δ_d, H_d from LSP Component. If yes, these parameters will be used to construct a preconditioning polynomial P_d, which can be used to generate a preconditioned residual x_d, then set the initial vector x_0 as x_d, and restart the basic GMRES, until the exit condition is satisfied. We reused PETSc's GMRES implementation and modified it to include sending and receiving data and calculating the new residual by Least Squares polynomial.

© 2019 Tous droits réservés.

lilliad.univ-lille.fr

Thèse de Xinzhe Wu, Université de Lille, 2019

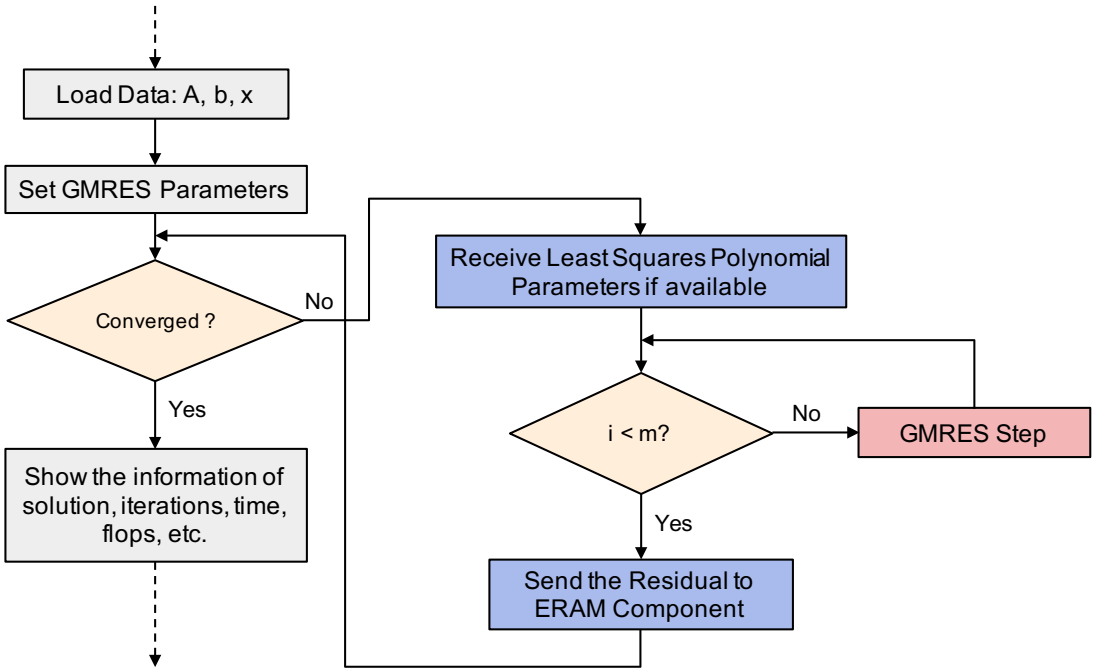

Figure 5.5 – GMRES Component.

5.4.1.2 ERAM Component

Fig. 5.6 gives the workflow of ERAM Component. ERAM Component loads the parameters m_a, v, r, ϵ_a and the operator matrix A, then launches ERAM function. When it receives a new vector X_TMP from GMRES Component, this vector will be stored in ERAM Component. This vector is updated with the continuous receiving of a new one from GMRES Component. If the r eigenvalues Λ_r are approximated by ERAM Component, it will send them to LSP Component, at the same time, it is able to save the eigenvalues into the local file. We reused SLEPc's ERAM implementation by adding the sending and receiving functionalities.

5.4.1.3 LSP Component

Fig. 5.7 gives the workflow of LSP Component. LSP Component will not start work until it receives the eigenvalues Λ_r sent from ERAM Component. Then it will use them to compute the parameters A_d, B_d, Δ_d, H_d, whose dimensions are related to d, the Least Squares polynomial degree, and send these parameters to GMRES Component. The Cholesky factorization inside LSP Component is implemented by the routine provided by LAPACK.

Algorithm 23 Implementation of Components

1: **function** LOADERAM(*input*: $A, m_a, \nu, r, \epsilon_a$)
2: **while** exit==False **do**
3: ERAM($A, r, m_a, \nu, \epsilon_a$, *output*: Λ_r)
4: Send (Λ_r) to LSP Component
5: **if** $saveflg == TRUE$ **then**
6: write (Λ_r) to file *eigenvalues.bin*
7: **end if**

© 2019 Tous droits réservés.

lilliad.univ-lille.fr

Thèse de Xinzhe Wu, Université de Lille, 2019

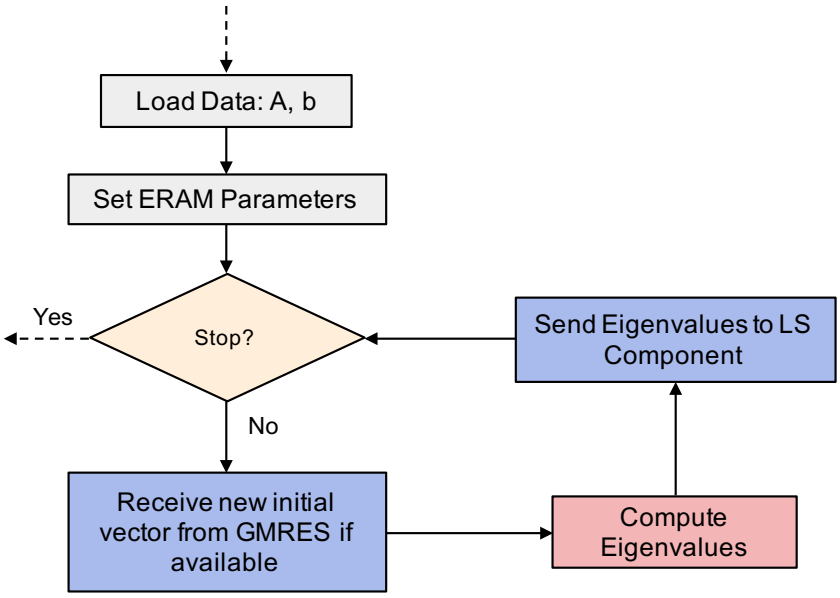

Figure 5.6 – ERAM Component.

8: **if** Recv (X_TMP) **then**
9: update X_TMP
10: **end if**
11: **if** Recv $(exit == TRUE)$ **then**
12: Send $(exit)$ to LSP Component
13: stop
14: **end if**
15: **end while**
16: **end function**
17: **function** LOADLS($input$: A, b, d)
18: **if** Recv(Λ_r) **then**
19: LSP-Pretreatment($input$: A, b, d, Λ_r, $output$: A_d, B_d, Δ_d, H_d)
20: Send $(A_d, B_d, \Delta_d, H_d)$ to GMRES Component
21: **end if**
22: **if** Recv $(exit == TRUE)$ **then**
23: stop
24: **end if**
25: **end function**
26: **function** LOADGMRES($input$: $A, m_g, x_0, b, \epsilon_g, freq, lsa$, $output$: x_m)
27: $count = 0$
28: BASICGMRES($input$: A, m, x_0, b, $output$: x_m)
29: $X\_TMP = x_m$
30: Send (X_TMP) to ERAM Component
31: **if** $||b - Ax_m|| < \epsilon_g$ **then**
32: **return** x_m
33: Send $(exit == TRUE)$ to ERAM Component

© 2019 Tous droits réservés.

lilliad.univ-lille.fr

Thèse de Xinzhe Wu, Université de Lille, 2019

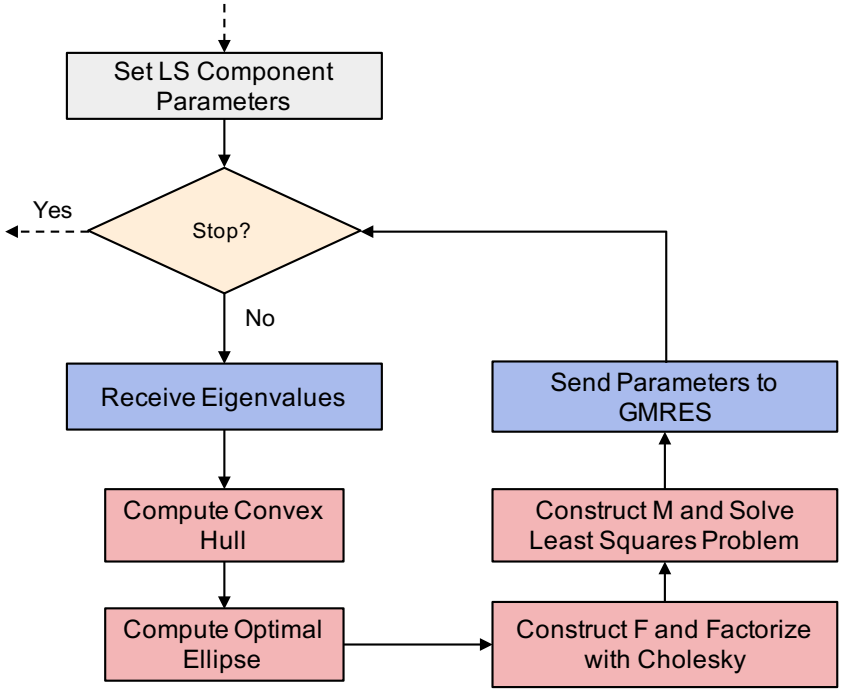

Figure 5.7 – LSP Component.

Stop
else
  if *count* | *freq* **then**
    if recv $(A_d, B_d, \Delta_d, H_d)$ **then**
      $r_0 = f - Ax_0$, $\omega_1 = r_0$ and $x_0 = 0$
      for $k = 1, 2, \cdots, lsa$ **do**
        for $i = 1, 2, \cdots, d-1$ **do**
          $\omega_{i+1} = \frac{1}{\beta_{i+1}}[A\omega_i - \alpha_i\omega_i - \delta_i\omega_{i-1}]$
          $x_{i+1} = x_i + \eta_{i+1}\omega_{i+1}$
        end for
      end for
      set $x_0 = x_d$, and GOTO 28
      $count++$
    end if
  else
    set $x_0 = x_m$, and GOTO 28
    $count++$
  end if
end if
if Recv $(exit == TRUE)$ **then**
  stop
end if
end function

© 2019 Tous droits réservés.

lilliad.univ-lille.fr

Thèse de Xinzhe Wu, Université de Lille, 2019

5.4.2 Parameters Analysis

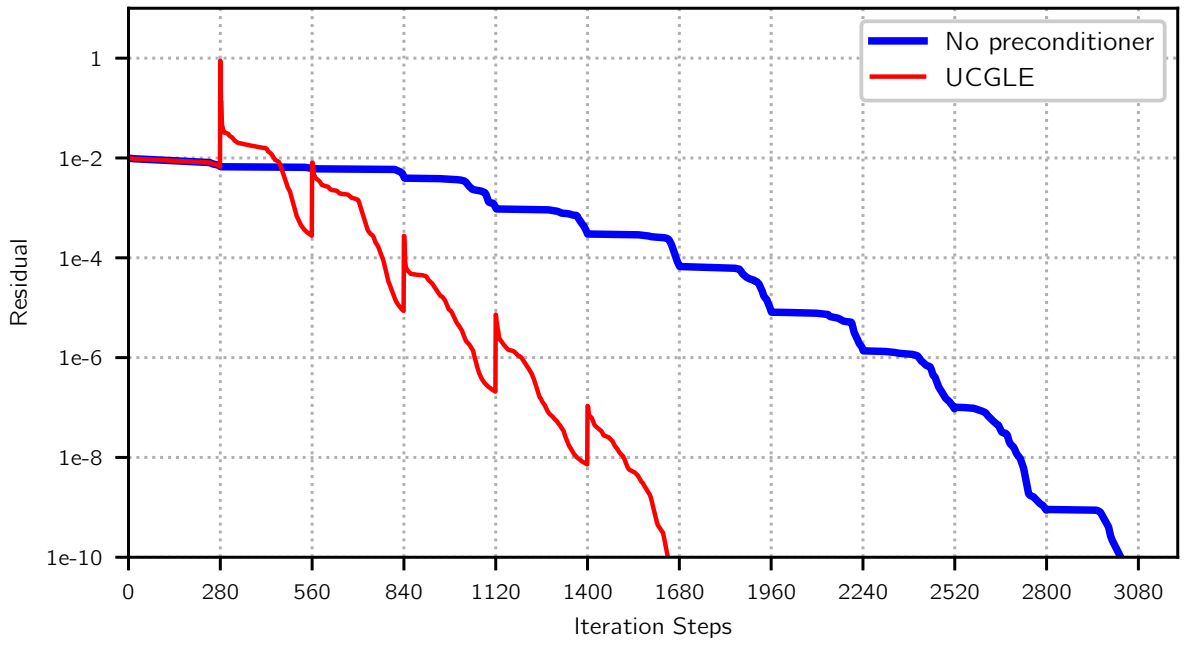

Figure 5.8 – Convergence comparison of UCGLE method vs classic GMRES.

UCGLE method is a combination of three different methods, there are a number of parameters, which have impacts on its convergence rate. We summarize these different related ones, and classify them according to their relations with different components.

1. GMRES Component
   (a) m_g: GMRES Krylov Subspace size
   (b) ϵ_g: absolute tolerance for the GMRES convergence test
   (c) P_g: GMRES core number
   (d) lsa: number of times that polynomial applied on the residual before taking account into the new eigenvalues
   (e) $freq$: number of GMRES restarts between two times of Least Squares polynomial preconditioning
2. ERAM Component
   (a) m_a: ERAM Krylov subspace size
   (b) r: number of eigenvalues required
   (c) ϵ_a: tolerance for the ERAM convergence test
   (d) P_a: ERAM core number
3. LSP Component
   (a) d: Least Squares polynomial degree

© 2019 Tous droits réservés.

lilliad.univ-lille.fr

Thèse de Xinzhe Wu, Université de Lille, 2019

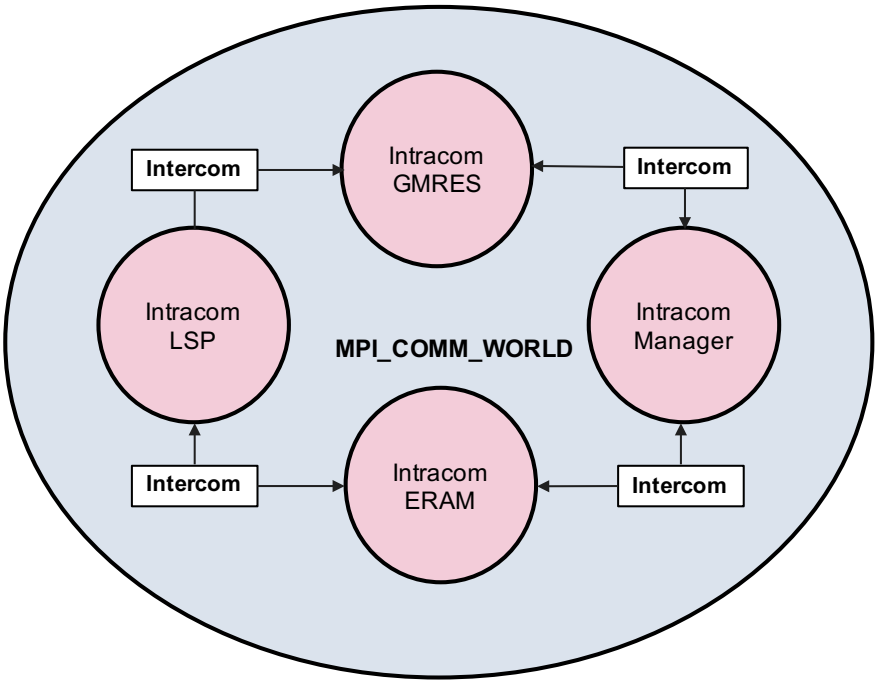

Figure 5.9 – Creation of Several Intra-Communicators in MPI.

Suppose that the convex hull constructed for Least Squares polynomial contains eigenvalues $\lambda_1, \cdots, \lambda_m$, the residual given by Least Square polynomial of degree $d-1$ is

$$r = \sum_{i=1}^{m} \rho_i R_d(\lambda_i) u_i + \sum_{i=m+1}^{n} \rho_i R_d(\lambda_i) u_i$$

In practice, it is limited for choosing the degree of polynomial degree by the fact that the moment matrix M_d becomes difficult to compute and to factor as the degree d increases. A classical solution to this problem is to compound lsa times a small degree polynomial. The residual given by Least Squares polynomial tends to be

$$r = \sum_{i=1}^{m} \rho_i (R_d(\lambda_i))^{lsa} u_i + \sum_{i=m+1}^{n} \rho_i (R_d(\lambda_i))^{lsa} u_i$$

The first part of this residual is minimized by the Least Square polynomial method using the eigenvalues inside convex hull H_m, and the second part is large since the related eigenvectors associated with the eigenvalues outside H_m. With the number of approximated eigenvalues increasing, the first part will be much closer to zero and the second part keeps enormous. The next restart process of GMRES can be still accelerated since it restarts with the combination of eigenvectors. The more eigenvalues are known, the more significant acceleration will be. The convergence comparison of UCGLE and classic GMRES is given in Fig. 5.8. The large peaks appear in the UCGLE curve for each time restart. It means that the residual turns to be large, and then will drop down very quickly with the acceleration of Least Squares polynomial method.

© 2019 Tous droits réservés.

lilliad.univ-lille.fr

Thèse de Xinzhe Wu, Université de Lille, 2019

5.4.3 Distributed and Parallel Manager Engine Implementation

GMRES method has been implemented by PETSc, and ERAM method is provided by SLEPc. Additional functions have been added to the GMRES and ERAM provided by PETSc and SLEPc to include the sending and receiving functions of different types of data. For the implementation of LSP Component, it computes the convex hull and the ellipse encircling the Ritz values of matrix A, which allows the generation of a new Gram matrix M_d based on the selected Chebyshev polynomial basis. This matrix should be factorized into LL^T by the Cholesky algorithm. The Cholesky method is ensured by PETSc as a preconditioner but can be used as a factorization method. Implementation based on these libraries allows recompilation of UCGLE code to accommodate CPU and GPU architectures. The experimentation in this chapter did not consider the OpenMP thread level of parallelism because the implementation of PETSc and SLEPc was not thread-safe due to its complex data structure. The data structures of PETSc and SLEPc makes it more difficult to partition the data among the threads to prevent conflict and to achieve good performance [26].

5.4.3.1 Implementation of the Inter-component Communication Network

In order to establish different computational components with asynchronous communications, the first solution is to create several communicators inside of *MPI_COMM_WORLD* and their inter-communication. The topology of communication among these groups is a circle shown in Figure 5.9. The total number of computing units supplied by the user is thus divided into four groups according to the following distribution: P_t is the total number of processes, then $P_t = P_g + P_a + P_l + P_m$, where P_g is the number of processes assigned to GMRES Component, P_a the number of processes to ERAM component, P_l the number of processes allocated to LSP Component and P_f the number of processes allocated to *Manager Process* proxy. P_g and P_a are greater than or equal to 1, P_l and P_m are both exactly equal to 1. LSP Component is a serial component. According to Section 3.5.3.4, the generation of Least Squares polynomial parameters by the Cholesky factorization and least squares problem are implemented by the subroutines provided by LAPACK with small size dense matrices, on process can fulfill the requirements.

P_t is thus divided into several MPI groups according to a color code. The minimum number of processes that our implementation requires is 4. We utilize the mechanism of standard MPI to fully support the communication of our application. The communication layer that does not depend on the application, which allows the replacement and scalability of various components provided.

5.4.3.2 Asynchronous Communication Mechanism

As shown in Figure 5.10, UCGLE has three levels of parallelism which is suitable for the modern supercomputers. In fact, the main characteristic of UCGLE method is its asynchronous communication. But the synchronous communication takes place inside of GMRES and ERAM components. Distributed and parallel communication involves different types of exchange data, such as vectors, scalar arrays, and signals among different components. When the data are sent and received in a distributed way, it is essential to ensure the consistency of data. In our case,

© 2019 Tous droits réservés.

lilliad.univ-lille.fr

Thèse de Xinzhe Wu, Université de Lille, 2019

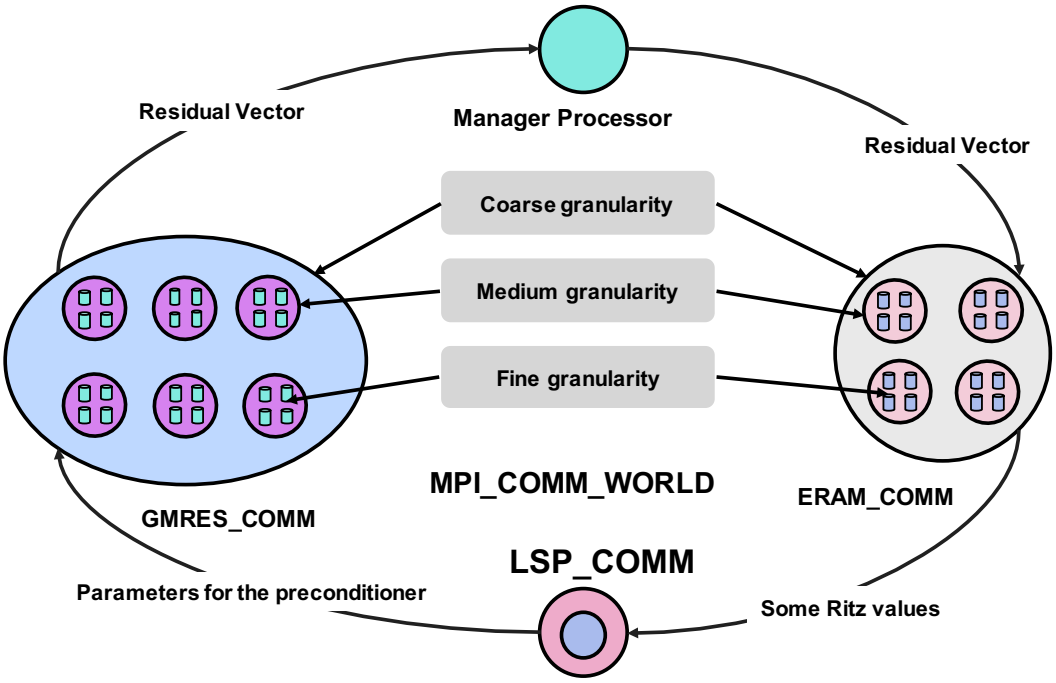

Figure 5.10 – Communication and different levels parallelism of UCGLE method

we choose to introduce an intermediate node as a proxy to carry out only several types of exchanges and thus facilitate the implementation of asynchronous communication. This proxy is called *Manager Process* as in Figure 5.10. One process can fulfil all the data exchanges.

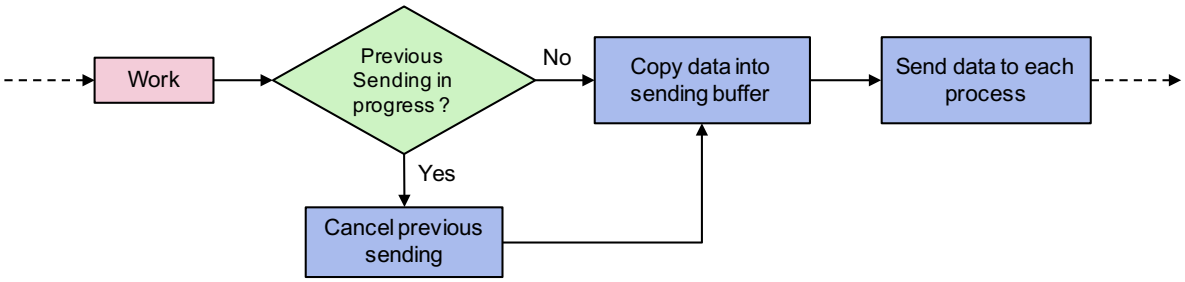

Figure 5.11 – Data sending scheme from one group of process to the other.

Asynchronous communication allows each computational component to conduct independently the work assigned to it without waiting for the input data. The asynchronous sending and receiving operations are implemented by the non-blocking communication of MPI. Sending takes place after the sender has completed the task assigned to it. Before any prior shipment, the component checks whether several sendings are now on the way. If yes, this task will be canceled to avoid the competition of different types of sending tasks. Sent data are copied into a buffer to prevent them from being modified while sending. For the asynchronous data receiving, before starting this task, the component will check if data is expected to be received. Once the receiving buffer is allocated, the component performs the receiving of data while respecting the distribution of data globally according to the rank of sending processes. It is also essential to validate the consistency of receiving data before any use of them by the tasks and components.

Asynchronous Sending: The sending operation (shown as Fig. 5.11), as we described, will start by verifying if the previous sending operations are pending or not. If some operations are

© 2019 Tous droits réservés.

lilliad.univ-lille.fr

Thèse de Xinzhe Wu, Université de Lille, 2019

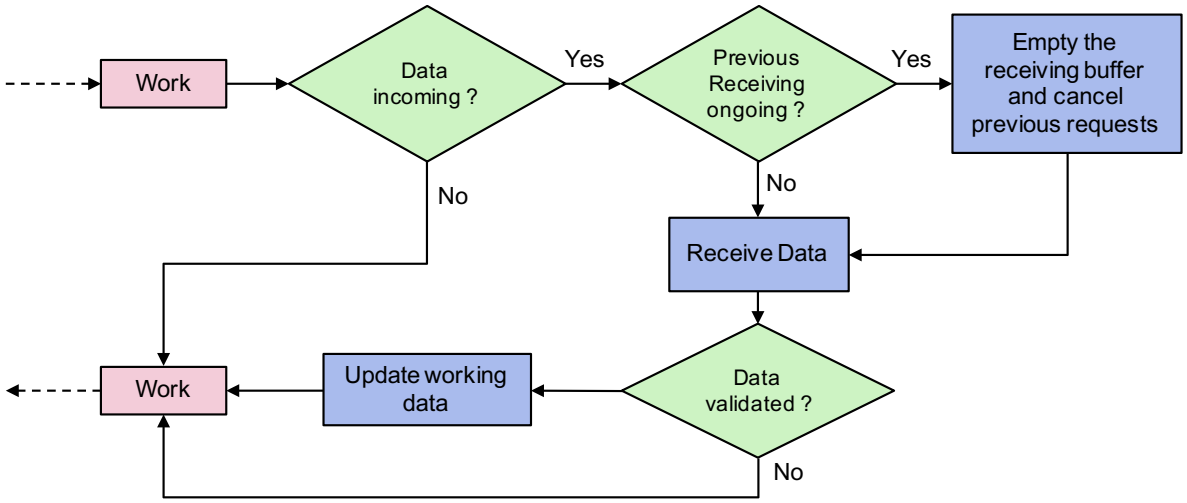

Figure 5.12 – Data receiving scheme from one group of process to the other.

not finished, they are canceled so as not to be in a state where several sending operations with different data are in competition. In the practical implementation, we use the MPI_Request to track the state of an asynchronous request. Once the verification is validated, then the data to be sent will be copied to a buffer to prevent them overwritten by other work operations. Then, this data is sent to the different nodes of the other components, respecting the distribution negotiated during the initialization of the communications via the standard asynchronous sending function MPI_Isend.

Asynchronous Receiving: In the context of send-and-receive communication mechanisms, the receiving operation (shown as Fig. 5.12) is often the most difficult to implement because it requires a synchronization point. As far as we are concerned, we have hidden this synchronization point thanks to an input verification step. Indeed, we have chosen to implement a test function before proceeding with asynchronous receiving operation instead of going through a purely asynchronous reception function. The data input test is done via the MPI_Iprobe function and the MPI_Recv reception. The latter is blocking or synchronous, that is, once called the computing node would wait for data to be received before returning to the calling function.

At first glance, it would seem wiser to go through the non-blocking receiving function MPI_Irecv. However, in practice, this function requires to know in advance the size of the data to be received, which is not the case where our components work with a dynamic receiving buffer, e.g., the receiving buffer for the eigenvalues should be resized with more and more eigenvalues approximated by ERAM. In our implementation, this dynamic buffer is allocated thanks to the information provided by the operation MPI_Get_count using structure MPI_Status filled in by the function MPI_Iprobe. Also, apart from this difference, our asynchronous receiving mechanism is fundamentally similar to the MPI_Irecv function in that it only receives data if it is available.

In addition to the implementation of asynchronous sending and receiving functions, we integrated a mechanism for checking the consistency of the received data. In order to allow different independent groups of computing nodes (our components), we have used the tools that are the intra-communications and inter-communicators MPI. The problem of this type of implementation is that it does not allow collective communications between the different nodes of two

© 2019 Tous droits réservés.

lilliad.univ-lille.fr

Thèse de Xinzhe Wu, Université de Lille, 2019

communicating groups. The communications between groups of nodes (or components) through the intercommunication only allow collective communications between one master process of a group and the nodes of others groups. It is therefore quite limited when the goal is to carry out entirely collective communications, that is to say, to allow all the nodes of a group to communicate with all the nodes of another group. Indeed, even if we go through the proxy to facilitate communication control, data consistency must be checked before any prior use. For example of a distributed vector, if a vector is partially received, it can not be used, otherwise, we could witness a disaster from a numerical point of view. Also, to avoid this kind of pitfall, we have integrated a validation mechanism that will check if the received data are consistent before they are used. The consistency check is conveniently performed by comparing the total size of the data received by each component node against the size of the data to be received at all. If this is consistent, then the receiving buffer data is placed in the working memory of each node of the receiving component.

5.5 Experiment and Evaluation

5.5.1 Hardware

In experiments, we implement UCGLE on the supercomputers *Tianhe-2* and *Romeo-2013*. The details of the two machines are already given in Section 4.6.1.

5.5.2 Parameters Evaluation

After the implementation of UCGLE, at first, we evaluate the influence of different parameters on its convergence. The selected parameters to be evaluated are:

(1) Krylov subspace size for GMRES;

(2) Least Squares polynomial degree;

(3) Least Squares polynomial applied times;

(4) Least Squares polynomial frequency;

(5) Number of eigenvalues.

5.5.2.1 Test Matrix Suite

UCGLE has been evaluated using the test matrices from Matrix Market collections, shown as Table 5.2. In this section, we select to use matrix *utm*300 to understand the influence of different parameters on the convergence of UCGLE.

The matrix *utm*300 is constructed from an electromagnetic problem, with its condition number number being 8.466435×10^5.

© 2019 Tous droits réservés.

lilliad.univ-lille.fr

Thèse de Xinzhe Wu, Université de Lille, 2019

Table 5.2 – Test Matrix from Matrix Market Collection.

Matrix	Size	NNZ	Domain
utm300	300	3155	$\mathbb{R}$
utm1700b	1700	21509	$\mathbb{R}$
pde2961	2961	14585	$\mathbb{R}$
young4c	841	4089	$\mathbb{C}$

5.5.2.2 Influence of Different Parameters on the Convergence

In order to highlight the impacts of different parameters inside UCGLE, we conducted several sets of experiments, which vary one parameter mentioned above, and keep the other parameters fixed. In this section, we will present the results of these experiments and then analyze the impact of each parameter on the preconditioning, thus the acceleration of convergence. We study the parameters including the Krylov subspace size of GMRES m_g, the times of Least Squares preconditioning applied on the GMRES lsa, the frequency of Least Squares preconditioning applied $freq$, the number of eigenvalues approximated by ERAM Component n_{eigen}, and the degree of Least Squares polynomial d.

Krylov subspace size: The parameter m_g, which means the restarted subspace size of GMRES, has important influence on the convergence of UCGLE. This effect is similar with the case on the conventional GMRES without preconditioning. For the experiments of UCGLE, we vary m_g from 50 to 180, and keep $l = 10$, $lsa = 10$, $freq = 1$. Moreover, we evaluate also the classic GMRES with m_g to be 100 and 150. The results are given in Fig. 5.13. First of all, we can conclude that in the case that m_g is too small (see UCGLE($m_g = 50$) in Fig. 5.13), even the Least Squares preconditioning is applied, the convergence cannot be achieved. With the augmentation of m_g, UCGLE is able to achieve the convergence with fewer iteration steps. Secondly, with the preconditioning of Least Squares polynomial, UCGLE can converge with $m_g = 100$, but the classic GMRES cannot converge using the same value of this parameter.

In conclusion, the Krylov subspace size of GMRES Component is a very important parameter of UCGLE. If this parameter is too small, it is difficult to get the convergence even with the Least Squares polynomial preconditioning. It is not practical to use very large m_g since the limitation of memory. Thus, it is essential to determine a good value of m_g which is able to able to accelerate the convergence by Least Squares polynomial preconditioning. Moreover, UCGLE is able to converge with smaller Krylov subspace size that classic GMRES cannot achieve the convergence with. The smaller Krylov subspace size is effective to reduce the number of global communications of SpMV inside Arnoldi reduction, and also the memory requirement.

Least Squares polynomial degree: The parameter d means the degree of Least Squares polynomial applied to the temporary residual of GMRES. If this polynomial is formulated by the polygon built by all the eigenvalues of operator A, the larger d is, the better the approximation of solution will be, theoretically. In the experiments, d are set respectively to be 5, 10, 15, 20 and 25, and the parameters m_g, lsa, and $freq$ are respectively fixed as 100, 10 and 1. Fig. 5.14 shows the convergence curves of all the tests. The influence of d is clear, with the increase of d, the residual norm of the restart vector produced by Least Squares polynomial will be enlarged,

© 2019 Tous droits réservés.

lilliad.univ-lille.fr

Thèse de Xinzhe Wu, Université de Lille, 2019

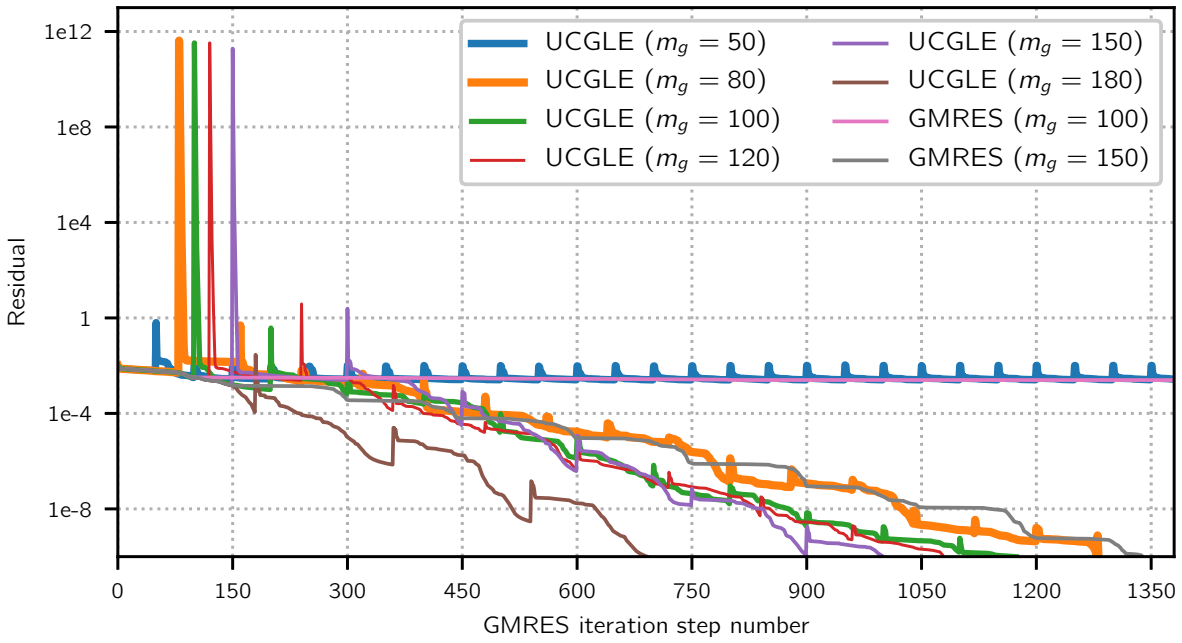

Figure 5.13 – Evaluation of GMRES subspace size m_g varying from 50 to 180. $d = 10$, $lsa = 10$, $freq = 10$.

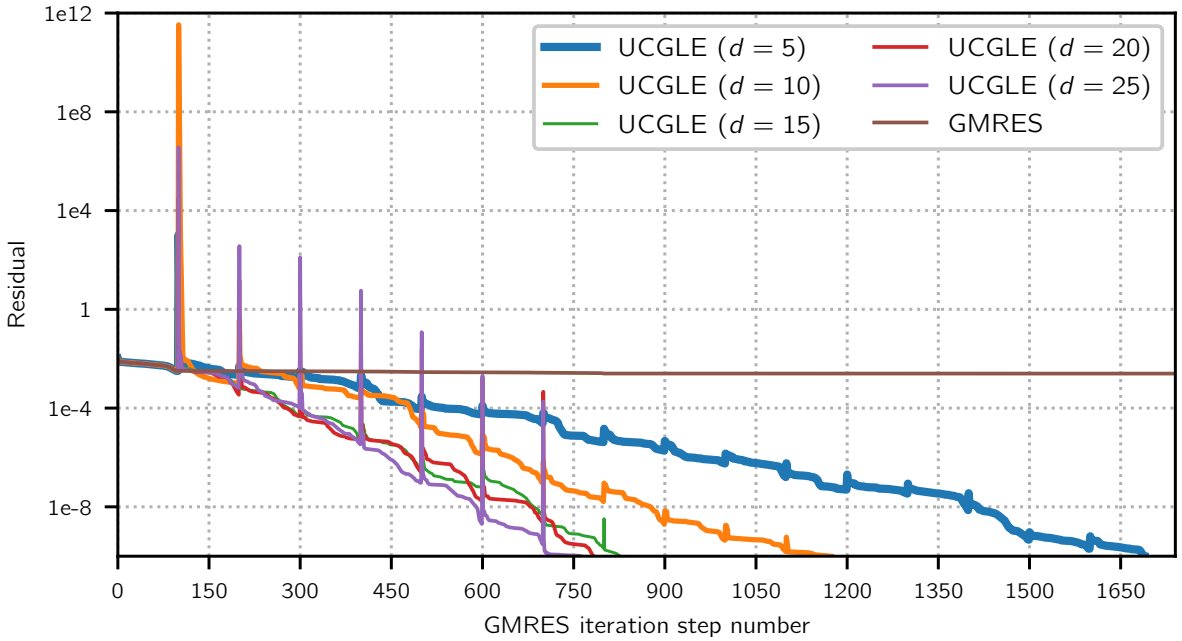

Figure 5.14 – Evaluation of Least Squares polynomial degree d varying from 5 to 25, and $m_g = 100$, $lsa = 10$, $freq = 1$.

© 2019 Tous droits réservés.

lilliad.univ-lille.fr

Thèse de Xinzhe Wu, Université de Lille, 2019

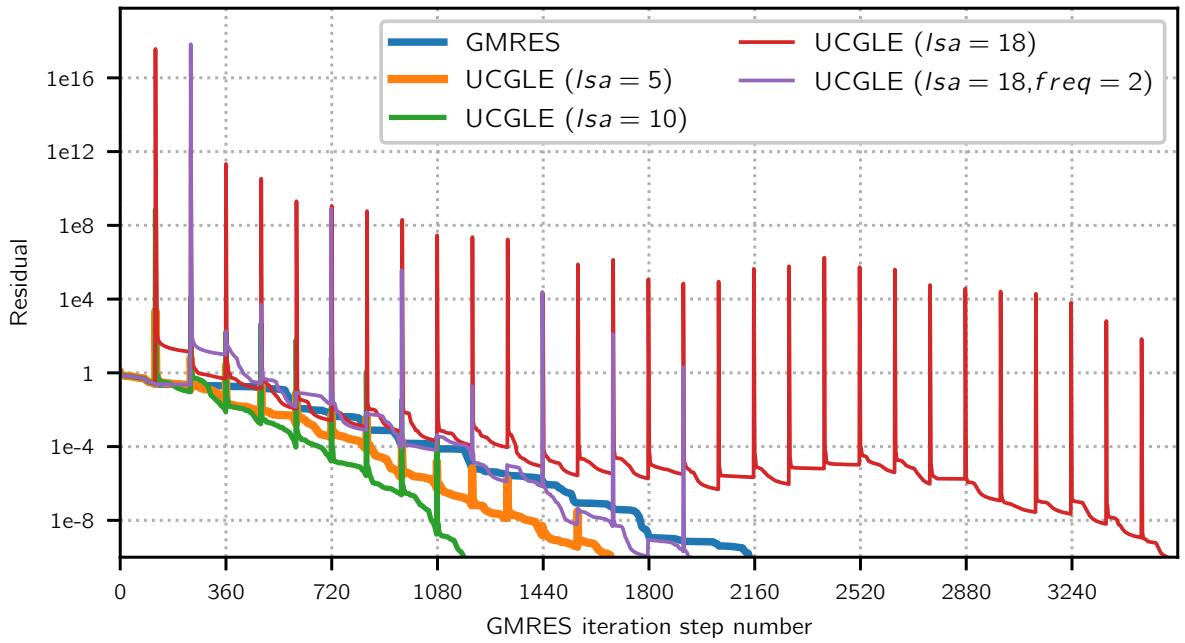

Figure 5.15 – Evaluation of Least Squares polynomial preconditioning applied times lsa varying from 5 to 18, and $m_g = 100$, $d = 10$, $freq = 1$.

and GMRES Component will be accelerated. UCGLE with $d = 25$ has more than 2× speedup than it with $d = 5$.

In conclusion, d is a very important parameter for the convergence of UCGLE. A good selection of this parameter should make a balance between the Least Squares polynomial preconditioning acceleration and the enlargement of the restarted residual norm. In practice, it is limited for choosing the degree of polynomial degree by the fact that the moment matrix M_d becomes difficult to compute and to factor as the degree d increases. The kernel operations for a d degree Least Squares polynomial are d-times SpMV, which involve with global communications. A classical solution to this problem is to compound several times a small degree polynomial. This is done by performing the iteration from line 39 to 44 in Algorithm 23 several times. We will evaluate this parameter lsa in the next step.

Least Squares polynomial applied times: The parameter Least Squares polynomial applied times lsa means the number of times the Least Squares polynomial preconditioning parameters will be applied to the temporary solution of GMRES Component before its restart after m_g iterations. In the experiments, lsa are set respectively to be 5, 10 and 18, and the parameters m_g, d, and $freq$ are respectively fixed as 120, 10 and 1. An additional test is done with lsa being 18 and $freq$ being 2. Fig. 5.15 shows the convergence curves of all the tests. Firstly, it is obvious that lsa has an effect on the peaks for each time Least Squares polynomial preconditioning. The greater it is, the bigger the peak will be. As talked in Section 5.4.2, these peaks mean the Euclidean norm of restart vector produced by Least Squares polynomial. By comparing the curves in Fig. 5.15, we can conclude that the augmentation of lsa will accelerate the convergence of UCGLE. The influence of lsa is clear, with the increase of lsa, the residual norm of the restart vector produced by Least Squares polynomial will be enlarged. In the beginning, the test with $lsa = 10$ performs better than $lsa = 5$, since Least Squares polynomial enlarges the norm of

© 2019 Tous droits réservés.

lilliad.univ-lille.fr

Thèse de Xinzhe Wu, Université de Lille, 2019

residual associated with dominant eigenvalues. However, if $lsa = 18$, the residual norm is too large, the speedup of Least Squares polynomial is covered, and the convergence might be slowed down. For the larger lsa, we could select a larger $freq$, which might reduce the influence of too large residual norm caused by lsa. This means lsa cannot be too large, otherwise it might lead to a too large norm of the residual of the restarted vector generated by Least Squares polynomial preconditioning process and finally, damage the convergence. We will give an auto-tuning scheme for this parameter later in Chapter 8.

To conclude on the effects of this parameter, it is necessary to select the best value with considering the selection of the setting of Least Squares polynomial power d. The two parameters seem particularly intricate together, and the choice of one will depend on the choice of the other. In the practical implementation, this parameter d implies a series of SpMV and AXPY operations in parallel. The larger d is, the more operations will be executed. Thus the more time will be occupied with more global communications. The good selection of the parameters lsa and d should make a balance between the reduction of iteration steps of GMRES components and additional time caused by these SpMV and AXPY operations.

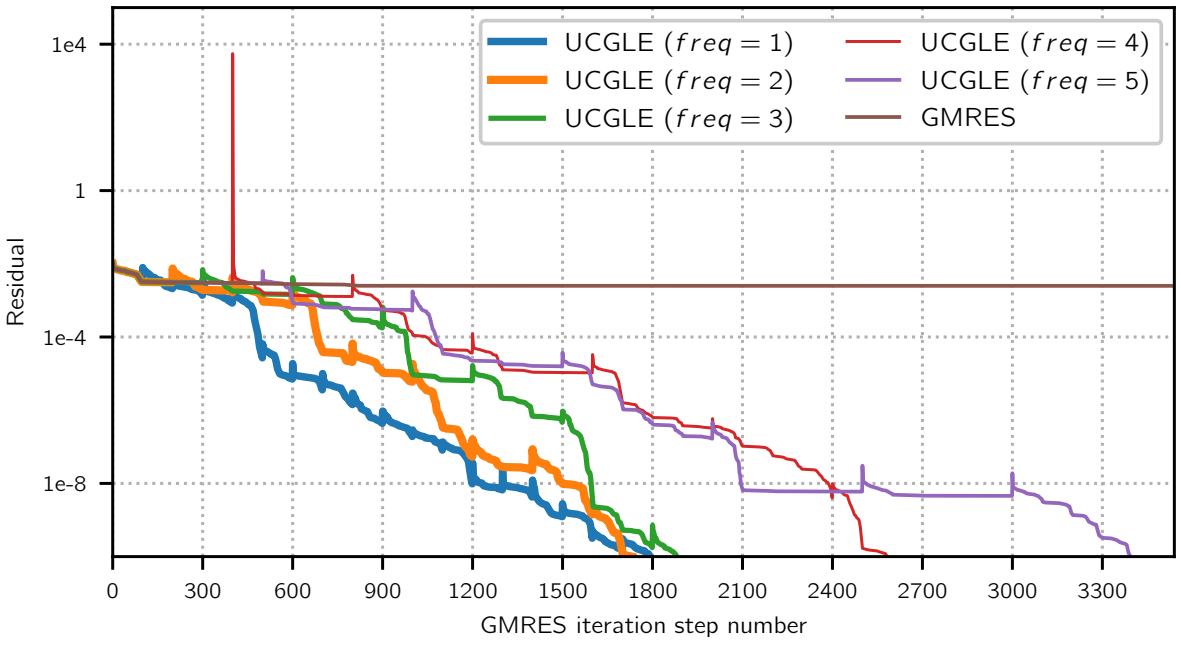

Figure 5.16 – Evaluation of Least Squares polynomial frequency $freq$ varying from 1 to 5, and $m_g = 100$, $lsa = 10$, $d = 10$.

Least Squares polynomial frequency: The Least Squares polynomial frequency $freq$ represents the number of restarts between which a GMRES preconditioning will take place by the Least Squares polynomial to the temporary solution. Also, we noticed in the previous experiments that after each preconditioning, a peak of the residual norm would be generated before the acceleration. This size of this peak depends on the influence of several parameters, and too large peak would damage the convergence. In order to characterize the latency parameter, the Krylov subspace m_g, lsa and d are respectively fixed as 100, 10, 10, and $freq$ ranges from 1 to 5. The results are shown in Fig. 5.16. For the cases with $freq$ being 1, 2 and 3, their convergence performances are similar. If $freq$ is too large, there will not enough Least Squares

© 2019 Tous droits réservés.

lilliad.univ-lille.fr

Thèse de Xinzhe Wu, Université de Lille, 2019

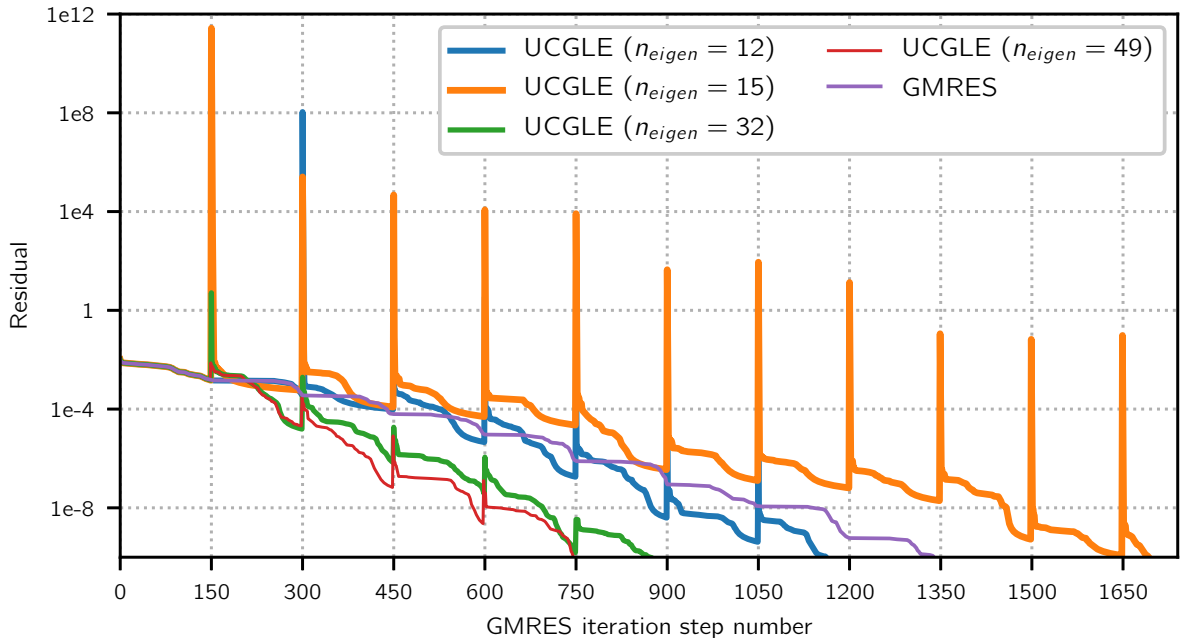

Figure 5.17 – Evaluation of eigenvalue number n_{eigen}, with and $m_g = 100$, $lsa = 10$, $d = 10$, $freq = 1$.

polynomial preconditioning applied to UCGLE, and their convergence might be heavily slowed down. Ultimately, the latency parameter must be chosen to allow sufficient consideration of the preconditioning in the successive cycles at this stage while not being too important so that the convergence can continue to benefit from its effect at a satisfactory pace. If the UCGLE with larger $freq$ can achieve a similar performance to the one with a smaller $freq$, the former is preferred since it employs less SpMV operations for the iterations.

Number of eigenvalues: The parameter n_{eigen} means the number of eigenvalues used to construct the polygon for the Least Squares preconditioning. We select to change the Krylov subspace size of ERAM m_a to control the number of eigenvalues applied to Least Squares preconditioning. In the experiments, the Krylov subspace m_g is fixed as 150. The parameters lsa, d, and $freq$ are respectively fixed as 10, 10 and 1. The numbers of eigenvalues approximated by ERAM with different Krylov subspace sizes are respectively 12, 15, 32 and 49. The convergence comparison is given in Fig. 5.17. We can conclude that with the augmentation of the number of eigenvalues applied to the Least Squares polynomial, the convergence of UCGLE can be accelerated, e.g., the test with 49 eigenvalues has more than 2× speedup compared with the one with 12 eigenvalues. Another phenomenon we can find is that the restart residual norm will be significantly decreased. The reason is that with the much larger number of eigenvalues, the polygon constructed by them will be able to approximate the spectrum of operator matrix A better. The solution of the minimum-maximum problem inside Least Squares preconditioning is better, which results in the decrease of restart residual norm. The Krylov subspace size of ERAM cannot be as large as we want since it is necessary for the ERAM Component to approximate enough number of eigenvalues and send them to GMRES Component in time.

© 2019 Tous droits réservés.

lilliad.univ-lille.fr

Thèse de Xinzhe Wu, Université de Lille, 2019

Table 5.3 – Test matrices information

Matrix Name	n	nnz	Matrix Type
$MEG1$	1.8×10^7	2.9×10^7	non-Symmetric
$MEG2$	1.8×10^7	1.9×10^8	non-Symmetric
$MEG3$	1.024×10^7	7.27×10^9	non-Hermitian
$MEG4$	5.1×10^6	3.64×10^9	non-Hermitian

5.5.3 Convergence Acceleration Evaluation

After the evaluation the effects of different parameters on the convergence of UCGLE, in this section, we will compare the acceleration of UCGLE with conventional preconditioned GMRES. We have selected four large-scale test matrices to evaluate the convergence speedup of UCGLE method. The test matrices $MEG1$ and $MEG2$ are built by placing several copies of the same small unsymmetrical matrix (*utm300*) onto the diagonal. For the generation of $MEG1$, several parallel lines with different values can be added to the off-diagonal. For $MEG2$, the first block column matrix as also filled by the small matrix *utm300*. The exact shapes of $MEG1$ and $MEG2$ are given in Fig. 5.18. The test matrix $MEG3$ and the second matrix $MEG4$ are all generated by SMG2S with the prescribed eigenvalues distributed randomly inside an annulus with the different scales which is symmetric to the real axis in the complex plane. The information of the fours tests matrices is given in Table 5.3.

The convergence of UCGLE is compared with:

(1) restarted GMRES without preconditioning;

(2) restarted GMRES with Jacobi preconditioner;

(3) restarted GMRES with SOR preconditioner.

We select the Jacobi and SOR preconditioners for the experimentations because they are implemented in parallel by PETSc. The parallel implementation of ILU preconditioner in PETSc is limited, which supports only the real scalar operations. The GMRES restarted parameter for $MEG1$, $MEG2$, $MEG3$ and $MEG4$ are respectively 250, 280, 30 and 40.

Table 5.4 – Summary of iteration number for convergence of 4 test matrices using SOR, Jacobi, non preconditioned GMRES,UCGLE_FT(G),UCGLE_FT(G) and UCGLE: red × in the table presents this solving procedure cannot converge to accurate solution (here absolute residual tolerance 1×10^{-10} for GMRES convergence test) in acceptable iteration number (20000 here).

Matrix Name	SOR	Jacobi	No preconditioner	UCGLE_FT(G)	UCGLE_FT(G)	UCGLE
$MEG1$	1430	×	1924	995	1073	900
$MEG2$	2481	3579	3027	2048	2005	1646
$MEG3$	217	386	400	81	347	74
$MEG4$	750	×	×	82	×	64

Fig 5.19, Fig 5.20, Fig 5.21 and Fig 5.22 present respectively the convergence experiments of $MEG1$, $MEG2$, $MEG3$ and $MEG4$. The numbers of iteration step for convergence are given

© 2019 Tous droits réservés.

lilliad.univ-lille.fr

Thèse de Xinzhe Wu, Université de Lille, 2019

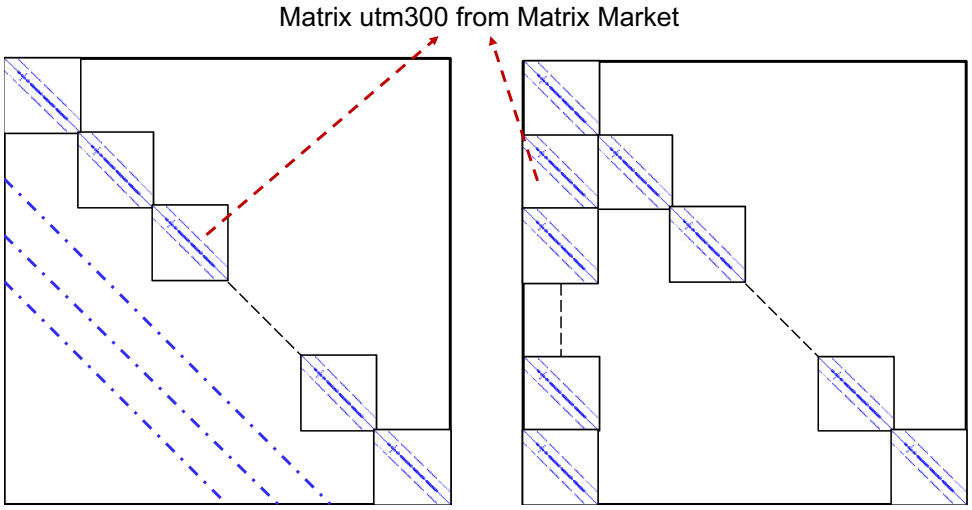

Figure 5.18 – Two strategies of large and sparse matrix generator by a original matrix utm300 of Matrix Market.

in Table 5.4. We find that UCGLE method has spectacular acceleration on the convergence rate compared these conventional preconditioners. It has almost two times of acceleration for $MEG1$, $MEG2$ and $MEG3$, and more than 10 times of acceleration for $MEG4$ than the conventional preconditioner SOR. The SOR preconditioner is already much better than the Jacobi preconditioner for the test matrices.

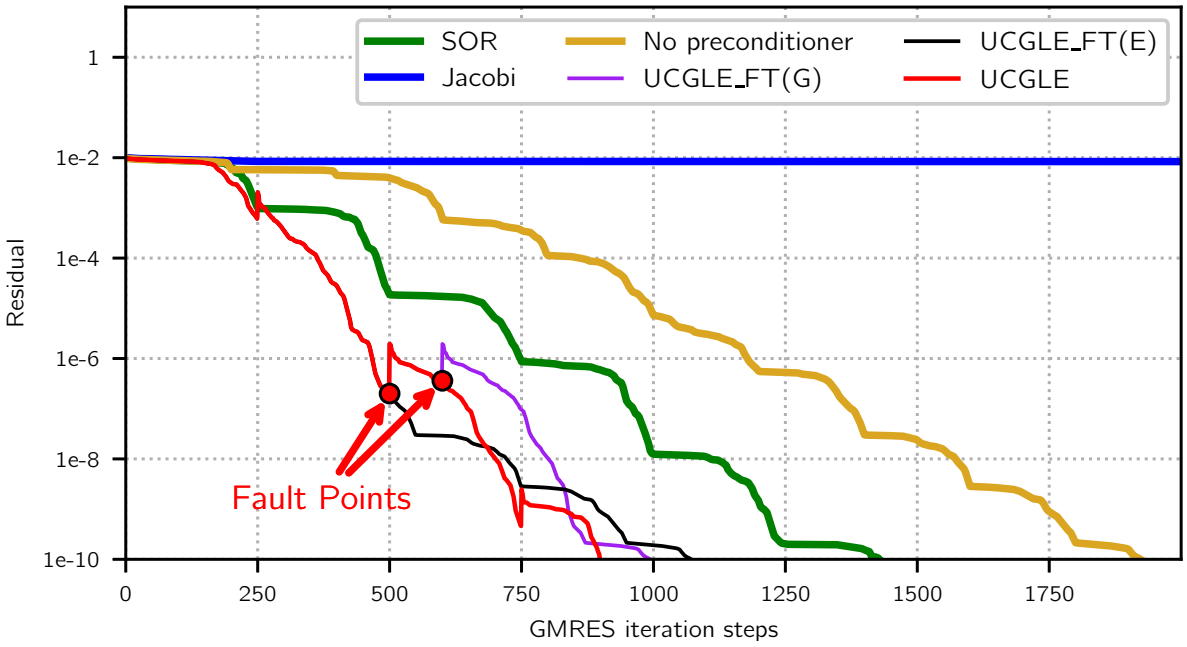

Figure 5.19 – $MEG1$: convergence comparison of UCGLE method vs conventional GMRES

5.5.4 Fault Tolerance Evaluation

The fault tolerance of UCGLE is studied by the simulation of the loss of either GMRES or ERAM Components. UCGLE_FT(G) in Fig. 5.19, Fig. 5.20, Fig. 5.21 and Fig. 5.22 represents the fault tolerance simulation of GMRES, and UCGLE_FT(E) implies the fault tolerance simulation of

© 2019 Tous droits réservés.

lilliad.univ-lille.fr

Thèse de Xinzhe Wu, Université de Lille, 2019

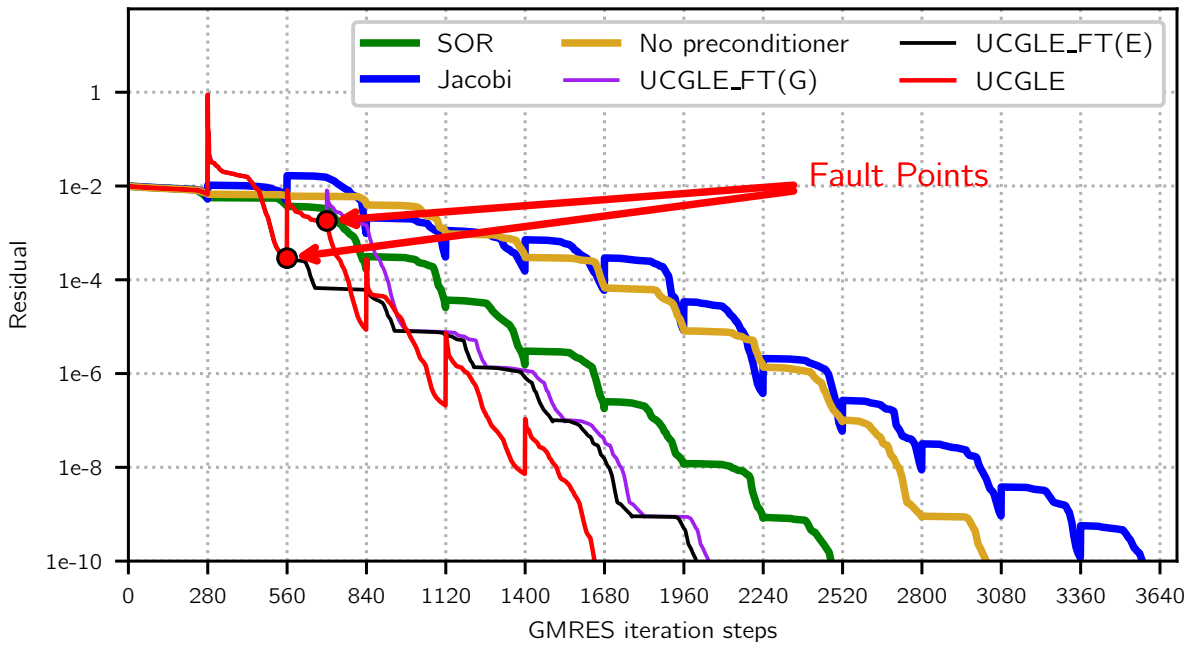

Figure 5.20 – $MEG2$: convergence comparison of UCGLE method vs conventional GMRES

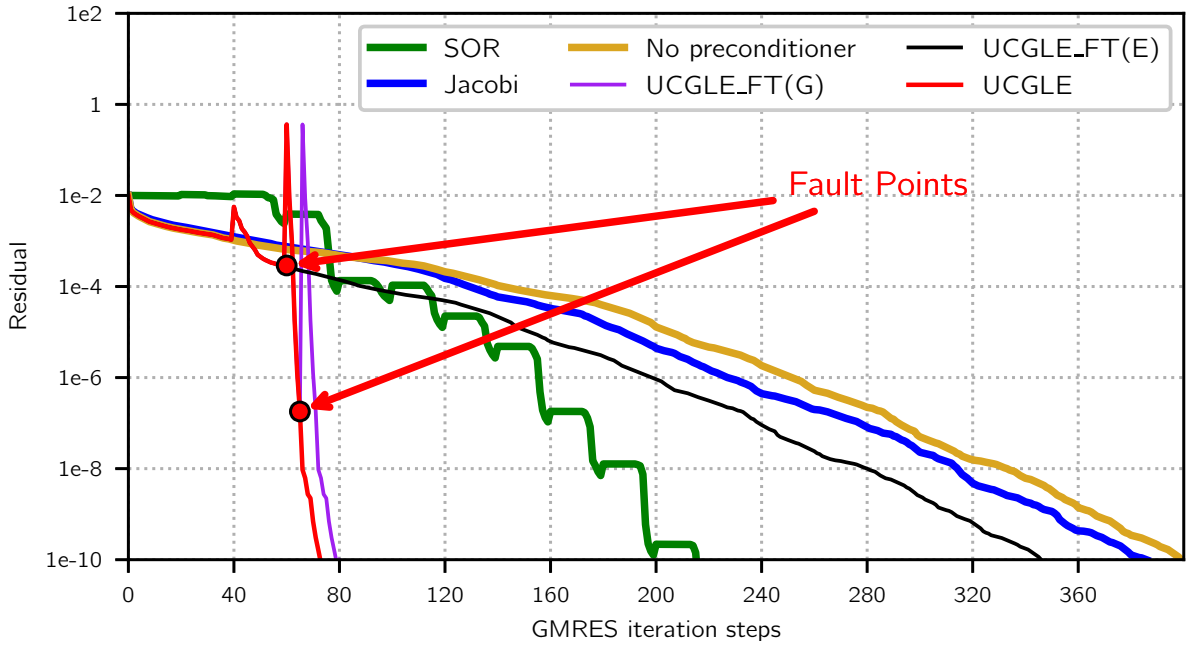

Figure 5.21 – $MEG3$: convergence comparison of UCGLE method vs conventional GMRES

© 2019 Tous droits réservés.

lilliad.univ-lille.fr

Thèse de Xinzhe Wu, Université de Lille, 2019

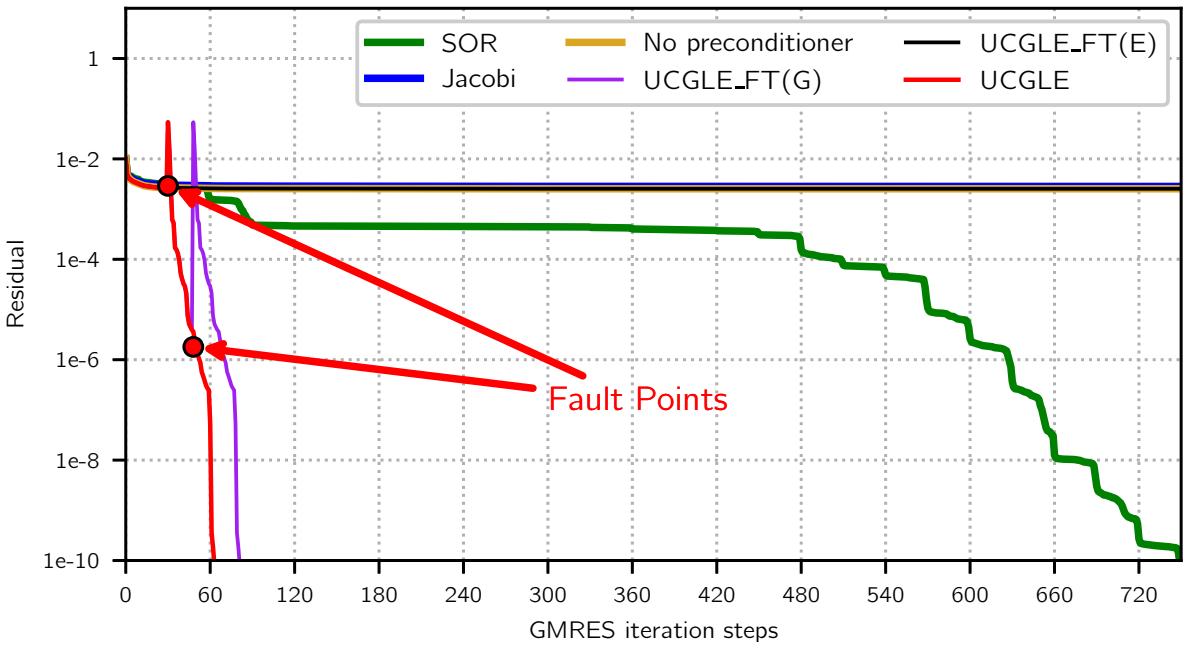

Figure 5.22 – *MEG4*: convergence comparison of UCGLE method vs conventional GMRES

ERAM.

The failure of ERAM Component is simulated by fixing the execution loop number of ERAM algorithm, in this case, ERAM exits after a fixed number of solving procedures. We mark the ERAM fault points of the two test matrices in Fig. 5.19, Fig. 5.20, Fig. 5.21 and Fig. 5.22 respectively 500, 560, 60 and 30 iteration step for each case. The UCGLE_FT(E) curves of the experimentations show that GMRES Component will continue to solve the systems without Least Squares polynomial preconditioning acceleration. Table 5.4 shows that the iteration number for convergence of UCGLE_FT(E) is greater than the normal UCGLE method but less than the GMRES method without preconditioning.

The failure of GMRES Component is simulated by setting the allowed iteration number of GMRES algorithm to be much smaller than the needed iteration number for convergence. The values of these cases are respectively 600, 700, 70 and 48. They are also marked in Fig. 5.19, Fig. 5.20, Fig. 5.21 and Fig. 5.22. We can find that after the quitting of GMRES Component without the finish of its task, ERAM computing units will automatically take over the jobs of GMRES component. The new GMRES solving procedure will use the temporary solution x_m as a new restarted initial vector received asynchronously from the previous restart procedure of GMRES Component before its failure. In this case, ERAM Component no longer exists. Thus the solving task can be continued as the classic GMRES without Least Squares polynomial preconditioning. In Fig. 5.19, Fig. 5.20, Fig. 5.21 and Fig. 5.22, we can find the difference between UCGLE_FT(E) and UCGLE_FT(G). In UCGLE_FT(G), the new GMRES Component takes x_m of previous restart procedure. Thus it will repeat the iteration steps of previous restart iterations until the failure of GMRES. Another fact of UCGLE_FT(G) which cannot be concluded, but can be easily obtained, is that the solving time will be different if the computing unit numbers of previous GMRES and ERAM Components are different.

© 2019 Tous droits réservés.

lilliad.univ-lille.fr

Thèse de Xinzhe Wu, Université de Lille, 2019

5.5.5 Impacts of Spectrum on Convergence

The Least Squares Polynomial uses the dominant eigenvalues to accelerate the convergence of iterative methods. With the help of SMG2S, we could study the impacts of spectral distribution on the convergence of UCGLE. In this section, we evaluate the acceleration of UCGLE with eight types of spectra, they are generated by the functions listed in Table 5.5. The dimension for all eight test matrices is fixed as 2000. The experimental results are given in Fig. 5.23 and Fig. 5.24. For all the tests, the Krylov subspace size m_a for ERAM Component is limited. Thus the accuracy of approximated eigenvalues is also low. However, the speedup of Least Squares polynomial preconditioning is still splendid. The purpose to limit m_a is to make sure generate enough eigenvalues for the first time restart of GMRES Component inside UCGLE. If this subspace size is too large, or the conditions for the eigenvalues to be accepted are too strict, there will be no acceleration by Least Squares polynomial preconditioning.

Table 5.5 – Spectrum generation functions: the size of all spectra is fixed as $N = 2000$, $i \in 0, 1, \cdots, N-1$ is the indices for the eigenvalues.

N^o	real part	imaginary part
I	$0.6 + (rand(0, 0.01) + 0.55)\cos(2\pi i/N - \pi)$	$(rand(0, 0.01) + 0.1)\sin(2\pi i/N - \pi)$
II	$0.3 + (rand(0, 0.01) + 0.55)\cos(2\pi i/N - \pi)$	$(rand(0, 0.01) + 0.1)\sin(2\pi i/N - \pi)$
III	$-0.6 + (rand(0, 0.01) + 0.55)\cos(2\pi i/N - \pi)$	$(rand(0, 0.01) + 0.1)\sin(2\pi i/N - \pi)$
IV	$0.6 + (rand(0, 0.01) + 0.55)\cos(4\pi i/N - \pi)$	$0.2 + (rand(0, 0.01) + 0.1)\sin(4\pi i/N - \pi)\ \forall i < 1000$ $-0.2 - (rand(0, 0.01) + 0.1)\sin(4\pi i/N - \pi)\ \forall i \geq 1000$
V	$0.006 + rand(0, 0.5)$	0.0
VI	$-0.006 + rand(0, 0.5)$	0.0
VII	$60.0 + (rand(0, 0.0001) + 0.00012)\cos(2\pi i/N - \pi)\ \forall i < 50$ $0.6 + (rand(0, 0.01) + 0.55)\cos(2\pi i/N - \pi)\ \forall i \geq 50$	$(rand(0, 0.0001) + 0.00012)\sin(2\pi i/N - \pi)\ \forall i < 50$ $(rand(0, 0.01) + 0.1)\sin(2\pi i/N - \pi)\ \forall i \geq 50$
VIII	$-60.0 - (rand(0, 0.0001) + 0.00012)\cos(2\pi i/N - \pi)\ \forall i < 50$ $-0.6 - (rand(0, 0.01) + 0.55)\cos(2\pi i/N - \pi)\ \forall i \geq 50$	$(rand(0, 0.0001) + 0.00012)\sin(2\pi i/N - \pi)\ \forall i < 50$ $(rand(0, 0.01) + 0.1)\sin(2\pi i/N - \pi)\ \forall i \geq 50$

The generated spectrum I is quasi-symmetric to the real axis, and all the real parts of these eigenvalues are positive, shown as Fig. 5.23a. The Ritz values approximated by ERAM are marked as the red cross in the figure. The parameters d and lsa for the Least Squares polynomial preconditioning are all set to be 10. In the experiments, m_g is the Krylov subspace size of GMRES Component. For UCGLE with $m_g = 20$, it has more than 3× speedup over the conventional GMRES for the convergence. But for the case UCGLE with larger Krylov subspace size $m_g = 80$ in GMRES Component, it only has about 1.4× over the conventional GMRES. In fact, for all the matrices with a spectral distribution similar to spectrum I, the Least Squares polynomial preconditioning is always very effective, and it is better to benefit from this preconditioning as soon as possible. Hence, GMRES Component with smaller m_g might converge much more rapidly than the case with larger m_g, since it can profit the Least Squares polynomial

© 2019 Tous droits réservés.

lilliad.univ-lille.fr

Thèse de Xinzhe Wu, Université de Lille, 2019

preconditioning in time.

The spectrum II is also quasi-symmetric to the real axis, its shape is nearly an ellipse. The real part of some eigenvalues in the spectrum is positive, and for the others, the real part is negative, shown as Fig. 5.23b. In this case, UCGLE cannot achieve the convergence even with much larger Krylov subspace size $m_g = 200$. When the original point is inside the spectrum of the operator matrix. As we presented in Chapter 3, the maximum-minimum problem of Least Squares polynomial method cannot be solved. In the current implementation of Least Squares polynomial preconditioning, for most cases with the origin point inside spectrum, UCGLE with Least Squares polynomial preconditioning is not applicable.

The spectrum III in Fig. 5.23c is also quasi-symmetric to the real axis, and the real part of all the eigenvalues are negative. The Ritz values approximated by ERAM Component are also marked as the red cross in the figure. This case is similar to the one in Fig. 5.23a. The acceleration of Least Squares polynomial preconditioning inside UCGLE is obvious, and this kind of spectral distribution is suitable for the polynomial preconditioning.

The spectrum IV in Fig. 5.23d consists of two ellipses which are symmetric to the real axis, and the real part of all eigenvalues are positive. The Ritz values approximated by ERAM are marked as the red cross in the figure. We could conclude that UCGLE is suitable for this case with almost 4× speedup compared the conventional GMRES.

The spectrum V in Fig. 5.24a is generated in random with all the eigenvalues located on the real axis, the imaginary part of all eigenvalues is zero, and the real part is positive. The Ritz values approximated by ERAM are complex, which are also marked by the red cross in this figure. UCGLE has more than 6× speedup for this spectrum, compared with the conventional GMRES.

The spectrum VI in Fig. 5.24b is also generated in random on the real axis using a different shift value with the one in Fig. 5.24a. The imaginary part of all the eigenvalues is also zero. However, the real part of a small number of eigenvalues are negative, and the real part of the others are positive. Since the origin point is inside of the spectrum, the convergence both for GMRES and UCGLE is hard to be obtained. However, UCGLE has still a little speedup over the conventional GMRES. If we enlarge the degree of Least Squares polynomial from 10 to 25, we can continue to have some acceleration.

The spectrum VII and VIII in Fig. 5.24c and Fig. 5.24d are also quasi-symmetric to the real axis, and the real parts of the eigenvalues for the two spectra are respectively all positive and negative. The two spectra are generated with a special manner which makes the eigenvalues be grouped into two separate clustered set with a relative long distance in the real-imaginary plane. With the change of Krylov subspace m_a of ERAM, different numbers of eigenvalues can be approximated. Three cases in the experiments are denoted as $eigen_1$, $eigen_2$ and $eigen_3$, which are marked with different colors in Fig. 5.24c and Fig. 5.24d. In the experiments, $eigen_1$ and $eigen_2$ are the Ritz values which approximate a few eigenvalues in both two clustered group. However, $eigen_3$ are only the Ritz values which approximate the eigenvalues in only one clustered group (the right clustered group in Fig. 5.24c, and the left clustered group in Fig. 5.24d). $eigen_1$ approximates more eigenvalues in the both two clustered group than $eigen_2$. We could conclude from Fig. 5.24c and Fig. 5.24d that UCGLE with $eigen_1$ converge the most rapid, with about

© 2019 Tous droits réservés.

lilliad.univ-lille.fr

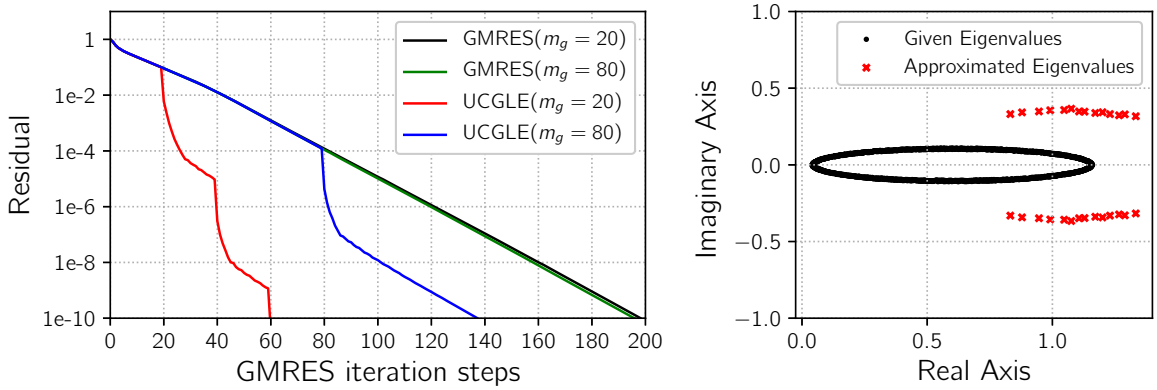

(a) Spectral Distribution I: matrix size = 2000, $d = 10$, $lsa = 10$, $freq = 1$.

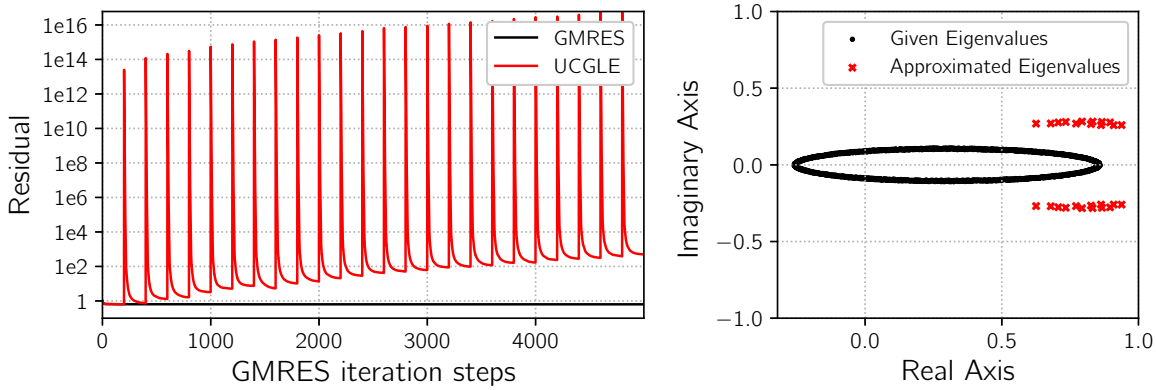

(b) Spectral Distribution II: matrix size = 2000, $m_g = 200$, $d = 10$, $lsa = 10$, $freq = 1$.

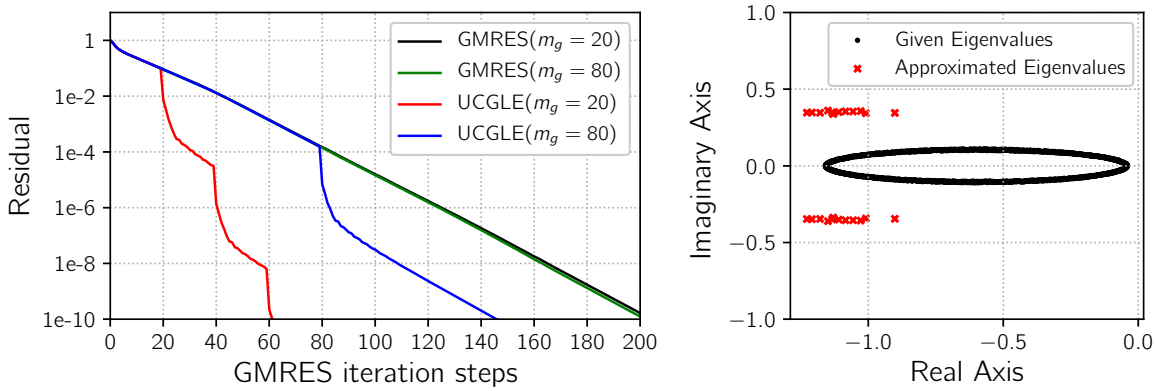

(c) Spectral Distribution III: matrix size = 2000, $m_g = 20$, $d = 10$, $lsa = 10$, $freq = 1$.

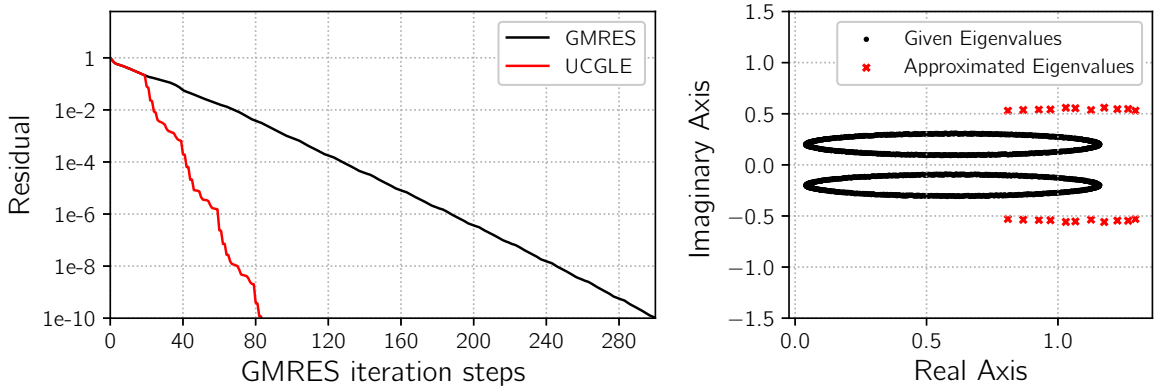

(d) Spectral Distribution IV: matrix size = 2000, $m_g = 20$, $d = 10$, $lsa = 10$, $freq = 1$.

Figure 5.23 – Impacts of Spectrum on Convergence.

© 2019 Tous droits réservés.

Thèse de Xinzhe Wu, Université de Lille, 2019

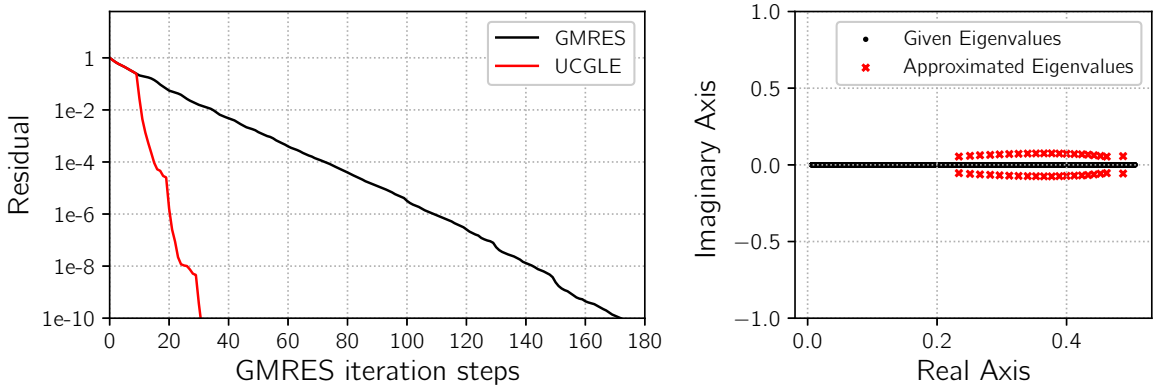

(a) Spectral Distribution V: matrix size = 2000, $m_g = 10$, $d = 10$, $lsa = 10$, $freq = 1$.

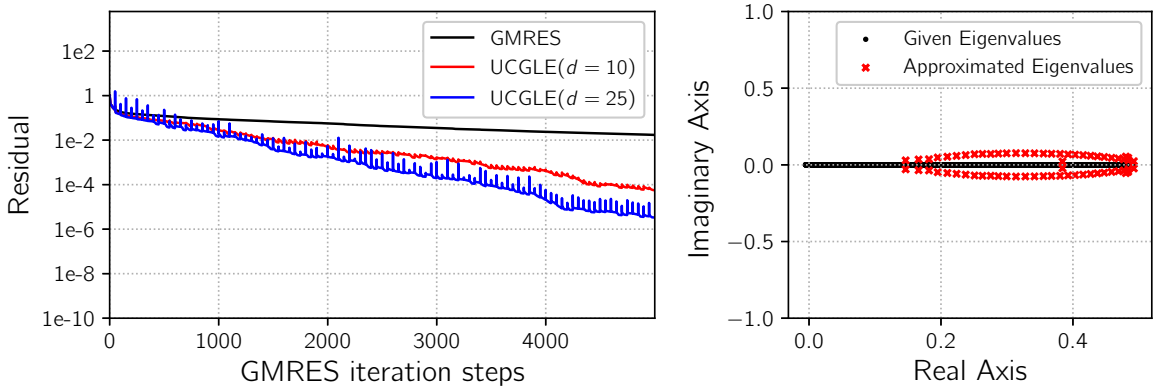

(b) Spectral Distribution VI: matrix size = 2000, $m_g = 50$, $lsa = 10$, $freq = 1$.

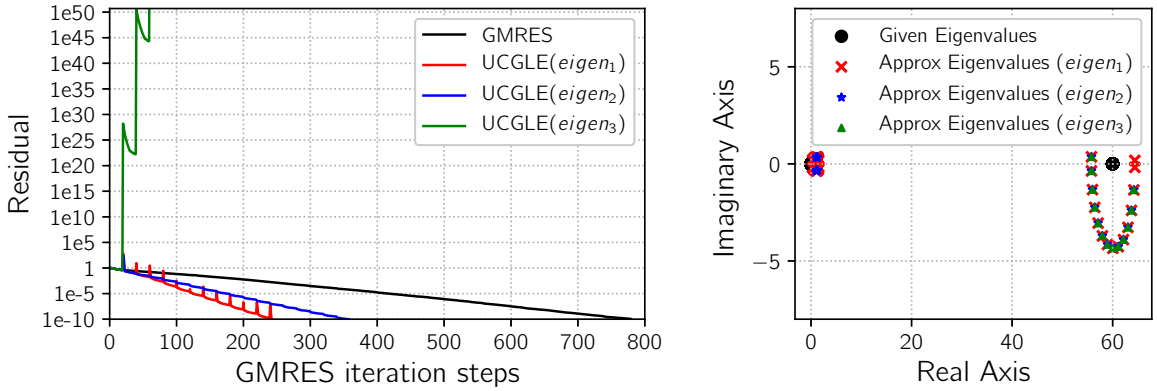

(c) Spectral Distribution VII: matrix size = 2000, $m_g = 20$, $d = 10$, $lsa = 10$, $freq = 1$.

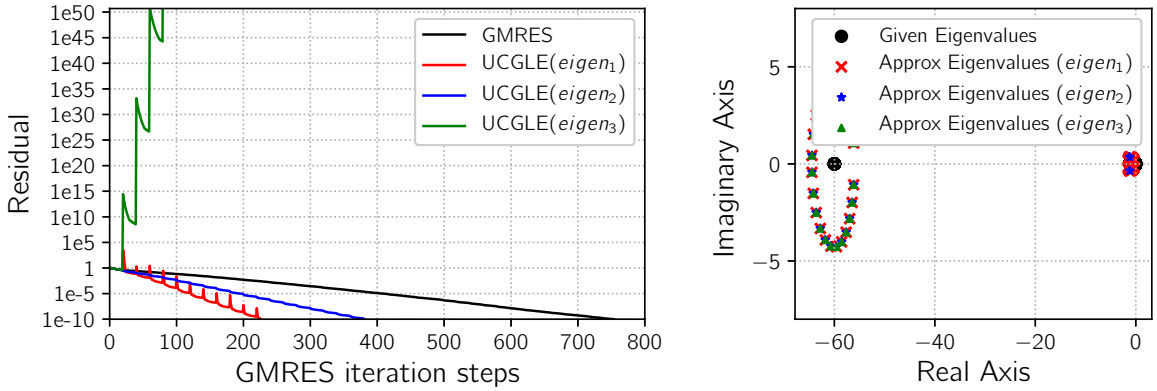

(d) Spectral Distribution VIII: matrix size = 2000, $m_g = 20$, $d = 10$, $lsa = 10$, $freq = 1$.

Figure 5.24 – Impacts of Spectrum on Convergence.

© 2019 Tous droits réservés.

lilliad.univ-lille.fr

Thèse de Xinzhe Wu, Université de Lille, 2019

3× speedup than the conventional GMRES, $eigen_2$ has almost 2× speedup, and $eigen_3$ diverge quickly in a few iteration steps. The reason is that $eigen_3$ approximates only one clustered group, and the polygon constructed by $eigen_3$ cannot represent the real spectral distribution, which makes the norm of residual vector generated by Least Squares polynomial explode in short time, and it is impossible to achieve the convergence.

We can conclude that:

(1) If the real part of the eigenvalues of the operator matrix is all positive or negative, and the spectrum is (quasi-)symmetric to the real axis, UCGLE can always accelerate the convergence.

(2) If the real part for some eigenvalues of the operator matrix is positive and for some is negative, the divergence of UCGLE can be easily achieved, UCGLE is not suitable for this case; however, it might exist some particular matrices which can obtain the speedup of UCGLE.

(3) For the matrices with a good spectral distribution as we talked in (1), the approximated eigenvalues do not need to be too accurate to allow the speedup by UCGLE.

(4) The more eigenvalues approximated to construct the Least Squares polynomial, the more acceleration UCGLE will achieve.

(5) For the eigenvalues distributed into the different clustered groups with their real part to be all positive or all negative, much more Ritz values are required for constructing the Least Squares polynomial preconditioning. At least, the Ritz values should be able to represent the different clustered groups of eigenvalues. If the different groups of clustered eigenvalues are very discrete, it is difficult for ERAM to approximate all of them with small Krylov subspace size. Thus the implementation of UCGLE with multiple ERAM Components is required. Each ERAM is executed with different shift value to approximate the different parts of eigenvalues with thick restarting. The difficulties are:

   (a) current implementation of manager engine does not allow adding more computational components since it is implemented by statically dividing MPI_COMM_World into four communicators;

   (b) for the matrices of real applications, we cannot know the clustering situations of their spectra. Thus the selection of shift value for different ERAM Components seems somehow blind. It is necessary to have the mechanism which can predict the distribution of clustered groups of eigenvalues with a relatively long distance.

(6) The implementation of Least Squares polynomial in UCGLE should be extended for the eigenvalues with both positive and negative real parts. One possible solution is to implement two separate LSP components to construct two Least Squares polynomials by the Ritz values with the positive and negative real part and exclude the origin point. Denote the two residual polynomial to be R_d and $R'_{d'}$ constructed by H_1 and H_2 in Fig. 5.25. R_d is constructed with m dominant eigenvalues with positive real parts, and $R'_{d'}$ is constructed

© 2019 Tous droits réservés.

lilliad.univ-lille.fr

Thèse de Xinzhe Wu, Université de Lille, 2019

with m' eigenvalues with largest magnitude and negative real part. The restarted residual vector generated by two Least Squares polynomials should be

$$r = \sum_{i=1}^{m} \rho_i(R_d(\lambda_i))^{lsa} u_i + \sum_{i=m+1}^{n} \rho_i(R_d(\lambda_i))^{lsa} u_i + \sum_{j=1}^{m'} \rho_j(R'_{d'}(\lambda_j))^{lsa} u_j + \sum_{j=m'+1}^{n} \rho_j(R'_{d'}(\lambda_j))^{lsa} u_j.$$

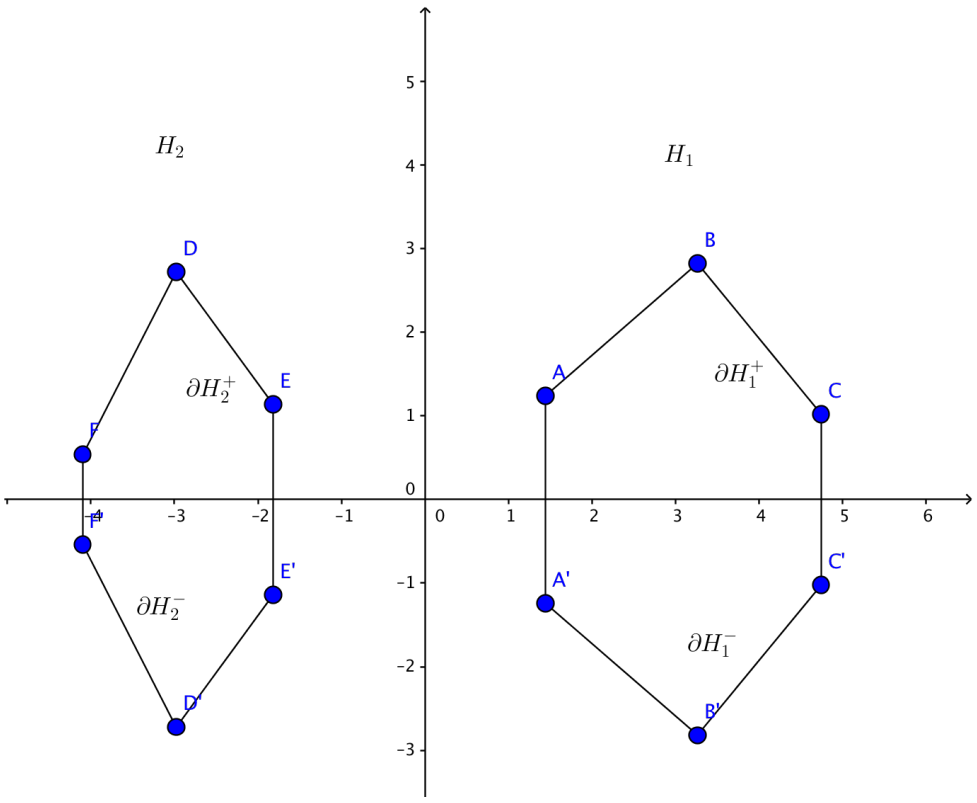

Figure 5.25 – Polygone region H with real part of eigenvalues positive and negative.

5.5.6 Scalability Evaluation

When solving large-scale linear systems on the modern supercomputing platforms, the main concern of the conventional preconditioned Krylov methods is the cost of global communications and synchronization overheads. We select the test matrix $MEG1$ for the scalability evaluation. The average time cost per iteration of these methods is computed by a fixed number of iterations. Time per iteration is suitable for demonstrating scaling behavior. The scaling performance of UCGLE is evaluated both on *Tianhe-2* and *Romeo-2013*.

For the evaluation of UCGLE on *Romeo-2013* with CPUs, the core amount of GMRES Component is set respectively to be 1, 2, 4, 8, 16, 32, 64, 128, 256, and both the core amount of LSP Component and Manager Component is 1. ERAM Component should ensure to supply the approximated eigenvalues in time for each time restart of GMRES Component. Thus the core amount is respectively 1, 1, 1, 1, 4, 4, 4, 10, 16, referring to different GMRES Component core number. For the evaluation with multi-GPU on *Romeo-2013*, both LSP Component and Manager Component allocate only one core on CPU. The GPU amount of GMRES Component is

© 2019 Tous droits réservés.

lilliad.univ-lille.fr

Thèse de Xinzhe Wu, Université de Lille, 2019

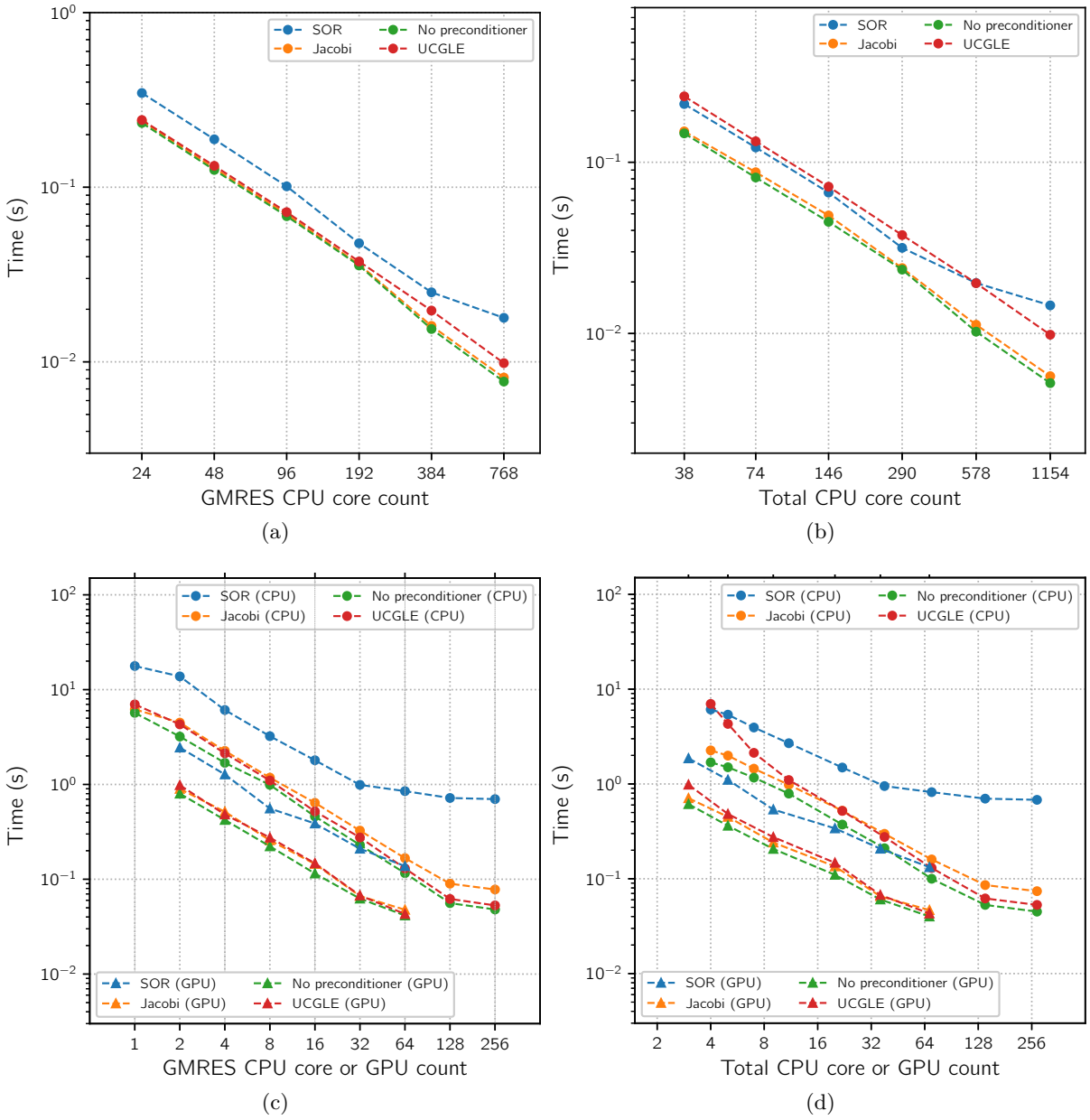

Figure 5.26 – Scalability per iteration comparison of UCGLE with GMRES with or without preconditioners on *Tianhe-2* and *Romeo-2013*. A base 10 logarithmic scale is used for Y-axis of (a); a base 2 logarithmic scale is used for Y-axis of (b).

© 2019 Tous droits réservés.

lilliad.univ-lille.fr

Thèse de Xinzhe Wu, Université de Lille, 2019

set respectively to be 2, 4, 8, 16, 32, 64, with the GPU amount of ERAM Component respectively 1, 1, 1, 4, 4, 4. The computing resource number of classic and preconditioned GMRES always keeps the same with the core number of GMRES Component in UCGLE. Thus it ranges from 1 to 256 for CPU performance evaluation, and from 2 to 64 for GPU performance evaluation.

For the evaluation of UCGLE on *Tianhe-2* with CPUs, the core number of GMRES Component is set respectively to be 24, 48, 96, 192, 384, 768, and both the core number of LSP Component and Manager Component is 1. Thus we select the core number is respectively 16, 32, 64, 128, 256, 512 referring to different GMRES Component core number. The GMRES core number of conventional GMRES is equal to the one of GMRES Component in UCGLE.

In Fig. 5.26a and Fig. 5.26c, we can find that these methods have good scalability with the augmentation of computing units except the SOR preconditioned GMRES. The classic GMRES has the smallest time cost per iteration. The Jacobi preconditioner is the simplest preconditioning form for GMRES, and its time cost per iteration is similar to the classic GMRES. The GMRES with SOR preconditioner has the largest time cost per iteration since SOR preconditioned GMRES has the additional matrix-vector and matrix-matrix multiplication operations in each step of the iteration. These operations have global communication and synchronization points. The communication overhead makes the SOR preconditioned GMRES more easily lose its good scalability with the augmentation of computing unit number. There is not much difference between the time cost per iteration of classic GMRES and UCGLE with the help of the asynchronous communication implementation of UCGLE method. Since the resolving part and preconditioning part of UCGLE work independently, its global communication and synchronize points is similar to the classic GMRES without preconditioning. That is the benefits UCGLE's asynchronous communication.

Since UCGLE requires additional computing units for the manager engine, LSP Component and especially ERAM Component, it is necessary to compare UCGLE with other methods when the total computing resource number of UCGLE and other methods keeps the same computing resource number of UCGLE and other methods the same. Thus we have tested the classic and conventional preconditioned GMRES on *Romeo-2013* with the CPU core number fixed respectively as 4, 5, 7, 11, 22, 38, 70, 140, 274 and the GPU number fixed respectively as 3, 5, 9, 20, 36, 68, referring to the previous scaling performance evaluation of UCGLE. In the evaluation on the GPU cluster, the two CPUs for LSP Component and Manager Component have been ignored because they have a minor influence. For the evaluation on *Tianhe-2*, the computing unit number is fixed as 38, 74, 146, 290, 578, 1154. The performance comparison on *Tianhe-2* and *Romeo-2013* are respectively given as Fig. 5.26b and Fig. 5.26d . We can find that if the computing resource number is small, the time per iteration of classic and conventional preconditioned GMRES is much better than UCGLE since the latter allocates extra computing resources for other components. With the augmentation of computing resources, the scalability of the SOR preconditioned GMRES trends to be bad, and the average time cost per iteration of UCGLE method tends to be better than the SOR preconditioned GMRES with good scalability. Although the scalability of classic and Jacobi is good, and their time per iteration is smaller than UCGLE, but since UCGLE can accelerate the convergence of solving linear systems, thus better performance can be expected. For test matrix $MEG1$ on *Romeo-2013*, UCGLE method has

© 2019 Tous droits réservés.

lilliad.univ-lille.fr

Thèse de Xinzhe Wu, Université de Lille, 2019

similar speedup on the solving time per iteration compared with the classic GMRES when the computing resource number is larger than 22 for CPUs and larger than 5 for GPUs, but it can decrease significantly more than 5× iteration step number for the convergence, thus about 5× acceleration for the time of the whole resolution. In the end, the better performance of UCGLE method compared with other methods can be concluded.

5.6 Conclusion

In this chapter, we have presented a distributed and parallel method UCGLE for solving large-scale non-Hermitian linear systems. This method has been implemented with asynchronous communication among different computational components. In the experimentation, we observed that UCGLE method has following features: 1) it has significant acceleration for the convergence than the conventional preconditioners as SOR and Jacobi; 2) the spectrum of different linear systems has influence on its improvement of convergence rate; 3) it has better scalability for the very large-scale linear systems; 4) it is able to speed up using GPUs; 5) it has the fault tolerance mechanism facing the failure of different computational components. We conclude that UCGLE method is a good candidate for emerging large-scale computational systems because of its asynchronous communication scheme, its multi-level parallelism, its reusability and fault tolerance, and its potential load balancing. The coarse grain parallelism among different computational components and the medium/fine grain parallelism inside each component can be flexibly mapped to large-scale distributed hierarchical platforms.

© 2019 Tous droits réservés.

lilliad.univ-lille.fr

© 2019 Tous droits réservés.

lilliad.univ-lille.fr

Chapter 6

UCGLE to Solve Linear Systems in Sequence with Different Right-hand Sides

Many problems in science and engineering often require to solve a long sequence of large-scale non-Hermitian linear systems with different RHSs but a unique operator. Efficiently solving such problems on extreme-scale platforms requires also the minimization of global communications, reduction of synchronization points and promotion of asynchronous communications. UCGLE method introduced in Chapter 5 is a suitable candidate with the reduction of global communications and the synchronization points of all computing units. In this chapter, we extend both the mathematical model and the implementation of UCGLE method to adapt to solve sequences of linear systems. The eigenvalues obtained in solving previous linear systems by UCGLE can be recycled, improved on the fly and applied to construct a new initial guess vector for subsequent linear systems, which can achieve a continuous acceleration to solve linear systems in sequence. Numerical experiments using different test matrices to solve sequences of linear systems on supercomputer indicate a substantial decrease in both computation time and iteration steps when the approximate eigenvalues are recycled to generate the initial guess vectors.

6.1 Demand to Solve Linear Systems in Sequence

In this chapter, we consider to solve a long sequence of general linear systems

$$Ax^{(i)} = b^{(i)}, i = 1, 2, \cdots, p \text{ with } p > 1 \tag{6.1}$$

where $A \in \mathbb{C}^{n\times n}$ is a fixed matrix, and the RHS $b^{(i)} \in \mathbb{C}^n$ which changes from one system to another. Moreover, these systems are typically not available simultaneously. Many scientific applications require to solve this kind of sequent linear systems, such as the finite element analysis in modeling fatigue [160, 106, 205], diffuse optical tomography [123, 14, 193], electromagnetic [30, 174, 231] and wave-propagation for the earthquake simulation [97, 146, 56], etc. Generally, these systems are formulated by the time-dependent applications, where the operator matrix A keeps the same, but the RHS $b^{(i)}$ cannot be gotten in the same time. In many fields, the next RHS of the linear system depends on the previous solution. Thus only one linear system

© 2019 Tous droits réservés.

lilliad.univ-lille.fr

Thèse de Xinzhe Wu, Université de Lille, 2019

is available at a time. Another type of applications to solve linear systems in sequence are the Newton methods for solving nonlinear equations (e.g., [45, 125, 34, 92, 6]). If the direct solvers are applicable, their decompositions can be shared and reused for the successive linear systems by the forward/backward solves. When the matrix has a large dimension or special sparsity pattern, and the direct solvers are not applicable, then the iterative methods based on Krylov subspace, such as CG for symmetric systems, and GMRES for non-Hermitian systems, are considerable. Obviously, this naive implementation is not efficient enough, since the sequence of linear systems shares the same matrix A. The intermediate information computed from the previous system's solution can be reused to speed up the solution of the next systems.

6.2 Existing Methods

There are already several methods proposed to take advantage of this temporary information in order to speed up the procedures to solve the sequences of linear systems.

6.2.1 Seed Methods

The first approach is to use the seed methods (e.g., [183, 168, 199, 105, 197, 1]). As an example of seed GMRES method shown by Algorithm 24, the seed methods select one seed system and solve it by the Krylov iterative method, and then a Galerkin projection of the other RHSs is performed onto the Krylov subspace generated by the seed system. It is efficient since the Krylov subspace generated by the previous time solving linear system develops a good approximation to the eigenvectors of small eigenvalues of A, and the projection of the other RHSs over this subspace can remove the components of their residual vectors in the directions these eigenvectors. The seed methods require more memory space to store the subspace of seed systems. The speedup cannot always be guaranteed for the uncorrelated RHSs. It can also be inefficient for the restarted methods, in this case, even the convergence of solving the seed system maybe stagnate.

6.2.2 Krylov Subspace Recycling Methods

Another more general approach is to improve the convergence of solving a sequence of linear systems by the process of Krylov Subspace Recycling (e.g. [169, 118, 123, 231]). For example, by recycling the Krylov subspace generated by previous solution, the GCRO-DR method proposed by Parks [169] allows to speed up the solution of systems from one RHS to another or even between two times restart of iterative methods through the maintain of the Arnoldi subspace orthogonalization and the deflation of smallest eigenvalues.

In this section, we choose GCRO-DR as an example to detail the idea of Krylov Subspace Recycling methods to solve sequences of linear systems with continuous improvement. This method is called GCRO-DR because it is a combination of GMRES-DR and GCRO [67]. The pseudocode of GCRO-DR is given as Algorithm 25. When solving a single linear system, GCRO-DR and GMRES-DR are algebraically equivalent. The primary advantage of GCRO-DR is its capability for solving sequences of linear systems.

The Krylov Subspace Recycling methods are proposed for the solution of sequences of general matrices, and do not assume that all matrices are pairwise close or that the sequence of matrices

© 2019 Tous droits réservés.

lilliad.univ-lille.fr

Thèse de Xinzhe Wu, Université de Lille, 2019

Algorithm 24 The seed-GMRES algorithm

1: Choose n_{max}, the maximum size of the subspace. For each RHS $b^{(i)}$, choose an initial guess $x_0^{(i)}$ and compute $r_0^{(i)} = b^{(i)} - Ax_0^{(i)}$. The recast problem is the error system $A(x^{(i)} - x_0^{(i)}) = r_0^{(i)}$, choose a RHS k, the first on which a cycle of GMRES is applied. Set $Z_p = (z_1, \cdots, z_p)$, p vectors of size m, to zero.

2: run one cycle of GMRES(n_{max}) on $r_0^{(k)}$, either it converges in $n = n_1$ step or stops after $n = n_{max}$ steps. This GMRES provides us with V_{n+1}, that has orthonormal columns, and $\underline{H}_{n+1,n}$ such that $AV_n = V_{n+1}\underline{H}_{n+1,n}$. The approximate solution for the k-th system writes $x_n = x_0^{(k)} + MV_n y_n^{(k)}$ but is not computed as such. The vector z_k is updated via $z_k = z_k + V_n y_n^{(k)}$ and the residual can be formatted via $x^{(k)} = x_0^{(k)} + Mz_k$. If all the systems have converged, stop.

3: For each RHS $i \neq k$ that has not converged, form $c^{(i)} = V_{n+1}^T r_0^{(i)}$ and compute $y_n^{(i)}$ the solution of the Least Squares problems $||\underline{H}_{n+1,n}y - c^{(i)}||_2$. Compute $z_i = z_i + V_n y_n^{(i)}$ and the residual $r_n^{(i)} = (I_m - V_{n+1}V_{n+1}^T)r_0^{(i)} + V_{n+1}(c^{(i)} - \underline{H}_{n+1,n}y_n^{(i)})$. If the system has i converged, form the approximate solution $x^{(i)} = x_0^{(i)} + Mz_i$. If all the systems have converged, stop.

4: For each RHS i that has not converged, set $r_0^{(i)} = r_n^{(i)}$. Choose a vector to run a cycle of GMRES. Traditionaly we take the first i in the list $k, k+1, \cdots p$, so that the system i has not converged and go to step 2.

converges to a particular matrix. The recycling techniques are effective under these assumptions that:

(1) the method must be able to identify and converge to an effective subspace for recycling (the recycle space) in a reasonable number of iterations, it must be able to converge to an effective recycle space over the solution of multiple linear systems. Otherwise, a good recycle space may never be found for a sequence of changing matrices;

(2) a significant convergence improvement for the linear solver should be obtained with a relatively small recycle space;

(3) the method must be able to converge quickly to an effective perturbed recycle space for an updated matrix, and it must provide an inexpensive mechanism for regularly updating the recycle space to reflect the changes in the linear systems.

The workflow of GCR-DO (shown as 6.1) for solving sequences of linear systems by recycling the Krylov subspaces is:

(1) Perform m steps of Arnoldi reduction in parallel, and generate the subspace V_{m+1} and Hessenberg matrix $\underline{H}_m$;

(2) Solve the Least Squares problem $||c - \underline{H}_m y||_2$ in sequence;

(3) solve the eigenvalue problem $(H_m + h_{m+1,m}^2 H_m^{-H} e_m e_m^H)z_\lambda = \theta_\lambda z_\lambda$ in sequence;

(4) perform the reduced QR factorization in sequence;

(5) compute U_k, V_{m+1}, W_{m+1} and $\underline{G}_m$ in parallel;

© 2019 Tous droits réservés.

lilliad.univ-lille.fr

Thèse de Xinzhe Wu, Université de Lille, 2019

(6) solve the Least Squares problem $||W_{m+1}^H r_{i-1} - \underline{G}_m y||_2$ and perform the reduced factorization in sequence;

(7) for the next iteration until the convergence;

(8) for the subsequent systems, the first step is recycling the matrices C_k and U_k in parallel, and then perform the iterations until the convergence.

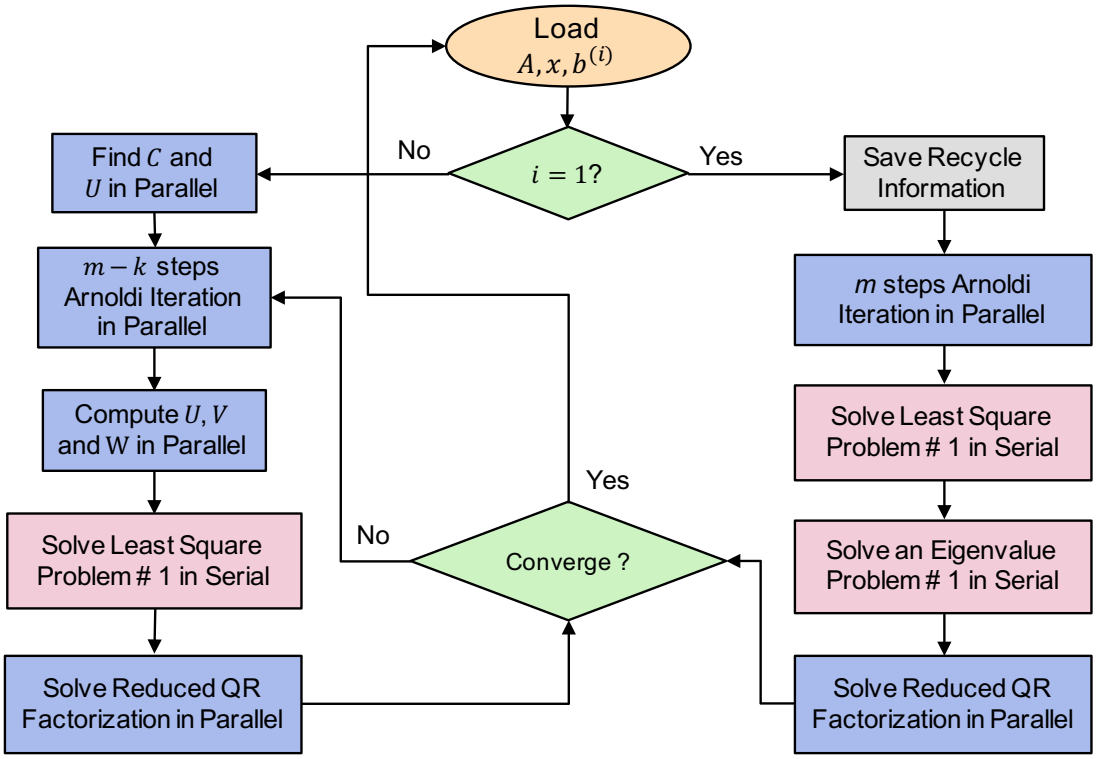

Figure 6.1 – GCR-DO workflow.

GCR-DO is a useful iterative methods to solve sequences of linear systems with acceleration by recycling the Krylov subspace. The only limitation of the different synchronization points introduced by the procedure of recycling. For the implementation of iterative methods on large-scale platforms, these synchronization points should be avoided.

GCR-DO is able to converted into distributed and parallel scheme based on the Unite and Conquer approach. But in this chapter, we prefer to extend our UCGLE with special strategy to solve long sequences of linear systems by recycling of approximated Ritz values.

6.3 UCGLE to Solve Linear Systems in Sequence by Recycling Eigenvalues

In this section, we introduce the extension of UCGLE to solve sequences of non-Hermitian linear systems for modern computer architectures. Inside of UCGLE, the dominant eigenvalues are used to accelerate the convergence of iterative methods. The more the eigenvalues are calculated, the more accurate these values are, the more significant the acceleration will be. When using UCGLE to solve sequences of linear systems, the eigenvalues computed during the solving procedures of

© 2019 Tous droits réservés.

lilliad.univ-lille.fr

Thèse de Xinzhe Wu, Université de Lille, 2019

Algorithm 25 GCRO-DR algorithm [169]

Choose m, the maximum size of the subspace, and k, the desired number of approximate eigenvectors. Let *tol* be tge convergence tolerance. Choose an initial guess x_0.
$r_0 = b - Ax_0$
set $i = 1$
if U_k is defined from solving previous systems **then**
  if $A_i \neq A_{i-1}$ **then**
    $[Q, R]$ = distributed qr$(A_i U_k)$
    $C_k = Q$
    $U_k = U_k R^{-1}$
  end if
  $x_1 = x_0 + U_k C_k^H r_0$
  $r_1 = r_0 - C_k C_k^H r_0$
else
  $v_1 = r_0 / ||r_0||_2$
  $c = ||r_0||_2 e_1$
  m steps of GMRES, solving min $||c - \underline{H}_m y||_2$ for y and generating V_{m+1} and H_m.
  $x_1 = x_0 + V_m y$
  $r_1 = V_{m+1}(c - \underline{H}_m y)$
  solve $(H_m + h_{m+1,m}^2 H_m^{-H} e_m e_m^H) z_\lambda = \theta_\lambda z_\lambda$
  store the k eigenvectors z_λ associated to the smallest eigenvalues in magnitude in P_k
  $[Q, R] = \text{qr}(\underline{H_m} P_k)$
  $C_k = V_{m+1} Q$
  $U_k = V_m P_k R^{-1}$
end if
while not converge **do**
  $i+ = 1$
  Perform m-k steps of GMRES with $(I - C_k C_k^H) A_i$, , thus generatingV_{m+1-k}, $\underline{H}_{m-k}$ and B_{m-k} and letting $v_i = r_{i-1}/||r_{i-1}||_2$.
  let D_k be a diagonal scaling matrix such that $U_k = U_k D_k$ with the columns having unit norm.
  $V_m = [U_k \quad V_{m-k}]$.
  $W_{m+1} = [C_k \quad V_{m-k+1}]$.
  $\underline{G}_m = \begin{bmatrix} D_k & B_{m-k} \\ 0 & \underline{H}_{m-k} \end{bmatrix}$
  find y such that min $||W_{m+1}^H r_{i-1} - \underline{G}_m y||_2$
  $x_i = x_{i-1} + V_m y$
  $r_i = r_{i-1} - W_{m+1} \underline{G}_m y$
  $R_j = B_i - A_i X_j$
  if $A_i \neq A_{i-1}$ **then**
    Compute the k eigenvectors z_i of $\underline{G}_m^H \underline{G}_m z_i = \theta_i \underline{G}_m^H W_{m+1}^H V_m z_i$ associated with smallest magnitude eigenvalues θ_i and store in P_k
    $Y_m = V_m P_k$
    $[Q, R] = \text{qr}(\underline{G_m} P_k)$
    $C_k = W_{m+1} Q$
    $U_k = Y_k R^{-1}$
  end if
end while
let $Y_k = U_k$ for the next system.

© 2019 Tous droits réservés.

lilliad.univ-lille.fr

Thèse de Xinzhe Wu, Université de Lille, 2019

previous linear systems can be reused, and sometimes improved, to solve the following different linear systems in sequence. Theoretically, the continuous amelioration of convergence for the rest of the linear systems can be achieved. Moreover, the eigenvalues computed from the procedure of solving previous linear systems can be used to construct an approximate solution for the subsequent linear systems by Least Squares polynomial method and serve as an initial guess vector to speedup up the solving procedure of next system.

6.3.1 Relation between Least Squares Polynomial Residual and Eigenvalues

In Section 5.4, we have already analyzed the relation between Least Squares polynomial residual and the computed eigenvalues $\lambda_1, \cdots, \lambda_m$ to construct the convex hull. The residual given by Least Squares polynomial of degree d is

$$r_d = \sum_{i=1}^{m} \rho_i (R_d(\lambda_i))^{lsa} u_i + \sum_{i=m+1}^{n} \rho_i (R_d(\lambda_i))^{lsa} u_i, \tag{6.2}$$

this residual can be divided into two parts. The first part is formulated with the first known m eigenvalues which are used to compute the convex hull by LSP Component. The second part represents the residual with unknown eigenpairs. In this chapter, we present this relation one more time in detail in order to illustrate the methology to solve sequences of linear systems by recycling of dominant eigenvalues.

In practice, for each time preconditioning by Least Squares polynomial method, it is often repeated for several times to improve its acceleration of convergence, that is the meaning of parameter lsa in Equation (6.2). The Least Squares polynomial preconditioning applies r_d as a restarted vector for each time GMRES restart process. Fig. 5.14 in Section 5.5 gives the comparison between classic GMRES and UCGLE with different values for the parameter lsa. As shown in this figure, the first part in Equation (6.2) is small since the Least Squares polynomial method finds R_d minimizing $|R_d(\lambda)|$ in the convex hull, but not with the second part, where the residual will be rich in the eigenvectors associated with the eigenvalues outside H_m. As the number of approximated eigenvalues m increasing, the first part will be much closer to zero, but the second part keeps still large. This results in an enormous increase of restarted GMRES preconditioned vector norm. Meanwhile, when GMRES restarts with the combination of a number of eigenvectors, the convergence will be faster even if the residual is enormous, and the convergence of GMRES can still be significantly accelerated. The peaks are shown in Fig. 5.14 for each time restart of UCGLE represent these enormous residuals. The lsa times repeat of r_d before applying to next time restart can still enlarge its norm, and the selection of lsa is important for the acceleration. In the example of Fig. 5.14, we conclude that if lsa is too large, the norm trends enormous, which slows down the speedup, if lsa is small, the acceleration may not be evident.

6.3.2 Eigenvalues Recycling to Solve Sequence of Linear Systems

After the analysis of relation between Least Squares polynomial residual and the approximated eigenvalues, it is apparent that these dominant eigenvalues used by LSP Component to accelerate the convergence, can be recycled and improved from the procedure of solving system with

© 2019 Tous droits réservés.

lilliad.univ-lille.fr

Thèse de Xinzhe Wu, Université de Lille, 2019

one RHS to another, which will introduce a potential continuous improvement for solving a long sequence of linear systems. Eigenvalues recycling technique proposed in this section is applicable for the series of linear systems with their operator matrices shared a portion of dominant eigenvalues. However, in this chapter, we only consider the case that A do not change.

In order to solve the sequence of linear systems $Ax = b^{(t)}$ with $t \in 1, 2, 3, \cdots$. We enlarge the Krylov subspace size m_a inside ERAM Component to approximate more eigenvalues. Suppose that $m_a^{(1)}$ for the first system, the exact implementation of ERAM Component for $t \in 2, 3, \cdots$ is shown in Equation (6.3), $m_a^{(t)}$ is equal to the sum of $m_a^{(t-1)}$ and a given constant a. And $k^{(t)}$, the number of eigenvalues computed by ERAM Component for $Ax = b^{(t)}$ can be described by a function f which maps the relation between $m_a^{(t)}$ and $k^{(t)}$. Obviously, $k^{(t)} \geq k^{(t-1)}$. The residual $r_d^{(t)}$ for each restart of $Ax = b^{(t)}$ with $t \in 2, 3, \cdots$ is also given in (6.3).

$$\begin{cases} m_a^{(t)} = (m_a)^{(t-1)} + a \\ k^{(t)} = f(m^{(t)}) \\ r_d^{(t)} = \sum_{i=1}^{k^{(t)}} (R_d(\lambda_i))^{lsa} \rho_i u_i + \sum_{i=k^{(t)}+1}^{n} (R_d(\lambda_i))^{lsa} \rho_i u_i s \end{cases} \tag{6.3}$$

With the enlargement of Krylov subspace size inside ERAM Component, the more eigenvalues are calculated, then the first part of $r_d^{(t)}$ in Equation (6.3) are more important, and the more significant the acceleration will be. The continuous amelioration of convergence for solving linear systems in sequence can be gotten. With the changing of ERAM component Krylov subspace size, it may not be guaranteed to get the demanded eigenvalues in time for each restart of GMRES component if this size is too large compared with GMRES Component Krylov subspace size. In order to improve the robustness of UCGLE, the previously calculated eigenvalues are kept in memory and updated if there come the new ones. These values in memory can be utilized in case that the failure of ERAM component when the parameters are too strict. In Equation (6.3), we did not define the upper limit for $m_a^{(t)}$, which depends on properties of operator matrices and P_g and P_a for GMRES and ERAM components.

For $t \in 2, 3, \cdots$, since the eigenvalues calculated when solving $Ax = b^{(t-1)}$ are kept in memory, they can be used to construct an approximative solution for the current linear system $Ax = b^{(t)}$ through the Least Squares polynomial method before its solve by GMRES. This approximative solution can be used as a non-zero initial guess vector $x_0^{(t)}$ to solve $Ax = b^{(t)}$. It will introduce an acceleration on the convergence for solving the linear systems in sequence. With the number of linear systems to be solved increasing, there will be more eigenvalues approximated, the initial guess vector constructed by LSP component will be more accurate, and thus the speedup for solves from one to another can be still gotten. The impact of the initial guess vector on the convergence is different from the restarted residual vector inside the iterative method. We propose a new parameter $(lsa')^{(t)}$ for the initial guess generation procedure which is different from the lsa in Least Squares polynomial preconditioning part. The residual vector $g_d^{(t)}$ for $Ax = b^{(t)}$ with $t \in 2, 3, \cdots$ is given in Equation (6.4), which is constructed by the $k^{(t-1)}$ number of eigenvalues calculated when solving $Ax = b^{(t)}$.

© 2019 Tous droits réservés.

lilliad.univ-lille.fr

Thèse de Xinzhe Wu, Université de Lille, 2019

$$g_d^{(t)} = \sum_{i=1}^{k^{(t-1)}} (R_d(\lambda_i))^{(lsa')^{(t-1)}} \rho_i u_i + \sum_{i=k^{(t-1)}+1}^{n} (R_d(\lambda_i))^{(lsa')^{(t-1)}} \rho_i u_i. \tag{6.4}$$

In this section, two parameters are added in order to solve linear systems in sequence using UCGLE. They are listed as below:

1. $m_a^{(t)}$: ERAM Krylov subspace size for solving $Ax = b^{(t)}$
2. $(lsa')^{(t)}$: times that Least Squares polynomial applied for the generation of initial guess vector for solving $Ax = b^{(t)}$

It is predictable that this speedup for solving successive systems will stagnate after the optimized values of m_a and $(lsa')^{(t)}$ are found. It is useless to use the ERAM Component to approximate the eigenvalues continuously. Thus P_a computing units allocated for ERAM Component can be redistributed to GMRES Component. It is expected to get an extra speedup on the performance with more computing resources.

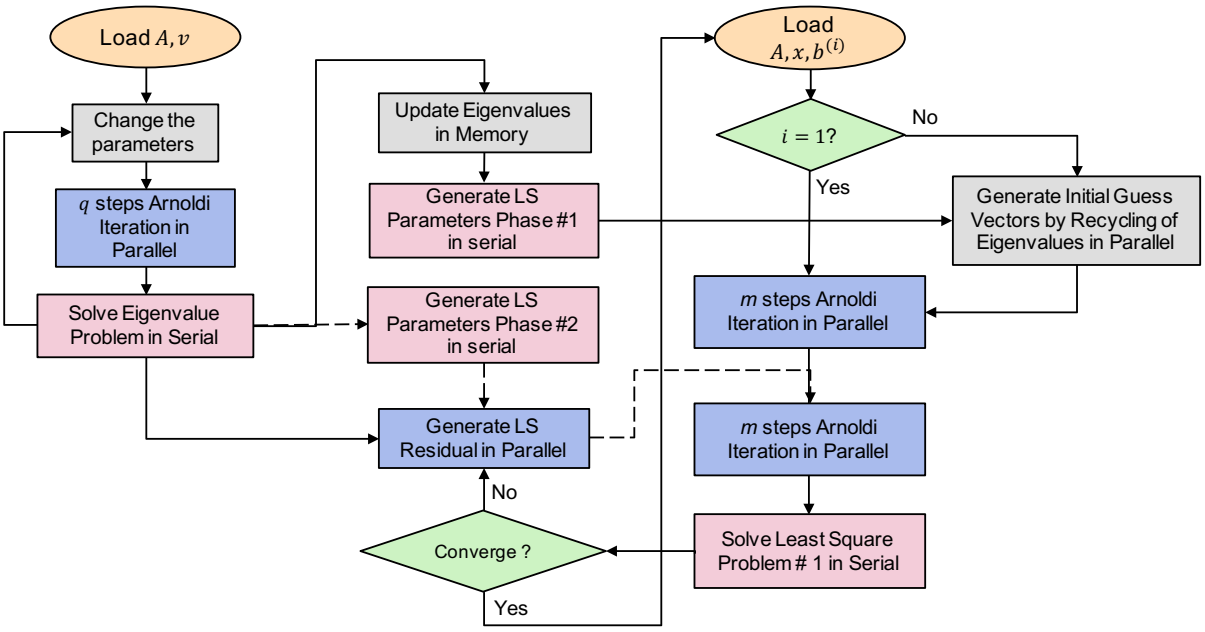

Figure 6.2 – Workflow of UCGLE to solve linear systems in sequence by recycling of eigenvalues.

6.3.3 Workflow to Recycle Eigenvalues

The Algorithm 26 and Fig. 6.2 give the procedure of UCGLE for solving a sequence of linear systems $Ax = b^{(t)}$ with $t \in 1, 2, 3, \cdots$. Initially, P_g and P_a are respectively set to be $proc_g$ and $proc_a$. If $t = 1$, UCGLE loads normally the three computational components with the ERAM component's Krylov subspace to be $m_a^{(1)}$, and the initial guess vector for GMRES component to be zero. For solving the successive linear systems, before the update of three components, a $INITIAL\_GUESS$ function is performed which is the same as the LSP component but with different parameter $(lsa')^{(t)}$. The $INITIAL\_GUESS$ function will generate an initial guess vector ${g_d}^{(t)}$. Inside the GMRES component, the initial guess vector is updated by ${g_d}^{(t)}$ before the

© 2019 Tous droits réservés.

lilliad.univ-lille.fr

Thèse de Xinzhe Wu, Université de Lille, 2019

Algorithm 26 UCGLE for sequences of linear systems

for $(t \in (1, 2, 3, \cdots))$ **do**
  if $(t = 1)$ **then**
    set $P_g = proc_g$ and $P_a = proc_a$
    $LOADERAM(input : A, m_a, v, r, \epsilon_a)$
    $LOADLS(input : A, b, d)$
    $LOADGMRES(input : A, m_g, x_0, b^{(1)}, \epsilon_g, freq, l, output : x_m)$
  else
    set $P_g = proc_g$ and $P_a = proc_a$
    $INITIAL\_GUESS(input : A, b^{(t)}, d, output : g_d^{(t)})$
    update $LOADGMRES(input : A, m_g, g_d^{(t)}, b^{(t)}, \epsilon_g, freq, l, output : x_m)$
    update $m_a^{(t-1)}$ by $m_a^{(t)}$ in $LOADERAM(input : A, m_a^{(t)}, v, r, \epsilon_a)$
    update $LOADLS(input : A, b^{(i)}, d)$
    if (optmized $m_a^{(op)}$ and $(lsa')^{(op)}$ found) **then**
      save the eigenvalues to *eigenvalues.bin*
      set $P_g = proc_g + proc_a - 1$ and $P_a = 1$
      $INITIAL\_GUESS(input : A, b^{(t)}, d, output : g_d^{(t)})$ by loading *eigenvalues.bin*
      $LOADGMRES(input : A, m_g, g_d{}^{(t)}, b^{(t)}, \epsilon_g, freq, (lsa')^{(op)}, output : x_m)$
      replace $LOADERAM$ by a simple useless function
      $LOADLS(input : A, b^{(i)}, d)$ by loading *eigenvalues.bin*
    end if
  end if
end for

start of solving procedure. Moreover, the Krylov subspace Size of ERAM Component is replaced by $(m_a)^{(t)}$. When the optimized values of $(m_a)^{(op)}$ and $(lsa')^{(op)}$ are found, the eigenvalues are kept into a local file *eigenvalue.bin*. The P_g and P_a are respectively updated as $proc_g + proc_a - 1$ and 1. The $INITIAL\_GUESS$ function executes by loading *eigenvalue.bin*. $LOADGMRES$ is restarted with the redeployment of its data onto $proc_g + proc_a - 1$ computing units. LSP Component also executes with *eigenvalue.bin*. The retainment of 1 computing unit for ERAM Component aims to ensure the distributed and parallel implementation of UCGLE with high fault tolerance. However, the inside kernel of ERAM Component is replaced by a simple function with keeping the data sending and receiving functionalities.

6.4 Experiments

In this section, we evaluate the UCGLE for solving the sequences of linear systems on the supercomputer using different test matrices generated by SMG2S. UCGLE with or without initial guess vector generation is compared with conventional restarted GMRES with or without available preconditioners (Jacobi and SOR) in our implementations. The parallel performance on different homogeneous and heterogeneous platforms is presented in Chapter 5. Thus this chapter concentrates on the numerical performance of UCGLE for solving non-Hermitian linear systems in sequence, and the parallel performance comparison will not be discussed. It is fair to prove the benefits of Unite and Conquer approach by comparing it with the implementations of classic solvers based on the same basic operations (distribution of matrix across the cores,

© 2019 Tous droits réservés.

lilliad.univ-lille.fr

Thèse de Xinzhe Wu, Université de Lille, 2019

Table 6.1 – $Mat1$: iterative step comparison for solving a sequence of linear systems.

Method	1	2	3	4	5	6	7	8	9
GMRES	509	505	501	505	527	510	523	516	518
GMRES+SOR	169	165	172	130	172	173	130	170	130
GMRES+Jacobi	274	273	270	276	269	274	280	276	273
UCGLE w/o initial guess	120	90	90	90	90	90	90	90	90
UCGLE with initial guess	120	36	35	35	36	36	36	33	35

parallel sparse matrix-vector operation, the orthogonalization in Arnoldi reduction, etc.) without specific optimization for different platforms. If we optimize the parallel implementation of classic solvers and also the components (especially GMRES Component) in UCGLE at the same time, the benefits of UCGLE by reducing the global communications and promoting the asynchronous communications are still there.

6.4.1 Hardware

UCGLE is implemented on the supercomputer *Tianhe-2*. The details of this machine is already given in Section 4.6.1.

6.4.2 Results

We evaluate UCGLE for solving sequences of linear systems using three test matrices of size 1.572×10^7 generated by SMG2S with different given spectra. They are respectively denoted as $Mat1$, $Mat2$ and $Mat3$. The different RHSs of these sequent linear systems are generated at random. The parameter lsa for all tests using UCGLE keeps the same as 10. The numbers of CPUs for GMRES and ERAM Components in UCGLE are respectively 768 and 384. Five methods are compared in the experiments, and their notations are given below:

- GMRES: classic restarted GMRES;
- GMRES+SOR or SOR: GMRES with SOR preconditioner;
- GMRES+Jacobi or Jacobi: GMRES with Jacobi preconditioner;
- UCGLE without (w/o) initial guess: UCGLE without using previously obtained eigenvalues to generate an initial guess vector for the next system by Least Squares polynomial method;
- UCGLE with initial guess: UCGLE using previously obtained eigenvalues to generate an initial guess vector for the next system by Least Squares polynomial method.

ERAM and LSP components in UCGLE demand additional computing units. It is unfair to test only the conventional methods of their numbers of CPUs equal to the number of GMRES components in UCGLE. Therefore, experiments have also been tested that the numbers of

© 2019 Tous droits réservés.

lilliad.univ-lille.fr

Thèse de Xinzhe Wu, Université de Lille, 2019

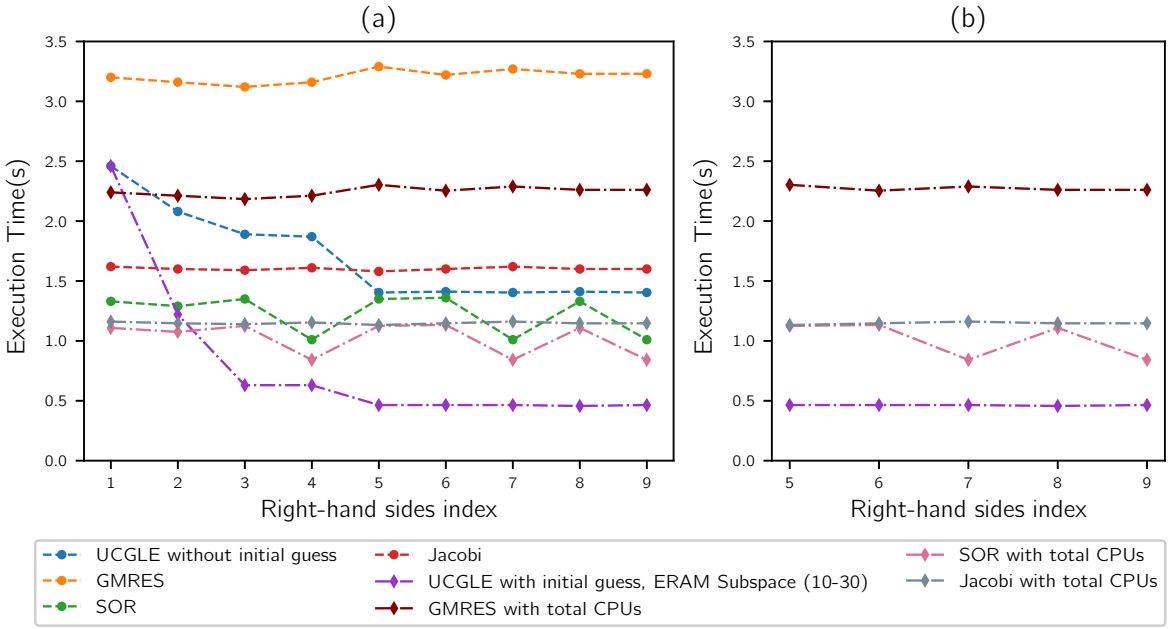

Figure 6.3 – $Mat1$: time comparison for solving a sequence of linear systems. (a) shows the solution time for 9 sequent linear systems; (b) shows the cases extracted from (a) after obtaining the optimal parameters in UCGLE.

computing units of the classical iterative method are equal to the total CPU in UCGLE (hence, the CPUs for GMRES and ERAM components are included). In the captions of figures, a given method "with total CPUs" means that its number of CPUs equals the total CPU in UCGLE. The time comparisons for solving nine sequent linear systems of $Mat1$, $Mat2$ and $Mat3$ are given respectively in Fig. 6.3a, Fig. 6.4a and Fig. 6.5a, the comparison of the number of iteration for convergence are respectively given in Table 6.1, Table 6.2 and Table 6.3. From these three tables, we conclude that UCGLE can speed up the convergence to solve linear systems with test matrices comparing with the conventional methods. The generation of initial vectors using the eigenvalues for subsequent linear systems can still speed up the convergence over the UCGLE without initial guess.

For the tests of $Mat1$, the GMRES restart size is 30, the Krylov subspace of ERAM Component for solving the first three linear systems are respectively 10, 20 and 30, the size of this subspace of ERAM for the remaining systems keeps being 30. For the tests of $Mat2$, the GMRES restart size is 300, the Krylov subspace of ERAM Component for solving the first three linear systems are respectively 100, 150 and 200, the size of this subspace of ERAM for the remaining systems keeps being 200. For the cases that UCGLE with initial guess, the parameter $(lsa')^{(t)}$ for $Mat1$ and $Mat2$ keeps 30. With the augmentation of the size of ERAM Krylov subspace, there will be more eigenvalues to be approximated, and we find that there is acceleration with the accumulation of more eigenvalues for both the case UCGLE with and without initial guess. The influence of subspace of ERAM can be found through the curves of UCGLE with/without initial guess in Fig. 6.3a and Fig. 6.4a. However, it is not practical to enlarge too much the Krylov subspace of ERAM to approximated more eigenvalues, since if it is too large, it takes too much time by ERAM, LSP Component cannot receive the eigenvalues in time, thus it will be

© 2019 Tous droits réservés.

lilliad.univ-lille.fr

Thèse de Xinzhe Wu, Université de Lille, 2019

difficult for the GMRES Component to perform the Least Squares polynomial preconditioning for its each time restart.

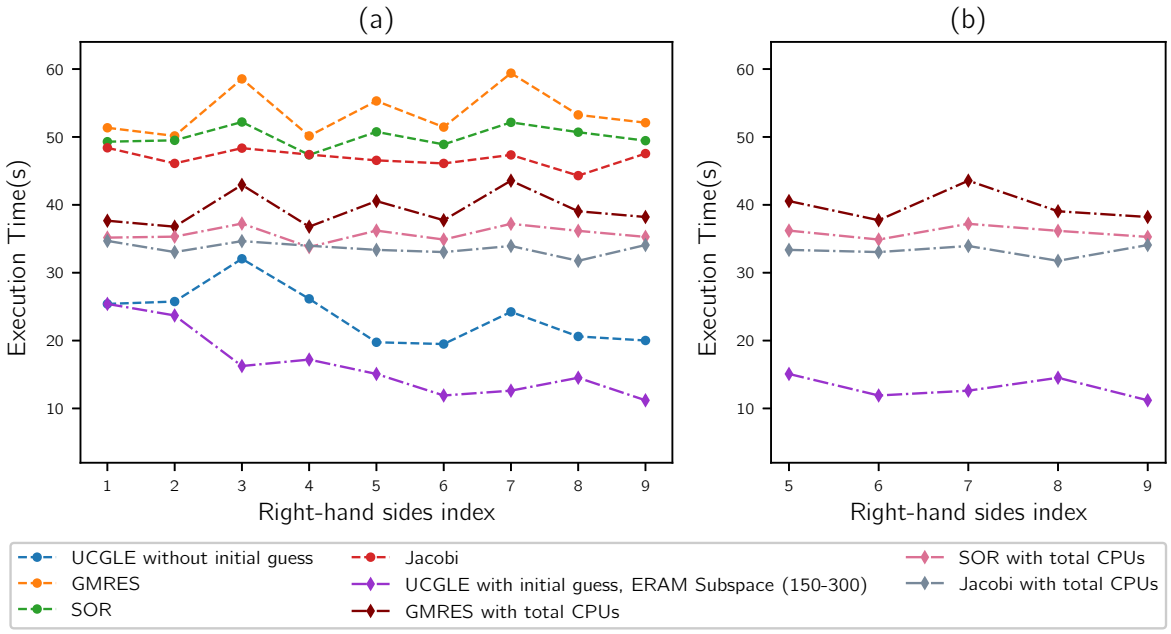

Figure 6.4 – $Mat2$: time comparison for solving a sequence of linear systems. (a) shows the solution time for 9 sequent linear systems; (b) shows the cases extracted from (a) after obtaining the optimal parameters in UCGLE.

For the tests of $Mat3$, the GMRES restart size is 150, and the Krylov subspace size of ERAM Components keeps the same to be 200. Meanwhile, for the 2nd, 3rd and 4th linear systems, the parameter $(lsa')^{(t)}$ of initial guess are respectively 20, 30 and 40, for the remaining linear systems, this parameter keeps 40. For solving the linear systems by UCGLE with initial guess, we can find that with the augmentation of $(lsa')^{(t)}$, the iteration numbers for the first four linear systems decrease quickly from 360 to 283 with approximately 1.3× speedup. For $Mat3$, SOR preconditioned GMRES is already good, but UCGLE with initial guess has still about 2.2× speedup of convergence. Even in the case that the computing unit number of SOR preconditioned GMRES equals the total number of UCGLE, UCGLE with initial guess can achieve 2.2× speedup of execution time. With the augmentation of the parameter $(lsa')^{(t)}$, there will be a strong impact on the convergence. Since the $Mat3$ is generated with the clustered eigenvalues which are randomly distributed inside a fixed region of the real-imaginary plain, if $(lsa')^{(t)}$ is larger, it can be seen as there are much more eigenvalues generated, even they are not very accurate compared with the real ones. The inaccuracy of eigenvalues can result in the enlargement the norm in Equation (6.3), but it can still very quickly converge. It is effective to generate an initial guess vector with very large $(lsa')^{(t)}$, but not the same case for the parameter lsa inside each preconditioning, since too many times of repeats for each time restart will amplify quickly this inaccuracy of norm, and it is easy to result in the difficulties for convergence.

In order to use UCGLE for solving a large number of linear systems in sequence, it is necessary to choose the suitable parameters by the evaluation of a small number of sequent linear systems. After the selection of parameters, we compare the best cases of each method

© 2019 Tous droits réservés.

lilliad.univ-lille.fr

Thèse de Xinzhe Wu, Université de Lille, 2019

Table 6.2 – *Mat*2: iterative step comparison for solving a sequence of linear systems.

Method	1	2	3	4	5	6	7	8	9
GMRES	1316	1277	1460	1278	1409	1325	1472	1369	1342
GMRES+SOR	1197	1219	1336	1173	1290	1194	1335	1289	1213
GMRES+Jacobi	1278	1185	1283	1220	1191	1184	1218	1159	1239
UCGLE w/o initial guess	666	671	831	689	701	685	837	736	714
UCGLE with initial guess	666	595	470	491	544	464	485	532	440

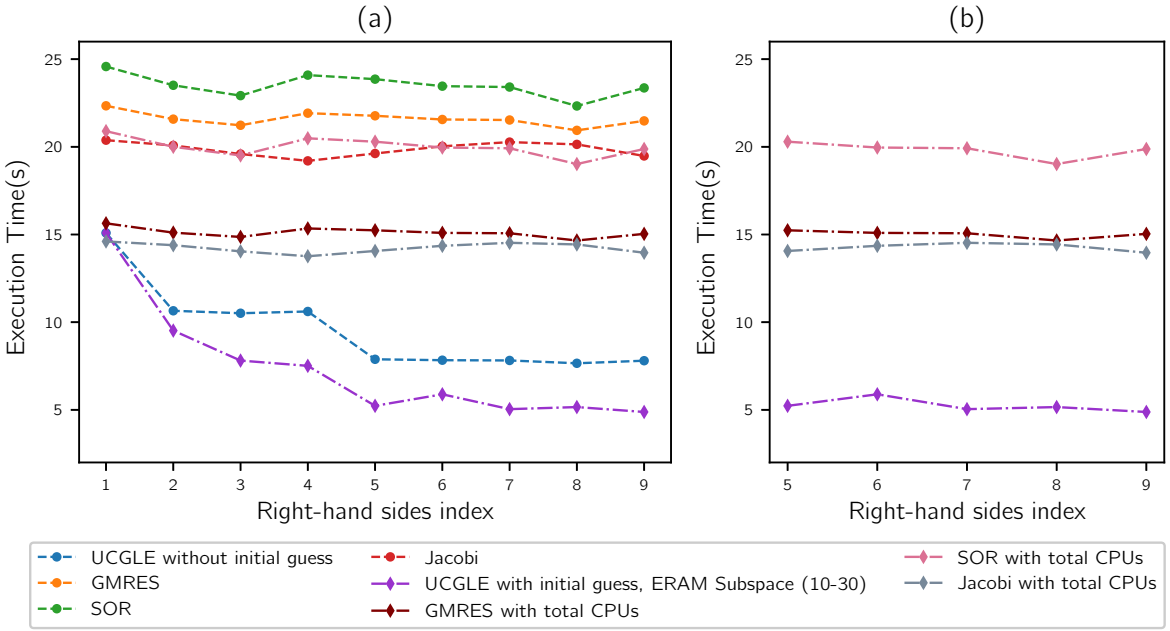

Figure 6.5 – *Mat*3: time comparison for solving a sequence of linear systems. (a) shows the solution time for 9 sequent linear systems; (b) shows the cases extracted from (a) after obtaining the optimal parameters in UCGLE.

with the least time-consumption. The results for three test matrices are shown in Fig. 6.3b, Fig. 6.5b and Fig. 6.4b. Except UCGLE with initial guess, the best methods for three tests are respectively GMRES+SOR, GMRES+Jacobi and GMRES+Jacobi. By comparing them with the tests of UCGLE with initial guess, we conclude that for *Mat*1, UCGLE with initial guess has about 4.4× for the acceleration of convergence and 1.7× for the speedup of execution time. For *Mat*2, it has about 2.6× acceleration for the convergence and 4.3× for the speedup of time. For *Mat*3, it has about 3.2× acceleration for the convergence and 2.7× for the speedup of time.

6.4.3 Analysis

In conclusion, UCGLE, especially it with the recycling eigenvalues to generate initial guess vector using the eigenvalues, can significantly accelerate the convergence and reduce the time consumption for solving a sequence of linear systems. However, the time employed by the Least Squares polynomial iterative recurrence, especially a small number of SpMV operations inside

© 2019 Tous droits réservés.

lilliad.univ-lille.fr

Thèse de Xinzhe Wu, Université de Lille, 2019

Table 6.3 – $Mat3$: iterative step comparison for solving a sequence of linear systems.

Method	1	2	3	4	5	6	7	8	9
GMRES	914	912	892	885	895	905	911	892	904
GMRES+SOR	895	871	856	885	879	870	868	838	868
GMRES+Jacobi	894	888	875	864	876	887	892	888	872
UCGLE w/o initial guess	673	364	355	360	367	363	363	351	364
UCGLE with initial guess	673	396	291	283	339	338	274	279	267

makes the time speedup not consistent with the convergence speedup. For example, in Table 6.3, UCGLE with initial guess has almost 3.0× acceleration on the convergence over the classic GMRES for solving the 3rd linear system. However, it has only about 2.0× acceleration on the performance in the case that the classic GMRES and GMRES Component inside UCGLE have the same number of computing units. It is caused by the recurrence of Least Squares polynomial iterations to perform the preconditioning on GMRES Component after receiving the parameters from LSP Component. Nevertheless, UCGLE is more efficient to solve the sequences of linear systems, and with its distributed and parallel communication framework, it is a good candidate for solving non-Hermitian linear systems in sequence on much larger machines.

6.5 Conclusion

In this chapter, we proposed an extended version of the distributed parallel method UCGLE, which is used to solve a large number of linear systems with unique matrix and different RHSs on a large platform. UCGLE method was proposed to solve large-scale linear systems on modern computing platforms, which is able to minimize the global communication, cover the synchronization points in the parallel implementation, improve the fault tolerance and reusability and speed up the convergence. In this chapter, it is proved this developed variant of UCGLE method can solve the linear systems with special spectral distribution in sequence more effectively than several preconditioned iterative methods. The recycling of a small group of dominant eigenvalues and generating initial guess vector using them by Least Squares polynomial method has a significant impact on the performance improvement for solving linear systems in sequence.

© 2019 Tous droits réservés.

lilliad.univ-lille.fr

Thèse de Xinzhe Wu, Université de Lille, 2019

Chapter 7

UCGLE to Solve Linear Systems Simultaneously with Multiple Right-hand Sides

Many problems in science and engineering often require to solve simultaneously large-scale non-Hermitian sparse linear systems with multiple RHSs. Efficiently solving such problems on extreme-scale platforms also requires the minimization of global communications, reduction of synchronization points and promotion of asynchronous communications. In this chapter, we develop another extension of UCGLE method by combining it with block GMRES method to solve non-Hermitian linear systems with multiple RHSs, using novel designed manager engine implementation. This engine is capable of allocating multiple block GMRES at the same time, each block GMRES solving the linear systems with a subset of RHSs and accelerating the convergence using the eigenvalues approximated by other eigensolvers. Dividing the entire linear system with multiple RHSs into subsets and solving them simultaneously with different allocated linear solvers allow localizing calculations, reducing global communication, and improving parallel performance. Meanwhile, the asynchronous preconditioning using eigenvalues can speed up the convergence and improve the fault tolerance and reusability. Numerical experiments using different test matrices on supercomputer *Romeo-2018* indicate that the proposed method achieves a substantial decrease in both computation time and iterative steps with good scaling performance.

7.1 Demand to Solve Linear Systems with Multiple RHSs

In this chapter, we consider solving the system

$$AX = B, \tag{7.1}$$

where $A \in \mathbb{C}^{n\times n}$ is a large, sparse and non-Hermitian matrix of order n, $X = [x^{(1)}, \cdots, x^{(s)}] \in \mathbb{C}^{n\times s}$ and $B = [b^{(1)}, \cdots, b^{(s)}] \in \mathbb{C}^{n\times s}$ are rectangular matrices of dimension $n \times s$ with $s \leq n$. In this chapter, the rectangular matrices such as B is also called block vector, which can be

© 2019 Tous droits réservés.

lilliad.univ-lille.fr

Thèse de Xinzhe Wu, Université de Lille, 2019

seen as the combination of s vectors b_i, with $i \in 1, 2, \cdots, s$. This kind of linear systems with multiple RHSs arise from a variety of applications in different scientific and engineering fields, such as the QCD [191, 157, 91], the wave scattering and propagation simulation [141], dynamics of structures [28, 90, 162], etc. The block Krylov methods are good candidates if we want to solve these large linear systems at the same time, because the block methods can expand the search space associated with each RHS and may accelerate the convergence. Another feature of block Krylov methods is that they can be implemented using the subroutines of BLAS3, which improves the locality and reusability of data and reduces the memory requirement on modern computer architectures [4]. The block Krylov methods replace the SpMV in each iterative step of the conventional Krylov methods with the SpGEMM.

7.2 Block GMRES Method

This section details block Krylov subspace and block GMRES to solve linear systems with multiple RHSs.

7.2.1 Block Krylov Subspace

In linear algebra, the m-order block Krylov subspaces $K^{\square}_{m\times s}$ [107] generated by an operator matrix $A \in \mathbb{C}^{n\times n}$ and a vector $B \in \mathbb{C}^{n\times s}$ is

$$K^{\square}_{m\times s}(A, B) = Block\ span\{B, AB, \cdots, A^{m-1}B\} \in \mathbb{C}^{n\times s}. \tag{7.2}$$

A block Krylov subspace method for solving the linear systems (7.1) is an iterative method that generates an approximate solution X_n such that

$$X_n - X_0 \in K^{\square}_{m\times s}(A, R_0), \tag{7.3}$$

where $R_0 = B - AX_0$ is the block vector of initial guess residual. For each RHS $b^{(i)}$ with $i \in 1, 2, \cdots, s$, its Krylov subspace generated by the block operation of A and R_0 can be defined as

$$\begin{aligned} K_{m\times s}(A, R_0) &= K_m(A, r_0^{(1)}) + \cdots + K_m(A, r_0^{(s)}) \\ &= Span\{r_0^{(1)}, \cdots, r_0^{(s)}, Ar_0^{(1)}, \cdots, Ar_0^{(s)}, \cdots, A^{m-1}r_0^{(1)}, \cdots, A^{m-1}r_0^{(s)}\}. \end{aligned} \tag{7.4}$$

Thus $K^{\square}_{m\times s}(A, R_0)$ is just the Cartesian product of s copies of $K_{m\times s}$

$$K^{\square}_{m\times s} = \bigtimes_{s \text{ times}} K_{m\times s}. \tag{7.5}$$

Thus $x_0^{(i)} + K_{m\times s}$ is the affine space where the approximation solution $x_n^{(i)}$ of the solution of the i-th systems $Ax^{(i)} = b^{(i)}$ is constructed from

$$x_m^{(i)} \in x_0^{(i)} + K_{m\times s}. \tag{7.6}$$

© 2019 Tous droits réservés.

lilliad.univ-lille.fr

Thèse de Xinzhe Wu, Université de Lille, 2019

Clearly, if all the ms vectors $A^k b^{(i)} \in \mathbb{C}^n$ are linearly independent,

$$dim\ K_{m\times s} = ms. \tag{7.7}$$

But this may not always be true, especially for different $b^{(i)}$ that are correlated. However even for the case that $dim\ K_{m\times s} < ms$, the searching space for each RHS $b^{(i)}$ can be enlarged, and a potential acceleration might be achieved. More exactly: block methods are most effective if

$$dim\ K_{m\times s}(A, R_0) \ll \sum_{k=1}^{s} dim\ K_m(A, r_0^{(k)}). \tag{7.8}$$

7.2.2 Block Arnoldi Reduction

In this section, we introduce the block version of Arnoldi reduction. Firstly, we define *block-orthogonal* and *block-normalized*. Denote the zero and unit matrix in $\mathbb{C}^{s\times s}$ by o and ι. The block vectors X and $Y \in \mathbb{C}^{n\times s}$ is *block-orthogonal* if $X * Y = o$, and we call X *block-normalized* if $X * X = \iota$. A set of block vectors $\{X_n\}$ is block orthonormal if these block vectors are block-normalized and mutually block-orthogonal. So, a set of block-orthonormal block vectors has the property that all the columns in this set are normalized vectors that are orthogonal to each other (even if they belong to the same block).

For matrix $A \in \mathbb{C}^{n\times n}$ and $V \in \mathbb{C}^{n\times s}$, a block Arnoldi reduction is able to generate nested block-orthonormal basis for the block Krylov subspace $K^{\square}_{m\times s}(A, V)$. Each column in the basis of $K^{\square}_{m\times s}(A, V)$ form at the same time an orthonormal basis of at most ms-dimensional space $K_{m\times s}(A, V)$. A version of block Arnoldi reduction with modified Gram-Schmit orthogonalization is given as Algorithm 27. The initialization step with a QR factorization generate an orthonormal baisis of $K_{1\times s}$ as V_0. For the subsequent m steps yield nests orthonormal bases for $K_{2\times s}, \cdots, K_{(m+1)\times s}$.

Algorithm 27 Block Arnoldi Algorithm

function BLOCK ARNOLDI(*input*:$A, m, V \in \mathbb{C}^{n\times s}$ of full rank, *output*: H_m, Ω_m)
  $V_0 P_0 := V$ ▷ QR factorization: $P_0 \in \mathbb{C}^{s\times s}, V_0 \in \mathbb{C}^{n\times s}, V_0^* V_0 = I$
  for $j = 0, 1, 2, \cdots, m$ **do**
    $U_j = AV_j$
    for $i = 1, 2, 4, \cdots, j$ **do**
      $H_{i,j} = V_i^T U_j$
      $U_j = U_j - V_i H_{i,j}$
    end for
    $U_j = V_{j+1} H_{j+1,j}$ ▷ QR factorization: $H_{j+1,j} \in \mathbb{C}^{s\times s}, V_{j+1} \in \mathbb{C}^{n\times s}, V_{j+1}^* V_{j+1} = I$
  end for
end function

Then we define the $n \times m$ matrices

$$\bar{V}_m = (V_0 \quad V_1 \quad \cdots \quad V_{m-1})$$

and the $(m+1)s \times ms$ matrix as Fig. 7.1, with block matrix $H_{1,0}, \cdots, H_{m,m-1}$ in the band

© 2019 Tous droits réservés.

lilliad.univ-lille.fr

Thèse de Xinzhe Wu, Université de Lille, 2019

to be upper triangle.

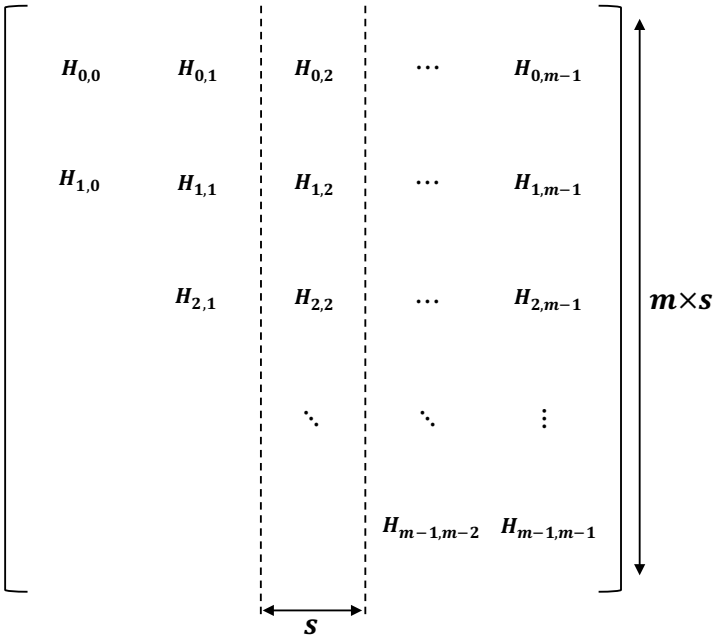

Figure 7.1 – Structure of block Hessenberg matrix.

Finally the Arnoldi relation can be obtained as:

$$AV_m = V_{m+1}\underline{H}_m. \tag{7.9}$$

7.2.3 Block GMRES Method

The block GMRES is constructed based the block Arnoldi reduction (shown as Algorithm 27) to solve the linear systems with multiple RHSs. Similar with the standard GMRES, block GMRES starts with a given initial guess solution $X_0 \in \mathbb{C}^{n\times s}$ of Equation (7.1), the related residual is of form

$$R_0 = B - AX_0 \tag{7.10}$$

The temporary solution X_m in the m-dimensional block Krylov subspace is

$$X_m = X_0 + V_m Y_m, \tag{7.11}$$

and the m-th block residual vector R_m can be obtained as

$$R_m = B - AX_m = R_0 - AV_m Y_m. \tag{7.12}$$

With the relation (7.9) of Arnoldi reduction, and $R_0 = V_{m+1}e_1 P_0$, we have

$$R_m = V_{m+1}(\underline{e_1}P_0 - \underline{H}_m Y_m). \tag{7.13}$$

where

- $\underline{e_1}$ the first s columns of the $(m+1)s \times (m+1)s$ unit matrix,

© 2019 Tous droits réservés.

lilliad.univ-lille.fr

Thèse de Xinzhe Wu, Université de Lille, 2019

- $P_0 \in \mathbb{C}^{s\times s}$ upper triangular, obtained in Arnoldi's initialization step,
- $\underline{H}_m$ the leading $(m+1)s \times ms$ submatrix of $\underline{H}_m$,
- $Y_m \in \mathbb{C}^{ms\times s}$ the "block coordinates" of $X_m - X_0$,

In order to get Y_m, a least squares problem should be solved

$$\min ||R_m||_F \text{ with } X_m - X_0 \in K^{\square}_{m\times s}. \tag{7.14}$$

where the operation $||.||_F$ for a block vector $Q \in \mathbb{C}^{n\times s}$ is defined as

$$||Q||_F = \sqrt{\sum_{j=1}^{s} ||x^{(j)}||_2^2} = \sqrt{\sum_{j=1}^{s}\sum_{i=1}^{n} |x_i^{(j)}|^2}. \tag{7.15}$$

But this least square problem is equivalent to

$$\min ||r_m^{(i)}||_2 \text{ with } x_m^{(i)} - x_0^{(i)} \in K_{m\times s}, \forall i = 1, 2, \cdots, s. \tag{7.16}$$

Since V_m has orthonormal columns, finally, we have

$$\min ||\underline{e_1} p_0^{(i)} - \underline{H}_m y_m^{(i)}||_2 \text{ with } y_m^{(i)} \in \mathbb{C}^{m\times s}, \forall i = 1, 2, \cdots, s. \tag{7.17}$$

These s least squares problems with the same matrix $\underline{H}_m$ can be solved efficiently by recursively computing the QR factorization of $\underline{H}_m$. An example of block MGRES is shown as Algorithm 28.

Algorithm 28 Block GMRES Algorithm

function BLOCK GMRES(*input*:$A, m, B, X_0 \in \mathbb{C}^{n\times s}$ of full rank, *output*: X)
  $R = B - AX_0$
  $V_0 R_0 := R$ ▷ QR factorization: $P_0 \in \mathbb{C}^{s\times s}, V_0 \in \mathbb{C}^{n\times s}, V_0^* V_0 = I$
  for $j = 0, 1, 2, \cdots, m$ **do**
    $U_j = AV_j$
    for $i = 1, 2, 4, \cdots, j$ **do**
      $H_{i,j} = V_i^T U_j$
      $U_j = U_j - V_i H_{i,j}$
    end for
    $U_j = V_{j+1} H_{j+1,j}$ ▷ QR factorization: $H_{j+1,j} \in \mathbb{C}^{s\times s}, V_{j+1} \in \mathbb{C}^{n\times s}, V_{j+1}^* V_{j+1} = I$
  end for
  $W_m = [V_1, V2, \cdots, V_m]$, $H_m = \{H_{i,j}\}_{0\le i\le j; 1\le j\le m}$
  Find Y_m, s.t. $||\beta - H_m Y_m||_2$ is minimized
  $X = X + W_m Y_m$
end function

7.2.4 Cost Comparison

In this section, we list the computational cost of the block Arnoldi process and block GMRES, and compare it with the cost of solving each system separately.

© 2019 Tous droits réservés.

lilliad.univ-lille.fr

Thèse de Xinzhe Wu, Université de Lille, 2019

Here is a table of the cost of m steps of block Arnoldi compared with s times the cost of m steps of conventional Arnoldi. Clearly, block Arnoldi is more costly than s times Arnoldi.

Table 7.1 – Operation Cost [107].

Operations	Block Arnoldi	s times Arnoldi
MVs	ms	ms
SDOTs	$\frac{1}{2}m(m+1)s^2+\frac{1}{2}ms(s+1)$	$\frac{1}{2}m(m+1)s$
SAXPYs	$\frac{1}{2}m(m+1)s^2+\frac{1}{2}ms(s+1)$	$\frac{1}{2}m(m+1)s$

The next table shows the storage requirements of m steps of block Arnoldi compared with those of m steps of Arnoldi:

Table 7.2 – Storage Requirement [107].

Operations	Block Arnoldi	s times Arnoldi
$y_0,\cdots,y_m$	$ms(s+1)n$	$(m+1)n$
ρ_0, H_m	$\frac{1}{2}s(s+1)+\frac{1}{2}ms(ms+1)+ms^2$	$1+\frac{1}{2}m(m+1)+m$

If we apply conventional Arnoldi s times, we can always use the same memory if the resulting orthonormal basis and Hessenberg matrix need not be stored. However, if we distribute the s columns of V_0 on s processors with distributed memory architecture, then block Arnoldi requires a lot of communication.

The extra cost of m steps of block GMRES on top of block Arnoldi compared with s times the extra cost of m steps of GMRES is given in the following table:

Table 7.3 – Extra cost of Block GMRES comparing with s times GMRES [107].

Operations	Block GMRES	s times GMRES
MVs	s	s
SDOTs	ms^2	ms
scalar work	$\mathcal{O}(m^2s^3)$	$\mathcal{O}(m^s)$

In particular, in the $(k+1)$-th block step we have to apply first ks^2 Givens rotations to the k-th block column (of size $(k+1)s\times s$) of $\underline{H}_m$, which requires $\mathcal{O}(ks^3)$ operations. Summing up over k yields $\mathcal{O}(m^2s^3)$ operations. Moreover, s times back substitution with a triangular $ms\times ms$ matrix requires also $\mathcal{O}(m^2s^3)$ operations.

Table 7.4 summarizes these numbers and gives the mean cost per iteration of block GMRES compared with s times the mean cost per iteration of GMRES:

© 2019 Tous droits réservés.

lilliad.univ-lille.fr

Thèse de Xinzhe Wu, Université de Lille, 2019

Table 7.4 – Extra cost of Block GMRES comparing with s times GMRES. [107]

Operations	Block GMRES	s times GMRES	ratio
MVs	$(1+\frac{1}{m})s$	$(1+\frac{1}{m})s$	1
SDOTs	$\frac{1}{2}(m+1)s^2+\frac{1}{2}s(s+1)$	$\frac{1}{2}(m+1)s$	$s+\frac{s+1}{m+1}$
SAXPYs	$\frac{1}{2}(m+3)s^2+\frac{1}{2}s(s+1)$	$\frac{1}{2}(m+3)s$	$s+\frac{s+1}{m+3}$
scalar work	$\mathcal{O}(ms^3)$	$\mathcal{O}(ms)$	$\mathcal{O}(s^2)$

Recall that the most important point in the comparison of block and ordinary Krylov space solvers is that the dimensions of the search spaces $K_{m\times s}$ and K_m differ by a factor of up to s. This could mean that block GMRES may converge in roughly s times fewer iterations than GMRES. Ideally, this might even be true if we choose

$$m_{block\ GMRES} = \frac{1}{s} m_{GMRES}. \tag{7.18}$$

This assumption would make the memory requirement of both methods comparable. Unfortunately, the numerical experiments indicate that it is rare to fully achieve this factor $\frac{1}{s}$.

7.2.5 Challenges of Exising Methods for Large-scale Platforms

However, nowadays, HPC cluster systems continue to scale up not only the number of compute nodes and CPU cores but also the heterogeneity of components by introducing GPUs and many-core processors. These hierarchical supercomputers can be seen as the intersection of distributed and parallel computing. The communication of overall reduction operations and global synchronization of applications are the bottleneck. When solving linear systems by block Krylov methods on large-scale distributed memory platforms, the cost of using BLAS3 operations to enlarge search space and reduce the memory requirement is apparent: the communication bound of SpGEMM in each step of Arnoldi projection damages heavily their performance, which cannot be compensated by the advantages of the block methods. Even using classic Krylov methods, such as GMRES, to solve a large-scale problem on parallel clusters, the cost per iteration of them becomes the most significant concern, typically caused by communication and synchronization overheads. Consequently, large scalar products, overall synchronization, and other operations involving communication among all cores have to be avoided.

7.3 m-UCGLE to Solve Linear Systems with Multiple Right-hand Sides

We propose to combine the block GMRES with UCGLE [225] to solve Equation (7.1) in parallel on modern computer architectures. In this chapter, firstly, we develop a block version of Least Squares polynomial method based on [184], then replace the three computational components

© 2019 Tous droits réservés.

lilliad.univ-lille.fr

Thèse de Xinzhe Wu, Université de Lille, 2019

of UCGLE respectively by the block GMRES, Shifted Krylov-Schur and block Least Squares polynomial methods. Thus, the three types of computational components in m-UCGLE are:

(1) *BGMRES Component* to solve the linear systems with multiple RHSs. Multiple BGMRES Components can be allocated, and each solve the linear systems with a subset of RHSs;

(2) *s-KS Component* to approximate the dominant eigenvalues of operator matrix. Multiple s-KS Components can also be allocated to compute more eigenvalues with thick restarting;

(3) *B-LSP Component* perform the pretreatement for the block Least Squares polynomial preconditioning for block GMRES.

Additionally, in order to solve linear systems with multiple RHSs and reduce the global communication produced by SpGEMM inside block methods, we design and implement a new manager engine to replace the former one in UCGLE. This novel engine allows to allocate and deploy multiple BGMRES and/or s-KS Components at the same time and support their asynchronous communications. Each allocated BGMRES Component is assigned to solve the linear systems with a subset of RHSs. This extension is denoted as multiple-UCGLE or m-UCGLE even though the ERAM Component is replaced by Shifted Krylov-Schur method.

7.3.1 Shifted Krylov-Schur Algorithm

UCGLE uses the dominant eigenvalues to accelerate the convergence of GMRES, and theoretically, the more eigenvalues are applied, the acceleration of Least Squares polynomial will be more significant. In order to approximate more eigenvalues by ERAM Component, the easiest way is to enlarge the size of related Krylov Subspace. In m-UCGLE, we replace ERAM Component by Shifted Krylov-Schur method which is another variant of the Arnoldi algorithm with an effective and robust restarting scheme and numerical stability [204]. The Krylov subspace of Shifted Krylov-Schur method cannot be too large. Otherwise BGMRES Component is not able to receive the eigenvalues in time to perform the block Least Squares polynomial acceleration. With the novel developed manager engine of m-UCGLE in this chapter, several different s-KS components can be allocated at the same time to approximate efficiently the different part of dominant eigenvalues of matrix A, by the shift with different values and thickly restarting with smaller Krylov subspace sizes. The algorithm of Shifted Krylov-Schur method is given in Algorithm 29.

Algorithm 29 Shifted Krylov-Schur Method

1: **function** s-KS(*input*: A, x_1, m, σ, *output*: Λ_k with $k \leq p$)
2: $A \leftarrow A - \sigma I$
3: Build an initial Krylov decomposition of order m
4: Apply orthogonal transformations to get a Krylov-Schur decomposition
5: Reorder the diagonal blocks of the Krylov-Schur decomposition
6: Truncate to a Krylov-Schur decomposition of order p
7: Extend to a Krylov decomposition of order m
8: If not satisfied, go to step 3
9: **end function**

© 2019 Tous droits réservés.

lilliad.univ-lille.fr

Thèse de Xinzhe Wu, Université de Lille, 2019

7.3.2 Block Least Squares Polynomial for Multiple Right-hand Sides

The Least Squares polynomial method is an iterative method proposed by Saad [184] to solve linear systems. It is applied to calculate a new preconditioned residual for restarted GMRES in UCGLE. In this section, we will present the block Least Squares polynomial method, which is a block extension of Least Squares polynomial method to solve linear systems with multiple RHSs at the same time. The iterates of block Least Squares polynomial method can be written as $X_d = X_0 + \mathcal{P}_d(A)R_0$, where $X_0 \in \mathbb{C}^{n\times s}$ is a selected initial guess to the solution, $R_0 \in \mathbb{C}^{n\times s}$ the corresponding residual block vector, and $\mathcal{P}_d$ a polynomial of degree $d-1$. We set a polynomial of degree d as $\mathcal{R}_d$ such that

$$\mathcal{R}_d(\lambda) = 1 - \lambda\mathcal{P}_d(\lambda)$$

.

The residual of d^{th} steps iteration R_d can be expressed as equation $R_d = \mathcal{R}_d(A)R_0$, with the constraint $\mathcal{R}_d(0) = 1$. We want to find a kind of polynomial which can minimize

$$||\mathcal{R}_d(A)R_0||_F. \tag{7.19}$$

Similarly for the Least Squares problem (7.14) in block GMRES, the maximum-minmum problem (7.19) is equivalent to

$$||R_0^{(p)}||_2 \max_{\lambda\in\sigma(A)} |\mathcal{R}_d(\lambda)|, \quad \forall p \in 0, 1, \cdots, s-1. \tag{7.20}$$

Suppose A is a diagonalizable matrix with its spectrum denoted as $\sigma(A) = \lambda_1, \cdots, \lambda_n$, and the associated eigenvectors $u_1, \cdots, u_n$. Expanding the each component of R_d in the basis of these eigenvectors as $R_d^{(p)} = \sum_{i=1}^{n} \mathcal{R}_d(\lambda_i)\rho_i u_i$, which allows to get the upper limit of $||R_d^{(p)}||_2$ with $p \in 0, 1, \cdots, s-1$ as:

$$||R_0^{(p)}||_2 \max_{\lambda\in\sigma(A)} |\mathcal{R}_d(\lambda)| \tag{7.21}$$

In order to minimize the norm of R_d, it is possible to find a polynomial $\mathcal{P}_d$ which can minimize the Equation (7.21). Therefore, for all s linear systems with different RHSs, they share the same best Least Squares polynomial $\mathcal{R}_d$. As presented in Section 3.5.3, $\mathcal{P}_d$ can be expanded with a basis of Chebyshev polynomial $t_j(\lambda) = \frac{T_j\frac{\lambda-c}{f}}{T_j\frac{c}{f}}$, where t_i is constructed by an ellipse englobing the convex hull formulated by the computed eigenvalues, with c the center of ellipse, and f the focal distance of this ellipse. $\mathcal{P}_d$ is under form that $\mathcal{P}_d = \sum_{i=0}^{d-1} \eta_i t_i$. The selected Chebyshev polynomials t_i meet still the three terms recurrence relation (7.22).

$$t_{i+1}(\lambda) = \frac{1}{\beta_{i+1}}[\lambda t_i(\lambda) - \alpha_i t_i(\lambda) - \delta_i t_{i-1}] \tag{7.22}$$

For the computation of parameters $H_d = (\eta_0, \eta_1, \cdots, \eta_{d-1})$, we construct a modified gram matrix M_d with dimension $d \times d$, and matrix T_d with dimension $(d+1) \times d$ by the three terms recurrence of the basis t_i. M_d can be factorized to be $M_d = LL^T$ by the Cholesky factorization. The parameters H_d can be computed by a least squares problem of the formula:

© 2019 Tous droits réservés.

lilliad.univ-lille.fr

Thèse de Xinzhe Wu, Université de Lille, 2019

$$min\|l_{11}e_1 - F_dH_d\| \tag{7.23}$$

With the definition of $\Omega_i \in R^{n\times s}$ by $\Omega_i = t_i(A)R_0$, we can obtain the Equation (7.24), and in the end iteration (7.25).

$$\Omega_{i+1} = \frac{1}{\beta_{i+1}}(A\Omega_i - \alpha_i\Omega_i - \delta_i\Omega_{i-1}) \tag{7.24}$$

$$X_n = X_0 + \mathcal{P}_d(A)R_0 = X_0 + \sum_{i=1}^{n-1}\eta_i\Omega_i \tag{7.25}$$

The pre-treatement of this method to obtain the parameters $A_d = (\alpha_0, \cdots, \alpha_{d-1})$, $B_d = (\beta_1, \cdots, \beta_d)$, $\Delta_d = (\delta_1, \cdots, \delta_{d-1})$, and $H_d = (\eta_0, \cdots, \eta_{d-1})$ is already presented by Algorithm 13 in Section 3.5.3, where A is a $n \times n$ matrix, d is the degree of Least Squares polynomial, Λ_r the collection of approximate eigenvalues, a, c, f the required parameters to fix an ellipse in the plan, with a the distance between the vertex and center, c the center position and b the focal distance. The iterative recurrence implementation of Equation (7.24) and (7.25) using the parameters gotten from the pre-treatement procedure to construct the restarted residual for block GMRES by block Least Squares polynomial method is given in Algorithm 30. In this algorithm, X_0 is the temporary solution in block GMRES before performing the restart. Compared with Least Squares polynomial method for single RHS, the difference in block Least Squares polynomial method is to replace the SpMV in each iteration step with SpGEMM, as shown in Equation (7.25).

Algorithm 30 Update block GMRES residual by block Least Squares polynomial

function LSUpdateResidual($input$:$A, B, A_d, B_d, \Delta_d, H_d$)
  Get X_0, which is temporary solution in block GMRES
  $R_0 = B - AX_0$, $\Omega_1 = R_0$
  for $k = 1, 2, \cdots, l$ **do**
    for $i = 1, 2, \cdots, d-1$ **do**
      $\Omega_{i+1} = \frac{1}{\beta_{i+1}}[A\Omega_i - \alpha_i\Omega_i - \delta_i\Omega_{i-1}]$
      $X_{i+1} = X_i + \eta_{i+1}\Omega_{i+1}$
    end for
  end for
  Update GMRES restarted residual by X_d
end function

7.3.3 Analysis

Suppose that the computed convex hull by block Least Squares polynomial method contains eigenvalues $\lambda_1, \cdots, \lambda_m$, the restarted residual for block GMRES generated by block Least Squares polynomial method for solving Equation (7.1) can be also divided into two parts:

$$R_n = \sum_{i=1}^{m}\sum_{j=1}^{s}\rho((\mathcal{R}_d^{(j)})(\lambda_i)^{lsa})u_i + \sum_{i=m+1}^{n}\sum_{j=1}^{s}\rho((\mathcal{R}_d^{(j)})(\lambda_i)^{lsa})u_i \tag{7.26}$$

The first part is constructed with the m known eigenvalues used to compute the convex hull

© 2019 Tous droits réservés.

lilliad.univ-lille.fr

Thèse de Xinzhe Wu, Université de Lille, 2019

in B-LSP Component, and the second part represents the residual with unknown eigenpairs. In the practical implementation, for each time preconditioning by the block Least Squares polynomial method, it is often repeated for several times to improve its acceleration of convergence, that is the meaning of parameter lsa in Equation (7.26). The block Least Squares polynomial preconditioning applies R_d as a deflation vector for each time restart of block GMRES. The first part in Equation (7.26) is small since the block Least Squares polynomial finds R_d minimizing $|\mathcal{R}_d(\lambda)|$ in the convex hull, but not with the second part, where the residual will be rich in the eigenvectors associated with the eigenvalues outside H_m. As the number of approximated eigenvalues m increasing, the first part will be much closer to zero, but the second part keeps still large. This results in an enormous increase of restarted block GMRES preconditioned vector norm. Meanwhile, when block GMRES restarts with the combination of some eigenvectors, the convergence will be faster even if the residual is enormous, and the convergence of block GMRES can still be significantly accelerated.

Similar to the block GMRES, the block Least Squares polynomial is also able to enlarge the search space with a maximum factor s. Compared with Least Squares polynomial preconditioning with one RHS, this block version of Least Squares polynomial preconditioning might have further speedup. For a small operator matrix, the selection of the degree d and the applied times lsa of Least Squares polynomial preconditioning in m-UCGLE should be different with the ones in UCGLE, since the combination of multiple RHSs can already enlarge the Euclidean norm of residual produced by the block Least Squares polynomial preconditioning. The optimal values for the two parameters might be different with the ones for UCGLE with single RHS.

7.4 Implementation of m-UCGLE and Manager Engine

In this section, we give the implementation of the newly designed manager engine, which is able to allocate multiple computational components at the same time, and manager the asynchronous communications, checkpointing and fault tolerance. Then, we give the practical implementation of m-UCGLE using this new manager engine.

7.4.1 Component Allocation

The manager engine allocates the components through MPI_Comm_Spawn. One process can fulfill the operations of this manager engine. Each component is identified with a unique identified number as long as its creation by the manager engine. All the data and messages on the manager engine are respectively stored according to their identified number, which facilitates the control of different components. A private MPI intra-communicator between the manager engine and each component is created, which conduct the asynchronous exchanges of data between them. The CPUs are assigned by MPI_Comm_Spawn to each component using a specified *hostfile* which lists the related hostnames.

7.4.2 Asynchronous Communication

Distributed and parallel communication among components involves different types of data, such as vectors, arrays, and signals. The manager engine serves as a proxy to carry out these exchanges

© 2019 Tous droits réservés.

lilliad.univ-lille.fr

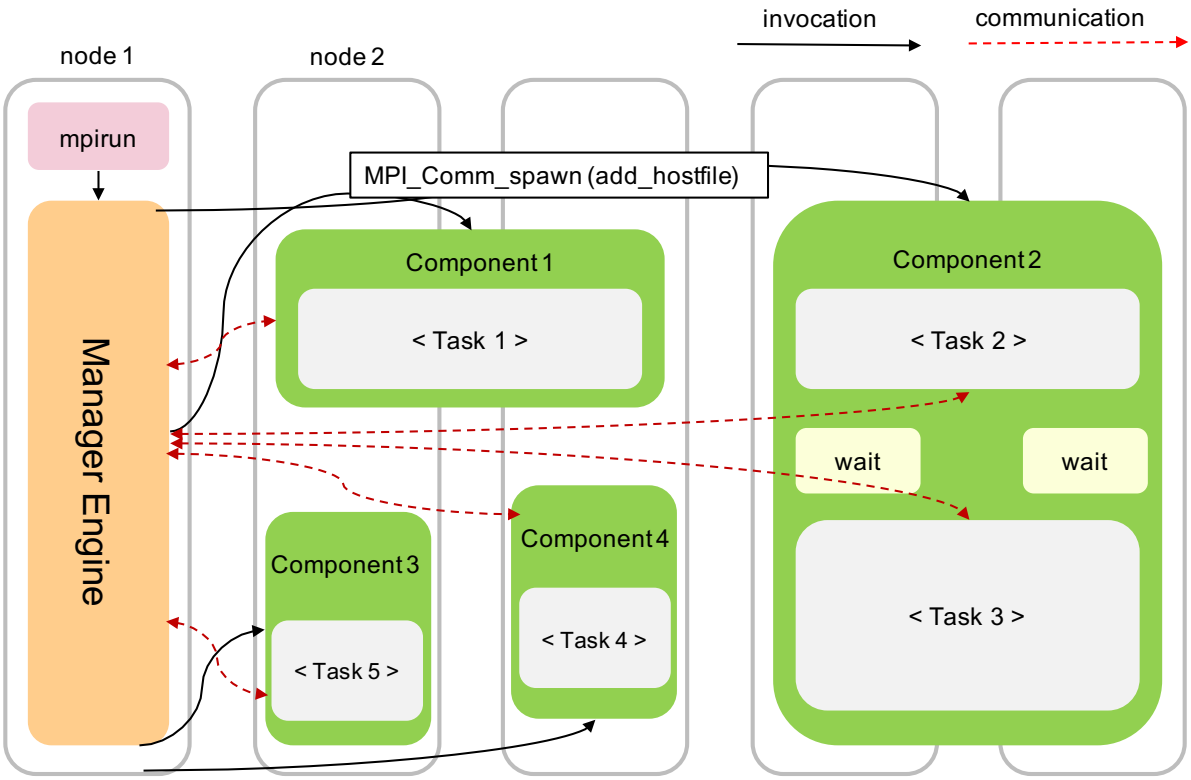

Figure 7.2 – Manager Engine Implementation.

with asynchronous communications. The asynchronous data sending and receiving operations are implemented by the non-blocking communication of MPI. The asynchronous communication is implemented with the same manner for the static manager engine introduced in Section 5.4.3. However, for the newly designed manager engine, these communications only take place between the manager engine and each component inside their private communicator.

7.4.3 Implementation on Hetergeneous Platforms with GPUs

For the implementation on heterogeneous platforms of iterative solvers based on the proposed paradigm, each component spawned by MPI can automatically select the GPU devices binded to it. In order to avoid the competition of different nodes of various computational components for the same GPUs, it is necessary to use the *hostfiles* to manually allocate the computing nodes for each component. In practice, the BGMRES and s-KS components prefer to be implemented with multi-GPUs, and it is enough for the B-LSP to use on MPI process, since it only performs the LAPACK operations with small matrices.

7.4.4 Checkpointing, Fault Tolerance and Reusability

The fault tolerance of the proposed paradigm can be guaranteed by the combination of a *checkpoint function* and an *error detection function*.

The *checkpoint function* takes the backup of necessary data of different components onto the manager engine, e.g., the temporary solution of each restart of linear solvers or the obtained Ritz values. These data on the manager engine are frequently updated. If some computational

© 2019 Tous droits réservés.

Thèse de Xinzhe Wu, Université de Lille, 2019

components are in fault, these data can be redistributed to new allocated components and recover the state before failures.

The *error detection function* is guaranteed by the frequent messages from the components to the manager engine, which can be seen as a *push technique* introduced by Chen et al.[55]. For the manager engine, if there is no news updated from one component for a fixed time interval, this component will be marked as failed. If it is BGMRES Component, it will be recovered using the computing units of s-KS components and checkpoint data saved on the manager engine. If s-KS components are detected in fault, BGMRES components can still work using the checkpoint data from the manager engine, but without the continuous improvement of preconditioning information.

The *reusability* of iterative solvers based on this new paradigm can be improved. Since the preconditioning and solving parts are separated, the information used for the preconditioning can be saved into local files and reused to solve the subsequent problems sharing the same operator.

7.4.5 Practical Implementation of m-UCGLE

The previous implementation of manager engine for UCGLE in Chapter 5, based on MPI_Split cannot meet the requirement of m-UCGLE. Thus, in order to extend UCGLE method to solve non-Hermitian linear systems and to reduce the global communication and synchronization points, we design and implement a new manager engine for m-UCGLE. As shown in Figure 7.3, the new engine allows creating a number of different computational components at the same time. Suppose that we have allocated n_g BGMRES Components, n_k s-KS Components and 1 B-LSP Component. The exact implementation for s-KS, B-LSP, BGMRES Components and manager process are respectively given in Algorithm 31, 32, 33 and 34. Denote the BGMRES Components as BGMRES[k] with $k \in 1, 2, \cdots, n_g$, and the s-KS Components as s-KS[q] with $q \in 1, 2, \cdots, n_a$. The matrix B in Equation (7.1) can be decomposed as:

$$B = [B_1, B_2, \cdots, B_k, \cdots, B_{n_g}] \tag{7.27}$$

Each BGMRES[k] will solve the linear systems with multiple RHSs B_k, which is a subgroup of B:

$$AX_k = B_k \tag{7.28}$$

Table 7.5 gives the comparison of memory and communication complexity of SpGEMM operation inside m-UCGLE and block GMRES with the same number of RHSs. The factors n, nnz, s, P_g and n_g represent respectively the matrix size, the number of non-zero entries of matrix, the number of multiple RHSs, the total number of computing units for block GMRES, and the number of BGMRES Components allocated by the manager engine of m-UCGLE. The average memory requirement for block GMRES on each computing unit is $\mathcal{O}(\frac{nnz(1+s)}{P_g})$. For m-UCGLE, the matrix is duplicated n_g times into different allocated linear solvers. Thus the required memory to store the matrix should be scaled with the factor n_g compared with block GMRES. Due to the localization of computation inside m-UCGLE, the total number global

© 2019 Tous droits réservés.

lilliad.univ-lille.fr

Thèse de Xinzhe Wu, Université de Lille, 2019

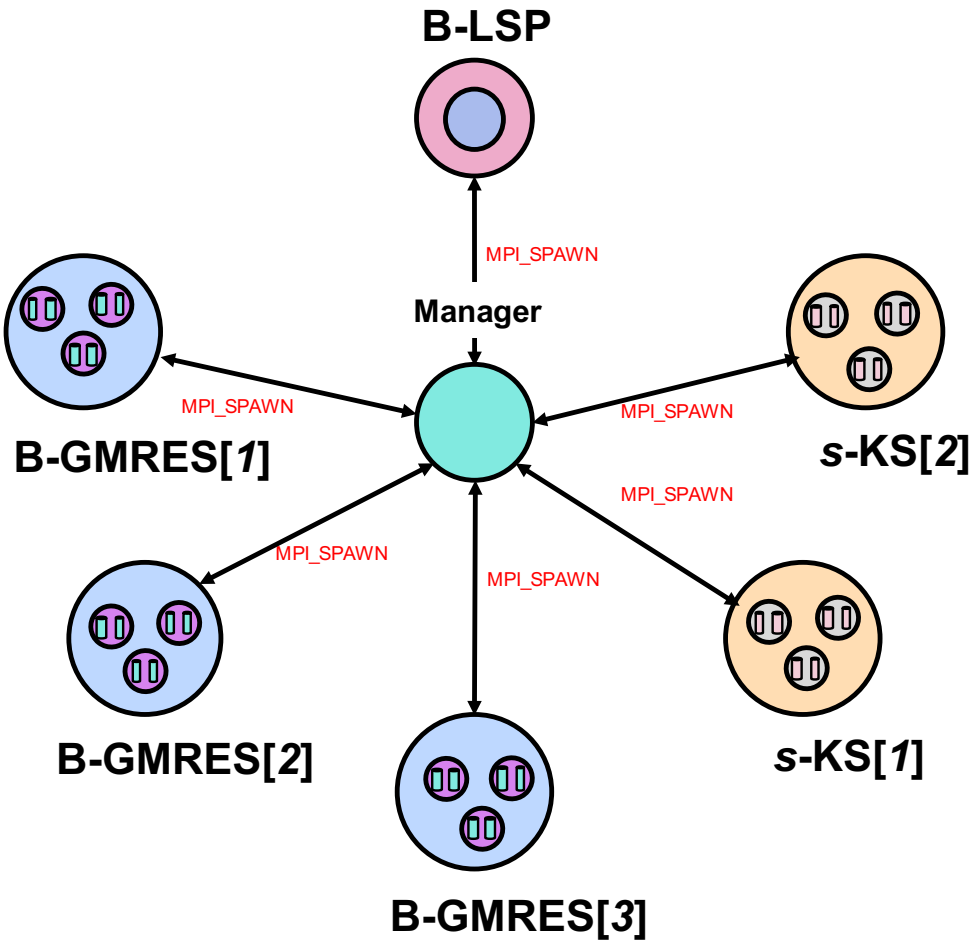

Figure 7.3 – Manager Engine Implementation for m-UCGLE. This is an example with three block GMRES components, and two s-KS components, but these numbers can be customized for different problems.

communication can be reduced with a factor $\frac{1}{n_g}$ compared with block GMRES. In practice, the selection of the number to allocate the BGMRES Components should make a balance between the increase of memory requirement and the reduction of global communication.

Here we present in detail the workflow of this new engine. At the beginning, the manager engine will simultaneously allocate the required number of three kinds of computational components. For each BGMRES[k], it will load a full matrix A and its related subgroup B_k, and then start to solve Equation (7.28) separately. Meanwhile, each s-KS[q] load a full matrix A from local, and start to find the required part of eigenvalues of A, through the Shifted Krylov-Schur method, using different parameters such as the shift value σ_q, the Krylov subspace size $(m_a)_q$, etc. If the eigenvalues of the required number are approximated on s-KS[q], these values will be asynchronously sent to the manager process. The manager process will always check if new eigenvalues are available from different s-KS Components, if yes, it will collect and update the new coming eigenvalues together and send them to B-LSP Component. B-LSP Component will use all the eigenvalues received from manager process to do the pre-treatment of the block Least Squares polynomial preconditioning, the parameters gotten will be sent back to the manager process. Immediately, these parameters will be distributed to BGMRES[k]. BGMRES[k] can use

© 2019 Tous droits réservés.

lilliad.univ-lille.fr

Thèse de Xinzhe Wu, Université de Lille, 2019

Table 7.5 – Memory and communication complexity comparison between m-UCGLE and block GMRES.

	m-UCGLE	block GMRES	ratio
Memory	$\mathcal{O}(\frac{nnz(n_g+s)}{P_g})$	$\mathcal{O}(\frac{nnz(1+s)}{P_g})$	$\frac{n_g+s}{1+s}$
Communication	$\mathcal{O}(\frac{nnzsP_g}{n_g})$	$\mathcal{O}(nnzsP_g)$	$\frac{1}{n_g}$

Algorithm 31 s-KS Component

```
1: function s-KS-EXEC(input: A, m_a, ν, r, ε_a)
2:     while exit==False do
3:         s-KS(A, r, m_a, ν, ε_a, output: Λ_r)
4:         Send (Λ_r) to B-LSP Component
5:         if Recv (exit == TRUE) then
6:             Send (exit) to B-LSP Component
7:             stop
8:         end if
9:     end while
10: end function
```

the block Least Squares polynomial residual constructed by these parameters to speed up the convergence. If the exit signals from all BGMRES Components are received by manager process, it will send a signal to all other components to terminate their executions.

The allocation of a different number of computational components is implemented with MPI_SPAWN, and their asynchronous communication is assured by the MPI non-blocking sending and receiving operations between the manager process and each computational components.

Algorithm 32 B-LSP Component

```
1: function B-LSP-EXEC(input: A, b, d)
2:     if Recv(Λ_r) then
3:         LSP-Pretreatment(input: A, b, d, Λ_r, output: A_d, B_d, Δ_d, H_d)
4:         Send (A_d, B_d, Δ_d, H_d) to GMRES Component
5:     end if
6:     if Recv (exit == TRUE) then
7:         stop
8:     end if
9: end function
```

Same as UCGLE, m-UCGLE has multiple levels of parallelism for distributed memory systems:

(1) Coarse Grain/Component level: it allows the distribution of different numerical components, including the preconditioning part (B-LSP and s-KS) and the solving part (BGMRES) on different platforms or processors;

(2) Medium Grain/Intra-component level, BGMRES and s-KS components are both deployed

© 2019 Tous droits réservés.

lilliad.univ-lille.fr

Thèse de Xinzhe Wu, Université de Lille, 2019

Algorithm 33 BGMRES Component

```
1: function BGMRES-EXEC(input: A, m_g, X_0, B, ε_g, L, l, output: X_m)
2:     count = 0
3:     BGMRES(input: A, m, X_0, B, output: X_m)
4:     if ||B − AX_m|| < ε_g then
5:         return X_m
6:         Send (exit == TRUE) to manager process
7:         Stop
8:     else
9:         if count | L then
10:            if recv (A_d, B_d, Δ_d, H_d) then
11:                LSUpdateResidual(input:A, B, A_d, B_d, Δ_d, H_d)
12:                count + +
13:            end if
14:        else
15:            set X_0 = X_m
16:            count + +
17:        end if
18:    end if
19:    if Recv (exit == TRUE) then
20:        stop
21:    end if
22: end function
```

in parallel;

(3) Fine Grain/Thread parallelism for shared memory: the OpenMP thread-level parallelism, or the accelerator level parallelism if GPUs or other accelerators are available.

7.5 Parallel and Numerical Performance Evaluation

In this section, we evaluate the numerical performance of m-UCGLE for solving non-Hermitian linear systems compared with conventional block GMRES.

7.5.1 Hardware Settings

After the implementation of m-UCGLE, we test it on the supercomputer with selected test matrices. The purpose of this section is to give the details about the hardware/software settings and test sparse matrices.

Experiments were obtained on the supercomputer *Romeo-2018*, a system located at University of Reims Champagne-Ardenne, France. Made by Atos, this cluster relies on totally 115 the Bull Sequana X1125 hybrid servers, powered by the Xeon Gold 6132 (products formerly Skylake) and NVidia P100 cards. Each dense Bull Sequana X1125 server accommodates 2 Xeon Scalable Processors Gold bi-socket nodes, and 4 NVidia P100 cards connected with NVLink. In total, this supercomputer includes 3,220 Xeon cores and 280 Nvidia P100 accelerators. *Romeo-2018* is updated version of *Romeo-2013*, which was used to evaluate the numerical and parallel performance of UCGLE for single RHS in Chapter 5.

© 2019 Tous droits réservés.

lilliad.univ-lille.fr

Thèse de Xinzhe Wu, Université de Lille, 2019

Algorithm 34 Manger of m-UCGLE with MPI Spawn

```
1: function MASTER(Input : n_g, n_a)
2:     for i = 1 : n_g do
3:         MPI_Spawn executable BGMRES-EXEC[i]
4:     end for
5:     for j = 1 : n_k do
6:         MPI_Spawn executable s-KS-EXEC[j]
7:     end for
8:     MPI_Spawn executable B-LSP-EXEC
9:     for j = 1 : n_k do
10:        if Recv array[j] from s-KS-EXEC[j] then
11:            Add array[j] to Array
12:        end if
13:    end for
14:    if Array ≠ NULL then
15:        Send Array to B-LSP-EXEC
16:    end if
17:    if Recv LSArray from B-LSP-EXEC then
18:        for i = 1 : n_g do
19:            Send LSArray to BGMRES-EXEC[i]
20:        end for
21:    end if
22:    for i = 1 : n_k do
23:        if Recv flag[i] for BGMRES-EXEC[i] then
24:            if flag[i] == exit then
25:                flag = true
26:            else
27:                flag = false
28:            end if
29:        end if
30:    end for
31:    if flag == true then
32:        Kill B-LSP-EXEC
33:        for i = 1 : n_g do
34:            Kill BGMRES-EXEC[i]
35:        end for
36:        for j = 1 : n_k do
37:            Kill s-KS-EXEC[j]
38:        end for
39:    end if
40: end function
```

© 2019 Tous droits réservés.

lilliad.univ-lille.fr

Thèse de Xinzhe Wu, Université de Lille, 2019

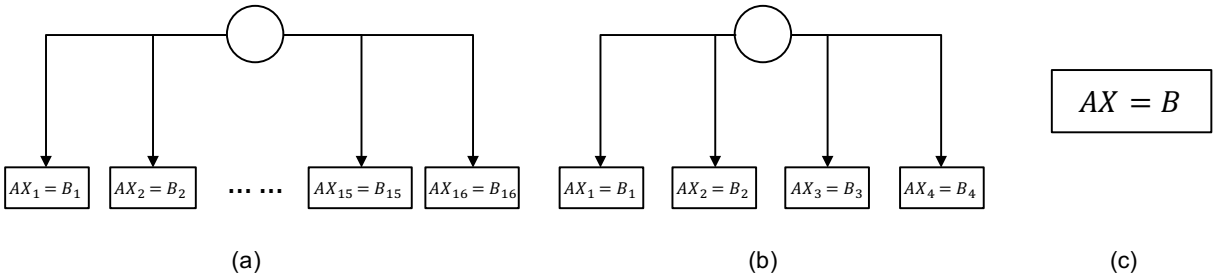

Figure 7.4 – Different strategies to divide the linear systems with 64 RHSs into subsets: (a) divide the 64 RHSs into to 16 different components of m-UCGLE, each holds 4 RHSs; (b) divide the 64 RHSs into to 4 different components of m-UCGLE, each holds 16 RHSs; (c) One classic block GMRES to solve the linear systems with 64 RHSs simultaneously.

Table 7.6 – Spectral functions to generate six test Matrices.

Name	*spec*
TEST 1	(rand(21.0, 66.0), rand(-21.0,24.0))
TEST 2	(rand(0.5, 3.0), rand(-0.5,2.0))
TEST 3	(rand(0.2, 5.2), rand(-2.5,2.5))
TEST 4	(rand(-5.2, -0.2), rand(-2.5,2.5))
TEST 5	(rand(-0.23, -0.03), rand(-0.2,0.2))
TEST 6	(rand(-9.3, -3.2), rand(-2.1,2.1))

7.5.2 Software Settings

The MPI used is the OpenMPI 3.1.2, all the shared libraries and binaries were compiled by *gcc* (version 6.3.0). The released scientific computational libraries Trilinos (version 12.12.1) and LAPACK (version 3.8.0) were also compiled and used for the implementation of m-UCGLE. m-UCGLE on multi-GPUs are boosted by Kokkos, compiled with its underlying compiler nvcc wrapper. The related CUDA version is 9.2.

7.5.3 Test Problems Settings

We use the SMG2S [226] to generate large-scale test matrices. In the experiments, the total number of RHSs for linear systems to be solved is fixed as 64. These RHSs are generated in random using different given seed states. The test matrices from TEST 1 to TEST 6 are all generated by SMG2S(*spec*). *spec* implies the spectral distribution functions, and their definition are shown in Table 7.6. For example, the *spec* of TEST 1 is given as (rand(21.0, 66.0), rand(-21.0,24.0)), the first part rand(21.0, 66.0) defines that the real parts of eigenvalues for TEST 1 are the floating numbers generated randomly in the fixed interval [21.0, 66.0], similarly its imaginary parts are randomly generated in the fixed interval [-21.0, 24.0].

© 2019 Tous droits réservés.

lilliad.univ-lille.fr

Thèse de Xinzhe Wu, Université de Lille, 2019

7.5.4 Specific Experimental Setup

Table 7.7 – Alternative methods for experiments, and the related number of allocated component, RHS number per component and preconditioners.

Method	Component nb	RHS nb per component	Preconditioner
BGMRES(64)	1	64	None
m-BGMRES(16)*4	4	16	None
m-BGMRES(4)*16	16	4	None
m-UCGLE(16)*4	4	16	block Least Squares polynomial
m-UCGLE(4)*16	16	4	block Least Squares polynomial

In the experiments, the total number of RHSs of linear systems to be solved for each test is fixed as 64. As shown in Figure 7.4, we propose three strategies to divide these systems into various subgroup:

(1) 4 allocated BGMRES Components in m-UCGLE with each holding 16 RHSs (shown by Figure 7.4(a));

(2) 16 allocated BGMRES Components in m-UCGLE with each holding 4 RHSs (shown in Figure 7.4(b));

(3) 1 group with all 64 RHSs solved by classic BGMRES (shown by Figure 7.4(c)).

Moreover, for m-UCGLE with 4 or 16 allocated components, they can be applied either with or without the preconditioning of block Least Squares polynomial using approximate eigenvalues. Denote the special variant of m-UCGLE without block Least Squares polynomial preconditioning as m-BGMRES. m-BGMRES is also able to reduce the global communications through allocating multiple BGMRES components by the manager engine. Table 7.7 gives the naming of the five alternatives to solve linear systems with 64 RHSs, the numbers of their allocated components and the numbers of RHSs per component.

7.5.5 Convergence Evaluation

Various parameters have impacts on the convergence of iterative methods. For all tests: Krylov subspace size m_g is fixed as 40. The number of times that block Least Squares polynomial applied in m-UCGLE and the degree of Least Squares polynomial are respectively set as 10 and 15. The relative tolerance is fixed as 1.0×10^{-8}. Fig. 7.5 and Table 7.8 give the iteration steps of different tests for convergence. We define the iteration steps for m-BGMRES(16)*4, m-BGMRES(4)*16, m-UCGLE(16)*4 and m-UCGLE(4)*16 as the maximal ones among their allocated components. Firstly, for TEST 1, 2, 3, and 6, the enlargement of searching subspace with more RHSs in BGMRES is effective to accelerate the convergence. However, for TEST 4 and 5, m-BGMRES(16)*4 with less RHSs converges much faster than BGMRES(64). Secondly,

© 2019 Tous droits réservés.

lilliad.univ-lille.fr

Thèse de Xinzhe Wu, Université de Lille, 2019

Table 7.8 – Iteration steps of convergence comparison (SMG2S generation suite SMG2S$(1, 3, 4, spec)$, relative tolerance for convergence test $= 1.0 \times 10^{-8}$), Krylov subspace size $m_g = 40$, $lsa = 10$, $d = 15$, $freq = 1$, $dnc =$ do not converge in 5000 iteration steps).

Method	m-BGMRES(4)*16	m-UCGLE(4)*16	m-BGMRES(16)*4	m-UCGLE(16)*4	BGMRES(64)
TEST 1	239	160	102	51	51
TEST 2	*dnc*	176	187	62	78
TEST 3	*dnc*	310	*dnc*	81	657
TEST 4	*dnc*	320	629	99	942
TEST 5	600	235	170	99	270
TEST 6	80	160	85	51	38

Table 7.9 – Consumption time (s) comparison on CPUs (SMG2S generation suite SMG2S$(1, 3, 4, spec)$, the size of matrices $= 1.792 \times 10^6$, relative tolerance for convergence test $= 1.0 \times 10^{-8}$), Krylov subspace size $m_g = 40$, $lsa = 10$, $d = 15$, $freq = 1$, $dnc =$ do not converge in 5000 iteration steps).

Method	m-BGMRES(4)*16	m-UCGLE(4)*16	m-BGMRES(16)*4	m-UCGLE(16)*4	BGMRES(64)
TEST 1	34.2	35.3	133.9	98.9	362.8
TEST 2	*dnc*	40.9	231.3	111.5	580.6
TEST 3	*dnc*	66.0	*dnc*	145.8	522.5
TEST 4	*dnc*	68.2	768.3	178.2	6829.3
TEST 5	132.3	50.1	209.4	120.5	1959.5
TEST 6	11.4	34.1	87.8	91.7	275.8

if we compare m-UCGLE and the related m-BGMRES with the same number of RHSs, we can conclude that B-LSP Component can splendidly accelerate the convergence, except for TEST 6. For TEST 2, 3, 4, and 5, m-UCGLE(16)*4 with less RHSs works even much better than BGMRES(64). TEST 4 is an extreme special case, where m-UCGLE(4)*16 and m-UCGLE(16)$*$4 converge respectively 3$\times$ and 9.5$\times$ faster over m-BGMRES(64).

In conclusion, m-UCGLE(16)*4 converges the fastest for most cases. The convergence of block methods can converge quickly with enough RHSs and the preconditioning by block Least Squares polynomial method. Compared with classic block GMRES, m-UCGLE with less RHSs and smaller searching space can still have better acceleration. Thus, the potential damages on the convergence caused by the reduction of global communications with less RHSs of each component inside m-UCGLE can be covered.

7.5.6 Time Consumption Evaluation

Time consumption for different methods with the same matrices and parameters as the previous section are also compared. The results are also given in Fig. 7.5 and Table 7.9. The dimension of all matrices are set as 1.792×10^6, the total numbers of CPU cores for Solver Components (either BGMRES Components in m-UCGLE and m-GMRES or conventional block GMRES) are

© 2019 Tous droits réservés.

lilliad.univ-lille.fr

Thèse de Xinzhe Wu, Université de Lille, 2019

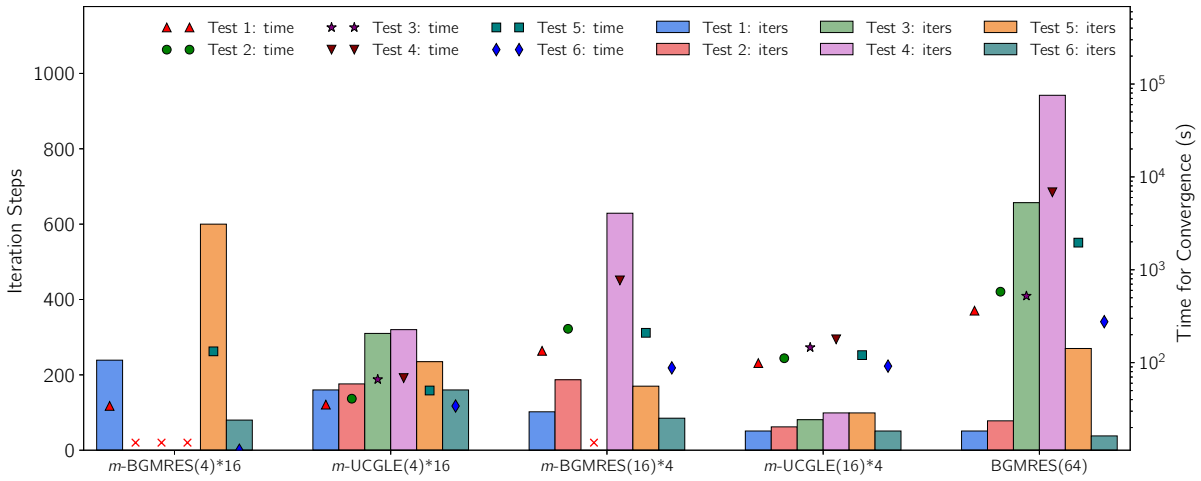

Figure 7.5 – Comparison of iteration steps and consumption time (s) of convergence and on CPUs. A base 10 logarithmic scale is used for Y-axis of Time. The × means the test do not converge in acceptable number of iterations.

respectively fixed as 1792. From Fig. 7.5, we can find that m-UCGLE(4)*16 take the least time to converge for TEST 2, 3, 4 and 5. For TEST 1 and 6, m-BGMRES(4)*16 takes a little less time than m-UCGLE(4)*16 for convergence. TEST 4 is an extreme case, where m-UCGLE(4)*16 has about 100× speedup in time consumption over BGMRES(64).

7.5.7 Strong Scalability Evaluation

The most import advantage of m-UCGLE is to reduce the global communications of SpGEMM and synchronization points of preconditioner by dividing the algorithms into components. In order to evaluate the parallel performance of m-UCGLE on both homogeneous and heterogeneous (multi-GPUs) systems, we compare the average time cost and speedup per iteration of five alternatives. For the evaluation with CPUs, the test matrix is generated by SMG2S with a fixed size of 1.792×10^6, and for the evaluation with multi-GPUs, the test matrix size is set as 3.2×10^5. No larger matrices are tested, due to the memory limitation during the Arnoldi projection of block GMRES. The Krylov subspace size m_g for all tests keeps still as 40. The average time per iteration is calculated after 100 iterative steps. The total CPU core number for both B-GMRES(64) and *Solver Component* in m-UCGLE and m-BGMRES ranges from 224 to 1792. Thus for each BGMRES Component of m-BGMRES(4)*16 and m-UCGLE(4)*16, this number ranges from 14 to 112. Similarly, for each BGMRES Component of m-BGMRES(16)*4 and m-UCGLE(16)*4, this number ranges from 56 to 448. The total GPU number ranges from 16 to 128. Thus for each BGMRES Component of m-BGMRES(4)*16 and m-UCGLE(4)*16, this number ranges from 1 to 8. This number ranges from 4 to 32 for each BGMRES Component of m-BGMRES(16)*4 and m-UCGLE(16)*4. All the tests allocate only 1 s-KS Component which always has the same number of CPU cores with one BGMRES Component inside m-UCGLE.

Figure 7.6a gives the comparison of average time per iteration on CPUs, and Figure 7.6b shows the related speedup. Firstly, we can conclude that the strong scaling of m-BGMRES(4)*16 and m-UCGLE(4)*16 perform well, the strong scalability of the rest are bad, especially BGMRES(64). At the beginning, the scalability of m-BGMRES(16)*4 and m-UCGLE(16)*4 is good,

© 2019 Tous droits réservés.

lilliad.univ-lille.fr

Thèse de Xinzhe Wu, Université de Lille, 2019

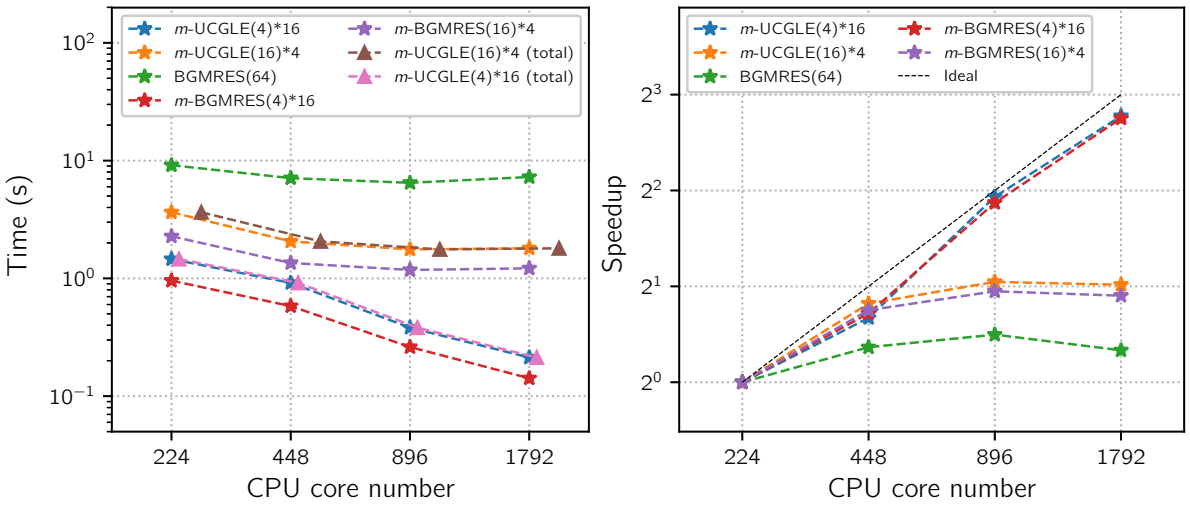

(a) Time per iteration on CPUs. Matrix size = 1.792×10^6.

(b) Speedup on CPUs. Matrix size = 1.792×10^6.

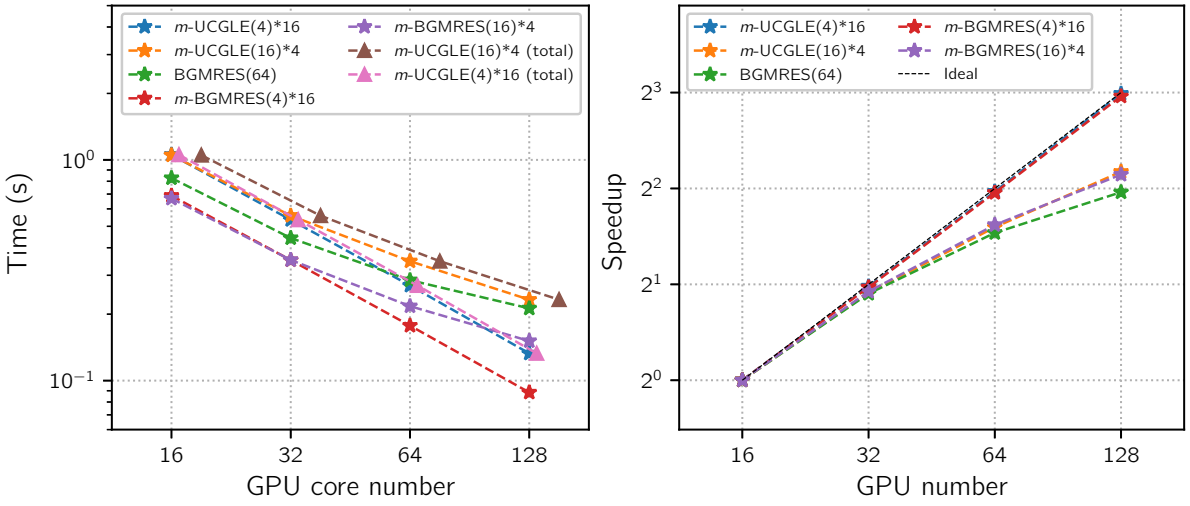

(c) Time per iteration on GPUs. Matrix size = 6.4×10^5.

(d) Speedup on GPUs. Matrix size = 6.4×10^5.

Figure 7.6 – Strong scalability and speedup on CPUs and GPUs of solving time per iteration for m-BGMRES(4)*16, m-UCGLE(4)*16, m-BGMRES(16)*4, m-UCGLE(16)*4, BGMRES(64). A base 10 logarithmic scale is used for Y-axis of (a) and (c); a base 2 logarithmic scale is used for Y-axis of (b) and (d).

© 2019 Tous droits réservés.

lilliad.univ-lille.fr

Thèse de Xinzhe Wu, Université de Lille, 2019

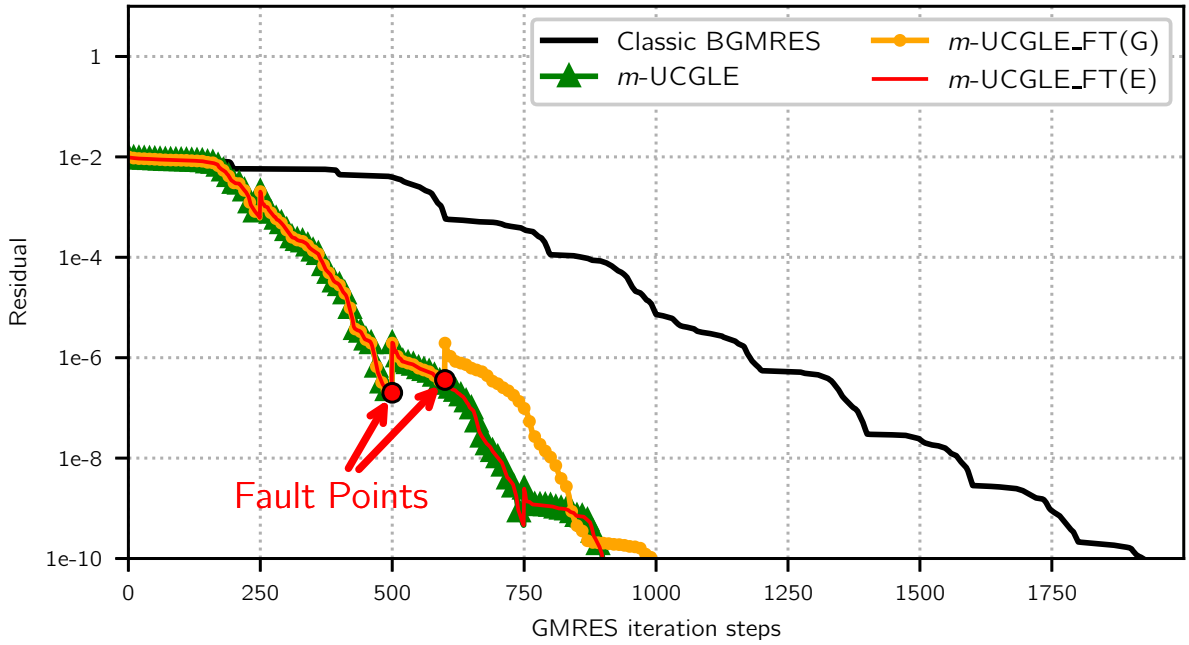

Figure 7.7 – Fault Tolerance Evaluation of m-UCGLE.

but it turns bad quickly with the increase of CPU number. It is well demonstrated that the advantages of m-UCGLE to promote the asynchronous communication and localize of computation can improve the parallel performance significantly to solve linear systems with multiple RHSs. Additionally, for the m-BGMRES and m-UCGLE with the same number of RHSs, the time per iteration of former is a little less the latter, since m-UCGLE introduces the iterative operations (SpGEMM) by block Least Squares polynomial preconditioning.

Figure 7.6c gives the comparison of average time per iteration on GPUs. Figure 7.6d shows the comparison of speedup. At the beginning, the scaling of all tests performs well. With the augmentation of GPU number, the scaling of BGMRES(64), m-UCGLE(16)*4 and m-GMRES(16)*4 tends worse, but the scaling of m-UCGLE(4)*16 and m-GMRES(4)*16 keeps good.

Since m-UCGLE uses additional computing units for other components especially s-KS Component, it is unfair only to compare the scaling performance that total CPU/GPU number of all BGMRES Components in m-UCGLE equals to these numbers of m-GMRES and BGMRES(64). Thus we plot two more curves of m-UCGLE(4)*16 and m-UCGLE(16)*14 with all their CPU/GPU numbers (including the ones of s-KS Component) in Figure 7.6a and 7.6c. The two additional curves are the ones with the marker set as the triangle. It is shown that m-UCGLE(4)*16 and m-UCGLE(16)*4 can still have respectively up to 35× and 4× speedup per iteration against BGMRES(64) on multi-CPUs. For the tests on multi-GPUs, at the beginning, each iteration of them takes longer time than BGMRES(64), but it tends better with the augmentation of GPU number, and the scaling of BGMRES(64) becomes bad.

7.5.8 Fault Tolerance Evaluation

Similar to the fault tolerance evaluation of UCGLE in Chapter 5, the fault tolerance of m-UCGLE is also studied by the simulation of the loss of either GMRES or s-KS Components. m-UCGLE_FT(G) in Fig. 7.7 represents the simulation of BGMRES Components in fault, and

© 2019 Tous droits réservés.

lilliad.univ-lille.fr

Thèse de Xinzhe Wu, Université de Lille, 2019

m-UCGLE_FT(E) implies the fault simulation of s-KS. The curves of m-UCGLE and classic BGMRES represent the normal m-UCGLE and BGMRES without preconditioning, respectively.

The failure of s-KS Component is simulated by fixing the execution loop number of s-KS algorithm, it exits after a fixed number of iterations. We mark the s-KS fault point of tests in Fig. 7.7. The m-UCGLE_FT(E) curves of the experimentations show that BGMRES Component will continue to solve the systems with Least Squares polynomial preconditioning using the eigenvalues stored on the manager engine. There is not much difference between the curves of m-UCGLE_FT(E) and m-UCGLE.

The failure of BGMRES Component (marked in Fig. 7.7) is simulated by fixing a small number of iterations before the achievement of convergence. We can find that after the fault of BGMRES Component, s-KS computing units will automatically take over the jobs of BGMRES component. This new BGMRES Component is recovered from the stat of the previous backup of the temporary solution x_m, and then continue to solve the linear systems with the checkpoint data. Thus in the curve of UCGLE_FT(G), the linear solver repeats a few steps of previous iterations from the fault point.

For the classic BGMRES, if it is in fault, its execution will be totally exit, and it is not possible to continue to solve the linear systems, even with lower performance.

7.5.9 Analysis

In conclusion, m-UCGLE(4)*16 and m-GMRES(4)*16 with the most decrease of global communications have the best strong scaling performance. m-UCGLE cost a little more time per iteration compared with m-BGMRES with the same number of RHSs, but this might be made up by its decrease of iterative steps with block Least Squares polynomial preconditioning. The experiments in this section demonstrate the benefits of m-UCGLE to reduce global communication and promote the asynchronization. Two more important points that cannot be concluded from the experiments in this chapter are:

(1) The increase of memory requirement should be considered when dividing the whole RHSs into subsets;

(2) The number of RHSs per component of m-UCGLE to enlarge the search space and the computation time per iteration should be balanced to achieve the best performance.

7.6 Conclusion

This chapter presents m-UCGLE, an extension of distributed and parallel method UCGLE to solve large-scale non-Hermitian sparse linear systems with multiple RHSs on modern supercomputers. m-UCGLE is implemented with three kinds of computational components which communicate by the asynchronous communication. A special engine is proposed to manger the communication and allocate multiple different components at the same time. m-UCGLE is able to accelerate the convergence, minimize the global communication, cover the synchronous points for solving linear systems with multiple RHSs on large-scale platforms. The experiments on supercomputers prove the good numerical and parallel performance of this method. The fault

© 2019 Tous droits réservés.

lilliad.univ-lille.fr

Thèse de Xinzhe Wu, Université de Lille, 2019

tolerance and reusability of m-UCGLE is also proved by the simulation of failures of different components. Various parameters have impacts on the convergence. Thus, the auto-tuning scheme is required in the next step, where the systems can select the dimensions of Krylov subspace, the numbers of eigenvalues to be computed, the degrees of Least Squares polynomial according to different linear systems and cluster architectures. Different deflation and polynomial preconditioned iterative methods could be transformed according to this proposed paradigm, and further study should be done to compare them. A complete runtime for this paradigm should be developed to replace the prototype implementation of this chapter.

© 2019 Tous droits réservés.

lilliad.univ-lille.fr

© 2019 Tous droits réservés.

lilliad.univ-lille.fr

Thèse de Xinzhe Wu, Université de Lille, 2019

Chapter 8

Auto-tuning of Parameters

Different optimization techniques were developed to accelerate convergence of Krylov iterative methods in order to reduce the number of iterations and calculate solutions in the shortest possible time. UCGLE and m-UCGLE are more complicated because it is a combination of several different computational components. Thus, a large number of parameters affect their numerical and parallel performance. The purpose of this chapter is to design adaptive methods to automatically optimize and select these parameters so that they can be adapted to different systems and hardware. In this chapter, we will at first study different auto-tuning schemes and optimizations that have contributed to them. Then we will focus on the proposition of heuristic algorithm to automatically select the parameters of Least Squares polynomial preconditioning of UCGLE at runtime.

8.1 Auto-tuning Techniques

Current supercomputer have hierarchical architectures, with millions of cores utilizing non-uniform memory access and hierarchical caches. The introduction of GPUs and other accelerators has increased the heterogeneity of computers. Therefore, it is increasingly difficult to tune the performance of software. Moreover, the science and industrial applications on the supercomputing systems tend to be more and more complex. It is necessary to propose strategies and methods to automatically adjust them for optimal performance. Auto-tuning refers to the automatic generation of a search space of possible implementations of a computation that are evaluated through models and/or empirical measurement to identify the most desirable implementation [22]. The main goal of auto-tuning is the minimization of execution time of applications. If the auto-tuning schemes with different objectives are combined together, this might achieve to optimize the numerical and parallel performance, the energy efficiency and reliability of applications.

8.1.1 Different Levels of Auto-tuning

Different aspects affect the performance of applications on supercomputers. In this section, we will discuss different levels of auto-tuning that are relatively different in appearance but have

© 2019 Tous droits réservés.

lilliad.univ-lille.fr

Thèse de Xinzhe Wu, Université de Lille, 2019

the same goal: reduce computation time to achieve a solution.

8.1.1.1 Algorithm Auto-tuning

The first level is to auto-tune the algorithm for a fixed application. Different numerical methods have been designed for problems with different characteristics. These methods have their own unique advantages and limitations. Numerical toolkits such as PETSc/SLEPc and Trilinos provide a large number of parallel implementation of solvers for large sparse linear systems and eigenvalue problems, including the direct methods and iterative methods with different preconditioning techniques. It is difficult for the user to select the routines to correctly and efficiently solve their problems. Thus different auto-tuning schemes should be proposed to classify numerical methods. Lighthouse Project [161] use the machine learning methods to classify the solvers and preconditioners based on a small number of features of applications. These classifiers are trained based on a large number of training set of linear systems and eigenvalue problems. For the users, the features of applications are used as the input, and the output is a collection of solvers and their configurations that may perform well. In [156], the development of this project is described, with an emphasis on the analysis of the sparse eigensolvers provided by SLEPc.

8.1.1.2 Code Variant Auto-tuning

The second level is to auto-tune the code variants inside the selected algorithm. Code variants in complex applications represent alternative implementations of a computational operation. For each code variant, it has the same interface, and its functionality equivalent to the other variants but may employ fundamentally different algorithms or implementations strategies [154]. A well-known example is the implementation of SpMV operation, which is the kernel of Arnoldi reduction of Krylov iterative methods. In Tpetra package of Trilinos, the SpMV operation is implemented with different matrix storage format across different parallel architectures, e.g., MPI for distributed-memory systems, OpenMP and Pthreads for shared memory platforms, and CUDA for GPUs. Aquilanti et al. [12] proposed the auto-tuning strategy for the incomplete orthogonalization inside parallel GMRES. OSKI (Optimized Sparse Kernel Interface) library implemented by Vuduc et al. [216] is a collection of low-level primitives that provide automatically tuned computational kernels on sparse matrices, for use by solver libraries and applications. A fully run-time auto-tuned sparse iterative solver with OpenATLib was introduced by Naono et al. [158]. Using APIs of OpenATLib, a fully auto-tuned sparse iterative solver called Xabclib was developed, which provides numerical computation policy that can optimize memory space and computational accuracy.

Different Domain Specific Languages and code generation strategies are also provided, which are able to generate the parallel optimized code variant specified for different computing architectures from a serial algorithm, e.g., PATUS [57] presented by Christen et al., which is a code generation and auto-tuning framework for parallel iterative stencil computations on modern microarchitectures; and Pochoir [207] a Domain Specific Language in which the user only specifies a stencil (computation kernel and access pattern), boundary conditions and a space-time domain while all optimizations are handled by a compiler.

© 2019 Tous droits réservés.

lilliad.univ-lille.fr

Thèse de Xinzhe Wu, Université de Lille, 2019

8.1.1.3 Hardware Auto-tuning

The third level is to auto-tune the applications according different computer architectures. In order to achieve performance portability of algorithms, decisions on parallelization and memory hierarchy optimizations (e.g., data placement, blocking/tiling and tile size) will necessarily depend on the architecture, e.g., Chen et al. [53] proposed a model-guided empirical optimization for memory hierarchy; Ren at al. [178] introduced a tuning framework for software-managed memory hierarchies, and Katagiri et al. [121] presented a smart tuning strategy for restart frequency of GMRES with hierarchical cache sizes.

8.1.1.4 Parameter Auto-tuning

This last level is the auto-tuning of various complex numerical parameters of algorithms. The modern applications on supercomputers are complex, both their numerical and parallel performance depends on different parameters, e.g., for the Krylov iterative methods with restart strategy, if the Krylov subspace size m is small, their parallel performance is good, since the limitation of the requirement of memory and the reduction of global communications of SpMV operations, but small m might slow down even diverge the iterative methods for solving selected linear systems, which results in the increase of time and energy consumptions. Thus for the parameter m, an auto-tuning strategy should be proposed to make a balance between its numerical and parallel performance. Iterative methods reconstructed based on Unite and Conquer approach are the combination of different computational components. The separation of the solving and preconditioning parts increase the flexibility of applications, and the auto-tuning scheme is critical for them to get the optimal performance. The proposition of auto-tuning scheme for multiple parameters is not easy. In [11, 10], Aquilanti et al. tried to propose an auto-tuning for the Krylov subspace size and the incomplete orthogonalization inside Arnoldi reduction at the same time. Boillod-Cerneux [38, 39, 37] investigated the possibility to propose auto-tuning scheme by mixing multiple restarting strategies.

8.1.2 Selection Modes

The different levels of alternatives for auto-tuning are selected by different search modes. In this section, we discuss the empirical search, the machine learning based and the automatic contextual selection.

8.1.2.1 Empirical Search Selection

The simplest approach for the selections is to execute each code variant, measure its runtime (or other objective function), evaluate the performance of all variants, select the best one, and include that variant in the final code to be run. These are called empirical auto-tuners. For a compute kernel of a sparse matrix, the search space is the set of data structures and the operation implementation corresponding to these structures. Each structure is designed to improve the locality (thus improving computational performance) by exploiting a class of sparse matrix format with specific characteristics: blocks, diagonals, bands, symmetry or the combination of

© 2019 Tous droits réservés.

lilliad.univ-lille.fr

Thèse de Xinzhe Wu, Université de Lille, 2019

all this. Thus, the analysis is based on heuristic and empirical data taking into account not only the data used at runtime, but also the mathematical context.

8.1.2.2 Machine Learning Based Selection

When analytical performance models based on empirical search become too difficult for a given complicated scientific workload and HPC architecture, machine learning based selection is an effective alternative. In this approach, a small subset of parameter configurations (code variants) are evaluated on the target machine to measure the required performance metrics, and a predictive model is built by using machine learning approaches. Here, the choice of the supervised machine learning algorithm for building the surrogate performance model is crucial. Often this choice is driven by an exploratory analysis of the relationship between the parameter configurations and their corresponding runtimes. Bergstra et al. [35] presented a method for predictive auto-tuning based on boosted regression trees. They showed that machine learning methods for non-linear regression can be used to estimate timing models from data, capturing the best of both approaches. Nitro [153] is a framework for adaptive code variant tuning, which provides a library interface that permits programmers to express code variants along with meta-information trained by a machine learning model that aids the system in selecting among the set of variants at runtime. MasiF introduced by Collions et al. [59] is a tool to auto-tune the parallelization parameters of skeleton parallel programs. It reduces the size of the parameter space using a combination of machine learning, via nearest neighbor classification, and linear dimensionality reduction using PCA.

8.1.2.3 Automatic Contextual Selection

For most numerical methods, their performance depends on several parameters. The effects of these parameters might change in different manners at runtime, especially for the restarted iterative methods. It is impossible for the users to select the optimal parameters in advance. These optimal parameters for each restart might vary, depending on the many factors, such as the selected preconditioners, the convergence rate, etc. The automatic contextual selection means that certain parameters of the restarted iterative method are dynamically adjusted based on the selected criteria and heuristics. This kind of selection is always in real-time. These techniques used at runtime depend on heuristics computed in real-time without dependence on the data or on the computing environment (whether software or hardware). In addition, these techniques also have the role of assisting the users during the parameterization by proposing tuners for specific purposes, e.g., minimizing the calculation time, maximizing numerical accuracy. All of this will be explored in the following sections through the auto-tuning of internal parameters of UCGLE, which have significant impacts on the convergence of GMRES Component. The approach we have just discussed focuses on the contextual optimization of computation, but this optimization also exists in terms of computing resources, data structures, and so on.

© 2019 Tous droits réservés.

lilliad.univ-lille.fr

Thèse de Xinzhe Wu, Université de Lille, 2019

8.2 UCGLE Auto-tuning by Automatic Selection of Parameters

As presented in Section 5.4.2, many parameters affect the convergence performance of UCGLE. The impacts of selected parameters are also evaluated in Section 5.5.2, including the Krylov subspace size of GMRES Component m_g, the Least Squares polynomial degree d, the Least Squares polynomial preconditioning applied times lsa, the Least Squares polynomial preconditioning applied frequency $freq$, the number of eigenvalues approximated by ERAM Component n_{eigen}. These comparison results help us well understand the way of different parameters to influence the convergence of GMRES Component inside UCGLE. However, the selection of optimal value for each parameter is an arduous mission. Since the selected values vary from one application to another. Moreover, some parameters also depend on the hardware systems. It is necessary to propose an auto-tuning scheme for UCGLE which is able to automatically select the best values for all parameters at runtime. In this section, we select one of the most important parameters in UCGLE, and propose an auto-tuning scheme which adjusts this parameter at runtime, and makes sure the performance with the least loss compared with the case using the best parameter that we have manually selected. The auto-tuning of parameters for UCGLE should be proposed based on the automatic contextual selection.

8.2.1 Selection of Parameter for Auto-tuning

The Krylov subspace size m_g is an important factor for both numerical and parallel performance of UCGLE. However, the auto-tuning of this parameter is simple. In [10], Aquilanti introduced the bi-directional scheme based on the hierarchical cache sizes for the auto-tuning of Krylov subspace in GMRES. It is better to choose the most representative parameters in UCGLE for the auto-tuning tests, which are the ones related to the Least Squares polynomial preconditioning. The most relevant parameters are the Least Squares polynomial degree d and the Least Squares preconditioning applied times lsa. Theoretically, it is better to select high Least Squares polynomial degree, since the larger d is, the better approximation of Least Squares residual will be, and the more acceleration will occur on the GMRES Component. However, in practice, this parameter is limited by the fact that the moment matrix M_d is difficult to construct with the increase of Least Squares polynomial degree. Additionally, there will also much more SpMV operations for the Least Squares preconditioning, which introduce more global communications across all the computing units of GMRES Component. lsa is a complementary to improve the speedup of Least Squares polynomial preconditioning by performing several times a small degree polynomial. Compared with d, the increase of lsa is cheap, which introduces more AXPY operations without global communications. Hence, we decide to propose an auto-tuning scheme for lsa in the next section.

8.2.2 Multi-level Criteria

Fig. 5.15 in Section 5.5.2 evaluate the influence of lsa on the convergence of GMRES Component. In this figure, we can find that when lsa is small, with the increase of its value, there will be more acceleration on the convergence. At the same time, the residual norm for restarting will also be enlarged. With the several times repeat of Least Squares polynomial before applying on the

© 2019 Tous droits réservés.

lilliad.univ-lille.fr

Thèse de Xinzhe Wu, Université de Lille, 2019

restarting, the acceleration of Least Squares polynomial preconditioning will also be enhanced. Meanwhile, as presented in Section 5.3, the Least Squares polynomial is constructed with a few dominant eigenvalues, and the ones excluded the polygon will make the algorithm numerically instable. This instability will be still amplified if the Least Squares polynomial is repeated lsa times. That is the reason that the peaks in Fig. 5.15 is enlarged with the augmentation of lsa. In the end, if this amplification of instable errors cannot be compensated by the acceleration of Least Squares polynomial, the speedup becomes weak, and the GMRES Component might even obtain the divergence.

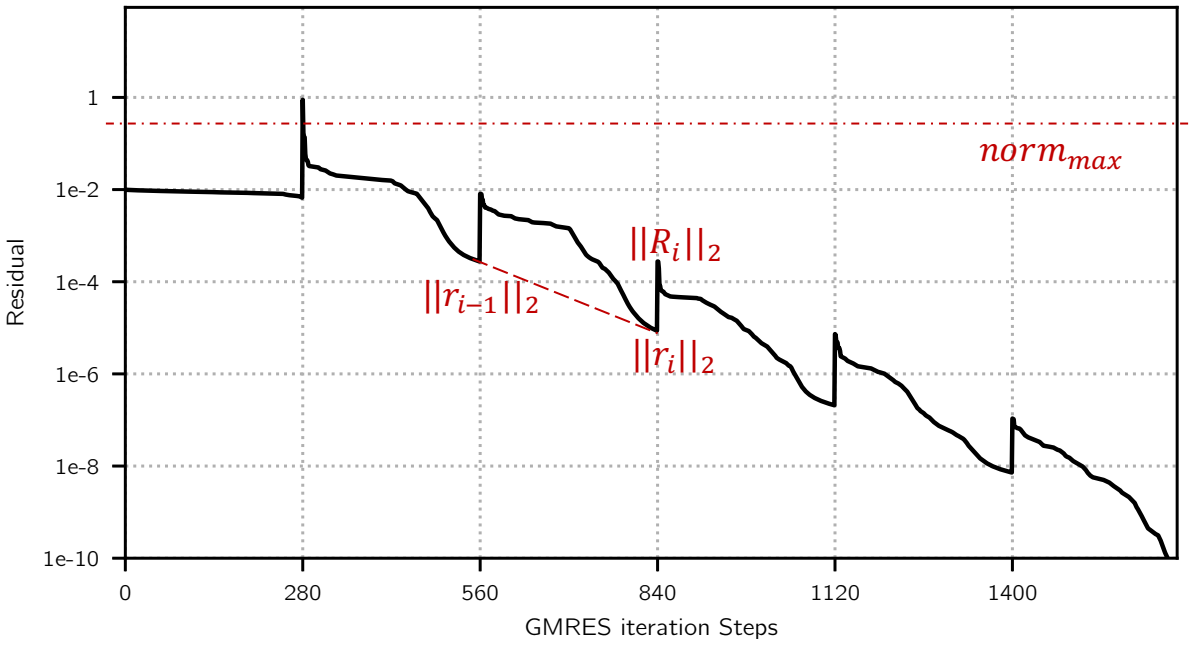

Figure 8.1 – Heuristic of lsa in UCGLE.

It is necessary to select suitable value of lsa for different linear systems. The auto-tuning proposed should be able to vary this parameter inside a given interval depending on several predefined criteria. In this dissertation, we implement two modes to vary the value of lsa, which is to reduce or increase this parameter value by a fixed step size for each Least Squares polynomial preconditioning from a given maximum or minimum value. As shown in Fig. 8.1, we list three important parameters to define the multi-level criteria as follows:

(1) $||r_{i-1}||_2$: Euclidean norm of previous time restarting residual vector before the Least Squares polynomial preconditioning;

(2) $||r_i||_2$: Euclidean norm of this time restarting residual vector before the Least Squares polynomial preconditioning;

(3) $||R_i||_2$: this time restarting residual norm after the Least Squares polynomial preconditioning.

In order to auto-tune the parameter lsa, we define three different criteria.

1^{st} **criterion:** The first criterion cr_i is defined as follows, with i indexing different restart times of GMRES Component.

© 2019 Tous droits réservés.

lilliad.univ-lille.fr

Thèse de Xinzhe Wu, Université de Lille, 2019

$$cr_i = \frac{||r_i||_2}{||r_{i-1}||_2}. \tag{8.1}$$

This parameter is defined as a ratio between $||r_i||_2$ and $||r_{i-1}||_2$. $||r_i||_2$ and $||r_{i-1}||_2$ represent respectively the Euclidean norm of this and previous time restarting residual vector before the Least Squares polynomial preconditioning, shown as Fig. 8.1. This criterion is defined to quantify the acceleration rate (see the slope of the red dashed line in Fig. 8.1 which connects two restarting points) of UCGLE with previous value of lsa, and the modification of this parameter for this time of Least Squares polynomial preconditioning should depend on the evaluation of cr_i. $cr_i < 1$ means the convergence of GMRES component, and the smaller it is, the more significant the acceleration will be. If $cr_i = 1$, there is no convergence for last time m steps of GMRES. If $cr_i > 1$ which means $||r_{i-1}||_2 > ||r_i||_2$, and the GMRES Component diverge. This first criterion is weak, which assures the convergence of GMRES, but it is impossible to control the acceleration rate by Least Square polynomial preconditioning.

2^{nd} **criterion:** The second criterion $ratio_i$ is defined as follows, with i indexing different restart times of GMRES Component.

$$ratio_i = \frac{||R_i||_2}{||r_i||_2}. \tag{8.2}$$

This parameter is defined as a ratio between $||R_i||_2$ and $||r_i||_2$. $||R_i||_2$ represents the restarted residual norm after the Least Squares polynomial preconditioning, shown as the peaks of the residual norms for the restarting in Fig. 8.1. The parameter $ratio_i$ defines the amplification of Least Squares polynomial preconditioning residual norm over the residual norm before the preconditioning. In other words, the value of $ratio_i$ determines the length of peaks in Fig. 8.1. In UCGLE, the peaks cannot be too large, otherwise the convergence will be slowed down, and GMRES Component might easily obtain the divergence. The definition of this criterion gives an relative upper limit for the residual norm generated by Least Squares polynomial preconditioning, and it will select the optimal value of parameter lsa for each restarting at runtime. This parameter can be seen as a strong factor to evaluate the quality of Least Squares polynomial preconditioning.

3^{rd} **criterion:** The third criterion $||R_i||_2$ is defined as follows, with i indexing different restart times of GMRES Component.

$$||R_i||_2. \tag{8.3}$$

The definition of this criterion is really simple, which is just the absolute residual norm generated by Least Squares polynomial for each restarting. This parameter determines that the absolute norm of Least Squares polynomial preconditioning should not be too enormous. The second criterion $ratio_i$ and $||R_i||_2$ can be seen as a complementary for each other. The former defines a relative amplification of residual norm caused by lsa, and the latter introduces a roof for the absolute enlargement of this residual norm. The combination of the two criteria can control the Least Squares polynomial preconditioning norm always in a good situation, and avoid the possibility of slowing down or divergence. The good selections of thresholds for them are really important.

© 2019 Tous droits réservés.

lilliad.univ-lille.fr

Thèse de Xinzhe Wu, Université de Lille, 2019

8.2.3 Heuristic and Auto-tuning Algorithm

After the definition of criteria, in this section, we present the heuristic and auto-tuning algorithm for selecting lsa at runtime. We give respectively the algorithm and workflow in Algorithm 35 and Fig . 8.2. Before the introduction of the heuristic in detail, different parameters of auto-tuning are listed as below:

- lsa: the initial value of applied times of Least Squares polynomial preconditioning predefined by users, the automatic selection this parameter at runtime will start from this value, by two different modes.
- $cr_i = \frac{||r_i||_2}{||r_{i-1}||_2}$: the 1^{st} criterion to control the convergence rate of GMRES Component. The threshold of this criterion can be prescribed by the users, which will define the acceptable of convergence rate. However, in this dissertation, we fix it to be 1, which means this criterion judge only if GMRES Component converge or not.
- $ratio_i = \frac{||R_i||_2}{||r_i||_2}$: the 2^{nd} criterion to determine the length of peaks generated by Least Squares polynomial preconditioning. This criterion the relative amplification of residual norm.
- $||R_i||_2$: the 3^{nd} criterion to determine the absolute amplification of residual norm produced by Least Squares polynomial preconditioning.
- lsa_i: the value of lsa determined by the 1^{st} criterion cr_i for the restart indexing by i. Hence, the initial given value $lsa_1 = lsa$.
- $\overline{lsa_i}$: the value of lsa determined by the 2^{nd} criterion $ratio_i$ and 3^{rd} criterion $||R_i||_2$. Thus it is the final determined value which will be applied to the Least Squares polynomial preconditioning.
- lsa_{min}: the minimum value that lsa should not break in max mode.
- lsa_{max}: the maximum value that lsa should not break in min mode.
- $ratio_{max}$: the threshold of $ratio_i$, and the acceptable value should not exceed it.
- $mode$: two modes to vary the value of lsa at runtime:
  - max: maximum mode which decreases lsa_i starting from lsa.
  - min: minimum mode which increases lsa_i starting from lsa..
- $norm_{max}$: the threshold of $||R_i||_2$, and the acceptable value should not exceed it.
- $length$: the step length to vary the value of lsa_i, either in max or min mode.
- m: the Krylov subspace of GMRES Component. this parameter is fixed when auto-tuning lsa.
- d: the degree of Least Squares polynomial. This parameter is also fixed to a given value during the procedure of auto-tuning.

© 2019 Tous droits réservés.

lilliad.univ-lille.fr

Thèse de Xinzhe Wu, Université de Lille, 2019

Algorithm 35 GMRES Component Implementation for Auto-tuing UCGLE

function AT-UCGLE($mode$, lsa, lsa_{max}, lsa_{min}, $length$, $norm_{max}$, $ratio_{max}$)
  $i = 1$, $lsa_1 = lsa$ and give initial guess x_0
  while not converged **do**
    $r_{i-1} = b - Ax_{x-1}$
    $r_i = b - A_{x_i}$, and $v_i = \frac{r_{i-1}}{||r_{i-1}||_2}$
    for $q = 1, 2, \cdots, m$ **do**
      Compute $h_{p,q} = (Av_q, v_p)$ for $p = 1, 2, \cdots, q$
      Compute $v_{q+1} = AV_q - \sum_{p=1}^{q} h_{p,q}v_p$, $h_{q+1,q} = ||v_{q+1}||_2$, and $v_{q+1} = v_{q+1}/h_{q+1,q}$
    end for
    $x_i = x_{i-1} + V_m y_m$, with y_m minimize $||\beta e_1 - H_m y||_2$
    if use Least Squares polynomial preconditioning **then**
      if i > 1 **then**
        $cr_i = \frac{||r_i||2}{||r_{i-1}||_2}$
        if $cr < 1$ **then**
          switch $mode$ **do**
            case max
              $lsa_i = lsa - length \times (i - 1)$
              if $lsa_i < lsa_{min}$ **then**
                $lsa_i = lsa_{min}$
              end if
            end case
            case min
              $lsa_i = lsa + length \times (i - 1)$
              if $lsa_i > lsa_{max}$ **then**
                $lsa_i = lsa_{max}$
              end if
            end case
          end switch
        end if
      end if
      for $j = 0, 1, \cdots, lsa_i - 1$ **do**
        for $i = k, 2, \cdots, d - 1$ **do**
          $\omega_{k+1} = \frac{1}{\beta_{k+1}}[A\omega_k - \alpha_k\omega_k - \delta_k\omega_{k-1}]$
          $x_{k+1} = x_k + \eta_{k+1}\omega_{k+1}$
        end for
        $x_i = x_i + x_l$
        $R_i = b - Ax_i$
        $ratio = \frac{||R_i||_2}{||r_i||_2}$
        if $ratio < ratio_{max}$ and $||R_i||_2 < norm_{max}$ **then**
          continue
        else
          $\overline{lsa_i} = j + 1$
          break
        end if
      end for
    end if
    $i = i + 1$
    Go to 4 to restart GMRES
  end while
end function

© 2019 Tous droits réservés.

lilliad.univ-lille.fr

Thèse de Xinzhe Wu, Université de Lille, 2019

After the introduction of parameters in the auto-tuning algorithm, here we present the auto-tuning scheme in detail. This auto-tuning can be divided into two parts. This first part is to varying the value lsa in either max or min mode according to the 1^{st} criterion cr_i. After a m-step GMRES indexing by i, if the convergence achieves, GMRES Component will exit. Otherwise, if Least Squares polynomial preconditioning is not available, GMRES will be restarted in a standard way using x_i as a initial vector for the next m-step GMRES. If the preconditioning is applicable, and $i = 1$, the value of lsa_1 is given as lsa. For $i > 1$, the lsa_{i-1} will be evaluated by calculating cr_i. If $cr_i < 1$, which means the GMRES with lsa_{i-1} is able to converge. We can continue to try to generate a new lsa_i based on the different modes. If the lsa_i is either too large or too small for the two modes, lsa_i will be fixed to be lsa_{min} and lsa_{max}, respectively. In a word, this part of auto-tuning will produce a value lsa_i based on the condition of cr_i.

The second part of the auto-tuning is more important, since it is directly linked to the iterations of Least Squares polynomial preconditioning. For each i, the loop from line 31 to 45 in Algorithm 35, is the operation that applies lsa_i times Least Squares polynomial. In this loop, for each $j \in 0, 1, 2, \cdots, lsa_i - 1$, a temporary solution x_l will be generated by a d degree Least Squares polynomial. Then x_l will be continuously added to x_i. For each j, current residual R_i can be defined as $b - Ax_i$, and a $ratio = \frac{||R_i||_2}{||r_i||_2}$ will also be calculated. If the condition that $ratio < ratio_{max}$ and $||R_i||_2 < norm_{max}$ are both satisfied at the same time, it means that both the peak and absolute residual norm sizes are acceptable. Thus the loop can continue until the end of loop. In this case, we have $\overline{lsa_i} = lsa_i$. If at least one of the two conditions cannot be satisfied, it means that either the peak size or the absolute residual Least Squares polynomial preconditioning is too large, and the loop will be immediately broken. In this case, we have $\overline{lsa_i} < lsa_i$. In summary, the real value of lsa applied for the Least Squares polynomial preconditioning is $\overline{lsa_i}$. The combination of criteria $ratio_i$ and $||R_i||_2$ can really select the good value of lsa_i at runtime, which assures the rapidest convergence produced by Least Squares polynomial preconditioning.

8.2.4 Experiments

After the proposition of heuristic, we will evaluate this auto-tuning scheme in this section.

8.2.4.1 Test Methods Setting

Since we have evaluated the influence of different parameters on the convergence using the test matrix $utm300$ from the Matrix Market collection, we continue to use it for the auto-tuning tests. The Krylov subspace size m for GMRES Component in different methods is fixed as 90, and the degree of Least Squares polynomial is set to be 10. The parameters $length$, $ratio_{max}$, $norm_{max}$ are respectively given as 2, 1.0×10^5 and 1.0×10^4 for UCGLE with auto-tuning scheme (denote it as AT-UCGLE). We list the test methods as below.

- UCGLE($lsa = 4$): UCGLE implementation without auto-tuning scheme, and $lsa = 4$;
- UCGLE($lsa = 10$): UCGLE implementation without auto-tuning scheme, and $lsa = 10$;
- UCGLE($lsa = 20$): UCGLE implementation without auto-tuning scheme, and $lsa = 20$;

© 2019 Tous droits réservés.

lilliad.univ-lille.fr

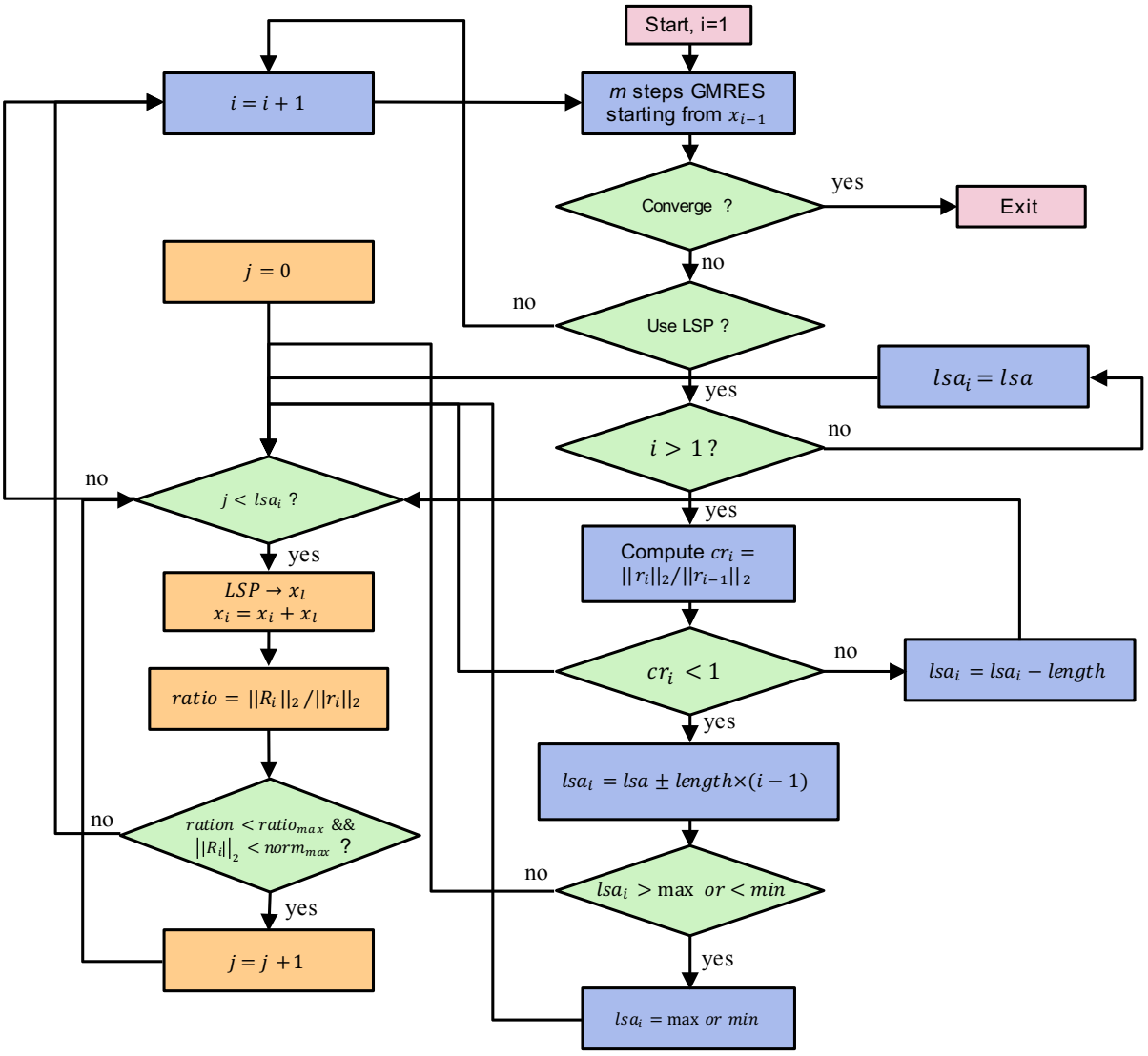

Figure 8.2 – Auto-tuning workflow for UCGLE.

- AT-UCGLE(max, $lsa = 20$): UCGLE implementation with auto-tuning scheme, varying the value of lsa in max mode, and initial value of lsa is set to be 20;
- AT-UCGLE(max, $lsa = 30$): UCGLE implementation with auto-tuning scheme, varying the value of lsa in max mode, and initial value of lsa is set to be 30;
- AT-UCGLE(min, $lsa = 4$): UCGLE implementation with auto-tuning scheme, varying the value of lsa in min mode, and initial value of lsa is set to be 4.

8.2.4.2 Convergence Comparison

The convergence comparison for UCGLE with and without auto-tuning is given as Fig. 8.3. In this figure, firstly we can find that UCGLE($lsa = 10$) has the fastest convergence. However, it is difficult for UCGLE($lsa = 4$) and UCGLE($lsa = 20$) to achieve the convergence. For the former, the peak for each restarting is relative small, and the acceleration of Least Squares polynomial preconditioning is weak. For the latter, the absolute norm of restart residual generated by Least

© 2019 Tous droits réservés.

Thèse de Xinzhe Wu, Université de Lille, 2019

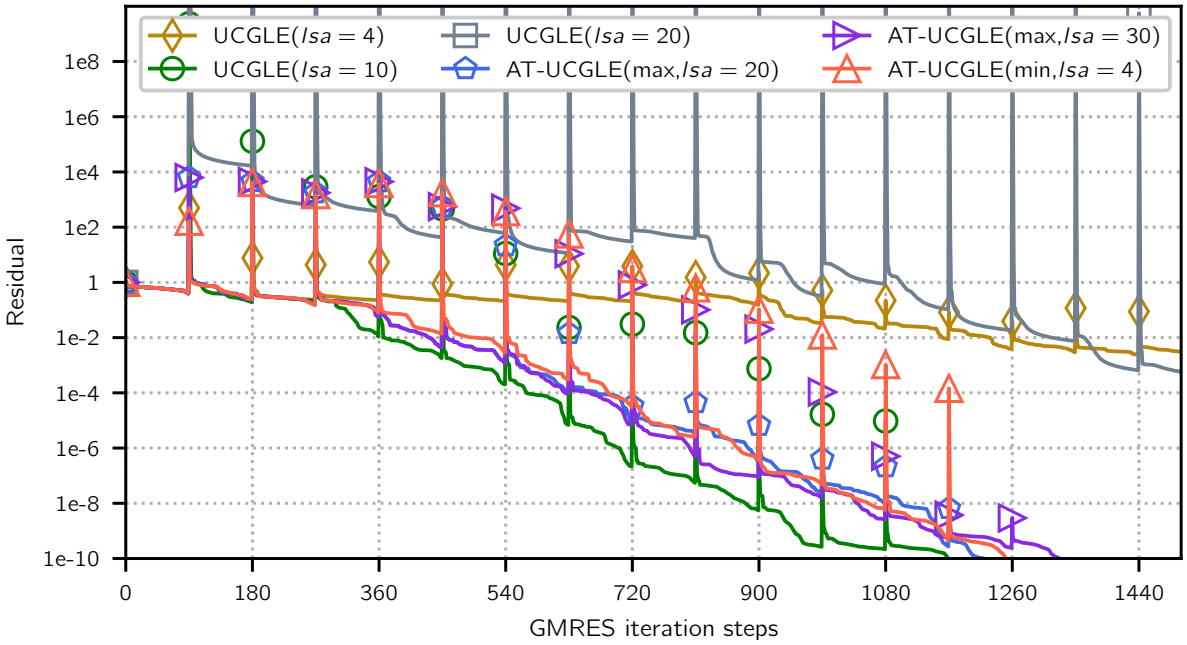

Figure 8.3 – Convergence Comparison for UCGLE with and without Auto-tuning.

Squares polynomial is too large which exceeds 1.0×10^{15}, and it is also difficult for UCGLE to quickly converge. It is not marked in Fig. 8.3, but a large number of tests indicate that $lsa = 10$ is the optimal value for UCGLE without auto-tuning scheme if all the other parameters are fixed.

In practice, for a given application, the users are unable to directly select the optimal value for lsa in advance. Thus the auto-tuning scheme is proposed to automatically select the best value inside a given interval at runtime. For AT-UCGLE(max, $lsa = 20$) and AT-UCGLE(max, $lsa = 30$) which start the iterations with a very large value for lsa (respectively 20 and 30), they can obtain the convergence much more quickly than UCGLE($lsa = 20$). They need a little more steps for the convergence compared with the best case UCGLE($lsa = 10$). For AT-UCGLE(min, $lsa = 4$) which starts the iteration with a small pre-defined $lsa = 4$, its iteration steps for convergence is also competitive with the best case UCGLE($lsa = 10$). For AT-UCGLE in *max* starts from a very large lsa, it will produce an enormous residual normal which damages the convergence (see UCGLE($lsa = 20$) and AT-UCGLE(max, $lsa = 20$) in Fig. 8.3). The constraint of $||R_i||_2$ can ensure this norm always in an acceptable condition, and the speedup of convergence is obvious. In a word, two modes of varying lsa are both effective to approximate the best numerical performance with a too large or small prescribed lsa.

Table. 8.1 shows the exact number of iterations and time of execution for different methods. Moreover, both the effectiveness of iterations and time are also given in this table. The iteration effectiveness is defined as the ratio between the iteration number of the best case UCGLE($lsa = 10$) and the one of the method to be compared. The time effectiveness can be also defined in a similar way. In this table, we can find that AT-UCGLE(max, $lsa = 20$) achieve 95.8% iteration effectiveness and 97.2% time effectiveness. AT-UCGLE(min, $lsa = 4$) can achieve respectively 93.4% and 92.1% for the iteration and time effectiveness. The effectiveness of iteration and time for AT-UCGLE(max, $lsa = 30$) are respectively 88% and 85.3%.

© 2019 Tous droits réservés.

lilliad.univ-lille.fr

Thèse de Xinzhe Wu, Université de Lille, 2019

Table 8.1 – Iteration steps and Time Comparison.

Methods	Iterations	Iteration Effectiveness	Time (s)	Time Effectiveness
UCGLE($lsa = 10$)	1169	100%	0.35	100%
UCGLE($lsa = 4$)	2513	46.5%	0.72	48.6%
UCGLE($lsa = 20$)	3226	36.2%	1.08	32.4%
AT-UCGLE(max, $lsa = 20$)	1220	95.8%	0.36	97.2%
AT-UCGLE(max, $lsa = 30$)	1328	88%	0.41	85.3%
AT-UCGLE(min, $lsa = 4$)	1252	93.4%	0.38	92.1%

In summary, two modes are both meaningful with high iteration and time effectiveness compared with the best case of UCGLE without auto-tuning. However, the selection of initial value of lsa value is still a factor which influences the convergence. In *max* mode, if lsa is extreme large, the effectiveness might be a little low. That is the reason that AT-UCGLE(max, $lsa = 30$) achieves only 88% iteration effectiveness, but AT-UCGLE(max, $lsa = 20$) can achieve about 95.8%.

8.2.4.3 Analysis

The auto-tuning scheme proposed in this dissertation is able to select a good value for the parameter lsa in two steps for each time Least Squares polynomial preconditioning. For each restarting indexing i, the first step is to generate a lsa_i using a simple heuristic based on cr_i. This parameter can ensure the convergence for the next m-steps GMRES not worse than the previous one, but it cannot make decision for the speedup of Least Squares polynomial preconditioning, which is the kernel of UCGLE. The second step is to select a best $\overline{lsa_i}$ according $ratio_i$ and $||R_i||_2$. Table 8.2 gives the comparison of lsa_i and related $\overline{lsa_i}$ at each restarting inside AT-UCGLE. In this table, we can find the benefits of the criteria $ratio_i$ and $||R_i||_2$, which can limit the value of lsa_i always in a good situation.

Table 8.2 – lsa_i vs $\overline{lsa_i}$ for each restart in AT-UCGLE.

Method \ Restarting times	1	2	3	4	5	6	7	8	9	10	11	12	13	14
AT-UCGLE(max, $lsa = 20$) lsa_i	20	18	16	14	12	10	8	6	4	4	4	4	4	
AT-UCGLE(max, $lsa = 20$) $\overline{lsa_i}$	5	8	8	9	10	8	6	6	4	4	4	4	4	
AT-UCGLE(max, $lsa = 30$) lsa_i	30	28	26	24	22	20	18	16	14	12	10	8	6	4
AT-UCGLE(max, $lsa = 30$) $\overline{lsa_i}$	5	8	8	9	10	10	10	10	11	10	10	8	6	4
AT-UCGLE(min, $lsa = 4$) lsa_i	4	6	8	10	12	14	16	18	20	22	24	26	28	
AT-UCGLE(min, $lsa = 4$) $\overline{lsa_i}$	4	6	8	10	11	10	9	11	10	11	11	10	11	

8.3 Conlusion

In this chapter, we investigated the different auto-tuning modes for the iterative methods. We implement an automatic contextual selection scheme for the selected parameter of UCGLE. This

© 2019 Tous droits réservés.

lilliad.univ-lille.fr

Thèse de Xinzhe Wu, Université de Lille, 2019

auto-tuning heuristic is established with the definition of multiple level criteria and a workflow for the selection of best value for parameters at runtime. The effectiveness of proposed auto-tuning scheme is proved by the experimental results using one test matrix. The experiments show the importance of auto-tuning for UCGLE method. The proposed scheme should be verified with more test matrices. In the future, a more flexible workflow should be proposed to vary the value inside a given interval. Moreover, UCGLE has a large number of parameters which have impact on its numerical and parallel performance, hence the final goal is to implement an adaptive version of UCGLE, which can auto-tune various parameters at the same time.

© 2019 Tous droits réservés.

lilliad.univ-lille.fr

Chapter 9

YML Programming Paradigm for Unite and Conquer Approach

After the validation of numerical and parallel performances of m-UCGLE, a major difficulty to profit from Unite and Conquer methods including m-UCGLE is to implement the manager engine which can well handle their fault tolerance, load balance, asynchronous communication of signals, arrays and vectors, the management of different computing units such as GPUs, etc. In Chapter 7, we tried to give a naive implementation of an engine to support the management computational components on the homogeneous/heterogeneous platforms based on MPI_SPAWN and MPI non-blocking sending and receiving functionalities. The stability of this implementation of the engine cannot always be guaranteed. Thus we are also thinking about to select the suitable workflow/-task based environments to manage all these aspects in the Unite and Conquer approach. YML[1] is a good candidate, which is a workflow environment to provide the definition of the parallel application independently from the underlying middleware used. The special middleware and workflow scheduler provided by YML allows defining the dependencies of tasks and data on the supercomputers [69]. YML, including its interfaces and compiler to various programming languages and libraries, will facilitate the implementation of Unite and Conquer based methods with different numerical components. In this chapter, firstly we give a quick summary of the YML framework and then analyze the limitations of existing YML implementation for Unite and Conquer approach. In the end, we propose related solutions.

9.1 YML Framework

YML is a workflow environment dedicated to the execution of parallel and distributed applications on different Grid platforms and supercomputers. The YML framework enables the description of the complicated parallel applications based on the tasks. The task-based application written based on YML language can be executed on several runtime systems or middleware without changes. YML is a software layer between the end-user and the runtime system of a

1. http://yml.prism.uvsq.fr/

© 2019 Tous droits réservés.

lilliad.univ-lille.fr

Thèse de Xinzhe Wu, Université de Lille, 2019

supercomputer and/or the middleware of a distributed system, which is in charge of communication.

9.1.1 Structure of YML

YML is composed of three main parts: an IDL, a kernel and a backend allowing interactions with the runtime system or middleware. As shown in Fig. 9.1, the kernel of YML consists of a high-level workflow language, a just-in-time scheduler and a system of service integration. The high-level language (YvetteML) which is XML-based permits the description of the graph of application with dependencies or communications. The language integrates the ability to describe computation and their workflow on the same time. This language provides a way to specify the communication between components during the execution of the application. The graph can contain parallel and sequential sections and standard construction of most languages including branching, exceptions, and loops. The graph language describes the dependencies between the components during the execution by the notion of events. The compiler translates the graph of components of applications in an internal representation containing a set of components calls. The scheduler manages application execution and acts as a client for the underlying runtime system accurately requiring computing resources. During the execution, the scheduler detects tasks ready for execution and solves their dependencies at runtime. Each scheduling step may generate different types of tasks (parallel or serial), which are supported dedicated middleware and backends. With the component-oriented design of YML, a service in YML can be any kind of components such as a library, a data repository, or a catalog of binary components. The computational components can be written in different programming languages like C, C++ and XcalableMP.

9.1.2 YML Design

The aim of YML is to provide users with an easy-of-use method to run parallel applications on different Grid platforms and supercomputers. The framework can be divided into three parts which are the *end-users interface*, *frontend*, and *backend*. The end-users interface is used to provide an intuitive way to submit their applications, which are described using a workflow language YvetteML. Frontend is the main part of YML which includes a compiler, scheduler, data repository, abstract and implementation components (shown as Fig. 9.1). The backend is the part to connect different Grid, P2P and cluster middlewares.

The development of a YML application is based on the components approach, and then we will discuss the three kinds of components in detail.

- **Abstract component** defines the communication interface with the other components. This definition gives the name, and the communication channels correspond to a data input, data output or both and are typed. This component is used in the code generation step and to create the graph.

- **Implementation component** is the implementation of an abstract component. It describes computations through YvetteML language. The implementation is done by using

© 2019 Tous droits réservés.

lilliad.univ-lille.fr

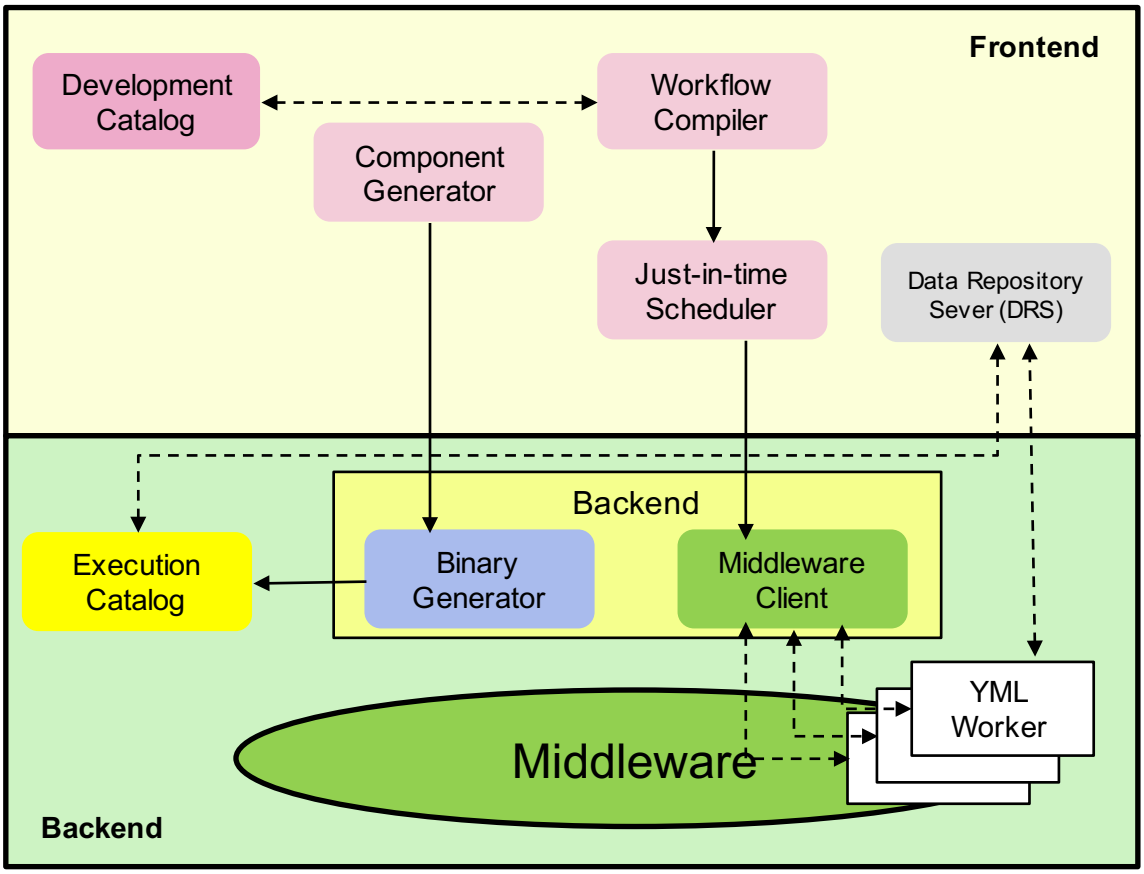

Figure 9.1 – YML Architecture.

common languages like C or C++. They can have several implementations for the same abstract component.

- **Graph component** carries a graph expressed in YvetteML instead of a description of computation. It provides the parallel and sequential parts of an application and the synchronization events between dependent components. It is a straightforward way for scientific researchers to develop their application.

Moreover, those three components are independent of middleware, which can be reused on various platforms. In order to run an application on other computing environments with a different middleware, the user needs to compile each component for the selected middleware. YML eases components creation. Existing codes can be reused by importing libraries as some new components without any adaptation. Those components are called by the application when computational tasks have to be started. Moreover, the notions of abstract and implementation descriptions of components bring three interesting features for the scheduler that can be included in the framework.

- **data migration** can be easily quantified at the start and at the end of the application thanks to the abstract definition.
- **data used** by a component is clearly defined in the abstract and implementation definitions, therefore this can be used in a checkpointing feature to move a component from a

© 2019 Tous droits réservés.

Thèse de Xinzhe Wu, Université de Lille, 2019

node to an other.

- **computation time** of a component can be evaluated thanks to the implementation definition.

The use of Data Repository Servers hides the data migrations to the developer and ensure that necessary data are always available to all components of the application.

9.1.3 Workflow and Dataflow

The workflow programming environment YML facilitates the expression of parallelism for the user, which is able to implement the applications in a way very close to the algorithms. YvetteML, the high-level language provided by YML, is able to describe easily the complex workflow of applications. The *Abstract* provides the interface of components including the input and output data. When a graph of tasks is constructed, the dataflow can be deduced by the input/output data types defined in the *Abstract* of components. As shown in Fig. 9.2, YML enables the optimization combining two aspects:

- workflow;
- dataflow

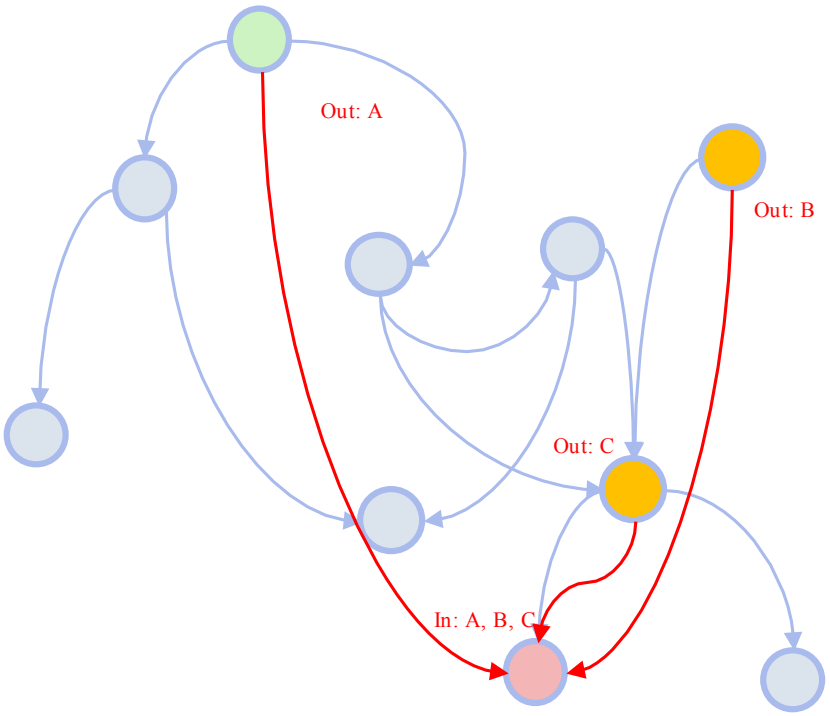

Figure 9.2 – YML workflow and dataflow.

9.1.4 YvetteML Language

The YvetteML language provides different features for creating applications. These features are described as below:

© 2019 Tous droits réservés.

lilliad.univ-lille.fr

Thèse de Xinzhe Wu, Université de Lille, 2019

- **Parallel Section:** they are used to explicitly define sections which will be executed in parallel. The formule of this operation is given as: *par section 1 // ... // section N endpar*;
- **Sequential loop:** they are loops with iterators, which are executed sequentially. The formule of this operation is given as: *seq (i:=begin;end) do ... enddo*;
- **Parallel loop:** they are loops with iterators, which are executed in parallel. The formule of this operation is given as: *par (i:=begin;end) do ... enddo*;
- **Conditional structure:** they are the condition structure to control the execution of tasks by the condition. The formule of this operation is given as: *if (condition) then ... else ... endif*;
- **Synchronization:** The formule of this operation is given as: *wait(event) / notify(event)*;
- **Component calls:** the role of component calls is to submit a new task to the Local Ressource Manger providing the name of the component defined earlier and the different input parameters. The formule of this operation is given as: *compute NameOfComponent(args,...,...)*.

9.1.5 YML Scheduler

In computing, scheduling is a method in which work specified in some way is assigned to resources that complete work. The scheduler performs scheduling activities, and the scheduler is usually implemented to keep all computing resources busy. A scheduler may aim to one of many goals, maximizing throughput (the total amount of work completed per time unit), minimizing response time (time from work becoming enabled until the first point it begins executing resources), minimizing latency (the time between work becoming enabled and its subsequent completion) or maximizing fairness (equals CPU time to each process, or more generally appropriate times according to the priority and workload of each process).

9.1.5.1 Scheduler Architecture

For the scheduling, the YML environment is defined in two parts:

(1) The first part is what we call the *frontend*. Its mission is to analyze the application code written by YvetteML and dispatch the tasks for the backend and middlewares.

(2) The second part is the *backend*. It deals with the distribution of tasks onto different computing units.

9.1.5.2 Frontend

Now we are talking about the scheduler of YML. It is responsible for reading the dependency graph by compiling the graph of application. This graph contains all inner-steps dependencies. The scheduler is closely linked to the worker component. Indeed the worker component is a component responsible for the execution of a service. Services represent computations needed

© 2019 Tous droits réservés.

lilliad.univ-lille.fr

Thèse de Xinzhe Wu, Université de Lille, 2019

for the realization of a workflow process, the execution of a service can be decomposed in the following steps:

(1) When the worker component is started, it first analyzes a work description. This work description contains all the information needed to execute the service. It consists of a list of resources to retrieve from the data repository component, the parameter of the service as well as the destination of the results. The resources retrieved are the service and its input. The service is then executed.

(2) It generates a set of results as well as some meta-information such as the status reported by the service, the list of results produced and a trace of the execution of a service.

(3) The information is published to the data repository component together with the results of the service.

(4) The worker finally cleans up the peer and finishes its execution. The workflow scheduler component is responsible for executing workflow processes.

As shown by Algorithm 36, the scheduler executes two main operations sequentially. Firstly, it schedules the execution of workflow by solving the dependencies among its activities and submit them to the backend. The generation of new tasks is following a new schedule rule updated from the scheduler. The second operation is the monitoring of the task currently being executed. Once tasks have started their execution, the scheduler of the application regularly checks if new works have entered the finished state. The scheduler interacts with the backend layer through the data repository and backend components. Every time a work status changed to ready, the scheduler prepares the execution of a service by creating a script describing the work. This script is processed by the worker component of the backend layer. In the meantime, the work channels are stored in an archive in order to be easily exchanged between the data repository and the worker. If a task is finished, it will be deleted, and its status will be updated to the scheduler. Besides, the scheduler is able to manage the execution errors of computational components.

9.1.5.3 Backend

The backend component is responsible for the interaction with the resource scheduler service of the middleware. It translates the abstract work description composing a workflow into requests to the resource scheduler of a middleware. Each middleware has its own backend component. The backend component acts as a client of the middleware. The abstract work request which is processed by the backend component leads to the execution of a worker component on a peer selected by the middleware resource scheduler. The worker component analyzes the work description and is responsible for its execution. Its means the acquisition of the concrete service used to do the computation and the data required for the computation. Then, the worker executes the concrete service corresponding to the work. And finally, the worker as well as the kernel layer interact with the data repository component. This component is responsible for the acquisition as well as the publishing of data in the workflow environment. The model thus defines two operations:

© 2019 Tous droits réservés.

lilliad.univ-lille.fr

Thèse de Xinzhe Wu, Université de Lille, 2019

Algorithm 36 YML Scheduler

```
1: while status == EXECUTING do
2:     while task == finished do
3:         ++taskFinished
4:         delete(task)
5:     end while
6:     UpdateStatus
7:     if status==ERROR then
8:         continue                    ▷ Task terminates with error, execution stopped
9:     end if
10:    UpdateSchedulingRule
11:    while (task = nextTaskReady) !=0 do
12:        ++taskSubmitted
13:        queue(task)
14:    end while
15:    if !SchedulingPendingTask then
16:        break                       ▷ Execution finished with error
17:    end if
18:    updateStatus
19: end while
20: finalizeExecution
```

- **put**: this operation is used to publish data within a data repository or a network of repositories. Publishing data is similar to write operation on a memory area;
- **get**: this operation is used to acquire data stored in a data repository. Acquiring a data is similar to read operation on a memory area.

The backend component allows the submission of asynchronous invocation of applications on peers. The resource scheduler selects arbitrary a peer and assigns it to the execution of the request. The content of the request varies significantly from one middleware to another. The backend component translates YML service execution into requests understandable by the resource scheduler of the middleware currently used. A backend component maintains a list of active requests and a list of finished requests. The polling of the middleware allows the backend to move requests from the active queue to the queue of finishde requests. In YML, a request consists in the execution of the worker component by a peer, thus the backend allows YML to ask the middleware to execute many instances of the YML worker and to be notified when one terminates.

9.1.6 Multi-level Programming Paradigm: YML/XMP

A multi-level programming model on the supercomputing systems is established by combing YML and XMP. YML/XMP programming model requires a specific middleware *OmniRPC-MPI*. The multi-level parallelism including:

- High level: communication inter nodes/group of nodes
  - YML - coarse grain parallelism - asynchronous communication

© 2019 Tous droits réservés.

lilliad.univ-lille.fr

Thèse de Xinzhe Wu, Université de Lille, 2019

- Low level: group of nodes / cores
  - PGAS language XMP programming with pragma

The multi-level programming paradigm YML/XMP is supported by the *OmniRPC-MPI* middleware. *OmniRPC* is a thread-safe remote procedure call (RPC) system, based on Ninf, for cluster and grid environment. It supports typical master/worker grid applications. Workers are listed in an XML file named as the host file. For each host, the maximum number of job, the path of OmniRPC, the connection protocol (ssh, rsh) and the user can be defined.

An OmniRPC application contains a client program which calls remote procedures through the OmniRPC agent. Remote libraries which contain the remote procedures are executed by the remote computation hosts. There are implemented like an executable program which contains a network stub routine as its main routine. The declaration of a remote function of the remote library is defined by an interface in the Ninf IDL. The implementation can be written in familiar scientific computation language like FORTRAN, C or C++. There are two versions of OmniRPC. One is for the Grid computing and distributed architecture of large numbers of computers and the other for supercomputer (OmniRPC-MPI). The scheduler of OmniRPC is simple. It is just a classic Round-Robin scheduling algorithm. As the term is generally used, time sliced are assigned to each process in equal portions and circular order, handling all processes without priority (also known as the cyclic executive).

9.1.7 YML Example

In this section, we give an example to understand the grammar and implementation of YML. The workflow of this example is given as Fig. 9.3. Its scenario is: firstly two seperate sum operations of four given floating numbers are executed, which result in two different floating numbers, these two numbers are added together to output the final results.

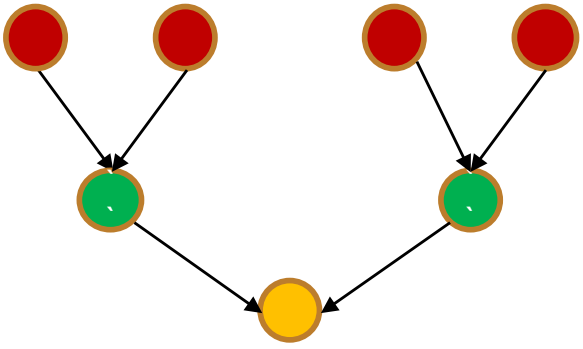

Figure 9.3 – Workflow of Sum Application.

9.1.7.1 Abstract

The *Abstract* defines the communication interface with the other components. This definition gives the name, and the communication channels correspond to a data input, data output or both and are typed. This component is used in the code generation step and to create the graph. As shown in the Listing 4, the *sum* operation requires two input parameters a and b, and an output parameter res. These three parameters are all of scalar type *real*.

© 2019 Tous droits réservés.

lilliad.univ-lille.fr

Listing 4 *Abstract Component* Example

```
<?xml version="1.0" encoding="utf-8"?>
<component type="abstract" name="test_abstract"
description="sum of two doubles">
  <param type="real" mode="out" name="res" />
  <param type="real" mode="in" name="a" />
  <param type="real" mode="in" name="b" />
</component>
```

9.1.7.2 Implementation

The *Implementation Component* is the implementation of an abstract component. It provides the description of computations through YvetteML language. The implementation is done by using common languages like C, C++ or XMP. As shown by the Listing 5, this *sum* operation is implemented with C++ to sum the input parameters a and b into the output parameter res.

Listing 5 *Implementation Component* Example

```
<?xml version="1.0" encoding="utf-8"?>
<component type="impl" name="test_impl" description="sum of two doubles">
  <impl lang="CXX" libs="">
    <header><![CDATA[
        #include <stdlib.h>
      ]]>
    </header>
    <source lang="CXX" libs="">
       res = a + b;
    </source>
    <footer></footer>
  </impl>
</component>
```

9.1.7.3 Application

The *Application* carries a graph expressed in YvetteML. It provides the parallel and sequential parts of an application and the synchronization events between dependent components. The Listing 6 below describes the workflow given in Fig. 9.3, the two first *sum* operations are executed in parallel, and the output of these operations *res[0]* and *res[1]* are added together by the subsequent sum operation, which gives the final output value *result*.

© 2019 Tous droits réservés.

lilliad.univ-lille.fr

Thèse de Xinzhe Wu, Université de Lille, 2019

Listing 6 *Application Component* Example

```
<?xml version="1.0" encoding="utf-8"?>
<application name="test_app">
  <description> sum application </description>
  <params></params>
  <graph>
    nb:=2;
    par (i:=0; nb-1)
    do
      compute test(res[i], 1.0, 2.0); #res[0 or 1]= 3.0
    enddo
    endpar
    compute test(result, res[0], res[1]); #result = 6.0
  </graph>
</application>
```

9.2 Limitations of YML for Unite and Conquer Approach

In this section, we analyze the limitations of YML for the implementation of the Unite and Conquer approach.

9.2.1 Possibility Analysis to Implement UCGLE using YML

In order to analyze the possibility to implement Unite and Conquer methods by YML framework, in this section, we give the workflow of m-UCGLE as an example (shown as Fig. 9.4). When the application starts, various number of components/tasks are allocated (e.g., three GMRES, two s-KS and one B-LSP components in Fig. 9.4). The algorithm of m-UCGLE is decomposed into a number of computational tasks as below:

- *bgmres_init*;
- *bgmres_check*;
- *ks_eigen*;
- *bgmres_ar*;
- *bgmres_restart*;
- *ks_update*;
- *bgmres_ls*;
- *ks_init*;
- *ks_restart*;
- *bgmres_precond*;
- *ks_ar*;
- *lsp_pretreatment*.

The first state for BGMRES and s-KS components are the *bgmres_init* and *ks_init* (denoted as I in Fig. 9.4) which loads the matrix and vectors. Then the *ks_ar* and *bgmres_ar* are executed, which are respectively the Arnoldi reduction inside s-KS and BGMRES components (denoted as A in Fig. 9.4). For BGMRES, temporary solutions can be approached by *bgmres_ls* which solves a Least Squares problem (denoted as L in 9.4). These temporary solutions are checked for the acceptable tolerance by *bgmres_check* (denoted as C in Fig. 9.4). If the condition to stop is satisfied, BGMRES components will exit. For s-KS Components, a number of eigenvalues can be approximated by *ks_eigen* (denoted as E in the figure). These eigenvalues are asynchronously

© 2019 Tous droits réservés.

lilliad.univ-lille.fr

Thèse de Xinzhe Wu, Université de Lille, 2019

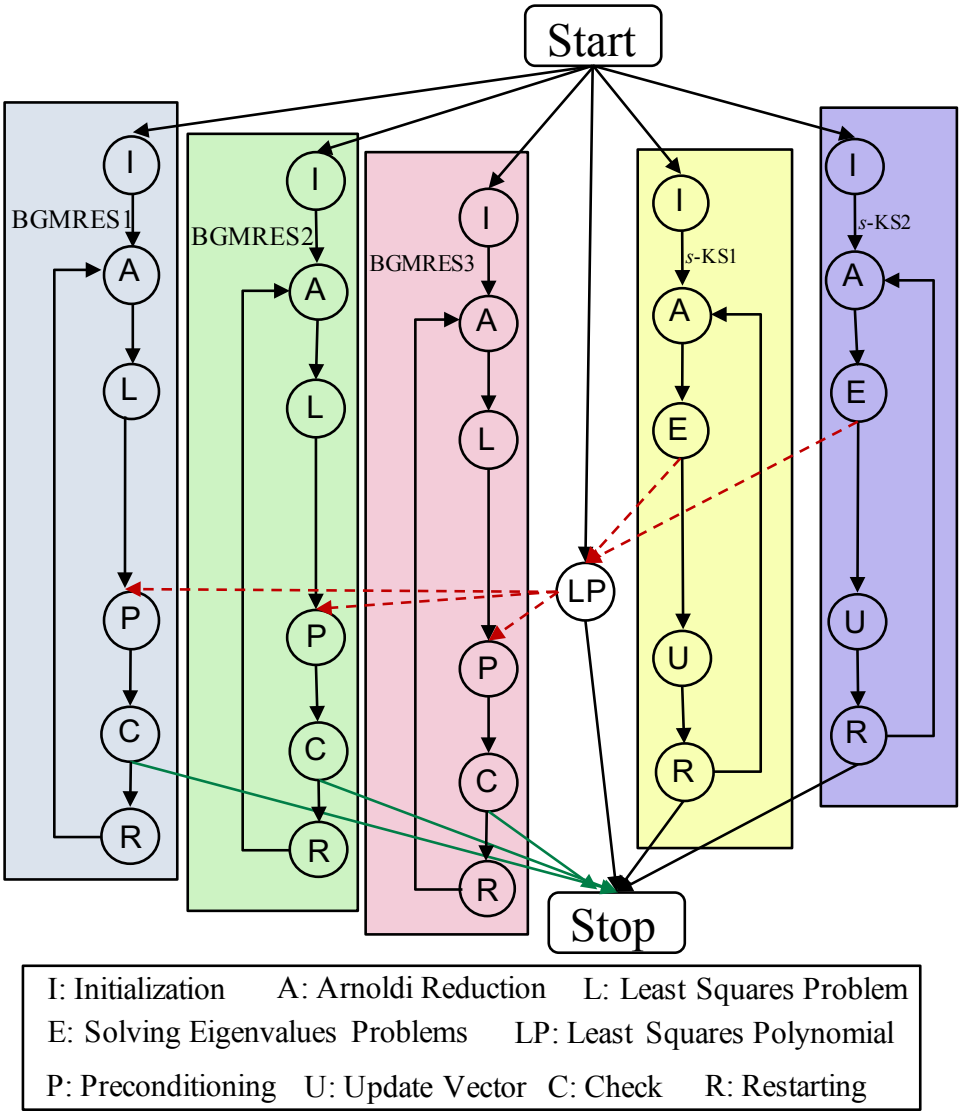

Figure 9.4 – Tasks and workflow of m-UCGLE.

sent to B-LSP component and it generates the Least Squares polynomial preconditioning parameters by *lsp_pretreatment* (denoted as LP in Fig. 9.4). If the convergence of BGMRES are not achieved, these parameters are asynchronously sent to BGMRES and perform the iterative steps to generate a new preconditioned residual vector by *bgmres_precond* (denoted as P in 9.4), and then restart BGMRES by *bgmres_restart* (denoted as R in 9.4); if no parameters received from B-LSP component, BGMRES are restarted with the residual vector gotten from L. For s-KS Components, after each cycle, a new vector is generated by *ks_update* which is used as a new initial vector for the next cycle restarted by *ks_restart*.

We would like to implement these components inside m-UCGLE and manage their workflow by the YvetteML language and the related scheduler. However, the actual version of YML has several limitations of the implementation of restarted iterative methods based on the Unite and Conquer approach. The first limitation is the lack of a mechanism to handle the asynchronous communication between the components, and the second is the lack of a mechanism to check the convergence of restarted iterative methods. In the following sections, we discuss in detail the

© 2019 Tous droits réservés.

lilliad.univ-lille.fr

Thèse de Xinzhe Wu, Université de Lille, 2019

two limitations.

9.2.2 Asynchronous Communications

The first limitation of YML framework for Unite and Conquer approach is that it does not support the special asynchronous communications (shown as the red dashed arrows in Fig. 9.4) for the three operations *bgmres_precond*, *ks_eigen* and *lsp_pretreatment*. They send and receive the eigenvalues asynchronously and preconditioning parameters between different computational components. In details, this type of operations can be summarized as:

- check the receiving of data asynchronously from other components;
- if received, operate with these data; if not, perform another operation without these data.

9.2.3 Mechanism for Convergence

The second limitation of YML framework for Unite and Conquer approach is the lack of a mechanism to check the convergence of iterative methods. In detail, for the BGMRES components in Fig. 9.4, they all perform the loop of Arnoldi reduction until the convergence criteria are satisfied or they exceeded the maximum number of iterations allowed. YML does not allow the mechanism to break the loop in halfway with some given condition. The iterative methods can only be implemented with a fixed number of iterative steps. This kind of implementations is inefficient for the iterative methods, and the convergence cannot always be guaranteed. In the acutal implementation of YML, it is not possible to exit the parallel section/loop of multiple operations until all of them are finished.

9.3 Proposition of Solutions

We reviewed the grammar and scheduler implementations of YML framework, and propose the solution of its limitations for Unite and Conquer approach discussed in Section 9.2.

9.3.1 Dynamic Graph Grammar in YML

The special asynchronous communications of Unite and Conquer approach be expressed with extending YML grammar to support the dynamic graphs.

9.3.1.1 Variable for Dynamic Graph

The dynamic graphs are the types of graph modifiable depends on the variables and/conditions. The dynamic graph can be supported with the introduction of a new variable for the dynamic graph in the *Abstract* components:

```
<param type="var_graph" mode="inout" name="foo">
```

© 2019 Tous droits réservés.

lilliad.univ-lille.fr

Thèse de Xinzhe Wu, Université de Lille, 2019

The variable for the dynamic graph can be the mode of *in*, *out* or *inout*. These parameter may be evaluated and modified inside a task, or only as logical into Yvette "if (logical) then ··· else ···".

9.3.1.2 Scheduler Component for Dynamic Graph

If the computation to evaluate the logical is too complex, we may use a task with a special indication, added on the Implementation component, such as "graph_scheduler_evaluation": then the scheduler may manage those tasks as others, or run it "itself".

9.3.1.3 Implementation for m-UCGLE

For the implementation of asynchronous communication, it is enough for creating variables to manage the dynamic grammar. In this section, we give the templates to implement the three computational components: *bgmres_precond*, *ks_eigen* and *lsp_pretreatment*. This is only an example to show the implementation of variables and the related logic inside the components, so no further detailed information is given. For the rest components without asynchronous dependencies, they can be normally implemented by YML, and we have no intention to give the details in this section.

Abstract: three types of *Abstract* components are constructed as the codes below. In *ks_eigen* (shown as Listing 7), a dynamic graph variable *eigen* is created with the mode "out". In *lsp_pretreatment* (shown as Listing 8), a dynamic graph variable *lp* is created with the mode "out", and another variable *eigen* is also created with the mode "in". In *bgmres_precond* (shown as Listing 9), a dynamic graph variable *lp* is also created with the mode "inout".

Listing 7 *ks_eigen Abstract Component* Implementation

```
<?xml version="1.0" encoding="utf-8"?>
<component type="abstract" name="ks_eigen_abstract"
description="Eigensolver">
... //defintion of other parameters
<param type="vector_complex" mode="out" name="eigenvalues" />
<param type="var_graph" mode="out" name="eigen" />
</component>
```

Implementation: three *Implementation* components are respetively constructed as Listing 10, 11 and 12 . We only give the logic inside each component to manage the dynamic graphs. In *ks_eigen*, a eigenvalue problem is solved by LAPACK functions. If enough eigenvalues are approximated, the dynamic graph variable will be set as "true", if not, it will be as "false". This variable is output into *lsp_pretreatment*. In *lsp_pretreatment*, if the input dynamic graph variable *eigen* is "true", Least Squares polynomial pretreatment operation is executed generate the array *lsparams*, and *lp* is set to be "true". The dynamic graph variable in *bgmres_precond* is *lp* input from *lsp_pretreatment*. If this variable is true, a new Least Squares preconditioning residual will be generated using *lsparams*.

© 2019 Tous droits réservés.

lilliad.univ-lille.fr

Thèse de Xinzhe Wu, Université de Lille, 2019

Listing 8 *lsp_pretreatment Abstract Component* Implementation

```
<?xml version="1.0" encoding="utf-8"?>
<component type="abstract" name="lsp_pretreatment_abstract"
description="Least Square Pretreatement">
... //defintion of other parameters
<param type="vector_complex" mode="in" name="eigenvalues" />
<param type="var_graph" mode="in" name="eigen" />
<param type="var_graph" mode="out" name="lp" />
<param type="vector_real" mode="out" name="lsparams" />
</component>
```

Listing 9 *bgmres_precond Abstract Component* Implementation

```
<?xml version="1.0" encoding="utf-8"?>
<component type="abstract" name="bgmres_precond_abstract"
description="Least Square Preconditioning">
... //defintion of other parameters
<param type="vector_real" mode="in" name="lsparams" />
<param type="var_graph" mode="in" name="lp" />
<param type="vector_complex" mode="inout" name="residual" />
</component>
```

9.3.2 Exiting Parallel Branch

The implementation of exiting parallel branch needs the optimization of scheduler. In this section, we propose novel implementation of YML scheduler and the related policies for different types of exiting parallel branch.

9.3.2.1 Different Types of Exiting Parallel Branch

In YML, it provides the parallel section and loop, which are able to define explicitly the sections and tasks to be executed in parallel. Inside m-UCGLE, the first level parallel sections are the different types of computational components, including BGMRES, s-KS, and B-LSP. For each parallel section, a number of tasks can be also executed in parallel, e.g., for a number of BGMRES components can be generated in parallel to solve the linear systems with a subset of RHSs, that is the second level of parallel sections inside m-UCGLE. Inside each second level task, a series sub-tasks are executed in sequence. For the example of restarted iterative methods with YML, a mechanism for checking the convergence should be established which allows the exiting of parallel section if some conditions are satisfied. In practice, different modes to exit a parallel branch are required, as shown by Fig. 9.5. Here we list these modes as below:

(1) the application may exit the parallel branch if all the running tasks are completed (shown as Fig. 9.5a), e.g., if there are several BGMRES components in parallel to solve linear

© 2019 Tous droits réservés.

lilliad.univ-lille.fr

Thèse de Xinzhe Wu, Université de Lille, 2019

Listing 10 *ks_eigen Implementation Component* Implementation

```
<?xml version="1.0" encoding="utf-8"?>
<component type="impl" name="ks_eigen_impl" description="Eigensolver">
<impl lang="CXX" libs="">
<header><![CDATA[ ]] ></header>
<source lang="CXX" libs="">
</source>
/*solving eigenvalue problem in sequence*/
eigen = false;
eigensolver(&eigenvalues);
if (enough eignevalues){
        eigen = true;
}
<footer></footer>
</impl>
</component>
```

systems, this parallel section should be exit if all the BGMRES component achieve the convergence;

(2) the application may exit the parallel branch if only one task among all are completed (shown as Fig. 9.5b), e.g., in the MERAM algorithm, several ERAM components are executed in parallel to approximate the eigenvalues of a matrix, if one of these components approximates enough eigenvalues, the whole parallel section should be exited;

(3) the application may exit the parallel branch if only several tasks among all are completed (shown as Fig. 9.5c);

(4) for the application with multi-level parallelism, we may decide to exit several levels of parallel branch, (shown as Fig. 9.5d, which has three levels of the parallel branch);

(5) the application may exit with saving selected data into the local filesystems, which will improve its fault tolerance and reusability, e.g., *lsparams* generated by the B-LSP Component could be saved into local, which will be used for solving the linear systems in future.

9.3.2.2 Optimization of YML Scheduler

In order to handle the mechanism to exit the parallel branch, a *exit* feature for YvetteML should be implemented to support the different modes of exiting a parallel branch:

(1) *exit(complete=all)*: all the running tasks of the level are finished before to exit;

(2) *exit(level=p,auto)*: we add to each abstract components if the task has to be finished, data saved or not, we exit the parallel branch (</exit finish = “yes” />) ;

© 2019 Tous droits réservés.

lilliad.univ-lille.fr

Thèse de Xinzhe Wu, Université de Lille, 2019

Listing 11 *lsp_pretreatment Implementation Component* Implementation

```
<?xml version="1.0" encoding="utf-8"?>
<component type="impl" name="lsp_pretreatment_impl" description="LSP">
<impl lang="CXX" libs="">
<header><![CDATA[ ]] ></header>
<source lang="CXX" libs="">
</source>
 lp = false;
/*generating Least Squares polynomial parameters if the eigenvalues available*/
if(eigen){
        LS_Pretreatement(eigenvalues, &lsparams);
        lp = true;
}
<footer></footer>
</impl>
</component>
```

(3) *exit(level=p)*: we exit p levels of parallelism (p loops if it is parallel loops);

(4) we can also add a "save_exit" type in the asbtract component for the selected parameter as <param type="real" mode="inout" name="A" save_exit="yes"/>. This parameter will be saved into local file before exiting the branch.

The different types defined above can be used together, which introduces the more flexible logic.

(1) *exit(complete=all, auto)*: all the running tasks of the level are finished before to exit, except the tasks defined with (</exit finish = “no” />);

(2) *exit(complete=all, level=p)*: we exit p levels of parallelism if all the tasks in this level are finished;

It is necessary to optimize the YML scheduler policies to support the *exit* grammar. Algorithm 37 gives the YML scheduler optimization. The scheduler algorithm is modified as shown by Algorithm 36. For each task in the parallel branch, its execution status is frequently updated to the scheduler. The scheduler make the decision according grammar and the newest status of these tasks in a same parallel branch. This generated exiting rule by the scheduler will be updated to all the tasks in the same parallel branch. Each task will be determined to exit or not according to this rule.

For the parallel branch with multiple BGMRES components, they will be exit when all the tasks in this parallel level are finished. For the s-KS and B-LSP components, their tasks will be exited if only all the BGMRES components are finished, and they also keep the eigenvalues and *lsparams* into local filesystems, respectively. We give the tentative graph implementation of m-UCGLE with the *exit* feature in Listing 13. In this implementation, for the second level of

© 2019 Tous droits réservés.

lilliad.univ-lille.fr

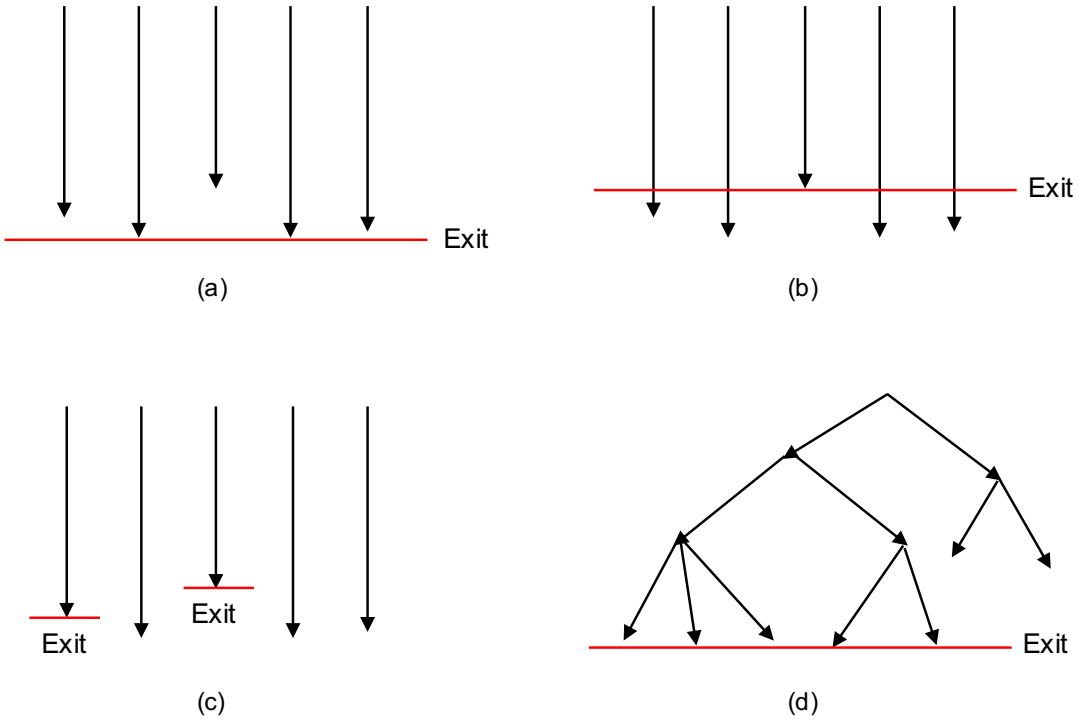

Figure 9.5 – Exiting Parallel Branch.

the parallel branch with various BGMRES components in execution at the same time, we add *exit(complete=all)*. This means that these BGMRES tasks should be exited until all the tasks are completed with all BGMRES components achieving the convergence.

For the tasks of B-LSP and *s*-KS components, they should be exited only if all the tasks of BGMRES Components are finished. Thus in the implementation of their *Abstract Components*, we add the parameter (</exit finish = "no">), which means these tasks need not be finished before exiting. In the *Abstract Components* of *ks_eigen*, the definition of the parameter *eigenvalues* is modified to be <param type="vector_complex" mode="out" name="eigenvalues" save_exit="yes"/>, which means that the approximated eigenvalues should be saved into local file before exiting. Similarly, the parameter *lsparams* should also be saved, and its definition is changed to be <param type="vector_real" mode="out" name="lsparams" save_exit="yes"/>. In order to exit the parallel branch of level 1 which express the parallel execution of BGMRES, B-LSP and *s*-KS, we add *exit(complete=all, auto)*. In this level of the parallel branch, the tasks will be executed until all the tasks are finished, except the tasks are defined with (</exit finish = "no">). Hence the logic is: if all the tasks in second level of the parallel branch of BGMRES are finished, they will exit this level of the branch. For the branch of first level, all the tasks completed means the finish of all tasks of BGMRES, thus, if all the BGMRES obtain the convergence, they will exit the level 2, and then immediately exit the level 1, and *m*-UCGLE is exit.

© 2019 Tous droits réservés.

lilliad.univ-lille.fr

Thèse de Xinzhe Wu, Université de Lille, 2019

Listing 12 *bgmres_precond Implementation Component* Implementation

```
<?xml version="1.0" encoding="utf-8"?>
<component type="impl" name="bgmres_precond_impl"
description="LSP Preconditioning">
<impl lang="CXX" libs="">
<header><![CDATA[ ]] ></header>
<source lang="CXX" libs="">
</source>
if(lp){
        /*updating Least Squares polynomial residual by lsparams*/
        residual=lspreconditioning(lsparams);
}
<footer></footer>
</impl>
</component>
```

9.4 Demand for MPI Correction Mechanism

For the multi-level parallel programming paradigm YML/XMP, it is necessary to investigate the application of scalable correctness checking methods to YML, XMP and selected features of MPI. This will result in a clear guideline how to limit the risk to introduce errors and how to best express the parallelism to catch errors that for principle reasons can only be detected at runtime, as well as extended and scalable correctness checking methods. MUST[2] is a good candidate which detects usage errors of the MPI and reports them to the user. As MPI calls are complex and usage errors common, this functionality is extremely helpful for application developers that want to develop correct MPI applications. To detect errors, MUST intercepts the MPI calls that are issued by the target application and evaluates their arguments. The two main usage scenarios for MUST arise during application development and when porting an existing application to a new system. When a developer adds new MPI communication calls, MUST can detect newly introduced errors, especially also some that may not manifest in an application crash. Further, before porting an application to a new system, MUST can detect violations to the MPI standard that might manifest on the target system. MUST reports errors in a log file that can be investigated once the execution of the target executable finishes. On the large-scale computing systems, it is necessary to use MUST as a tool to check all kinds of MPI errors during the whole life cycle of YML/XMP applications.

9.5 Conclusion

In this chapter, we investigate the prossibility to implement the iterative methods based on Unite and Conquer approach using the YML workflow runtime. There are two limitations of current implementation: 1) asynchronous communication between the computational components; 2)

2. https://tu-dresden.de/zih/forschung/projekte/must

© 2019 Tous droits réservés.

lilliad.univ-lille.fr

Thèse de Xinzhe Wu, Université de Lille, 2019

Algorithm 37 YML Scheduler Optimization

```
1: while status == EXECUTING do
2:     while task == finished do
3:         ++taskFinished
4:     end while
5:     UpdateStatus
6:     UpdateSchedulingRuleForExiting
7:     if SchedulingRuleForExiting == true then
8:         delete(task)
9:     end if
10:    UpdateStatus
11:    if status==ERROR then
12:        continue                    ▷ Task terminates with error, execution stopped
13:    end if
14:    UpdateSchedulingRule
15:    while (task = nextTaskReady) !=0 do
16:        ++taskSubmitted
17:        queue(task)
18:    end while
19:    if !SchedulingPendingTask then
20:        break                       ▷ Execution finished with error
21:    end if
22:    updateStatus
23: end while
24: finalizExecution
```

exit the parallel branch. We propose the solution by adding variable to handle the dynamic graphs, and optimize the scheduler rules to manage different modes of exiting parallel branches. These proposed solution should be embedded into YML in the future.

© 2019 Tous droits réservés.

lilliad.univ-lille.fr

Listing 13 Tentaive implememtation of m-UCGLE's graph

```
<?xml version="1.0" encoding="utf-8"?>
<application name="dyntest_app">
<description> m-UCGLE prototype </description>
<params></params>
<graph>
ngmres: = 3; neram: = 2;
par
do
        par(gid: = 0; ngmres-1)
        do
                compute bgmres_init(gid, ... );
                seq(g_restart: =0; max_restart_nb-1)
                do
                        compute bgmres_ar(gid, ... );
                        compute bgmres_ls(gid, ... );
                        compute bgmres_precond(gid, ... );
                        compute bgmres_check(gid, ... );
                        compute bgmres_restart(gid, ... );
                        exit(complete=all);
                enddo
        enddo
        endpar
        par(eid: = ngmres; ngmres+neram-1)
        do
                compute ks_init(eid, ... );
                seq(e_restart: =0; max_restart_nb-1)
                do
                        compute ks_ar(eid, ... );
                        compute ks_eigen(eid, ... );
                        compute ks_update(eid, ... );
                        compute ks_restart(eid, ... );
                enddo
        enddo
        endpar
        compute lsp_pretreatment(ngmres+neram, ... );
        exit(complete=all, auto);
enddo
endpar
</graph>
</application>
```

© 2019 Tous droits réservés.

Thèse de Xinzhe Wu, Université de Lille, 2019

Chapter 10

Conclusion and Perspective

10.1 Synthesis

The contributions of this thesis address several interconnected problems in the fields of HPC and the numerical iterative methods for linear systems and eigenvalue problems. This dissertation focuses on the proposition and analysis a distributed and parallel programming paradigm for smart hybrid Krylov methods targeting at the exascale computing.

In the first part, we gave the state-of-the-art of HPC, including the modern computing architectures for supercomputers and the parallel programming models. We also discussed the current challenges of HPC facing the coming of exascale supercomputers.

In the second part, we summarized Krylov iterative methods for the linear systems and eigenvalues problems. We introduced the algorithms of these methods and then analyze the relation between their convergence performance and the spectral information of the operator matrix. We presented different preconditioning techniques to accelerate the convergence of restarted iterative methods, including the preconditioning by matrix, deflation and a selected polynomial. We explained how to implement the iterative methods and their preconditioners in parallel on distributed memory supercomputers. We identified also the correlated goals for the research of parallel implementation of numerical methods facing the upcoming of exascale computing.

In the third part, the parallel implementation and evaluation of SMG2S were given. SMG2S can generate large-scale non-Hermitian test matrices using the user-defined spectrum and ensuring their eigenvalues as the given ones with high accuracy. SMG2S was implemented in parallel both on homogeneous and heterogeneous platforms with good scaling performance. SMG2S is released as an open source software to benchmark the numerical and parallel performance of iterative methods. The proposition of SMG2S was an essential factor for the continuation of my thesis on the evaluation of Krylov methods.

In the fourth part, we supplied the initial implementation of UCGLE and its manager engine based on the scientific libraries PETSc and SLEPc for both CPUs and GPUs. We described the implementation of components, the manager engine, and the distributed and parallel asynchronous communications. The selected parameters, the convergence, scalability and fault tolerance were evaluated on several supercomputers. We analyzed the impacts of spectral distributions on the convergence of UCGLE using different test matrices generated by SMG2S. UCGLE method was proved to be a good candidate for large-scale computing systems because

© 2019 Tous droits réservés.

lilliad.univ-lille.fr

Thèse de Xinzhe Wu, Université de Lille, 2019

of its asynchronous communication scheme, its multi-level parallelism, its reusability and fault tolerance, and its potential load balance. The multi-level parallelism of UCGLE can be flexibly mapped to large-scale distributed hierarchical platforms.

In the fifth part of this dissertation, we have extended UCGLE to solve a series of linear systems in sequence with different RHSs, and showed how to improve the acceleration for solving subsequent linear systems by recycling the dominant eigenvalues. This extension of UCGLE recycles the eigenvalues obtained in solving previous systems, improves them on the fly and constructs a new initial guess vector for subsequent linear systems. Numerical experiments using different test matrices indicated a substantial decrease in both computation time and iteration steps.

In the sixth part, we revisited the implementation of UCGLE and proposed a new variant to solve simultaneously linear systems with multiple RHSs, that is m-UCGLE. It was implemented with a newly designed manager engine, which can allocate various GMRES components at the same time. The Solver Component was implemented with block GMRES algorithm, which was intended to solve the linear systems with a subset of RHSs. A mathematical extension of Least Squares polynomial was also proposed for the linear systems with multiple RHSs. m-UCGLE was implemented with the packages Belos and Anasazi packages of Trilinos. Its implementation on multi-GPUs was boosted by Kokkos. The experiments on supercomputers proved its good numerical and parallel performance.

In the seventh part, we proposed an adaptive scheme for the selection of the applied times of Least Squares polynomial preconditioning for each restarting, which is one of the most critical parameters for the Least Squares polynomial preconditioning inside UCGLE.

In the last part, we investigated the possibility of UCGLE using the workflow programming environment YML. Two limitations of the actual version of YML were found; 1) it does not support the special asynchronous communications between different computation tasks; 2) the lack of a mechanism to check the convergence of iterative methods. We propose the solution by adding a variable to handle the dynamic graphs and optimize the scheduler rules to manage different modes of exiting parallel branches.

10.2 Future Research

The initial goals of the thesis have been completed, but there are still a lot of problems that should be further explored for the current work.

Since the GPU version of SMG2S was implemented with the data structures and functions provided by PETSc, a specific optimized version for GPUs could be implemented based on CUDA and packaged into the open source software SMG2S in the future.

With the help of SMG2S, the relationship between different existing hybrid and deflated iterative methods and preconditioners for solving non-Hermitian linear systems and the spectral information of operator matrices can be investigated. This work will guide users to select suitable iterative methods according to their applications from the real world.

For UCGLE, a new version should be developed for the case that some eigenvalues of the operator matrix have the positive real part, and the others have the negative part. The possible solution is to construct to two Least Squares polynomials using two polygons built by the

© 2019 Tous droits réservés.

lilliad.univ-lille.fr

Thèse de Xinzhe Wu, Université de Lille, 2019

eigenvalues either with the all positive or negative real part, separately. This modification can exclude the origin point and might accelerate the convergence of this kind of spectral distribution.

YML, including its grammar and the scheduler policies, should be re-developed to support the implementation of Unite and Conquer approach, then the performance of UCGLE implemented based on workflow can be evaluated. An autotuning scheme can be provided for adaptive selections of all the complicated parameters of UCGLE at runtime.

Finally, the implementation of UCGLE with distributed and parallel programming paradigm is only the beginning of a long adventure. It is necessary to test the Unite and Conquer methods on the upcoming exascale machines with much more computing units. More deflated or hybrid methods can also be transformed into the Unite and Conquer scheme, and implemented with a distributed and parallel manner. Further research should study both the numerical and parallel performance of other iterative methods with Unite and Conquer scheme.

© 2019 Tous droits réservés.

lilliad.univ-lille.fr

© 2019 Tous droits réservés.

lilliad.univ-lille.fr

Bibliography

[1] Abdou M Abdel-Rehim, Ronald B Morgan, and Walter Wilcox. Improved seed methods for symmetric positive definite linear equations with multiple right-hand sides. Numerical Linear Algebra with Applications, 21(3):453–471, 2014.

[2] Nabil FT Abubaker, Kadir Akbudak, and Cevdet Aykanat. Spatiotemporal graph and hypergraph partitioning models for sparse matrix-vector multiplication on many-core architectures. IEEE Transactions on Parallel and Distributed Systems, 2018.

[3] Loyce Adams and J Ortega. A multi-color sor method for parallel computation. In ICPP, pages 53–56. Citeseer, 1982.

[4] Emmanuel Agullo, Luc Giraud, and Y-F Jing. Block gmres method with inexact breakdowns and deflated restarting. SIAM Journal on Matrix Analysis and Applications, 35(4): 1625–1651, 2014.

[5] José I Aliaga, Hartwig Anzt, Maribel Castillo, Juan C Fernández, Germán León, Joaquín Pérez, and Enrique S Quintana-Ortí. Unveiling the performance-energy trade-off in iterative linear system solvers for multithreaded processors. Concurrency and Computation: Practice and Experience, 27(4):885–904, 2015.

[6] Heng-Bin An and Zhong-Zhi Bai. A globally convergent newton-gmres method for large sparse systems of nonlinear equations. Applied Numerical Mathematics, 57(3):235–252, 2007.

[7] Gabriel Antoniu, Taisuke Boku, Christophe Calvin, Philippe Codognet, Michel Dayde, Nahid Emad, Yuyaka Ishikawa, Satoshi Matsuoka, Kengo Nakajima, Hiroshi Nakashima, et al. Towards exascale with the anr-jst japanese-french project fp3c (framework and programming for post-petascale computing). In 9th International Conference on Computer Science and Information Technologies, 2013.

[8] Hartwig Anzt, Stanimire Tomov, and Jack Dongarra. Energy efficiency and performance frontiers for sparse computations on gpu supercomputers. In Proceedings of the sixth international workshop on programming models and applications for multicores and manycores, pages 1–10. ACM, 2015.

[9] Hartwig Anzt, Jack Dongarra, Goran Flegar, and Enrique S Quintana-Ortí. Batched gauss-jordan elimination for block-jacobi preconditioner generation on gpus. In Proceedings of

© 2019 Tous droits réservés.

lilliad.univ-lille.fr

the 8th International Workshop on Programming Models and Applications for Multicores and Manycores, pages 1–10. ACM, 2017.

[10] Pierre-Yves Aquilanti. Méthodes de Krylov réparties et massivement parallèles pour la résolution de problèmes de Géoscience sur machines hétérogeènes dépassant le pétaflop. PhD thesis, Université Lille 1, 2011.

[11] Pierre-Yves Aquilanti, Serge Petiton, and Henri Calandra. Parallel auto-tuned gmres method to solve complex non-hermitian linear systems. In Workshop iWapt10, VECPAR10 Conference, USA, 2010.

[12] Pierre-Yves Aquilanti, Serge Petiton, and Henri Calandra. Parallel gmres incomplete orthogonalization auto-tuning. Procedia Computer Science, 4:2246–2256, 2011.

[13] Walter Edwin Arnoldi. The principle of minimized iterations in the solution of the matrix eigenvalue problem. Quarterly of applied mathematics, 9(1):17–29, 1951.

[14] SR Arridge, M Schweiger, M Hiraoka, and DT Delpy. A finite element approach for modeling photon transport in tissue. Medical physics, 20(2):299–309, 1993.

[15] Arash Ashari, Naser Sedaghati, John Eisenlohr, and P Sadayappan. An efficient two-dimensional blocking strategy for sparse matrix-vector multiplication on gpus. In Proceedings of the 28th ACM international conference on Supercomputing, pages 273–282. ACM, 2014.

[16] Thomas J Ashby, Pieter Ghysels, Wim Heirman, and Wim Vanroose. The impact of global communication latency at extreme scales on krylov methods. In International Conference on Algorithms and Architectures for Parallel Processing, pages 428–442. Springer, 2012.

[17] Cédric Augonnet, Samuel Thibault, Raymond Namyst, and Pierre-André Wacrenier. Starpu: a unified platform for task scheduling on heterogeneous multicore architectures. Concurrency and Computation: Practice and Experience, 23(2):187–198, 2011.

[18] Owe Axelsson. A generalized ssor method. BIT Numerical Mathematics, 12(4):443–467, 1972.

[19] Zhaojun Bai, David Day, James Demmel, and Jack Dongarra. A test matrix collection for non-hermitian eigenvalue problems. Prof. Z. Bai, Dept. of Mathematics, 751:40506–0027, 1996.

[20] Chris G Baker, Ulrich L Hetmaniuk, Richard B Lehoucq, and Heidi K Thornquist. Anasazi software for the numerical solution of large-scale eigenvalue problems. ACM Transactions on Mathematical Software (TOMS), 36(3):13, 2009.

[21] Christopher G Baker and Michael A Heroux. Tpetra, and the use of generic programming in scientific computing. Scientific Programming, 20(2):115–128, 2012.

[22] Prasanna Balaprakash, Jack Dongarra, Todd Gamblin, Mary Hall, Jeffrey K Hollingsworth, Boyana Norris, and Richard Vuduc. Autotuning in high-performance computing applications. Proceedings of the IEEE, (99):1–16, 2018.

© 2019 Tous droits réservés.

lilliad.univ-lille.fr

[23] Jairo Balart, Alejandro Duran, Marc Gonzàlez, Xavier Martorell, Eduard Ayguadé, and Jesús Labarta. Nanos mercurium: a research compiler for openmp. In Proceedings of the European Workshop on OpenMP, volume 8, page 56, 2004.

[24] Satish Balay, Kris Buschelman, William D Gropp, Dinesh Kaushik, Matthew G Knepley, L Curfman McInnes, Barry F Smith, and Hong Zhang. Petsc web page, 2001.

[25] Satish Balay, Shrirang Abhyankar, M Adams, Peter Brune, Kris Buschelman, L Dalcin, W Gropp, Barry Smith, D Karpeyev, Dinesh Kaushik, et al. Petsc users manual revision 3.7. Technical report, Argonne National Lab.(ANL), Argonne, IL (United States), 2016.

[26] Satish Balay, Shrirang Abhyankar, Mark F. Adams, Jed Brown, Peter Brune, Kris Buschelman, Lisandro Dalcin, Victor Eijkhout, William D. Gropp, Dinesh Kaushik, Matthew G. Knepley, Lois Curfman McInnes, Karl Rupp, Barry F. Smith, Stefano Zampini, Hong Zhang, and Hong Zhang. PETSc users manual. Technical Report ANL-95/11 - Revision 3.7, Argonne National Laboratory, 2016. URL http://www.mcs.anl.gov/petsc.

[27] Randolph E Bank, Todd F Dupont, and Harry Yserentant. The hierarchical basis multigrid method. Numerische Mathematik, 52(4):427–458, 1988.

[28] Gianluca Barbella, Federico Perotti, and V Simoncini. Block krylov subspace methods for the computation of structural response to turbulent wind. Computer Methods in Applied Mechanics and Engineering, 200(23-24):2067–2082, 2011.

[29] Achim Basermann. Qmr and tfqmr methods for sparse nonsymmetric problems on massively parallel systems. In AMS-SIAM Summer Seminar in Applied Mathematics, number FZJ-2014-04512. Zentralinstitut für Angewandte Mathematik, 1996.

[30] João Pedro A Bastos and Nelson Sadowski. Electromagnetic modeling by finite element methods. CRC press, 2003.

[31] Eric Bavier, Mark Hoemmen, Sivasankaran Rajamanickam, and Heidi Thornquist. Amesos2 and belos: Direct and iterative solvers for large sparse linear systems. Scientific Programming, 20(3):241–255, 2012.

[32] Nathan Bell and Michael Garland. Efficient sparse matrix-vector multiplication on cuda. Technical report, Nvidia Technical Report NVR-2008-004, Nvidia Corporation, 2008.

[33] Nathan Bell and Michael Garland. Implementing sparse matrix-vector multiplication on throughput-oriented processors. In Proceedings of the conference on high performance computing networking, storage and analysis, page 18. ACM, 2009.

[34] Stefania Bellavia and Benedetta Morini. A globally convergent newton-gmres subspace method for systems of nonlinear equations. SIAM Journal on Scientific Computing, 23(3): 940–960, 2001.

[35] James Bergstra, Nicolas Pinto, and David Cox. Machine learning for predictive auto-tuning with boosted regression trees. In Innovative Parallel Computing (InPar), 2012, pages 1–9. IEEE, 2012.

© 2019 Tous droits réservés.

lilliad.univ-lille.fr

[36] Pietro Berkes. Handwritten digit recognition with nonlinear fisher discriminant analysis. In Proceedings of the 15th international conference on Artificial neural networks: formal models and their applications-Volume Part II, pages 285–287. Springer-Verlag, 2005.

[37] France Boillod-Cerneux. Nouveaux algorithmes numériques pour l'utilisation efficace des architectures de calcul multi-coeurs et hétérogènes. PhD thesis, Université Lille 1, 2014.

[38] France Boillod-Cerneux, Serge Petition, Christophe Calvin, and Dubois Jérôme. Toward smart-tuned asynchronous krylov eigenvalue computing with multi-restarted strategies. In Parallel Matrix Algorithms and Applications (PMAA), London, UK, 2012.

[39] France Boillod-Cerneux, Serge Petition, Christophe Calvin, and Leroy Drummond. Toward restarting strategies tuning for krylov solver. In the 9th International Workshop on Automatic Performance Tuning, USA, 2014.

[40] Ronald F Boisvert, Roldan Pozo, Karin Remington, Richard F Barrett, and Jack J Dongarra. Matrix market: a web resource for test matrix collections. In Quality of Numerical Software, pages 125–137. Springer, 1997.

[41] George Bosilca, Aurelien Bouteiller, Anthony Danalis, Thomas Herault, Pierre Lemarinier, and Jack Dongarra. Dague: A generic distributed dag engine for high performance computing. Parallel Computing, 38(1-2):37–51, 2012.

[42] Achi Brandt. Algebraic multigrid theory: The symmetric case. Applied mathematics and computation, 19(1-4):23–56, 1986.

[43] Marian Brezina, Andrew J Cleary, Robert D Falgout, Van Enden Henson, Jim E Jones, Thomas A Manteuffel, Stephen F McCormick, and John W Ruge. Algebraic multigrid based on element interpolation (amge). SIAM Journal on Scientific Computing, 22(5): 1570–1592, 2001.

[44] Claude Brezinski and M Redivo-Zaglia. Hybrid procedures for solving linear systems. Numerische Mathematik, 67(1):1–19, 1994.

[45] Peter N Brown and Youcef Saad. Hybrid krylov methods for nonlinear systems of equations. SIAM Journal on Scientific and Statistical Computing, 11(3):450–481, 1990.

[46] Annalisa Buffa, Patrick Ciarlet, and Erell Jamelot. Solving electromagnetic eigenvalue problems in polyhedral domains with nodal finite elements. Numerische Mathematik, 113 (4):497–518, 2009.

[47] Kevin Burrage, Jocelyne Erhel, Bert Pohl, and Alan Williams. A deflation technique for linear systems of equations. SIAM Journal on Scientific Computing, 19(4):1245–1260, 1998.

[48] Xiao-Chuan Cai and Marcus Sarkis. A restricted additive schwarz preconditioner for general sparse linear systems. Siam journal on scientific computing, 21(2):792–797, 1999.

© 2019 Tous droits réservés.

lilliad.univ-lille.fr

[49] Carmen Campos and Jose E Roman. Strategies for spectrum slicing based on restarted lanczos methods. Numerical Algorithms, 60(2):279–295, 2012.

[50] Erin Claire Carson. Communication-avoiding Krylov subspace methods in theory and practice. PhD thesis, UC Berkeley, 2015.

[51] Umit V Catalyurek and Cevdet Aykanat. Hypergraph-partitioning based decomposition for parallel sparse-matrix vector multiplication. IEEE Transactions on parallel and distributed systems, 10(7):673–693, 1999.

[52] Andrew Chapman and Yousef Saad. Deflated and augmented krylov subspace techniques. Numerical linear algebra with applications, 4(1):43–66, 1997.

[53] Chun Chen. Model-guided empirical optimization for memory hierarchy. University of Southern California, 2007.

[54] Langshi Chen, Serge G Petiton, Leroy A Drummond, and Maxime Hugues. A communication optimization scheme for basis computation of krylov subspace methods on multi-gpus. In International Conference on High Performance Computing for Computational Science, pages 3–16. Springer, 2014.

[55] Wei Chen, Sam Toueg, and Marcos Kawazoe Aguilera. On the quality of service of failure detectors. IEEE Transactions on computers, 51(5):561–580, 2002.

[56] Xiaojun Chen, Carolin Birk, and Chongmin Song. Transient analysis of wave propagation in layered soil by using the scaled boundary finite element method. Computers and Geotechnics, 63:1–12, 2015.

[57] Matthias Christen, Olaf Schenk, and Helmar Burkhart. Patus: A code generation and autotuning framework for parallel iterative stencil computations on modern microarchitectures. In Parallel & Distributed Processing Symposium (IPDPS), 2011 IEEE International, pages 676–687. IEEE, 2011.

[58] Hakan Ciftci, Richard L Hall, and Nasser Saad. Asymptotic iteration method for eigenvalue problems. Journal of Physics A: Mathematical and General, 36(47):11807, 2003.

[59] Alexander Collins, Christian Fensch, Hugh Leather, and Murray Cole. Masif: machine learning guided auto-tuning of parallel skeletons. In 20th Annual International Conference on High Performance Computing, pages 186–195. IEEE, 2013.

[60] Siegfried Cools and Wim Vanroose. The communication-hiding pipelined bicgstab method for the parallel solution of large unsymmetric linear systems. Parallel Computing, 65:1–20, 2017.

[61] Christophe Croux and Gentiane Haesbroeck. Principal component analysis based on robust estimators of the covariance or correlation matrix: influence functions and efficiencies. Biometrika, 87(3):603–618, 2000.

© 2019 Tous droits réservés.

lilliad.univ-lille.fr

[62] Leonardo Dagum and Ramesh Menon. Openmp: an industry standard api for shared-memory programming. IEEE computational science and engineering, 5(1):46–55, 1998.

[63] Timothy A Davis and Yifan Hu. The university of florida sparse matrix collection. ACM Transactions on Mathematical Software (TOMS), 38(1):1, 2011.

[64] David Day and Michael A Heroux. Solving complex-valued linear systems via equivalent real formulations. SIAM Journal on Scientific Computing, 23(2):480–498, 2001.

[65] Michel J Dayde and Iain S Duff. The use of computational kernels in full and sparse linear solvers, efficient code design on high-performance risc processors. In International Conference on Vector and Parallel Processing, pages 108–139. Springer, 1996.

[66] Michel J Daydé and Iain S Duff. The risc blas: A blocked implementation of level 3 blas for risc processors. ACM Transactions on Mathematical Software (TOMS), 25(3):316–340, 1999.

[67] Eric de Sturler. Nested krylov methods based on gcr. Journal of Computational and Applied Mathematics, 67(1):15–41, 1996.

[68] Eric De Sturler. Truncation strategies for optimal krylov subspace methods. SIAM Journal on Numerical Analysis, 36(3):864–889, 1999.

[69] Olivier Delannoy. YML: un workflow scientifique pour le calcul haute performance. PhD thesis, Université de Versailles Saint-Quentin, France, 2008.

[70] Olivier Delannoy and Serge Petiton. Block linear algebra on the peer to peer xtremweb/yml plateform. In SIAM conference on Computational Science and Engineering, USA, 2003.

[71] Olivier Delannoy and Serge Petiton. A peer to peer computing framework; design and performance evaluation of yml. In HeteroPar 2004, Irland, 2004.

[72] Olivier Delannoy, Nahid Emad, and Serge Petiton. Workflow global computing with yml. In Proceedings of the 7th IEEE/ACM International Conference on Grid Computing, pages 25–32. IEEE Computer Society, 2006.

[73] James Demmel and Alan McKenney. A test matrix generation suite. In Courant Institute of Mathematical Sciences. Citeseer, 1989.

[74] Jack Dongarra, Jeffrey Hittinger, John Bell, Luis Chacon, Robert Falgout, Michael Heroux, Paul Hovland, Esmond Ng, Clayton Webster, and Stefan Wild. Applied mathematics research for exascale computing. Technical report, Lawrence Livermore National Laboratory (LLNL), Livermore, CA, 2014.

[75] Jack Dongarra, Michael A Heroux, and Piotr Luszczek. Hpcg benchmark: a new metric for ranking high performance computing systems. Knoxville, Tennessee, 2015.

[76] Jack J Dongarra, Piotr Luszczek, and Antoine Petitet. The linpack benchmark: past, present and future. Concurrency and Computation: practice and experience, 15(9):803–820, 2003.

© 2019 Tous droits réservés.

lilliad.univ-lille.fr

[77] IS Duff, RG Grimes, and JG Lewis. Users' guide for the hawell–boeing sparse matrix collection. Technical report, Technical Report RAL-92-086, Rutherford Applton Laboratory, Chilton, UK, 1992.

[78] Alejandro Duran, Eduard Ayguadé, Rosa M Badia, Jesús Labarta, Luis Martinell, Xavier Martorell, and Judit Planas. Ompss: a proposal for programming heterogeneous multi-core architectures. Parallel Processing Letters, 21(02):173–193, 2011.

[79] Guy Edjlali, Nahid Emad, and Serge Petiton. Hybrid methods on network of heterogeneous parallel computers. In Proceedings of the 14th IMACS World Congress, Atlanta, USA, 1994.

[80] Guy Edjlali, Serge Petiton, and Nahid Emad. Interleaved parallel hybrid arnoldi method for a parallel machine and a network of workstations. In Conference on Information, Systems, Analysis and Synthesis (ISAS'96), pages 22–26, 1996.

[81] H Carter Edwards, Christian R Trott, and Daniel Sunderland. Kokkos: Enabling manycore performance portability through polymorphic memory access patterns. Journal of Parallel and Distributed Computing, 74(12):3202–3216, 2014.

[82] Howard C Elman, Youcef Saad, and Paul E Saylor. A hybrid chebyshev krylov subspace algorithm for solving nonsymmetric systems of linear equations. SIAM Journal on Scientific and Statistical Computing, 7(3):840–855, 1986.

[83] Nahid Emad and Serge Petiton. Unite and conquer approach for high scale numerical computing. Journal of Computational Science, 14:5–14, 2016.

[84] Nahid Emad, Serge Petiton, and Guy Edjlali. Multiple explicitly restarted arnoldi method for solving large eigenproblems. SIAM Journal on Scientific Computing, 27(1):253–277, 2005.

[85] Jocelyne Erhel, Kevin Burrage, and Bert Pohl. Restarted gmres preconditioned by deflation. Journal of computational and applied mathematics, 69(2):303–318, 1996.

[86] Azeddine Essai, Guy Bergére, and Serge G Petiton. Heterogeneous parallel hybrid gmres/ls-arnoldi method. In PPSC, 1999.

[87] Michael Feldman. Top500 cea to deploy arm-powered supercomputer, 2018. URL https://www.top500.org/news/cea-to-deploy-arm-powered-supercomputer/.

[88] Michael Feldman. Top500 fujitsu completes prototype of arm processor that will power excascale supercomputer, 2018.

[89] Alexandre Fender, Nahid Emad, Serge Petiton, and Maxim Naumov. Parallel modularity clustering. Procedia Computer Science, 108:1793–1802, 2017.

[90] Fabio Guilherme Ferraz and José Maria C Dos Santos. Block-krylov component synthesis and minimum rank perturbation theory for damage detection in complex structures. Proceeding of the IX DINAME, Florianópolis-SC-Brazil, pages 329–334, 2001.

© 2019 Tous droits réservés.

lilliad.univ-lille.fr

[91] Peter Fiebach, Andreas Frommer, and Roland Freund. Variants of the block-qmr method and applications in quantum chromodynamics. In 15th IMACS World Congress on Scientific Computation, Modelling and Applied Mathematics, volume 3, pages 491–496, 1997.

[92] Alexander J Flueck and Hsiao-Dong Chiang. Solving the nonlinear power flow equations with an inexact newton method using gmres. IEEE Transactions on Power Systems, 13 (2):267–273, 1998.

[93] Valérie Frayssé, Luc Giraud, and Serge Gratton. Algorithm 881: A set of flexible gmres routines for real and complex arithmetics on high-performance computers. ACM Transactions on Mathematical Software (TOMS), 35(2):13, 2008.

[94] Roland W Freund and Noël M Nachtigal. Qmr: a quasi-minimal residual method for non-hermitian linear systems. Numerische mathematik, 60(1):315–339, 1991.

[95] Haohuan Fu, Junfeng Liao, Jinzhe Yang, Lanning Wang, Zhenya Song, Xiaomeng Huang, Chao Yang, Wei Xue, Fangfang Liu, Fangli Qiao, et al. The sunway taihulight supercomputer: system and applications. Science China Information Sciences, 59(7):072001, 2016.

[96] Seiji Fujino and Kosuke Iwasato. An estimation of single-synchronized krylov subspace methods with hybrid parallelization. In Proceedings of the World Congress on Engineering, volume 1, 2015.

[97] Kohei Fujita, Keisuke Katsushima, Tsuyoshi Ichimura, Masashi Horikoshi, Kengo Nakajima, Muneo Hori, and Lalith Maddegedara. Wave propagation simulation of complex multi-material problems with fast low-order unstructured finite-element meshing and analysis. In Proceedings of the International Conference on High Performance Computing in Asia-Pacific Region, HPC Asia 2018, pages 24–35, New York, NY, USA, 2018. ACM. ISBN 978-1-4503-5372-4. doi: 10.1145/3149457.3149474. URL http://doi.acm.org/10.1145/3149457.3149474.

[98] Hervé Galicher, France Boillod-Cerneux, Serge Petiton, and Christophe Calvin. Generate very large sparse matrices starting from a given spectrum. in lecture notes in computer science, 8969, springer (2014).

[99] André Gaul, Martin H Gutknecht, Jorg Liesen, and Reinhard Nabben. A framework for deflated and augmented krylov subspace methods. SIAM Journal on Matrix Analysis and Applications, 34(2):495–518, 2013.

[100] Pieter Ghysels and Wim Vanroose. Hiding global synchronization latency in the preconditioned conjugate gradient algorithm. Parallel Computing, 40(7):224–238, 2014.

[101] Pieter Ghysels, Thomas J Ashby, Karl Meerbergen, and Wim Vanroose. Hiding global communication latency in the gmres algorithm on massively parallel machines. SIAM Journal on Scientific Computing, 35(1):C48–C71, 2013.

© 2019 Tous droits réservés.

lilliad.univ-lille.fr

[102] Luc Giraud, Serge Gratton, Xavier Pinel, and Xavier Vasseur. Flexible gmres with deflated restarting. SIAM Journal on Scientific Computing, 32(4):1858–1878, 2010.

[103] Andrew Grimshaw, W Wulf, J French, A Weaver, and Paul F Reynolds Jr. A synopsis of the legion project. Technical report, Technical Report CS-94-20, Department of Computer Science, University of Virginia, 1994.

[104] William D Gropp, William Gropp, Ewing Lusk, Anthony Skjellum, and Argonne Distinguished Fellow Emeritus Ewing Lusk. Using MPI: portable parallel programming with the message-passing interface, volume 1. MIT press, 1999.

[105] Gui-Ding Gu. A seed method for solving nonsymmetric linear systems with multiple right-hand sides. International journal of computer mathematics, 79(3):307–326, 2002.

[106] Arne S Gullerud and Robert H Dodds Jr. Mpi-based implementation of a pcg solver using an ebe architecture and preconditioner for implicit, 3-d finite element analysis. Computers & Structures, 79(5):553–575, 2001.

[107] Martin H Gutknecht. Block krylov space methods for linear systems with multiple right-hand sides: an introduction. 2006.

[108] Azzam Haidar, Stanimire Tomov, Jack Dongarra, and Nicholas J Higham. Harnessing gpu tensor cores for fast fp16 arithmetic to speed up mixed-precision iterative refinement solvers. In Harnessing GPU Tensor Cores for Fast FP16 Arithmetic to Speed up Mixed-Precision Iterative Refinement Solvers, page 0. IEEE, 2018.

[109] Haiwu He, Guy Bergère, and Serge Petiton. A hybrid gmres/ls-arnoldi method to accelerate the parallel solution of linear systems. Computers & Mathematics with Applications, 51(11):1647–1662, 2006.

[110] V Hernandez, JE Roman, A Tomas, and V Vidal. Single vector iteration methods in slepc. Scalable Library for Eigenvalue Problem Computations, 2005.

[111] Vicente Hernandez, Jose E Roman, and Vicente Vidal. Slepc: A scalable and flexible toolkit for the solution of eigenvalue problems. ACM Transactions on Mathematical Software (TOMS), 31(3):351–362, 2005.

[112] Michael A Heroux. Epetra performance optimization guide. Sandia National Laboratories, Tech. Rep. SAND2005-1668, 2005.

[113] Michael A Heroux, Roscoe A Bartlett, Vicki E Howle, Robert J Hoekstra, Jonathan J Hu, Tamara G Kolda, Richard B Lehoucq, Kevin R Long, Roger P Pawlowski, Eric T Phipps, et al. An overview of the trilinos project. ACM Transactions on Mathematical Software (TOMS), 31(3):397–423, 2005.

[114] Michael Allen Heroux. Aztecoo user guide. Technical report, Sandia National Laboratories, 2004.

© 2019 Tous droits réservés.

lilliad.univ-lille.fr

[115] Ralf Hiptmair. Multigrid method for maxwell's equations. SIAM Journal on Numerical Analysis, 36(1):204–225, 1998.

[116] Mark Hoemmen. Communication-avoiding Krylov subspace methods. University of California, Berkeley, 2010.

[117] BR Hutchinson and GD Raithby. A multigrid method based on the additive correction strategy. Numerical Heat Transfer, Part A: Applications, 9(5):511–537, 1986.

[118] Pierre Jolivet and Pierre-Henri Tournier. Block iterative methods and recycling for improved scalability of linear solvers. In SC16-International Conference for High Performance Computing, Networking, Storage and Analysis, 2016.

[119] W Kahan. The rate of convergence of the extrapolated gauss-seidel iteration, presented at the conference on matrix computations, wayne state university, september 4, 1957. t. w. kahan. Gauss-Seidel methods of solving large systems of linear equations, 1958.

[120] M Ozan Karsavuran, Kadir Akbudak, and Cevdet Aykanat. Locality-aware parallel sparse matrix-vector and matrix-transpose-vector multiplication on many-core processors. IEEE Transactions on Parallel & Distributed Systems, (1):1–1, 2016.

[121] Takahiro Katagiri, Pierre-Yves Aquilanti, and Serge Petiton. A smart tuning strategy for restart frequency of gmres (m) with hierarchical cache sizes. In International Conference on High Performance Computing for Computational Science, pages 314–328. Springer, 2012.

[122] Serge A Kharchenko and A Yu. Yeremin. Eigenvalue translation based preconditioners for the gmres (k) method. Numerical linear algebra with applications, 2(1):51–77, 1995.

[123] Misha E Kilmer and Eric De Sturler. Recycling subspace information for diffuse optical tomography. SIAM Journal on Scientific Computing, 27(6):2140–2166, 2006.

[124] Rex B Kline. Principles and practice of structural equation modeling. Guilford publications, 2015.

[125] Dana A Knoll and David E Keyes. Jacobian-free newton–krylov methods: a survey of approaches and applications. Journal of Computational Physics, 193(2):357–397, 2004.

[126] Tomonori Kouya. A highly efficient implementation of multiple precision sparse matrix-vector multiplication and its application to product-type krylov subspace methods. arXiv preprint arXiv:1411.2377, 2014.

[127] Moritz Kreutzer, Georg Hager, Gerhard Wellein, Holger Fehske, and Alan R Bishop. A unified sparse matrix data format for efficient general sparse matrix-vector multiplication on modern processors with wide simd units. SIAM Journal on Scientific Computing, 36 (5):C401–C423, 2014.

[128] Takuro Kutsukake and Takashi Nodera. The deflated flexible gmres with an approximate inverse preconditioner. 2015.

© 2019 Tous droits réservés.

lilliad.univ-lille.fr

[129] L Lasdon, S Mitter, and A Waren. The conjugate gradient method for optimal control problems. IEEE Transactions on Automatic Control, 12(2):132–138, 1967.

[130] Jeonghwa Lee, Jun Zhang, and Cai-Cheng Lu. Incomplete lu preconditioning for large scale dense complex linear systems from electromagnetic wave scattering problems. Journal of Computational Physics, 185(1):158–175, 2003.

[131] Jinpil Lee and Mitsuhisa Sato. Implementation and performance evaluation of xcalablemp: A parallel programming language for distributed memory systems. In Parallel Processing Workshops (ICPPW), 2010 39th International Conference on, pages 413–420. IEEE, 2010.

[132] Koung Hee Leem, Suely Oliveira, and DE Stewart. Algebraic multigrid (amg) for saddle point systems from meshfree discretizations. Numerical linear algebra with applications, 11(2-3):293–308, 2004.

[133] Jörg Liesen and Zdenek Strakos. Krylov subspace methods: principles and analysis. Oxford University Press, 2013.

[134] Jörg Liesen and Petr Tichỳ. Convergence analysis of krylov subspace methods. GAMM-Mitteilungen, 27(2):153–173, 2004.

[135] Na Liu, Luis Eduardo Tobón, Yanmin Zhao, Yifa Tang, and Qing Huo Liu. Mixed spectral-element method for 3-d maxwell's eigenvalue problem. IEEE Transactions on Microwave Theory and Techniques, 63(2):317–325, 2015.

[136] Weifeng Liu and Brian Vinter. Csr5: An efficient storage format for cross-platform sparse matrix-vector multiplication. In Proceedings of the 29th ACM on International Conference on Supercomputing, pages 339–350. ACM, 2015.

[137] Yuxin Liu, Abdelkrim Talbi, Bahram Djafari-Rouhani, Lucie Drbohlavová, Vincent Mortet, El Houssaine El Boudouti, Olivier Bou Matar, and Philippe Pernod. Interaction of love waves with coupled cavity modes in a 2d holey phononic crystal. arXiv preprint arXiv:1811.03922, 2018.

[138] Yuxin Liu, Abdelkrim Talbi, Philippe Pernod, and Olivier Bou Matar. Highly confined love waves modes by defect states in a holey sio 2/quartz phononic crystal. Journal of Applied Physics, 124(14):145102, 2018.

[139] L Maio, V Memmolo, F Ricci, ND Boffa, E Monaco, and R Pecora. Ultrasonic wave propagation in composite laminates by numerical simulation. Composite Structures, 121: 64–74, 2015.

[140] Tahir Malas and Levent Gürel. Incomplete lu preconditioning with the multilevel fast multipole algorithm for electromagnetic scattering. SIAM Journal on Scientific Computing, 29(4):1476–1494, 2007.

[141] Manish Malhotra, Roland W Freund, and Peter M Pinsky. Iterative solution of multiple radiation and scattering problems in structural acoustics using a block quasi-minimal

© 2019 Tous droits réservés.

lilliad.univ-lille.fr

residual algorithm. Computer methods in applied mechanics and engineering, 146(1-2): 173–196, 1997.

[142] Thomas A Manteuffel. The tchebychev iteration for nonsymmetric linear systems. Numerische Mathematik, 28(3):307–327, 1977.

[143] Christopher M Maynard and David N Walters. Precision of the endgame: Mixed-precision arithmetic in the iterative solver of the unified model. arXiv preprint arXiv:1811.03852, 2018.

[144] Duane Merrill and Michael Garland. Merge-based sparse matrix-vector multiplication (spmv) using the csr storage format. In ACM SIGPLAN Notices, volume 51, page 43. ACM, 2016.

[145] Takeshi Mifune, Takeshi Iwashita, and Masaaki Shimasaki. New algebraic multigrid preconditioning for iterative solvers in electromagnetic finite edge-element analyses. IEEE transactions on magnetics, 39(3):1677–1680, 2003.

[146] Peter Moczo, Jozef Kristek, M Galis, P Pazak, and M Balazovjech. The finite-difference and finite-element modeling of seismic wave propagation and earthquake motion. Acta Physica Slovaca. Reviews and Tutorials, 57(2):177–406, 2007.

[147] Eurıpides Montagne and Anand Ekambaram. An optimal storage format for sparse matrices. Information Processing Letters, 90(2):87–92, 2004.

[148] Hannah Morgan, Matthew G Knepley, Patrick Sanan, and L Ridgway Scott. A stochastic performance model for pipelined krylov methods. Concurrency and Computation: Practice and Experience, 28(18):4532–4542, 2016.

[149] Ronald Morgan. On restarting the arnoldi method for large nonsymmetric eigenvalue problems. Mathematics of Computation of the American Mathematical Society, 65(215): 1213–1230, 1996.

[150] Ronald B Morgan. A restarted gmres method augmented with eigenvectors. SIAM Journal on Matrix Analysis and Applications, 16(4):1154–1171, 1995.

[151] Ronald B Morgan. Gmres with deflated restarting. SIAM Journal on Scientific Computing, 24(1):20–37, 2002.

[152] Aaftab Munshi. The opencl specification. In Hot Chips 21 Symposium (HCS), 2009 IEEE, pages 1–314. IEEE, 2009.

[153] Saurav Muralidharan, Manu Shantharam, Mary Hall, Michael Garland, and Bryan Catanzaro. Nitro: A framework for adaptive code variant tuning. In Parallel and Distributed Processing Symposium, 2014 IEEE 28th International, pages 501–512. IEEE, 2014.

[154] Saurav Muralidharan, Amit Roy, Mary Hall, Michael Garland, and Piyush Rai. Architecture-adaptive code variant tuning. ACM SIGPLAN Notices, 51(4):325–338, 2016.

© 2019 Tous droits réservés.

lilliad.univ-lille.fr

[155] Noël M Nachtigal, Lothar Reichel, and Lloyd N Trefethen. A hybrid gmres algorithm for nonsymmetric linear systems. SIAM Journal on Matrix Analysis and Applications, 13(3): 796–825, 1992.

[156] Ramya Nair, S Bernstein, ER Jessup, and Boyana Norris. Generating customized sparse eigenvalue solutions with lighthouse. In Proceedings of the Ninth International Multi-Conference on Computing in the Global Information Technology, 2014.

[157] Yoshifumi Nakamura, K-I Ishikawa, Y Kuramashi, Tetsuya Sakurai, and Hiroto Tadano. Modified block bicgstab for lattice qcd. Computer Physics Communications, 183(1):34–37, 2012.

[158] Ken Naono, Takao Sakurai, Mitsuyoshi Igai, Takahiro Katagiri, Satoshi Ohshima, Shoji Itoh, Kengo Nakajima, and Hisayasu Kuroda. A fully run-time auto-tuned sparse iterative solver with openatlib. In Intelligent and Advanced Systems (ICIAS), 2012 4th International Conference on, volume 1, pages 143–148. IEEE, 2012.

[159] Olavi Nevanlinna. Convergence of iterations for linear equations. Birkhäuser, 2012.

[160] James C Newman. A finite-element analysis of fatigue crack closure. In Mechanics of crack growth. ASTM International, 1976.

[161] Boyana Norris, Sa-Lin Bernstein, Ramya Nair, and Elizabeth Jessup. Lighthouse: A user-centered web service for linear algebra software. arXiv preprint arXiv:1408.1363, 2014.

[162] Bahram Nour-Omid and Ray W Clough. Short communication block lanczos method for dynamic analysis of structures. Earthquake engineering & structural dynamics, 13(2): 271–275, 1985.

[163] C Nvidia. Cuda c programming guide, version 9.1. NVIDIA Corp, 2018.

[164] CUDA Nvidia. Nvidia cuda c programming guide. Nvidia Corporation, 120(18):8, 2011.

[165] Edson Luiz Padoin, Laércio Lima Pilla, Francieli Zanon Boito, Rodrigo Virote Kassick, Pedro Velho, and Philippe OA Navaux. Evaluating application performance and energy consumption on hybrid cpu+ gpu architecture. Cluster Computing, 16(3):511–525, 2013.

[166] V Pagneux and A Maurel. Determination of lamb mode eigenvalues. The Journal of the Acoustical Society of America, 110(3):1307–1314, 2001.

[167] Christopher C Paige and Michael A Saunders. Solution of sparse indefinite systems of linear equations. SIAM journal on numerical analysis, 12(4):617–629, 1975.

[168] Manolis Papadrakakis and S Smerou. A new implementation of the lanczos method in linear problems. International Journal for Numerical Methods in Engineering, 29(1):141–159, 1990.

[169] Michael L Parks, Eric De Sturler, Greg Mackey, Duane D Johnson, and Spandan Maiti. Recycling krylov subspaces for sequences of linear systems. SIAM Journal on Scientific Computing, 28(5):1651–1674, 2006.

© 2019 Tous droits réservés.

lilliad.univ-lille.fr

[170] Serge Petiton. Parallelization on an mimd computer with real-time scheduler, gauss-jordan example. In Aspects of Computation on Asynchronous Parallel Processors, North-Holland, 1989.

[171] Serge Petiton. Parallel subspace method for non-hermitian eigenproblems on the connection machine (cm2). Applied Numerical Mathematics, 10(1):19–35, 1992.

[172] Judit Planas, Rosa M Badia, Eduard Ayguadé, and Jesús Labarta. Selection of task implementations in the nanos++ runtime. PRACE WP53, 2013.

[173] Gernot Plank, Manfred Liebmann, Rodrigo Weber dos Santos, Edward J Vigmond, and Gundolf Haase. Algebraic multigrid preconditioner for the cardiac bidomain model. IEEE Transactions on Biomedical Engineering, 54(4):585–596, 2007.

[174] DF Pridmore, GW Hohmann, SH Ward, and WR Sill. An investigation of finite-element modeling for electrical and electromagnetic data in three dimensions. Geophysics, 46(7): 1009–1024, 1981.

[175] Matt Probert. High performance computing - history of the supercomputer. University Lecture, 2018.

[176] Nikola Rajovic, Alejandro Rico, Filippo Mantovani, Daniel Ruiz, Josep Oriol Vilarrubi, Constantino Gomez, Luna Backes, Diego Nieto, Harald Servat, Xavier Martorell, et al. The mont-blanc prototype: an alternative approach for hpc systems. In High Performance Computing, Networking, Storage and Analysis, SC16: International Conference for, pages 444–455. IEEE, 2016.

[177] James Reinders. Intel xeon phi processor programming in a nutshell, 2017. URL https://insidehpc.com/2017/01/intel-xeon-phi-processor-programming-nutshell/.

[178] Manman Ren, Ji Young Park, Mike Houston, Alex Aiken, and William J Dally. A tuning framework for software-managed memory hierarchies. In Proceedings of the 17th international conference on Parallel architectures and compilation techniques, pages 280–291. ACM, 2008.

[179] John W Ruge and Klaus Stüben. Algebraic multigrid. In Multigrid methods, pages 73–130. SIAM, 1987.

[180] Karl Rupp, Josef Weinbub, Ansgar Jüngel, and Tibor Grasser. Pipelined iterative solvers with kernel fusion for graphics processing units. ACM Transactions on Mathematical Software (TOMS), 43(2):11, 2016.

[181] Y Saad. Sparsekit: a basic tool kit for sparse matrix computation (version2), university of illinois, 1994.

[182] Youcef Saad. Chebyshev acceleration techniques for solving nonsymmetric eigenvalue problems. Mathematics of Computation, 42(166):567–588, 1984.

© 2019 Tous droits réservés.

lilliad.univ-lille.fr

[183] Youcef Saad. On the lanczos method for solving symmetric linear systems with several right-hand sides. Mathematics of computation, 48(178):651–662, 1987.

[184] Youcef Saad. Least squares polynomials in the complex plane and their use for solving nonsymmetric linear systems. SIAM Journal on Numerical Analysis, 24(1):155–169, 1987.

[185] Youcef Saad and Martin H Schultz. Gmres: A generalized minimal residual algorithm for solving nonsymmetric linear systems. SIAM Journal on scientific and statistical computing, 7(3):856–869, 1986.

[186] Yousef Saad. Krylov subspace methods for solving large unsymmetric linear systems. Mathematics of computation, 37(155):105–126, 1981.

[187] Yousef Saad. Ilut: A dual threshold incomplete lu factorization. Numerical linear algebra with applications, 1(4):387–402, 1994.

[188] Yousef Saad. Iterative methods for sparse linear systems. Siam, 2003.

[189] Yousef Saad. Numerical Methods for Large Eigenvalue Problems: Revised Edition. SIAM, 2011.

[190] Yousef Saad and Maria Sosonkina. Distributed schur complement techniques for general sparse linear systems. SIAM Journal on Scientific Computing, 21(4):1337–1356, 1999.

[191] Tetsuya Sakurai, Hiroto Tadano, and Y Kuramashi. Application of block krylov subspace algorithms to the wilson–dirac equation with multiple right-hand sides in lattice qcd. Computer Physics Communications, 181(1):113–117, 2010.

[192] Patrick Sanan, Sascha M Schnepp, and Dave A May. Pipelined, flexible krylov subspace methods. SIAM Journal on Scientific Computing, 38(5):C441–C470, 2016.

[193] Martin Schweiger, SR Arridge, M Hiraoka, and DT Delpy. The finite element method for the propagation of light in scattering media: boundary and source conditions. Medical physics, 22(11):1779–1792, 1995.

[194] Kubilay Sertel and John L Volakis. Incomplete lu preconditioner for fmm implementation. Microwave and Optical Technology Letters, 26(4):265–267, 2000.

[195] Chang-Hoon Shim, Fumito Maruoka, and Reiji Hattori. Structural analysis on organic thin-film transistor with device simulation. IEEE Transactions on Electron Devices, 57 (1):195–200, 2010.

[196] Masanobu Shinozuka and Clifford J Astill. Random eigenvalue problems in structural analysis. AIAA journal, 10(4):456–462, 1972.

[197] Valeria Simoncini and Efstratios Gallopoulos. An iterative method for nonsymmetric systems with multiple right-hand sides. SIAM Journal on Scientific Computing, 16(4): 917–933, 1995.

© 2019 Tous droits réservés.

lilliad.univ-lille.fr

[198] Gerard LG Sleijpen and Diederik R Fokkema. Bicgstab (l) for linear equations involving unsymmetric matrices with complex spectrum. Electronic Transactions on Numerical Analysis, 1(11):2000, 1993.

[199] Charles F Smith, Andrew F Peterson, and Raj Mittra. A conjugate gradient algorithm for the treatment of multiple incident electromagnetic fields. IEEE Transactions on Antennas and Propagation, 37(11):1490–1493, 1989.

[200] Dennis Chester Smolarski. Optimum semi-iterative methods for the solution of any linear algebraic system with a square matrix. PhD thesis, University of Illinois at Urbana-Champaign, 1982.

[201] Danny C Sorensen. Implicitly restarted arnoldi/lanczos methods for large scale eigenvalue calculations. In Parallel Numerical Algorithms, pages 119–165. Springer, 1997.

[202] Gerhard Starke. Field-of-values analysis of preconditioned iterative methods for nonsymmetric elliptic problems. Numerische Mathematik, 78(1):103–117, 1997.

[203] Pyrrhos Stathis, Stamatis Vassiliadis, and Sorin Cotofana. A hierarchical sparse matrix storage format for vector processors. In Parallel and Distributed Processing Symposium, 2003. Proceedings. International, pages 8–pp. IEEE, 2003.

[204] Gilbert W Stewart. A krylov–schur algorithm for large eigenproblems. SIAM Journal on Matrix Analysis and Applications, 23(3):601–614, 2002.

[205] N Sukumar, DL Chopp, and B Moran. Extended finite element method and fast marching method for three-dimensional fatigue crack propagation. Engineering Fracture Mechanics, 70(1):29–48, 2003.

[206] Kasia Swirydowicz, Julien Langou, Shreyas Ananthan, Ulrike Yang, and Stephen Thomas. Low synchronization gmres algorithms. arXiv preprint arXiv:1809.05805, 2018.

[207] Yuan Tang, Rezaul Alam Chowdhury, Bradley C Kuszmaul, Chi-Keung Luk, and Charles E Leiserson. The pochoir stencil compiler. In Proceedings of the twenty-third annual ACM symposium on Parallelism in algorithms and architectures, pages 117–128. ACM, 2011.

[208] TheNextPlatform. TheNextPlatform argonne hints at future architecture of aurora exascale system, 2018. URL https://www.nextplatform.com/2018/03/19/argonne-hints-at-future-architecture-of-aurora-exascale-system/.

[209] top500. Top 500 list of november 2018, 2018. URL https://www.top500.org/lists/2018/11.

[210] Lloyd N Trefethen. Approximation theory and numerical linear algebra. In Algorithms for approximation II, pages 336–360. Springer, 1990.

[211] Raymond van Venetië and Jan Westerdiep. Induced dimension reduction. 2015.

[212] Petr Vaněk, Jan Mandel, and Marian Brezina. Algebraic multigrid by smoothed aggregation for second and fourth order elliptic problems. Computing, 56(3):179–196, 1996.

© 2019 Tous droits réservés.

lilliad.univ-lille.fr

[213] Brendan Vastenhouw and Rob H Bisseling. A two-dimensional data distribution method for parallel sparse matrix-vector multiplication. SIAM review, 47(1):67–95, 2005.

[214] John Von Neumann. First draft of a report on the edvac, 30 june 1945. Contract No W-670-ORD-492, Moore School of Electrical Engineering, University of Pennsylvania, Philadelphia. Google Scholar, 1945.

[215] Heinrich Voß. An arnoldi method for nonlinear eigenvalue problems. BIT numerical mathematics, 44(2):387–401, 2004.

[216] Richard Vuduc, James W Demmel, and Katherine A Yelick. Oski: A library of automatically tuned sparse matrix kernels. In Journal of Physics: Conference Series, volume 16, page 521. IOP Publishing, 2005.

[217] Olof Widlund. A lanczos method for a class of nonsymmetric systems of linear equations. SIAM Journal on Numerical Analysis, 15(4):801–812, 1978.

[218] Sandra Wienke, Paul Springer, Christian Terboven, and Dieter an Mey. Openacc—first experiences with real-world applications. In European Conference on Parallel Processing, pages 859–870. Springer, 2012.

[219] WikiChips. WikiChips matrix-2000 - nudt, 2017. URL https://en.wikichip.org/wiki/nudt/matrix-2000.

[220] Wikipedia. Fork–join model — from Wikipedia, the free encyclopedia, 2018. URL https://en.wikipedia.org/wiki/Fork\T1\textendashjoin_model. [Online; accessed 04-January-2019].

[221] Michael Wilde, Mihael Hategan, Justin M Wozniak, Ben Clifford, Daniel S Katz, and Ian Foster. Swift: A language for distributed parallel scripting. Parallel Computing, 37(9): 633–652, 2011.

[222] Markus Wittmann, Georg Hager, Thomas Zeiser, and Gerhard Wellein. An analysis of energy-optimized lattice-boltzmann cfd simulations from the chip to the highly parallel level. CoRR, vol. abs/1304.7664, 2013.

[223] Cornell Virtual Workshop. Cornell Virtual Workshop getting started on knl, 2019. URL https://cvw.cac.cornell.edu/knlstart/MemModes.

[224] Xinzhe Wu. Smg2s manual v1. 0. Technical report, 2018.

[225] Xinzhe Wu and Serge G Petiton. A distributed and parallel asynchronous unite and conquer method to solve large scale non-hermitian linear systems. In Proceedings of the International Conference on High Performance Computing in Asia-Pacific Region, pages 36–46. ACM, 2018.

[226] Xinzhe Wu, Serge Petiton, and Yutong Lu. A parallel generator of non-hermitian matrices computed from given spectra. In VECPAR 2018: 13th International Meeting on High Performance Computing for Computational Science, 2018.

© 2019 Tous droits réservés.

lilliad.univ-lille.fr

[227] Ichitaro Yamazaki, Stanimire Tomov, and Jack Dongarra. Mixed-precision cholesky qr factorization and its case studies on multicore cpu with multiple gpus. SIAM Journal on Scientific Computing, 37(3):C307–C330, 2015.

[228] Ichitaro Yamazaki, Mark Hoemmen, Piotr Luszczek, and Jack Dongarra. Improving performance of gmres by reducing communication and pipelining global collectives. In Parallel and Distributed Processing Symposium Workshops (IPDPSW), 2017 IEEE International, pages 1118–1127. IEEE, 2017.

[229] Ulrike Meier Yang et al. Boomeramg: a parallel algebraic multigrid solver and preconditioner. Applied Numerical Mathematics, 41(1):155–177, 2002.

[230] Xiyang IA Yang and Rajat Mittal. Acceleration of the jacobi iterative method by factors exceeding 100 using scheduled relaxation. Journal of Computational Physics, 274:695–708, 2014.

[231] Zuochang Ye, Zhenhai Zhu, and Joel R Phillips. Generalized krylov recycling methods for solution of multiple related linear equation systems in electromagnetic analysis. In Proceedings of the 45th annual Design Automation Conference, pages 682–687. ACM, 2008.

[232] Seokkwan Yoon and Antony Jameson. Lower-upper symmetric-gauss-seidel method for the euler and navier-stokes equations. AIAA journal, 26(9):1025–1026, 1988.

© 2019 Tous droits réservés.

lilliad.univ-lille.fr

Appendix

Construct the Optimal Ellipse

The Least Squares polynomial preconditioning in UCGLE method relies on the computation of a polynomial constructed from an optimal ellipse which enclosing the spectrum of operator matrix. This ellipse is constructed by the polygon H constructed by the dominant eigenvalues approximated from ERAM Component. A good selection of this optimal ellipse, therefore, a crucial algorithm for the implementation. Denote the optimal ellipse as $ellipse(a, c, d)$, with a the length of major axis, d the center, and c the focal of this ellipse. The optimal ellipse can be calculated by either two or three discrete points. The best ellipse is either an ellipse that passes through three vertices of H and encloses H or an ellipse of smallest area passing through two vertices of H. In practice, this ellipse is implemented to be symmetric about the real axis. We list the formulas used of the computation of optimal ellipses in our implementation of UCGLE. Both the two way of finding the optimal ellipse come from the existing literature.

Two-point Ellipse

The formules of two-point optimal ellipse are given by Saad in [189]. As shown in Fig. 1, suppose that two points $\lambda_1 = x_1 + iy_1$ and $\lambda_2 = x_2 + iy_2$ are used to construct an optimal $ellipse(a, c, d)$ of smallest area. Assume that $y1 \neq y2$.

Denote that

$$A = \frac{1}{2}(x_2 - x_1), \quad B = \frac{1}{2}(x_2 + x_1),$$

$$S = \frac{1}{2}(y_2 - y_1), \quad T = \frac{1}{2}(y_2 + y_1), \tag{1}$$

$$Q = \frac{1}{2}\Big(\frac{S}{T} + \frac{T}{S}\Big).$$

The three parameters a, c and d of the optimal ellipse can be calculated by the following formulas.

© 2019 Tous droits réservés.

lilliad.univ-lille.fr

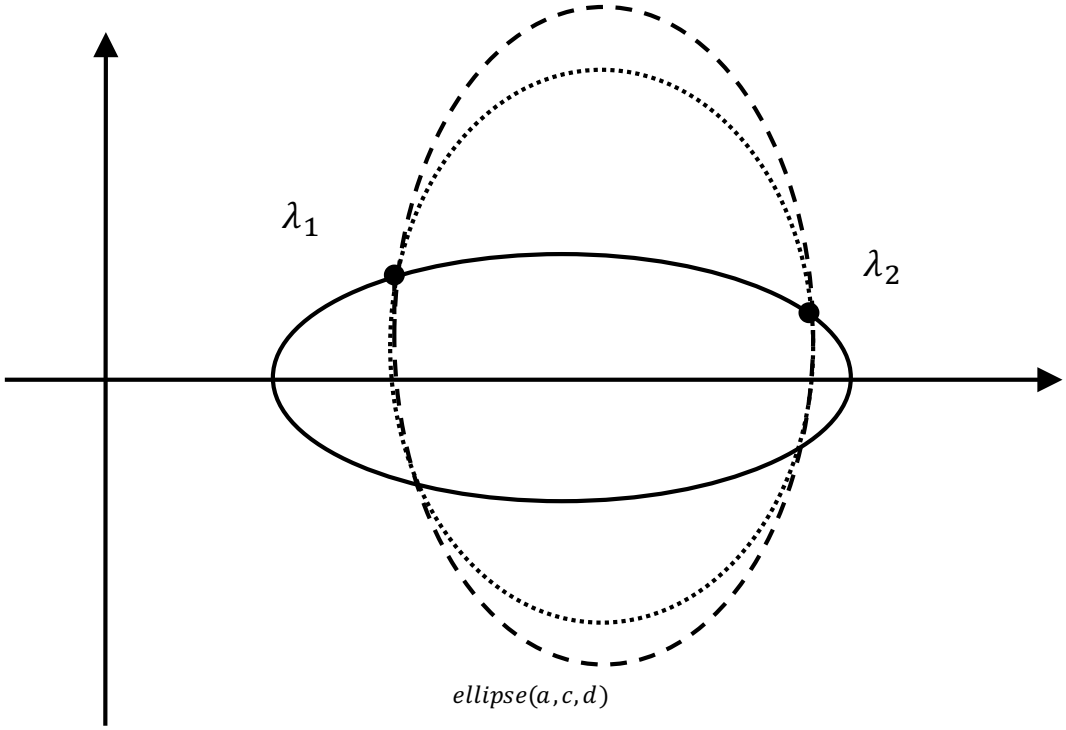

Figure 1 – Two-point $ellipse(a, c, d)$.

$$d = \frac{A}{\sqrt{Q^2+3} + \mathrm{sgn}(AS)Q} + B,$$

$$c^2 = \frac{1}{d-B}[(d-B+\frac{AT}{S})(d-B+\frac{AS}{T})(d-B-\frac{ST}{A})], \tag{2}$$

$$a^2 = (d-B+\frac{AT}{S})(d-B+\frac{AS}{T}).$$

Three-way Ellipse

Three points to construct is presented by Manteuffel in [142]. Shown as Fig. 2a and 2b, suppose that three points $\lambda_1 = x_1+iy_1$, $\lambda_2 = x_2+iy_2$, $\lambda_3 = x_3+iy_3$ are used to construct an $ellipse(a, c, d)$. Assume that $x_1 < x_2 < x_3$. The optimal ellipse can be determined by the following formules.

$$d = \frac{1}{2}\frac{(y_1^2(x_2^2-x_3^2)+y_2^2(x_3^2-x_1^2)+y_3^2(x_1^2-x_3^2))}{(y_1^2(x_2-x_3)+y_2^2(x_3-x_1)+y_3^2(x_1-x_3))},$$

$$a^2 = d^2 - \frac{(y_1^2x_2x_3(x_2-x_3)+y_2^2x_1x_2(x_3-x_1)+y_3^2x_1x_2(x_1-x_3))}{(y_1^2(x_2-x_3)+y_2^2(x_3-x_1)+y_3^2(x_1-x_3))}, \tag{3}$$

$$c^2 = a^2\left(1 - \frac{(y_1^2(x_2-x_3)+y_2^2(x_3-x_1)+y_3^2(x_1-x_3))}{(x_1-x_2)(x_2-x_3)(x_3-x_1)}\right).$$

© 2019 Tous droits réservés.

lilliad.univ-lille.fr

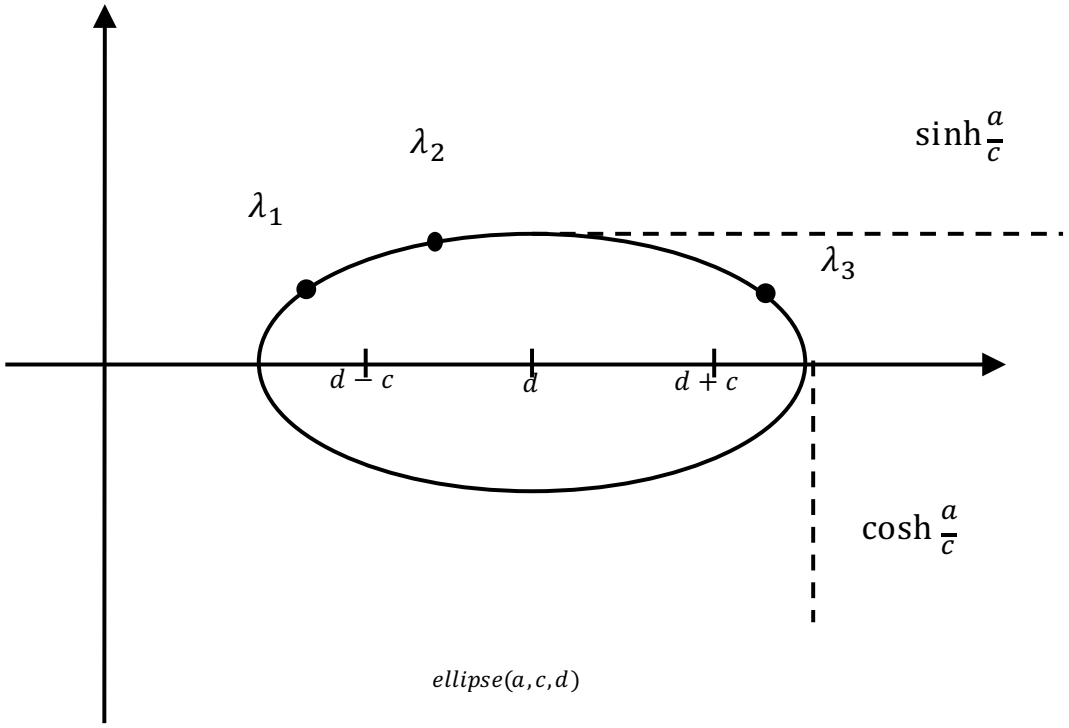

(a)

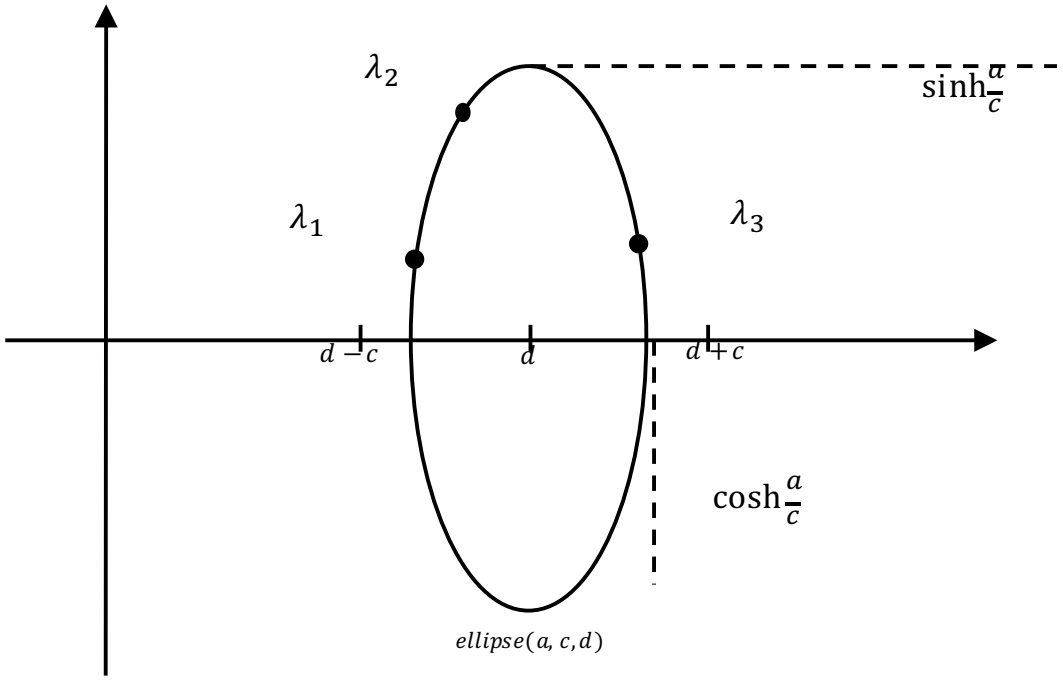

(b)

Figure 2 – Three-way $ellipse(a, c, d)$.

© 2019 Tous droits réservés.

© 2019 Tous droits réservés.

lilliad.univ-lille.fr

Appendix

Scientific Communication

Peer-reviewed publications

- Xinzhe Wu and Serge G. Petiton, "A Distributed and Parallel Asynchronous Unite and Conquer Method to Solve Large Scale Non-Hermitian Linear Systems" in HPC Asia 2018: International Conference on High Performance Computing in Asia-Pacific Region, Tokyo, Japan.

- Xinzhe Wu, Serge G. Petiton and Yutong Lu, "A Parallel Generator of Non-Hermitian Matrices computed from Given Spectra" in VECPAR 2018: 13th International Meeting on High Performance Computing for Computational Science, São Pedro, Brazil.

- Xinzhe Wu and Serge G. Petiton, "A Distributed and Parallel Unite and Conquer Method to Solve Sequences of Non-Hermitian Linear Systems". Submitted to Japan Journal of Industrial and Applied Mathematics. [Under Review].

- Xinzhe Wu and Serge G. Petiton, "A Distributed and Parallel Asynchronous Unite and Conquer Method to Solve Large Scale Non-Hermitian Linear Systems with Multiple Right-hand Sides". Submitted to Parallel Computing. [Under Review].

- Xinzhe Wu and Serge G. Petiton, "A parallel generator of non-Hermitian matrices computed from given spectra". Submitted to Concurrency & Computation: Practice & Experience. [Under Review].

Invited and Contributed Talks

- Serge G. Petiton and Xinzhe Wu, "An Asynchronous Distributed and Parallel Unite and Conquer Method to Solve Sequences of Non-Hermitian Linear systems" in MATHIAS 2018: Computational Science Engineering & Data Science by TOTAL, Serris, France.

- Xinzhe Wu, Serge G. Petiton and Yutong Lu, "A Parallel Generator of Non-Hermitian Matrices Computed from Given Spectra" in VECPAR 18: 13th International Meeting on High Performance Computing for Computational Science, São Pedro, Brazil.

© 2019 Tous droits réservés.

lilliad.univ-lille.fr

- Xinzhe Wu and Serge G. Petiton, "A Parallel Generator of Non-Hermitian Matrices Computed from Given Spectra" in PMAA18: 10th International Workshop on Parallel Matrix Algorithms and Applications, Zurich, Switzerland.
- Xinzhe Wu and Serge G. Petiton, "A Parallel Generator of Non-Hermitian Matrices Computed from Known Given Spectra" in 3rd Workshop on Parallel Programming Models - Productivity and Applications, Aachen, Germany.
- Xinzhe Wu and Serge G. Petiton, "A Parallel Generator of Non-Hermitian Matrices Computed from Known Given Spectra" in SIAM PP18: SIAM Conference on Parallel Processing for Scientific Computing, Tokyo, Japan.
- Serge G. Petiton and Xinzhe Wu, "The Unite and Conquer GMRES-LS/ERAM method to solve sequences of Linear Systems" in EPASA 2018: International Workshop on Eigenvalue Problems: Algorithms, Software and Applications, in Petascale Computing, Tsukuba, Japan.
- Xinzhe Wu and Serge G. Petiton, "A Distributed and Parallel Asynchronous Unite and Conquer Method to Solve Large Scale Non-Hermitian Linear Systems" in HPC Asia 2017: International Conference on High Performance Computing in Asia-Pacific Region, Tokyo, Japan.
- Serge G. Petiton, Xinzhe Wu and Tao Chang, "A Distributed and Parallel Asynchronous Unite and Conquer Method to Solve Large Scale Non-Hermitian Linear Systems" in Preconditioning 2017: International Conference On Preconditioning Techniques For Scientific And Industrial Applications, Vancouver, Canada.

Posters

- Xinzhe Wu and Serge G. Petiton, "Large Non-Hermitian Matrix Generation with Given Spectra" in EPASA 2018: International Workshop on Eigenvalue Problems: Algorithms, Software and Applications, in Petascale Computing, Tsukuba, Japan.

Software Manual/Technical Reports

- Xinzhe Wu, "SMG2S Manual" in Maison de la Simulation, France - Version 1.0, 2018.

© 2019 Tous droits réservés.

lilliad.univ-lille.fr

© 2019 Tous droits réservés.

lilliad.univ-lille.fr